Invited Speaker

595 Following low and high-temperature electrolysis processes with in-situ and cryo electron microscopy
Shibabrata Basak[1], Pritam Chakraborty[1], Jean-Pierre Poc[1], Tobias Mehlkoph[1], Junbeom Park[1], Eva Jodat[1], André Karl[1], Rüdiger-A Eichel[1]
[1]Institute of Energy and Climate Research, Fundamental Electrochemistry (IEK-9), Forschungszentrum Jülich GmbH, Jülich, Germany

Oral Presentation

32 In situ microscopic observations of zinc electrodeposition process in various electrolytes
Dr Kaname Yoshida[1], Dr. Yuki Sasaki[1], Dr. Akihide Kuwabara[1], Prof. Yuichi Ikuhara[1,2]
[1]Japan Fine Ceramics Center, Nagoya, Japan, [2]The University of Tokyo, Bunkyo-ku, Japan
239 Cation Vacancies Regulate the Electron Spin Configuration of Cathode Catalytic Additives towards Robust Li-S Batteries
PhD JING YU[1,2], Mr. Andreu Cabot[2], Mr. Jordi Arbiol[1]
[1]Catalan Institute of Nanoscience and Nanotechnology (ICN2), Bellaterra, 08193, Spain, [2]Catalonia Institute for Energy Research（IREC）, Sant Adrià de Besòs, 08930 , Spain
268 Operando ETEM study on solid oxide cells
Zhongtao Ma[1], Mr. Christodoulos Chatzichristodoulou[1], Mr. Kristian Speranza Mølhave[2], Mr. Søren Bredmose Simonsen[1]
[1]DTU Energy, Kongens Lyngby, Denmark, [2]DTU Nanolab, Kongens Lyngby, Denmark
420 MAX phase-based nanocomposites for LIBs negative electrodes investigated by multi-approach TEM analysis
Irene Ostroman[1], Dr. Cameron Duncan[1], Mrs. Beatrice Ferrari[1], Mrs. Maria Giulia Bravi[1], Dr. Antonio Gentile[2], Dr. Stefano Marchionna[2], Dr. Chiara Ferrara[1], Dr. Taewon Kim[3], Dr. Changhyun Park[3], Dr. Chanhee Lee[3], Prof. Hyun-Wook Lee[3], Prof. Riccardo Ruffo[1], Prof. Giovanni Maria Vanacore[1]
[1]Università degli Studi di Milano-Bicocca - UNIMIB, Milano, Italy, [2]Ricerca sul Sistema Energetico - RSE S.p.A, Milano, Italy, [3]Ulsan National Institute of Science and Technology - UNIST, Ulsan, Republic of Korea
706 3D Operando Monitoring of lithiation spatial composition in NMC-cathode electrode by X-ray nano-CT & XANES-techniques
Dr. Arnaud Demortière[1], Dr. Tuan-Tu Nguyen[1], Dr. Vincent De Andrade[2], Dr. Zeliang Su[1]
[1]Laboratoire de Réactivité et Chimie des Solides (LRCS), CNRS UMR7314, Amiens , France, [2]Argonne NL, Chicago, USA
721 Nanowire Triple-Junction GaInP/InP/InAsP Solar Cells Realized
Prof. Reine Wallenberg[1,2], Dr Lukas Hrachowina[2], Prof Magnus Borgström[2]
[1]national center for HREM, Lund University, Lund, Sweden, [2]NanoLund, Lund University, Lund, Sweden
48 (In-situ) 3DED and other TEM Techniques Unravel (Ca,Sr)(Mn,Fe)O3-δ and LaxSr2-xMnO4-δ Structure-Property Relations in Redox Conditions
Daphne Vandemeulebroucke[1], Dr. Maria Batuk[1], Mr. Amirhossein Hajizadeh[1], Dr. Pascal Roussel[2], Dr. Myriam Wastiaux[2], Prof. Dr. Joke Hadermann[1]
[1]EMAT, University of Antwerp, Antwerp, Belgium, [2]UCCS, CNRS, University of Lille, Lille, France
129 Exploring solid conversion products in lithium-sulfur batteries through cryo-TEM and machine-learning-supported small angle neutron scattering
Jean-marc Von Mentlen[1], Mrs. Ayca Senol[1], Mr. Thomas Demuth[3], Dr. Jürgen Belz[3], Dr. Alen Vižintin[4], Prof. Dr. Kerstin Volz[3], Prof. Dr. Vanessa Wood[1], Prof. Dr. Christian Prehal[2]

[1]ETH Zurich, Zurich, Switzerland, [2]Paris Lodron University Salzburg, Salzburg, Austria, [3]Phillips University Marburg, Marburg, Germany, [4]National Institute of Chemistry, Ljubljana, Slovenia

195 Operando structural and chemical imaging of lithium battery interfaces

Sayantan Sharma[1,2], Dr. Luca Cressa[1], Dr. Tom Wirtz[1], Dr. Santhana Eswara[1]
[1]Advanced Instrumentation for Nano-Analytics (AINA), Materials Research and Technology Department, Luxembourg Institute of Science and Technology (LIST), Belvaux, Luxembourg, [2]University of Luxembourg, Belval, Luxembourg

444 In-situ TEM reduction of a solid oxide cell with NiO/YSZ and NiO/BZCY fuel electrode materials

Dr Svetlana Korneychuk[1,2,3], Cedric Grosselindemann[4], Laura-Alena Schäfer[5], Dr.-Ing. Mariya E. Ivanova[5], Hon.-Prof. Dr.-Ing. Norbert H. Menzler[5], Prof. Dr. Olivier Guillon[5], PD Dr.-Ing. André Weber[4], Prof. Dr. rer. nat. Astrid Pundt[1]
[1]IAM-WK, Karlsruhe Institute of Technology, Karlsruhe, Germany, [2]INT, Karlsruhe Institute of Technology, Karlsruhe, Germany, [3]KNMFi, Karlsruhe Institute of Technology, Karlsruhe, Germany, [4]IAM-ET, Karlsruhe Institute of Technology, Karlsruhe, Germany, [5]Forschungszentrum Jülich GmbH, Institute of Energy and Climate Research (IEK), IEK-1: Materials Synthesis and Processing, Jülich, Germany

603 Operating a model Solid Oxide Fuel Cell in the Environmental Transmission Electron Microscope

Dr Matthieu Bugnet[1], Dr Thierry Epicier[2], Dr Cedric Frantz[3], Dr Stefan Diethelm[3], Dr Dario Montinaro[4], Dr Elizaveta Tyukalova[5], Dr Yevheniy Pivak[6], Prof Jan Van Herle[3], Prof Aïcha Hessler-Wyser[7], Prof Martial Duchamp[5], Dr Quentin Jeangros[7]
[1]CNRS, INSA Lyon, Université Caliude Bernard Lyon 1, MATEIS, UMR 5510 , Villeurbanne, France, [2]Université Claude Bernard Lyon 1, IRCELYON, UMR CNRS 5256, Villeurbanne, France, [3]Group of Energy Materials, Ecole Polytechnique Fédérale de Lausanne, Sion, Switzerland, [4]SolydEra S.p.A., Mezzolombardo, Italy, [5]Laboratory for In Situ & Operando Electron Nanoscopy, School of Materials Science, Nanyang Technological University, Singapore, Singapore, [6]DENSsolutions, Delft, The Netherlands, [7]Photovoltaics and Thin Film Electronics Laboratory, Ecole Polytechnique Fédérale de Lausanne, , Switzerland

615 In-situ TEM Investigation of Degradation Process in Ni-Rich Cathodes.

Mr Ioannis Siachos[1,2], Dr Xiaodong Liu[1], Dr Annalena Genreith-Schriever[2,3], Dr Tingting Yang[4], Dr Penghan Lu[4], Prof. Rafal Dunnin-Borkowski[4], Prof. Clare Gray[2,3], Prof. Layla Mehdi[1,2]
[1]Department of Materials, Design & Manufacturing Engineering, University of Liverpool, Liverpool, UK, [2]The Faraday Institution, Harwell Campus, Didcot, Oxford, UK, [3]Department of Chemistry, University of Cambridge, Cambridge, UK, [4]Ernst Ruska-Centre for Microscopy and Spectroscopy with Electrons, Research Centre Juelich, 52425, Juelich, Germany

634 Atomic-resolution mapping of phonon modes across Magnéli structures in thermoelectric (Al,Nb)-doped TiO2

Dr Shihao Wang[1,2], Dr Demie Kepaptsoglou[1,3], Dr Jan Rusz[4], Dr Paul Zeiger[4], Dr Xiaodong Liu[5,6], Dr Robert Freer[6], Dr Quentin Ramasse[1,2]
[1]SuperSTEM Laboratory, STFC Daresbury Campus, Daresbury WA4 4AD, United Kingdom, [2]School of Chemical and Process Engineering, University of Leeds, Leeds LS2 9JT, United Kingdom, [3]Department of Physics, University of York, York Yo10 5DD, United Kingdom, [4]Department of Physics and Astronomy, University of Uppsala, P.O. Box 516, 75120, Uppsala, Sweden, [5]Department of Mechanical, Materials & Aerospace Engineering, University of Liverpool, Liverpool L69 3BX, United Kingdom, [6]Department of Materials, University of Manchester, Manchester M13 9PL, United Kingdom

699 Unveiling degradation mechanisms in layered Li-rich cathode materials using combined operando neutron diffraction and 4D-STEM

Dr. Tingting Yang[1], Maolin Yang[2], Zhongyuan Huang[2], Dr. Rui Wang[3], Peng-han Lu[1], Prof. Rafal Dunin-Borkowski[1], Dr. Lei Jin[1], Prof. Yinguo Xiao[2]
[1]Forschungszentrum Juelich, Juelich, Germany, [2]Peking University Shenzhen Graduate School, ShenZhen, China, [3]Department of Engineering, University of Cambridge, Cambridge, UK

157 Unique in-situ characterization workflow of Cathode Components using AFM-in-SEM
Veronika Hegrova[1], Mr. Radek Dao[1], Dr. Vojtech Schanilec[1], Dr. Jan Neuman[1]
[1]NenoVision s. r. o., Brno, Czech Republic
437 Unraveling the original dissolution mechanism of LiFePO4 when treated for recycling
Dr. Adrien Boulineau[1], Julie Poulizac[1,2], Dr. Emmanuel Billy[1], Pr. Karien Masenelli-Varlot[2]
[1]Univ. Grenoble Alpes, CEA, LITEN, Grenoble, France, [2]Univ. Lyon, INSA Lyon, UCBL, CNRS, MATEIS, Villeurbanne, France
616 Identification of Chemical Segregation and Surface Twinning Structures in Electro-deposited Al Dendrites
Dr Xiaodong Liu[1], Dr Fatemehsadat Rahide[2], Dr Tingting Yang[3], Dr Penghan Lu[3], Dr Sonia Dsoke[2,4,5], Dr Helmut Ehrenberg[2], Professor Rafal E Dunin-Borkowski[3], Professor Layla Mehdi[1,6]
[1]Department of Materials, Design & Manufacturing Engineering, University of Liverpool, Liverpool, UK, [2]Institute for Applied Materials, Karlsruhe Institute of Technology, Eggenstein-Leopoldshafen, Germany, [3]Ernst Ruska-Centre for Microscopy and Spectroscopy with Electrons, Research Centre Juelich, Juelich, Germany, [4]Department of Sustainable Systems Engineering, Albert-Ludwigs-University of Freiburg, Freiburg, Germany, [5]Fraunhofer Institute for Solar Energy Systems, Department of Electrical Energy Storage, Freiburg, Germany, [6]Albert Crewe Centre, University of Liverpool, , UK
622 Stability insights of MnO2 electrocatalysts from identical location and in-situ electrochemical liquid cell electron microscopy
Dr. Raquel Aymerich Armengol[1], Lau Morten Kaas[1], Alba Bech Larsen[1], Marika Birkedal Norby[1], Christian Danvad Damsgaard[1,2], Peter Christian Kjærgaard Vesborg[1], Jakob Kibsgaard[1], Stig Helveg[1]
[1]Center for Visualizing Catalytical Processes (VISION), Technical University of Denmark (DTU), Kongens Lyngby, Denmark, [2]Nanolab, Technical University of Denmark (DTU), Kongens Lyngby, Denmark
662 Analyzing Lithiation Dynamics in LiFePO4 Cathode : Insights from TEM Experiments and Phase Field Modeling
Ahmed Yousfi[1], Justine Jean[1], Kevyn Gallegos Moncayo[1], Florent Magaud[1], Guillaume Boussinot[2], Arnaud Demortière[1]
[1]Laboratoire de Réactivité et Chimie des Solides(LRCS)/Centre National de Recherche Scientifique(CNRS)/Université de Picardie Jules Verne(UPJV)/RS2E, Amiens, France, [2]Access e.V Institute, Rheinisch-Westfälische Technische Hochschule (RWTH) Aachen University, Aachen, Germany
772 Microstructural Influence on Sodium Filament Growth in All Solid-state Batteries
Dr. Ziming Ding[1], Dr. Yushu Tang[1], Till Ortmann[2], Dr. Janis Kevin Eckhardt[2], Dr. Marcus Rohnke[2], Dr. Georgian Melinte[1], Prof. Dr. Christian Heiliger[2], Prof. Dr. Jürgen Janek[2], Prof. Dr. Christian Kübel[1,3]
[1]Institute of Nanotechnology (INT), Karlsruhe Institue of Techonology (KIT), Karlsruhe, Germany, [2]Institute for Physical Chemistry and Center for Materials Research, Justus Liebig University Giessen, Giessen, Germany, [3]Karlsruhe Nano Micro Facility (KNMF), Karlsruhe Institute of Technology (KIT), Germany
154 Oxidation states of IrOx characterised by EELS and ED-PDF
Dr. Trung-Dung Tran[1,2], Mr. Dogan Ozkaya[1,2]
[1]Johnson Matthey Technology Centre, Reading, UK, [2]ePSIC, Diamond Light Source, Didcot, UK
296 Electron Microscopy of Novel Lithium Alloy Anodes for Solid State Batteries
Dr Ed Darnbrough[1], Mrs Myra Ng[1], Dr Sreejith Olakkil Veedu[1], Prof David Armstrong[1], Prof Chris Grovenor[1], Prof Pete Nellist[1]
[1]University of Oxford, Oxford, United Kingdom
306 Mitigating radiation damage in beam sensitive battery materials by adapting scanning parameters
Mme. Hannah Nickles Jäkel[1], Mr Eric Gautron[1], Mr Maurice Peeman[2], Mr Philippe Moreau[1], Ms Patricia Abellan[1]

[1]Nantes Université, CNRS, Institut des Matériaux de Nantes Jean Rouxel, IMN, 44000 Nantes, France, [2]Thermo Fisher Scientific, Eindhoven, Netherlands

533 Investigating the formation of surface reconstruction layers in Ni-rich cathode materials using STEM

Lara Ahrens[1,2], Kilian Vettori[3], Dr. Shibabrata Basak[4], Prof. Dr. Rüdiger-A. Eichel[4], Prof. Dr. Joachim Mayer[1,2]
[1]Central Facility for Electron Microscopy (GFE), RWTH Aachen University, Aachen, Germany, [2]Ernst Ruska-Centre for Microscopy and Spectroscopy with Electrons, Forschungszentrum Jülich, Jülich, Germany, [3]Physical-Chemical Institute, Justus-Liebig-University, Gießen, Germany, [4]Institute of Energy and Climate Research (IEK-9), Forschungszentrum Jülich , Jülich, Germany

587 PFIB-preparation and STEM-characterization of electrochemically plated lithium at the interface to the solid electrolyte Li6PS5Cl

Franziska Hüppe[1], Juri Becker[2], Dr. Jürgen Belz[1], Dr. Shamail Ahmed[1], Dr. Till Fuchs[2], Dr. Burak Aktekin[2], Prof. Dr. Jürgen Janek[2], Prof. Dr. Kerstin Volz[1]
[1]Department of Physics, Philipps-Universität Marburg, Marburg, Germany, [2]Institute of Physical Chemistry and Center for Materials Research, Justus-Liebig-Universität Gießen, Gießen, Germany

619 Defect engineering of core-shell systems based on 2D transition metal dichocalgenides

Juan José Quintana González[1], Antonio Jesus Medina Olivera[1], Dr Ramon Manzorro[1], Dr Cédric Pardanaud[2], Dr Rong Sun[1], Dr Ana Belén Hungría[1], Dr Laura Cubillana Aguilera[3], Dr Jose María Palacios Santander[3], Dr Juan Carlos Hernández Garrido[1], Dr Luc Lajaunie[1]
[1]Department of Inorganic Chemistry, Faculty of Sciences. University of Cadiz, Puerto Real, Spain, [2]Aix-Marseille Université, CNRS, PIIM UMR 7345, Marseille, France, [3]Department of Analytical Chemistry, Faculty of Sciences. University of Cadiz,, Puerto Real, Spain

867 From design to « operando » experiments in the SEM: application to battery studies

Dr Neelam Yadav[1], Mrs Melissa HERMANN ALba[1], Dr Morcrette Mathieu[1,2], Dr Carine Davoisne[1,2]
[1]LRCS, UMR CNRS 7314, Amiens, France, [2]Réseau sur le Stockage Electrochimique de l'Energie (RS2E), FR CNRS 3459, , France

1126 Mapping Li in thin-films and heterostructures by EELS and ptychography: case of Li7La3Zr2O12 and LiCoO3

Dr Adam Kerrigan[2], Dr Connor Murril[2], Dr Demie Kepaptsoglou[1,3], Dr Chris Allen[4], Dr Mohsen Danaie[4], Dr Frederick Allars[4], Prof Vlado Lazarov[1,2]
[1]School of Physics, Engineering and Technology, University of York, York, UK, [2]The York-JEOL Nanocentre, University of York, York, UK, [3]SuperSTEM Laboratory, SciTech Daresbury, Daresbury, UK, [4]Electron Physical Science Imaging Centre, Diamond Light Source Ltd., Oxford, UK

Poster Presentation

22 Seeing the nanoscale dynamics in gas-based processes by using in-situ TEM

Tanmay Ghosh[1,3], Ms Tjiu Weng Weei[1], Mr. Khakimjon Saidov[2,3], Mr. Antoine Pacco[5], Mr Harold Philipsen[5], Mr Utkur Mirsaidov[2,3,4], Mr Zainul Aabdin[1]
[1]Institute of Materials Research and Engineering, A*STAR (Agency for Science, Technology, and Research), Singapore 138634, Singapore, Singapore, [2]Center for Advanced 2D Materials and Department of Physics, National University of Singapore, Singapore 117546, Singapore, Singapore, [3]Center for BioImaging Sciences and Department of Biological Sciences, National University of Singapore, Singapore 117557, Singapore, Singapore, [4]Department of Materials Science and Engineering, National University of Singapore, Singapore 117575, Singapore, Singapore, [5]imec, Kapeldreef 75, Leuven, B-3001, Belgium, Leuven, Belgium

30 Analyses of Observed Speciation of Cobalt in NMC cathodes Using Laboratory X-ray Absorption Spectroscopy (XAS)

Andreas Bergner[1], Simon John[1]

[1]Quantum Design GmbH, Pfungstadt, Germany

31 Observing Lithium Ion Battery Bonds During Charge Cycling Using Laboratory XAS

Andreas Bergner[1], Simon John[1]
[1]Quantum Design GmbH, Pfungstadt, Germany

39 Understanding strain and composition effects in fuel cell catalysts using advanced electron microscopy and DFT

Alessandro Zanre[1], Dr. Aaakash Varambhia[2], Dr. Dogan Ozkaya[2], Dr. Xiaonan Luo[3], Prof. Sergio Lozano-Perez[1], Prof. Rebecca J. Nicholls[1], Prof. Peter D. Nellist[1]
[1]Department of Materials, University of Oxford, , United Kingdom, [2]Johnson Matthey Technology Centre, , United Kingdom, [3]Contemporary Amperex Technology Co., Limited, , P. R. China

65 Quantification of Lithium in State-of-the-Art low Voltage STEM

Pr. Raynald Gauvin[1], Mr. Nicolas Brodusch[1], Mrs. Stéphanie Bessette[1]
[1]Mining and Materials Engineering,McGill University, Montréal, Canada

134 Structure analysis on the nm scale: The amorphous LiNbO3 coatings for solid state batteries

Johannes Haust[1], Dr. Jürgen Belz[1], Dr. Shamail Ahmad[1], Mrs. Narges Adeli[1], Mrs. Franziska Hüppe[1], Mrs. Yiran Guo[2], Mr. Linus Erhard[3], Dr. Jochen Rohrer[3], Dr. Anna-Lena Hansen[2], Dr. Valeriu Mereacre[2], Prof. Dr. Karsten Albe[3], Prof. Dr. Kerstin Volz[1]
[1]Philipps University Marburg, Marburg , Germany, [2]Karlsruhe Institute of Technology, Karlsruhe, Germany, [3]Technical University of Darmstadt, Darmstadt, Germany

166 In situ TEM/EELS and spatially resolved XAS/XRF analysis of CuO electrocatalyst for CO2 reduction

Dr Manfred Erwin Schuster[1], Dr Gea T. van de Kerkhof[2], Dr Angela E. Goode[1], Dr Urša Podbevšek[1]
[1]Johnson Matthey, Sonning Common, United Kingdom, [2]Diamond Light Source, Didcot, United Kingdom

183 Materials characterization of recycled batteries (black mass): automated quantitative phase classification in 3D

Ria Mitchell[1], Mr Andy Holwell[1], Dr Richard Taylor[1], Dr Eddy Hill[1]
[1]Carl Zeiss Microscopy Ltd, Cambourne, UK

187 Combining in-situ synchrotron and electron microscopy techniques to study NiFe catalysts for CO2 methanation

Dr Manfred Erwin Schuster[1], Dr Pilar Ferrer[2], Dr Rosa Arrigo[3]
[1]Johnson Matthey, Sonning Common, United Kingdom, [2]Diamond Light Source, Didcot, United Kingdom, [3]University of Salford, Manchester , United Kingdom

189 Identifying transient defects in exsolution of nanoparticles by semi-quantitative ABF STEM imaging

Andreas Rosnes[1,3], Mr. Holger von Wenchstern[1,3,4], Mr. Jonathan Polfus[2,3], Mr. Øystein Prytz[1,3]
[1]Department of Physics, University of Oslo, Oslo, Norway, [2]Department of Chemistry, University of Oslo, Oslo, Norway, [3]Center for Material Science and Nanotechnology, University of Oslo, Oslo, Norway, [4]Felix-Bloch-Institut, Universität Leipzig, Leipzig, Germany

210 A crystallographic aspect of Li metal anodes: Understanding the functionality of lithium-ion all-solid-state batteries

Dr Pawel Nowakowski[1], PhD Cecile Bonifacio[1], Mrs Mary Ray[1], Mr Paul Fischione[1]
[1]Fischione Instruments, Export, USA

230 New Workflows and Innovations for Maximizing Relevance of In Situ TEM Results for Liquid-Based Applications

Mrs. Jennifer Mcconnell[1], Dr. Madeline Dressel Dukes[1], Dr. Nynke Krans[1], Dr. Yaofeng Guo[1], Dr. Tim Eldred[1], Dr. Kate Stephens[1], Franklin Walden[1], Patrick Wellborn[1], Dr. David Nackashi[1], Dr. John Damiano[1]
[1]Protochips, Morrisville, United States of America

236 Electron Channeling Contrast Imaging (ECCI) of Ion Battery Cathode Materials

Ph.d. Candidate Meysam Naghizadeh[1], Dr. Chisu Kim[2], Pr. Raynald Gauvin[1]

[1]Department of Mining and Materials Engineering, McGill University, Montréal, Canada, [2]Center of Excellence in Transportation Electrification and Energy Storage Hydro Québec, Varennes, Canada

287 STEM, PED and EELS: A powerful combination for the investigation of cathode-active-materials for batteries

Thomas Demuth[1], Dr. Michael Malaki[1], Dr. Shamail Ahmed[1], Dr. Philipp Kurzhals[2,3], Dr. Andreas Beyer[1], Prof. Dr. Jürgen Janek[2], Prof. Dr. Kerstin Volz[1]
[1]Materials Science Center (WZMW) and Department of Physics, Philipps Universität Marburg, Marburg, Germany, [2]Institute of Physical Chemistry & Center for Material Research, Justus-Liebig-University, Gießen, Germany, [3]BASF SE, New Battery Materials and Systems, Ludwigshafen, Germany

290 A Real Space Understanding of Short Range Order in Disordered Rocksalt Cathodes

Dr Emma Hedley[1], Mr Liquan Pi[2], Prof. Peter G. Bruce[2,3,4], Prof. Peter D. Nellist[2]
[1]Monash University, Melbourne, Australia, [2]University of Oxford, Oxford, United Kingdom, [3]Faraday Institution, Didcot, United Kingdom, [4]The Henry Royce Institute, Oxford, United Kingdom

297 Unveiling the Optoelectronic and Thermal Properties of SnSe Polycrystals via EELS

Francesco Salutari[1], Dr. Sharona Horta[2], Mr. Marc Botifoll[1], Dr. Maria Chiara Spadaro[1,3,4], Dr. Maria Ibañez[2], Dr. Jordi Arbiol[1,5]
[1]Catalan Institute of Nanoscience and Nanotechnology (ICN2) , Campus UAB, Bellaterra, 08193 Barcelona, Spain, [2]Institute of Science and Technology Austria (ISTA), AM Campus 1, 3400 Klosterneuburg, Austria, [3]Department of Physics and Astronomy “Ettore Majorana”, University of Catania, via S. Sofia 64, Catania 95123, Italy, [4]CNR-IMM, via S. Sofia 64, Catania 95123, Italy, [5]ICREA, Pg Lluis Companys 23, 08010 Barcelona, Spain

334 Effect of preparation and oxygen evolution catalysis on CoNiFe oxide electrocatalysts revealed by STEM-EELS

Dr. Nils Rockstroh[1], Ms. Trang Pham[1], Mr. Carsten Kreyenschulte[1], Ms. Annette-Enrica Surkus[1], Mr. Robert Francke[1]
[1]Leibniz Institute for Catalysis e.V. (LIKAT), Rostock, Germany

359 Towards 3D quantitative imaging in FIB-SEM for applications in battery materials

Stephanie Bessette[1], Prof. Raynald Gauvin[1]
[1]McGill University, Montreal, Canada

391 Characterization of Solid Electrolyte-free Si anodes for all-solid-state batteries (ASSBs) using Cryo-STEM

Dr. Shamail Ahmed[1], Dr. Hanyu Huo[2], Mrs. Franziska Hüppe[1], Dr. Jürgen Belz[1], Prof. Dr. Jürgen Janek[3], Prof. Dr. Kerstin Volz[1]
[1]Structure and Technology Research Laboratory, Philipps University of Marburg, Marburg, Germany, [2]The Bruce Group, University of Oxford, Oxford , United Kingdom, [3]Institute of Physical Chemistry, Justus Liebig University Giessen, Giessen, Germany

404 Defects and alloy ordering in Pt-Cu nanoparticulate electrocatalysts

Ana Rebeka Kamsek[1,2], Dr. Francisco Ruiz-Zepeda[1], Anja Logar[1,3], Dr. Marjan Bele[1], Prof. Dr. Goran Dražić[1], Prof. Dr. Nejc Hodnik[1,3]
[1]Department of Materials Chemistry, National Institute of Chemistry, Ljubljana, Slovenia, [2]Faculty of Chemistry and Chemical Engineering, University of Ljubljana, Ljubljana, Slovenia, [3]University of Nova Gorica, Nova Gorica, Slovenia

543 Towards Quantitative Liquid Phase Electrochemistry for Understanding Electrochemical Processes

Shibabrata Basak[1], Junbeom Park[1], Hongyu Sun[2], Hugo Pérez Garza[2], Eva Jodat[1], André Karl[1], Rüdiger-A Eichel[1]
[1]Institute of Energy and Climate Research, Fundamental Electrochemistry (IEK-9), Forschungszentrum Jülich GmbH, Jülich, Germany, [2]DENSsolutions B.V., Delft, The Netherlands

562 Scale-bridging microscopic characterization of complex energy devices enabled by novel cross-sectional preparation routines

Marco Hepp[1], Charles Ogolla[1], Dominik Stepien[2], Dominik Bresser[2], Benjamin Butz[1], Tristan Zemke[1]

[1]Micro- and Nanoanalytics Group, University of Siegen, Siegen, Germany, [2]Helmholtz Institute Ulm, Ulm, Germany

644 Scale-Bridging Analysis of Hierarchical Mesoporous Transition Metal Foams

Jonas Frohne[1], Dr.-Ing. Julian Müller[1], Dr. Jean Marie Vianney Nsanzimana[1], Charles Otieno Ogolla[1], Prof. Benjamin Butz[1]
[1]Micro- and Nanoanalytics Group/University of Siegen, Siegen, Germany

700 In-Situ insights into Multivalent Metal Energy Storage:
A model system for calcium sulfur batteries

Marco Kögel[1], Prof. Jannik C. Meyer[1,2]
[1]NMI Natural and Medical Sciences Institute at the University of Tübingen, Reutlingen, Germany, [2]Institute of Applied Physics, University of Tübingen, Tübingen, Germany

714 Understanding the effect of Al:ZnO coating on the structural and chemical stabilities of LiNi1/3Mn1/3Co1/3O2 electrode

Ardavan Makvandi[1,5], Dr. Michael Wolff[2], Dr. Sandra Lobe[2], Bastian Heidrich[3], Dr. Martin Peterlechner[1,5], Dr. Christoph Gammer[4], Dr. Sven Uhlenbruck[2], Prof. Martin Winter[3,6], Prof. Gerhard Wilde[1]
[1]Institute of Materials Physics, University of Münster, Münster , Germany, [2]Forschungszentrum Jülich GmbH, Institute of Energy and Climate Research, Materials Synthesis and Processing (IEK-1) Jülich Aachen Research Alliance: JARA-Energy, Jülich, Germany, [3]MEET Battery Research Center, Institute of Physical Chemistry, University of Münster, Münster , Germany, [4]Erich Schmid Institute of Materials Science, Austrian Academy of Sciences, Leoben, Austria, [5]Laboratory for Electron Microscopy, Karlsruhe Institute of Technology, Karlsruhe, Germany, [6]Helmholtz Institute Münster, IEK-12 Forschungszentrum Jülich GmbH, Münster , Germany

725 Ultra-fast and facile synthesis of cathodes for rechargeable batteries using an organic syntehsis route

Dr Saul Rubio[2], Mr Julio E. de la Rosa-Melian[1], Dr Francisco J. Garcia-Garcia[1], Dr Eva M. Perez-Soriano[1], Dr Cristina Arevalo[1], Dr Isabel Montealegre-Melendez, Dr Ana M Beltrán[2], Dr Juan G. Lozano[1]
[1]Departamento de Ingeniería y Ciencia de los Materiales y del Transporte, Escuela Técnica Superior de Ingeniería, Universidad De Sevilla, Sevilla, Spain, [2]Departamento de Ingeniería y Ciencia de los Materiales y del Transporte, Escuela Politécnica Superior, Universidad De Sevilla, Sevilla, Spain

729 Visualization of binder mixtures in hard carbon composite electrodes using OsO4 and uranyl acetate staining

Gregor Neusser[1], Tom Philipp[1], Sven Daboss[1], Clarissa Read[2,3], Paul Walther[2], Christine Kranz[1]
[1]Institute of Analytical and Bioanalytical Chemistry, Ulm University, Ulm, Germany, [2]Central Facility for Electron Microscopy, Ulm University, Ulm, Germany, [3]Institute of Virology, Ulm University Medical Center, Ulm, Germany

731 Toward 3D imaging of the PEMFC electrode microstructure

Dr Laure GUETAZ[1], Mr Mamadou Sangare[1], Dr Thomas David[1], Dr Zineb Saghi[2], Dr Arnaud Morin[1], Dr Joël Pauchet[1]
[1]Université Grenoble Alpes, CEA, LITEN, Grenoble, France, [2]Université Grenoble Alpes, CEA, LETI, Grenoble, France

737 Investigating solar degradation mechanisms of the Ta3N5 photoelectrode by in-situ transmission electron microscopy

Dr. Annett Thøgersen[1], Dr. Øystein Dahl[4], Dr. Shima Kadkhodazadeh[2], Dr. Michael Seifner[2], Msc. Martin Fleissner Sunding[1], Dr. Ingeborg-Helene Svenum[4], Dr. Mathieu Grandcolas[1], Professor Thomas Willum Hansen[2], Dr. Ingvild Julie Thue Jensen[1], Dr. Athanasios Chatzitakis[3]
[1]SINTEF, Oslo, Norway, [2]DTU, Lyngby, Denmark, [3]UiO, Oslo, Norway, [4]SINTEF, Trondheim, Norway

785 Insights on the disordered nature in amorphous-based anode materials from Electron Pair Distribution Function

Dr. Anuj Pokle[1], Marte Orderud Skare[2], Shihui Feng[3], Dr Cheuk Wai Tai[3], Dr Asbjørn Ulvestad[2], Prof Xiaodong Zou[3], Prof Øystein Prytz[1]
[1]Department of Physics and Center for Materials Science and Nanotechnology, University of Oslo, Oslo, Norway, [2]Department of Battery Technology, Institute for Energy Technology, Kjeller, Norway, [3]Department of Materials and Environmental Chemistry, Arrhenius Laboratory, Stockholm University, Stockholm, Sweden

808 Operando Environmental TEM observations of SOEC Ni-YSZ fuel electrode dynamics

Mr. Magnus Björnsson[1], Mr. Søren Simonsen[1], Mr. Ming Chen[1]
[1]Department of Energy Conversion and Storage, The Danish Technical University, Kgs. Lyngby, Denmark

820 Transmission electron microscopy studies of ferroelectric ZrO2 thin films

Phd Student Marian Cosmin Istrate[1], Dr Corneliu Ghica[1], Dr Jose Pedro Basto Silva[2]
[1]National Institute of Materials Physics, 105 Bis Atomistilor, 077125, Magurele, Romania, [2]Physics Center of Minho and Porto Universities (CF-UM-UP), University of Minho, Campus de Gualtar, 4710-057, Braga, Portugal

821 Characterization of the structure and chemistry of solid electrolyte

Dr Kyung Song[1], Dr Abin Kim[2], Professor Byungwoo Kang[2]
[1]Korea Institute of Materials Science , Changwon, Republic of Korea, [2]Pohang University of Science and Technology , Pohang, Republic of Korea

824 Correlative study of hematite-based photoanodes for solar water splitting by transmission electron and X-ray microscopies

Léon Schmidt[1], Bilal Meddas[2], Walid Baaziz[1], Dana Stanescu[2], Stefan Stanescu[3], Ovidiu Ersen[1]
[1]IPCMS CNRS / Université de Strasbourg, Strasbourg, France, [2]SPEC CEA Saclay / CNRS, Gif sur Yvette, France, [3]Synchrotron SOLEIL, Saint-Aubin, France

842 Structural Probing of Charging Mechanism in LiNiO2 at High Voltage using Microscopy and Spectroscopy

Dr Jun Chen[1], Dr Mikkel Juelsholt[2], Dr Robert House[1], Prof Peter Bruce[1]
[1]Department of Materials, University of Oxford, Oxford, United Kingdom, [2]Department of Chemical Engineering. Columbia University, New York, United States

904 Investigation on photocorrosion of TiO2 during photoelectrochemistry process by electron microscopy together with operando ICP-MS

Dr. Yiqun Jiang[1], Dr. Martin Rabe[1], Dr. Ilias Efthimiopoulos[1], Prof. Christina Scheu[1], Dr. Siyuan Zhang[1]
[1]Max-Planck Institut für Eisenforschung GmbH, Düsseldorf, Germany

921 In-situ HAADF-STEM observation of phase transformation in microencapsulated Al-Cu-Si alloy

Dr Melbert Jeem[1], Dr Norihito Sakaguchi[1], Dr Takahiro Nomura[1]
[1]Faculty of Engineering, Hokkaido University, Sapporo, Japan

940 Innovative Nanoanalytical Approaches for Lithium Metal Interface Analysis

Clementine Warres[1], Philipp Karl Albrecht[1], Dr. Tarek Lutz[1], Dr. Wilfried Nisch[1]
[1]NMI Natural and Medical Sciences Institute at the University of Tuebingen, Reutlingen, Germany

980 Ultra-low voltage SEM observation for battery materials

Ph.D. Yutaka Nagaoka[1], Dr. Yoichiro Hashimoto[1], Mr. Toru Aiso[1], Mr. Shuhei Yabu[2], Mr. Masahiro Sasajima[3]
[1]Solution Development Dept., Hitachi High-Tech Corporation, Hitachinaka, Japan, [2]Electron Microscope Systems Design Dept., Hitachi High-Tech Corporation, Hitachinaka, Japan, [3]Software Design Dept., Hitachi High-Tech Corporation, Hitachinaka, Japan

1020 Leveraging FIB-SEM with Integrated ToF-SIMS for Comprehensive Characterization of Lithium-Ion Battery Materials

Dr. Tomáš Šamořil[1], Jiří Dluhoš[1], Jiří Honč[1], Dr. Tan Sui[2], Dr. Xuhui Yao[3]
[1]TESCAN GROUP, a.s., Brno, Czech Republic, [2]University of Surrey, Guildford Surrey, UK, [3]National Physical Laboratory, Teddington, UK

1030 Insights into Lithium-rich Oxides from Synthesis and Characterization Studies

Rabail Badar Abbasi[1,2,3], Dr Marjan Bele[1], Dr Giuliana Aquilanti[4], Dr Jasper Plaisier[4], Prof. dr Anton Meden[2], Dr Elena Tchernychova[1], Prof. dr Robert Dominko[1,2,3]
[1]Department of Materials Chemistry, National Institute of Chemistry, Ljubljana, Slovenia, [2]Faculty of chemistry and chemical technology, University of Ljubljana, Ljubljana, Slovenia, [3]ALISTORE-European Research Institute, Amiens, France, [4]Elettra-Sincrotrone Trieste S.C.p.A, Trieste, Italy

1035 Electron microscopy studies of Ni/GDC fuel electrode in solid oxide fuel cell

Ardavan Makvandi[1], Yanting Liu[2], Dr. Heike Störmer[1], Dr. André Weber[2], Dr. Martin Juckel[3], Prof. Norbert H. Menzler[3], Prof. Dagmar Gerthsen[1]
[1]Laboratory for Electron Microscopy (LEM), Karlsruhe Institute of Technology (KIT), Karlsruhe, Germany, [2]Institute for Applied Materials - Electrochemical Technologies (IAM-ET), Karlsruhe Institute of Technology (KIT), Karlsruhe, Germany, [3]Institute of Energy and Climate Research (IEK), IEK-1: Materials Synthesis and Processing, Forschungszentrum Jülich GmbH, Jülich, Germany

1078 Optimizing Soft X-ray Spectroscopy for Silicon Anode Lithium Mapping

M. Sc. Svenja Kalthoff[1]
[1]Fraunhofer ISE, Freiburg im Breisgau, Germany

1085 Electron microscopy characterization of grain boundaries in Nb1-xTixFeSb based half-Heusler thermoelectric materials

Dominique Mattlat[1], Dr. Ruben Bueno Villoro[1], Dr. Chanwon Jung[1], Raana Hatami Naderloo[2], Dr. Ran He[2], Prof. Dr. Kornelius Nielsch[2], Duncan Zavanelli[3], Prof. Dr. G. Jeffrey Snyder[3], Dr. Siyuan Zhang[1], Prof. Dr. Christina Scheu[1]
[1]Max-Planck-Institute for Iron Research, Düsseldorf, Germany, [2]Leibniz Institute for Solid State and Materials Research, Dresden, Germany, [3]Northwestern University, Chicago, United States of America

1131 In-situ synthesis of thin kesterite films using high voltage TEM

Professor Klaus Leifer[1], Mr Sharath Sathyanath[1], Professor Y Gong[2], Dr Alex J. Arguijo[2], Prof Edgardo Saucedo[2], Professor S Araj[3], Professor Shun Muto[3]
[1]Uppsala University, Uppsala, Sweden, [2]Univ. Politèc. de Catalunya, Barcelona, Spain, [3]Nagoya University, Nagoya, Japan

1145 Interplay between microstructural properties with ionic/electronic conductivity in Na3PS4-based composite cathodes for Na-SSBs

Rana Ucuncuoglu[1], Dr. Leticia Trezecik Silvano[1], Tim Schubert[1], Prof. Dr. Volker Knoblauch[1], Dr Pinar Kaya[1]
[1]Materials Research Institute (IMFAA), Aalen University of Applied Sciences, Aalen, Germany

Late Poster Presentation

1256 A systematic study on PtRu alloy composition for catalytic applications

Tonya Kloos[1], Dr. Ningyan Cheng[1], M.Sc. Miquel Vega Paredes[1], M.Sc. Alan Savan[2], Prof. Dr.-Ing. Alfred Ludwig[2], Prof. Dr. Christina Scheu[1]
[1]Max-Planck Institute for Sustainable Materials, Düsseldorf, Germany, [2]Ruhr-Universität Bochum, Bochum, Germany

1258 Synthesis, structural and electrochemical characterization of nanostructured Ir/TiO_2 for the oxygen evolution reaction

Yeeun Bang[1], Dr. Raquel Aymerich Armengol[2], Prof. Dr. Joohyun Lim[3], Prof. Dr. Christina Scheu[1]
[1]Max-Planck-Institute for Sustainable Materials, Düsseldorf, Germany, [2]Technical University of Denmark, Lyngby, Denmark, [3]Kangwon National University, Gangwon-do, South Korea

1263 Nano-characterization of Sodium-ion cathodes fabricated using economically and environmentally friendly organic routes

Dr Ana M Beltran[1], Dr. Saul Rubio[1], Dr. Francisco J Garcia-Garcia[2], Mr Julio E de la Rosa[2], Dr Eva M. Pérez[2], Dr Isabel Montealegre-Meléndez[1], Dr. Cristina Arévalo[2], Dr. Juan G. Lozano[2]

[1]Departamento de Ingeniería y Ciencia de los Materiales y del Transporte, Escuela Politécnica Superior, Universidad de Sevilla, Sevilla, Spain, [2]Departamento de Ingeniería y Ciencia de los Materiales y del Transporte, Escuela Técnica Superior de Ingeniería, Universidad de Sevilla, Sevilla, Spain

1264 Epitaxial LiNi0.33Mn0.33Co0.33O2 thin films as a model cathode material system for Li-ion batteries

Dr. Elena Tchernychova[1], Blaž Jaklič[2,3], Jan Žuntar[2,3], Gregor Kapun[1,4], Prof. Dr. Matjaž Spreitzer[2], Prof. Dr. Robert Dominko[1,4,5]

[1]National Institute of Chemistry, , Ljubljana, Slovenia, [2]Jozef Stefan Institute, Ljubljana, Slovenia, [3]Jozef Stefan Institute International Postgraduate School, Ljubljana, Slovenia, [4]4Faculty of chemistry and chemical technology, University of Ljubljana, Ljubljana, Slovenia, [5]ALISTORE-European Research Institute, Amiens, France

1276 Visualisation of tetrahedral Li in the alkali layers of Li-rich layered oxides

Dr Weixin Song[1,2,3], Dr Miguel Pérez-Osorio[1,2,3], Dr Jun Chen[1,2,3], Mr Zhiyuan Ding[1,3], Dr John Joseph-Marie[1,2,3], Dr Robert House[1,2,3], Prof Peter Bruce[1,2,3], Prof Peter Nellist[1,2,3]

[1]University of Oxford, Oxford, United Kingdom, [2]The Faraday Institution, Oxford, United Kingdom, [3]The Henry Royce Institute, Oxford, UK

595

Following low and high-temperature electrolysis processes with in-situ and cryo electron microscopy

Shibabrata Basak[1], Pritam Chakraborty[1], Jean-Pierre Poc[1], Tobias Mehlkoph[1], Junbeom Park[1], Eva Jodat[1], André Karl[1], Rüdiger-A Eichel[1]
[1]Institute of Energy and Climate Research, Fundamental Electrochemistry (IEK-9), Forschungszentrum Jülich GmbH, Jülich, Germany

PS-04 (3), Plenary, august 27, 2024, 10:30 - 12:30

Background incl. aims
Electrochemistry plays a crucial role in various hydrogen production technologies [1], yet understanding the intricate nanoscale processes that govern these reactions remains a significant challenge. To address this gap, we employ advanced electron microscopy techniques to visualize and unravel the nanoscale mechanisms behind electrochemical phenomena.
Methods
While the Plasma Focused Ion Beam (PFIB) tomography at room temperature allows us to visualize the evolution of solid oxide fuel cell (SOFC) [2] electrodes due to operation, and the cryo PFIB tomography allows characterizing proton exchange membrane (PEM) [3] of low-temperature water electrolysis. This coupled with the in-situ TEM allows us probing the mechanisms of low and high-temperature electrolysis.
Results
PFIB tomography enables us to generate high-resolution 3D reconstructions of SOFC materials, revealing the evolution of triple-phase boundaries and potential degradation sites that influence ion transport and catalytic activity. In situ TEM experiments, utilizing MEMS chips, allow us to monitor electrochemical processes in real time. By studying $Sr_{0.95}Fe_{0.9}Mo_{0.1}O_{3-\delta}$ (SFM) [4] and related materials, we demonstrate exsolution mechanisms that can impact the performance of SOFCs. Further, we showcase the application of MEMS-based chips in visualizing power-to-x processes, exemplified by methane generation on Ni catalysts.
For PEM MEAs, maintaining the original hydration level is crucial to understand degradation mechanisms. Our cryo workflow which includes largescale surface investigation using a laser scanning microscopy (LSM), preserves hydration throughout sample preparation, FIB tomography, TEM lamella preparation, and TEM characterization, ensuring optimal sample preservation for TEM imaging.
Conclusions
Our research highlights the transformative power of electron microscopy in unraveling the nanoscale secrets of hydrogen production. By visualizing these intricate processes, we gain a deeper understanding of the factors influencing material performance and optimize material design to enhance the efficiency and durability of hydrogen production technologies. This approach holds immense promise for advancing the H_2 value chain and driving the transition towards a clean energy future.
Acknowledgments
Authors acknowledge the funding provided by the BMBF (German Research Foundation) through the project DERIEL (03HY122C).

Keywords:

FIB-tomography, in-situ, and cryo TEM

Reference:

[1] Energies 2023, 16(3), 1141; https://doi.org/10.3390/en16031141
[2] ECS Trans. 2021 103 299; https://10.1149/10301.0299ecst
[3] Energy Environ. Sci. 2022, 15, 2288-2328; https://doi.org/10.1039/D2EE00790H
[4] ECS Trans. 2023, 111, 2119; https://10.1149/11106.2119ecst

32

In situ microscopic observations of zinc electrodeposition process in various electrolytes

Dr Kaname Yoshida[1], Dr. Yuki Sasaki[1], Dr. Akihide Kuwabara[1], Prof. Yuichi Ikuhara[1,2]
[1]Japan Fine Ceramics Center, Nagoya, Japan, [2]The University of Tokyo, Bunkyo-ku, Japan
PS-04 (1), august 26, 2024, 10:30 - 12:30

-Background and Aims-
Zinc anode batteries are expected as low-cost and high energy density batteries. While they have already been widely utilized as primary batteries, there are many problems in the application to a secondary battery [1]. In particular, the dendrite formation during the charging process is a major issue for development of rechargeable zinc anode batteries. Dendrite growth from the zinc anode is known to cause internal short-circuiting between the cathode and the anode. In order to suppress dendrite formation effectively, it is important to clarify the formation mechanism. However, electrochemical reactions in the liquid electrolytes involve many factors and they proceed through complex mechanisms. Clarifying ever-changing electrochemical reactions at the electrode (solid) – electrolyte (liquid) interface, in situ microscopic observations are advantageous. Because of such requests, we had started in situ observations of zinc electrodeposition process by using liquid-phase transmission microscope (LP-TEM). As a result, we succeeded in observing the dendrite formation at the early stage of zinc electrodeposition process [2]. However, in situ electrochemical observations with LP-TEM suffered from the problem of low reproducibility due to the severe limitation in liquid thickness. The condition of a liquid electrolyte surrounding a working electrode for LP-TEM can be changed drastically as the redox reaction proceeds. Furthermore, it was difficult for the LP-TEM method to handle a wide range of electrolytes, due to the restrictions on liquid properties.
Therefore, we devised noble setup of liquid-phase scanning electron microscope (LP-SEM) for in situ observations of electrochemical reaction in various liquid electrolytes [3]. Our LP-SEM setup for electrochemical reactions enables in situ observations in bulky liquid electrolytes and is expected to improve the reliability of reactions.
-Methods-
In situ electrochemical TEM (EC-TEM) observations of zinc electrodeposition in were carried out by combining the TEM (TITAN E-TEM, Thermo Fisher Scientific) and the liquid-cell holder (Poseidon Select, Protochips) under the accelerating voltage of 300 kV.
In situ electrochemical SEM (EC-SEM) was constructed based on atmospheric SEM (JASM-6200, JEOL). A noble electrochemical reaction vessel was created by using a commercially available electrochemical chip for LP-TEM (ECT-15WO, Protochips). Electrochemical reactions were controlled by an external potentio/galvanostat (SP-300, Bio-Logic Science Instruments) through the working electrode (WE) on the chip, metal wires as a counter electrode (CE) and a quasi-reference electrode (RE). Overview of our EC-SEM equipment shown in the figure.
-Results and Conclusions-
First, reliability of our EC-SEM setup was confirmed in a zinc electrodeposition reaction under similar conditions with EC-TEM observations. Compared with EC-TEM observations, reproducibility of zinc deposition processes and their electrochemical conditions were drastically improved. That is, EC-SEM observations can make it possible to reveal the correlation between electrochemical conditions and deposited zinc shape.
Next, zinc deposition processes in several kinds of electrolytes under different electrochemical conditions were compared by using EC-SEM observations. In comparing various constant current conditions, shape changes of deposited zinc depending on the current density were observed in EC-SEM. For example, in a 0.5 M zinc sulfate solution, a dendric zinc structure was formed at a current density of > 2 A/cm^2. The shape of the deposited zinc was found to depend not only on the

electrochemical conditions but also on the kind of counter anion and the concentration of zinc cation in liquid electrolytes. The details about the relationship between reaction conditions and deposited zinc shapes will be discussed.

-Acknowledgement-
This work was supported by the R&D Initiative for Scientific Innovation on the New Generation Batteries 3 (RISING3) Project administrated by the New Energy and Industrial Technology Development Organization (NEDO) (JPNP21006).

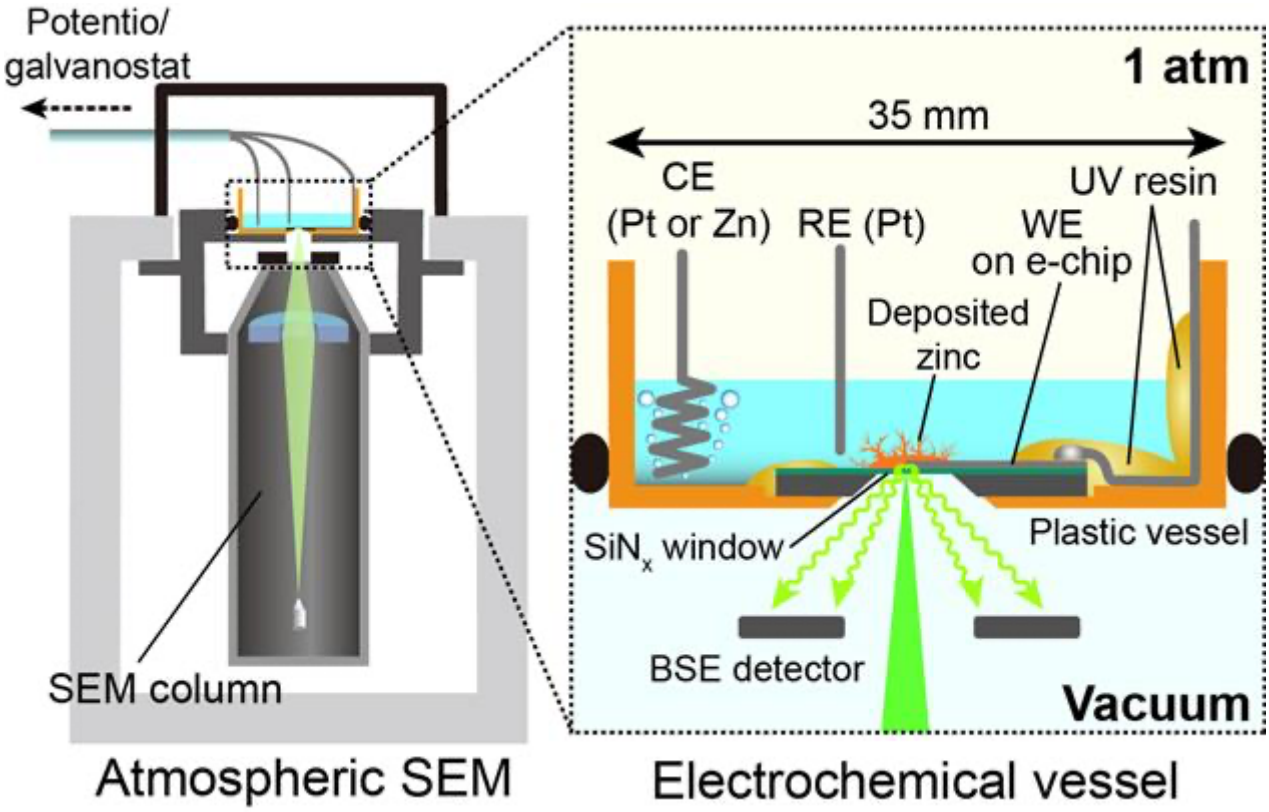

Keywords:

electrochemistry, LP-SEM, LP-TEM, liquid, batteries

Reference:

[1] Zhang, X. et al. InforMat 2022, 4 (7), e12306. DOI: 10.1002/inf2.12306
[2] Sasaki, Y. et al. J. Power Sources 2021, 481 (1), 228831. DOI: 10.1016/j.jpowsour.2020.228831
[3] Yoshida, K. et al. Microscopy 2022, 71 (5), 311-314. DOI: 10.1093/jmicro/dfac028

239

Cation Vacancies Regulate the Electron Spin Configuration of Cathode Catalytic Additives towards Robust Li-S Batteries

PhD JING YU[1,2], Mr. Andreu Cabot[2], Mr. Jordi Arbiol[1]
[1]Catalan Institute of Nanoscience and Nanotechnology (ICN2), Bellaterra, 08193, Spain, [2]Catalonia Institute for Energy Research（IREC）, Sant Adrià de Besòs, 08930 , Spain

PS-04 (1), august 26, 2024, 10:30 - 12:30

Background
Lithium-sulfur batteries (LSBs) are promising energy storage devices due to their high theoretical energy density (2600 Wh kg-1), large specific capacity (1675 mAh g-1), potential cost-effectiveness, and environmental friendliness.[1] However, the commercialization of LSBs is limited by factors such as polysulfide migration, sluggish kinetics of the sulfur redox reaction (SRR), and poor electronic and ionic cathode conductivities.[2] The use of defect-engineered catalysts, with tunable surface chemistry and electronic properties, as cathode additives in LSBs is a promising strategy to accelerate the Li-S redox reactions and thus promote LSB performance. In contrast to earlier research that predominantly concentrated on how defects influence the electronic density of states, the present work explores the impact of defects in modulating electronic spins and how these changes in spin configuration influence the macroscopic adsorption properties and activity of the catalytic additive.
Methods
In this study, a defect engineering strategy was used to tune the electron spin state of an SRR electrocatalyst. This strategy was showcased by introducing controlled amounts of cation vacancies within ultrathin CoSe nanosheets through plasma etching. Atomic resolution aberration-corrected high-angle annular dark-field scanning transmission electron microscopy (AC-HAADF-STEM) was used to gain in-depth insights into the spatial distribution of Co vacancies. 3D atomic models were obtained by using Rhodius and the corresponding AC-HAADF-STEM image simulations obtained by using STEM-CELL software.[3-4] XRD, EXAFS, XPS, Raman spectroscopy, XMCD, DFT calculations, EPR, in situ XRD combined with electrochemical test were conducted.
Results
Vacancies were also indirectly evidenced by an increase of disorder and reduced lattice spacing, Co-Se bond length, and Se coordination number using XRD, HRTEM, EXAFS, XPS, and Raman spectroscopy. XANES and XPS spectroscopy further showed an increase in the average oxidation state of cobalt with the introduction of vacancies and EELS pointed to a higher occupation of Co 3d states in v-CoSe. Beyond modifying the structural parameters and electronic state occupation, the presence of vacancies resulted in a polarization of the 3d electron spins as evidenced by an increase in the intensity of the satellite peak in the Co 2p XPS spectra, a strong Co dichroism signal obtained by XMCD and magnetic measurements that confirmed a large moment per Co ion of 2.8 muB in v-CoSe. EPR spectroscopy further confirmed the generation of additional electrons with unpaired spins by the introduction of Co vacancies.
DFT calculations showed these spin-polarized unpaired electrons to be easily transferred from v-CoSe to polysulfide. Computational results showed that the d band center shifts toward the Fermi level with the introduction of vacancies, which involves that electrons are more prone to disperse in the high-spin configuration. The altered spin configuration results in a swift transferability of additional unpaired electrons to the polysulfide. DFT calculations also showed v-CoSe to have significantly higher lithium polysulfide adsorption energies and to decrease the polysulfide stability upon adsorption, thus enhancing both polysulfide adsorption and conversion activity. Besides, computational results showed the modified spin configuration to result in a more favorable thermodynamic reduction process, particularly for the transition from soluble polysulfide to solid Li2S that showed a lower nucleation energy barrier.

Experimental measurements confirmed an enhanced adsorption of the lithium polysulfide on the v-CoSe surface. Symmetric cells showed v-CoSe to provide a low polarization voltage and sharper and more intense redox peaks. In situ XRD showed a very rapid and complete transformation of S8 and a high lithium polysulfide redox activity in v-CoSe. EIS analyses showed v-CoSe to be characterized by a low SRR activation energy, particularly for the liquid-solid conversion stage. Besides, the presence of vacancies resulted in promoted Li2S nucleation, reduced LSB polarization voltages, and higher Q2/Q1 ratios. v-CoSe cathodes not only demonstrated excellent electrocatalytic properties but also outstanding LSB electrochemical performance in terms of specific capacity, rate performance, and cycling stability, even at high sulfur loadings.
As a result, more uniform nucleation and growth of Li2S and an accelerated liquid-solid conversion in LSB cathodes are obtained. These translate into CoSe-based LSB cathodes exhibiting capacities up to 1089 mAh g-1 at 1C with 0.039% average capacity loss for 1500 cycles, and up to 5.2 mAh cm-2, with 0.16% decay per cycle after 200 cycles in high sulfur loading cells.
Conclusion
Overall, this study demonstrates the need for considering the electronic spin configuration in the design of electrocatalysts, particularly for developing robust LSBs. Thus, the spin engineering approach showcased here paves the way to the rational design of new generations of LSB cathodes based on defect-engineered SRR electrocatalysts, toward the development of a cost-effective LSB technology with market-ready potential.

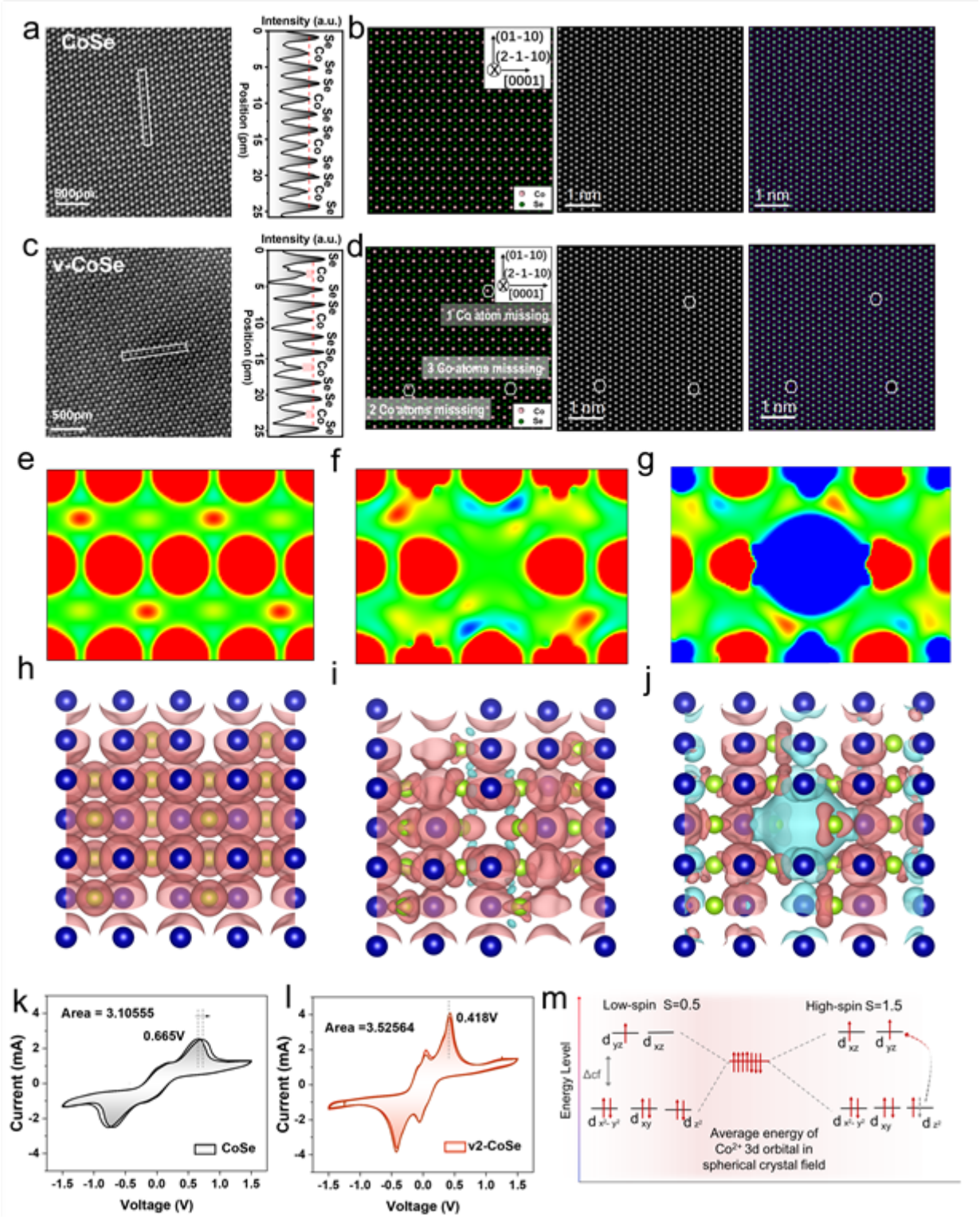

Keywords:

AC-HAADF-STEM, battery, vacancy, spin polarization

Reference:

[1] A. Manthiram, et al., Advanced Materials 2015, 27, 1980.
[2] Z. Liang, et al., Advanced Energy Materials 2021, 11, 2003507.
[3] J. Arbiol et al., Appl. Phys. Lett. 2002, 80, 2.
[4] S. Bernal, et al., Ultramicroscopy 1998, 72, 135-164.

268

Operando ETEM study on solid oxide cells

Zhongtao Ma[1], Mr. Christodoulos Chatzichristodoulou[1], Mr. Kristian Speranza Mølhave[2], Mr. Søren Bredmose Simonsen[1]
[1]DTU Energy, Kongens Lyngby, Denmark, [2]DTU Nanolab, Kongens Lyngby, Denmark

PS-04 (1), august 26, 2024, 10:30 - 12:30

Background incl. aims
Solid oxide electrolyzers and fuel cells (SOEC/SOFC) are crucial for reducing global carbon emissions. Understanding their degradation processes is key to making them more durable and cost-effective for widespread use [1]. Usually, researchers examine these cells after electrochemical tests, which limits insights into the ongoing degradation process. Our study introduces a new method that makes it possible to observe the cells in operation. This method combines the TEM characterization and the electrochemical test and correlates the structural and compositional evolution with electrochemical performance.

Methods
The presented method combines a TEM holder with a heating-biasing MEMS chip and an environmental TEM capable of introducing relevant reactive gases such as O_2, H_2, and H_2O, mirroring the operational conditions of SOEC/SOFC. We developed and utilized a special sample preparation procedure to apply three types of stimuli—heat, reactive gas, and electrical bias—directly to the SOEC/SOFC within TEM [2, 3]. The tested cells have lanthanum-strontium-cobalt oxide (LSC) electrodes and an yttrium-stabilized zirconia (YSZ) electrolyte. To study cell degradation, those cells are tested with polarization in an atmosphere of 2.7 mbar O_2 at 700 °C.

Results
STEM imaging revealed that degradation feature development in the negatively polarized LSC electrodes varies with polarization voltage. Crack formation was also observed at the interface between the positively polarized LSC electrode and the YSZ electrolyte. EELS analysis conducted simultaneously showed a Co valence state change, with lanthanum's state remaining constant. Subsequent analyses, including EDS, SAED, and HRTEM, suggested that the newly observed features in negatively polarized LSC are the result of LSC decomposing into Co_3O_4, La_2O_3, and La_2CoO_4. This decomposition process was particularly pronounced near the YSZ interface, indicating a direct correlation between structural changes and electrochemical performance.

Acknowledgements
This project has received funding from the European Research Council (ERC) under the European Union’s Horizon 2020 research and innovation programme (grant agreement No 850850)”

Keywords:

Operando; ETEM; SOEC; SOFC; degradation;

Reference:

[1] Hauch, Anne, et al. "Recent advances in solid oxide cell technology for electrolysis." Science 370.6513 (2020): eaba6118.
[2] Ma, Zhongtao, et al. "Experimental Requirements for High-Temperature Solid-State Electrochemical TEM Experiments." Small Methods (2024): 2301356.
[3] Ma, Zhongtao, et al. "Electrochemical impedance spectroscopy integrated with environmental transmission electron microscopy." Small Methods 7.7 (2023): 2201713.

420

MAX phase-based nanocomposites for LIBs negative electrodes investigated by multi-approach TEM analysis

Irene Ostroman[1], Dr. Cameron Duncan[1], Mrs. Beatrice Ferrari[1], Mrs. Maria Giulia Bravi[1], Dr. Antonio Gentile[2], Dr. Stefano Marchionna[2], Dr. Chiara Ferrara[1], Dr. Taewon Kim[3], Dr. Changhyun Park[3], Dr. Chanhee Lee[3], Prof. Hyun-Wook Lee[3], Prof. Riccardo Ruffo[1], Prof. Giovanni Maria Vanacore[1]
[1]Università degli Studi di Milano-Bicocca - UNIMIB, Milano, Italy, [2]Ricerca sul Sistema Energetico - RSE S.p.A, Milano, Italy, [3]Ulsan National Institute of Science and Technology - UNIST, Ulsan, Republic of Korea

PS-04 (1), august 26, 2024, 10:30 - 12:30

Background incl. aims
In a landscape where the global demand for clean and reliable energy sources, and the need to mitigate the environmental impacts of fossil fuels, are constantly growing, lithium-ion batteries (LIBs) represent the most widespread energy storage technology, due to their reliability and excellent electrochemical performance. Nonetheless, the drawbacks of graphite, the most used negative electrode in LIBs, pose the need to study materials that present better outputs. In the limited landscape of alternative anodic materials, one of the most interesting is the family of MXenes: 2D materials with Mn+1XnTx stoichiometry (M represents a transition metal, X carbon or nitrogen, T the functionalization of the layers). However, these materials are obtained by etching the corresponding MAX phase precursor with HF, a seriously hazardous operation. To overcome the issue, we changed the paradigm and thermally treated Sn-doped MAX phases with different levels of Sn doping, obtaining peculiar MAX nanocomposites, and employing them as anodic materials in LIBs. [1] Since the key to understanding their electrochemical behavior lies in the morphology, crystal structure, and formation mechanism of the nanostructures, a multi-approach Transmission Electron Microscopy (TEM) analysis has been the main character in the investigation of the materials, consisting of static High-Resolution TEM (HRTEM), Operando TEM upon electrochemical materials lithiation [2] and pump-probe dynamic Ultrafast TEM (UTEM). [3]
Methods
The Ti3Al(1-x)SnxC2 MAX phase samples with nominal x = 0, 0.4, and 0.7 were synthesized through Spark Plasma Sintering (SPS). They were heated in air at 600°C and studied as anodic materials in LIBs by galvanostatic cycling with potential limitation (GCPL) in two-electrode coin cells. The sample were characterized by neutron and X-ray diffraction, CHNS, thermal gravimetric analysis, Scanning Electron Microscopy and Raman spectroscopy. Static HRTEM was executed with a JEOL JEM 2100 Plus operated at 200 kV at UNIMIB; Operando electrochemical TEM measurements were obtained with a JEOL JEM 2100 Plus at 200 kV at UNIST coupled to a Nanofactory Instruments in-situ Dual-Probe sample-holder used to apply bias and execute the lithiation. The pump-probe UTEM measurements are going to be acquired with a JEOL JEM 2100 coupled with a fs PHAROS laser in stroboscopic mode: the 1030 nm IR laser is both used as the pump and upconverted into UV light used to generate the photoelectron pulses used as the probe.
Results
The electrochemical performances show a very large improvement for the oxidized samples; moreover, the cells show a remarkably increasing capacity for a higher Sn content: it reaches 200 mAh g-1 for Sn0.4_Ox and 250 mAh g-1 for Sn0.7_Ox at 1 C, more than double to the non-Sn-doped material. Moreover, the samples showed an excellent value of Coulombic Efficiency (99.6%) and good stability upon cycling. The structural analysis evidenced the appearance of rutile and SnyTi(1-y)O2 mixed oxides in the thermally treated samples, and the HRTEM imaging highlighted the morphology of such nanometric crystallites on the MAX phase surface as shown in Figure 1. Since the MAX phase is inert, the potential profiles from the GCPL suggest that for the LIBs the measured

capacity is due to mixed mechanisms of intercalation, conversion, and alloying in the nanostructured oxide composite. The main contribution of SnO2 conversion and alloying has been confirmed thanks to the operando electrochemical TEM analysis, which shows the enlargement of the surface structures (clearly depicted in Figure 2), typical of the mentioned mechanisms.
According to our analysis, the presence of Sn lowers the MAX phase resistance to oxidation, giving a lower oxidation temperature and a higher percentage of oxides, which is confirmed also by CHNS; for a complete understanding of the process, as sketched in Figure 3, pump-probe dynamic UTEM measurements will be crucial to unveil the onset of the transient structural modification upon laser heating which leads to oxidation in the presence of oxygen.

Conclusions

Our study has highlighted that the unaltered conductive MAX phase cores show a beneficial role to the surrounding oxide nanoparticles since they can ensure sufficient electrical contact. In addition, as testified by the good stability of the samples, the SnyTi(1-y)O2 solid solution prevents the huge volume changes that pure SnO2 particles typically show, which cause an important loss of capacity after a few cycles due to active material shattering. Our investigation underscores the indispensable role of a diverse TEM analysis in elucidating the electrochemical behavior and structural transformations of the Ti/Sn oxides and Sn-doped MAX phase composite, paving the way for the rational design and optimization of such nanocomposites for next-generation LIBs.

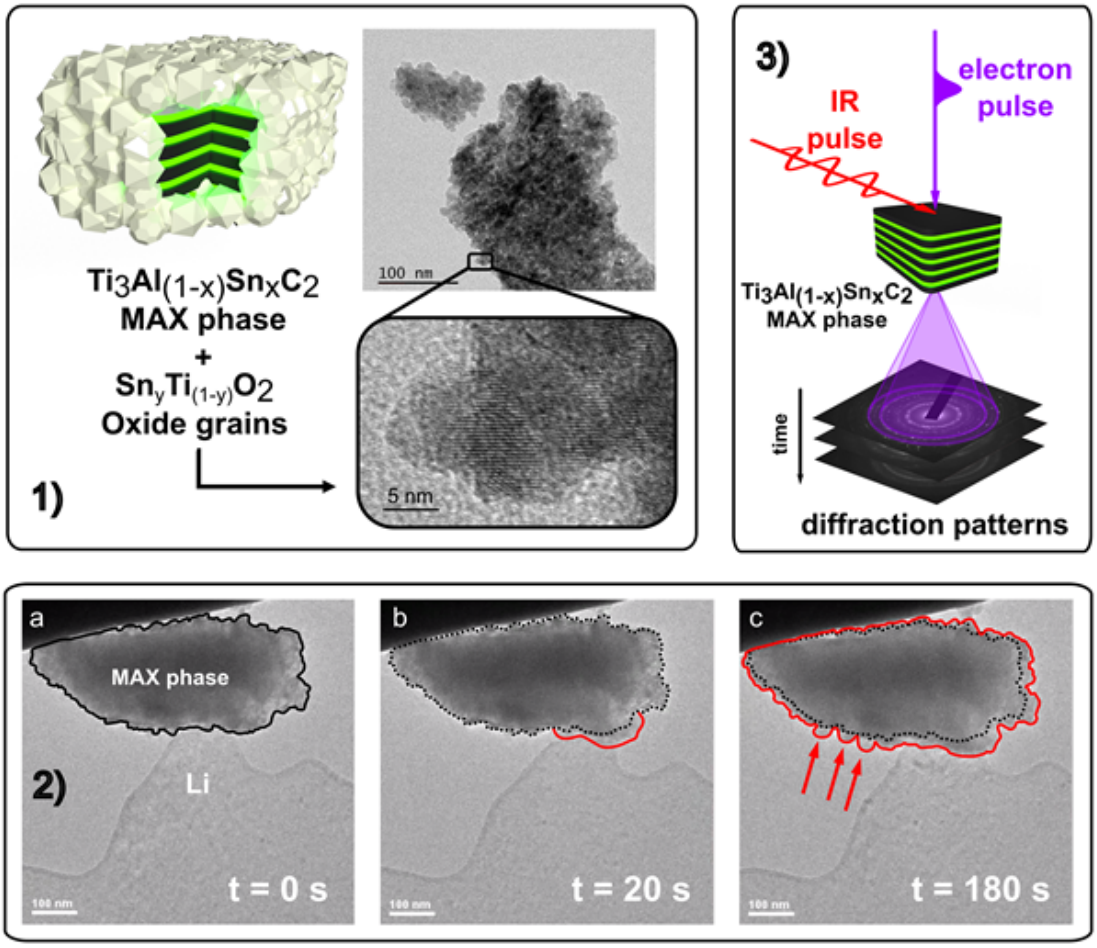

Figure 1. Sketch of an oxidized MAX phase grain and HRTEM images of the sample Sn0.7_Ox.
Figure 2. A sequence of images taken with operando TEM of a Sn0.7_Ox grain upon lithiation. a) No contact and no biasing; b) 20 s after starting bias, the oxide nanoparticles close to the contact spot show enlargement; c) 180 s after starting bias, all the nanoparticles are enlarged, three evident round nanoparticles marked with arrows.
Figure 3. Scheme of the pump-probe dynamic UTEM measurements. Transient structural modification (which leads to oxidation in the presence of oxygen) of a MAX phase grain is stimulated by laser heating.

Keywords:

Energy-Storage, lithium-metal-batteries, Ultrafast-TEM, pump-probe, operando-TEM

Reference:

[1] Ostroman, I., Ferrara, C., Marchionna, S., Gentile, A., Vallana, N., Sheptyakov, D., Lorenzi, R. & Ruffo, R. (2023). Highly Reversible Ti/Sn Oxide Nanocomposite Electrodes for Lithium Ion Batteries Obtained by Oxidation of Ti3Al (1-x) SnxC2 Phases. Small Methods, 7(10), 2300503.

[2] Li, S., Wi, T. U., Ji, M., Cui, Z., Lee, H. W., & Lu, Z. (2021). The Role of Polymer and Inorganic Coatings to Enhance Interparticle Connections Diagnosed by In Situ Techniques. Nano Letters, 21(3), 1530.

[3] Vanacore, G. M., Fitzpatrick, A. W. P., & Zewail, A. H. (2016). Four-dimensional electron microscopy: Ultrafast imaging, diffraction and spectroscopy in materials science and biology. Nano Today, 11(2), 228.

706

3D Operando Monitoring of lithiation spatial composition in NMC-cathode electrode by X-ray nano-CT & XANES-techniques

Dr. Arnaud Demortière[1], Dr. Tuan-Tu Nguyen[1], Dr. Vincent De Andrade[2], Dr. Zeliang Su[1]
[1]Laboratoire de Réactivité et Chimie des Solides (LRCS), CNRS UMR7314, Amiens , France, [2]Argonne NL, Chicago, USA

PS-04 (1), august 26, 2024, 10:30 - 12:30

Over the last decades, with increasing energy demand along with the shift towards greener energy solutions, Li-ion batteries have gained attraction for energy storage applications.[1] Due to the high complexity in the hierarchical architecture of composite electrodes, it is extremely challenging to ensure a homogenous electrode structure. The non-uniform distribution of phases, leading to microstructural heterogeneities, has been shown to induce a non-uniform electrochemical behavior, which can deteriorate the performance, and cause macroscopic failures.[2,3] Therefore, the identification of these microstructural heterogeneities and understanding their effects on the dynamics of (de)lithiation is crucial to improve electrode design.

Lithium compositional distributions in composite electrodes can also be investigated using various techniques such as Raman microscopy,[4] X-ray diffraction (XRD),[5] or 2D X-ray absorption near-edge structure spectroscopy (XANES).[6] However, these methods have been restricted to low spatial resolution or spatially integrated signal along the depth direction. These methods hence cannot accurately capture the spatial distributions and can lead to a limited interpretation of the mechanism. Recently, Finegan et al.[7] used Operando X-ray diffraction-computed tomography (XRD-CT) for characterizing, in 3D, the dynamic crystallographic structure between and within LMO particles during electrochemical operation.

Several works have combined XANES and X-ray tomography to generate a rich data set that allows a direct correlation of the chemical information and the microstructure. Meirer et al.[8] used 3D XANES to probe the conversion of NiO to Ni metal in a partly reduced electrode. They found significant inhomogeneities in terms of chemical states across particles as well as evidence of fracturing caused by volume expansion during the reaction. More recently, Wang et al. [9] collected a 46-point spectrum across the iron K-edge of a LiFePO4 cathode particle and developed a run-out correction system to enable automated tomography.

Here, we perform XANES coupled with transmission X-ray computed tomography (TXM-CT) at nanoscale in Operando mode to investigate LiNi0.5Mn0.3Co0.2O2 (NMC) positive electrodes[12]. The ability to probe battery materials in an operando mode provides significant advantages over ex situ approaches and allow characterizing the microstructure evolution while capturing the electrochemical reaction kinetics inside electrode and active materials (AM). In this work, we demonstrate that Operando XANES-TXM nanoCT allows access to the Li distribution (local Li concentration) at nanoscale within the LiB electrodes during the operation. We also proposed a method that relies on just three energy levels located at pre-edge, edge, post-edge for minimization of radiation damage to the sample. Also, a specific electrochemical cell and a sample preparation process were introduced, which make the use of electrodes typical to those used in real-life applications possible.

Our experimental results unveil the non-uniformity of the Li repartition throughout the LiB porous electrodes during operation [10]. As a result, there are regions being more active than the others as well as preference spots on the particle surface where the reactions are more likely to occur. The Li

repartition across the electrode depth is adequately uniform, which indicates a negligible effect from porous electrode. This is expected as we used EC:DMC solvent-based electrolyte at 1.2 M which reduces the limitation from ionic transport in liquid phase within the porous electrode. Thus, we can conclude that mass transport in the electrolyte is not rate limiting factor in this electrode under the applied cycling conditions. In addition, some of the reconstructed slices also revealed that the lithiation process could also happen from internal pores of the AM particles. This observation also implies that the electrolyte along with the carbon conductive can penetrate some internal pores through the AM grain boundaries and allow the (de)lithiation process to occur from the inside of the NMC secondary particles.

Finally, we expect that our analysis technique will provide a direct method to unveil the effects of the electrode microstructure on its electrochemical performance [11,13]. This multiscale insight can shed light to the optimization of the electrode design to improve the electrode performance.

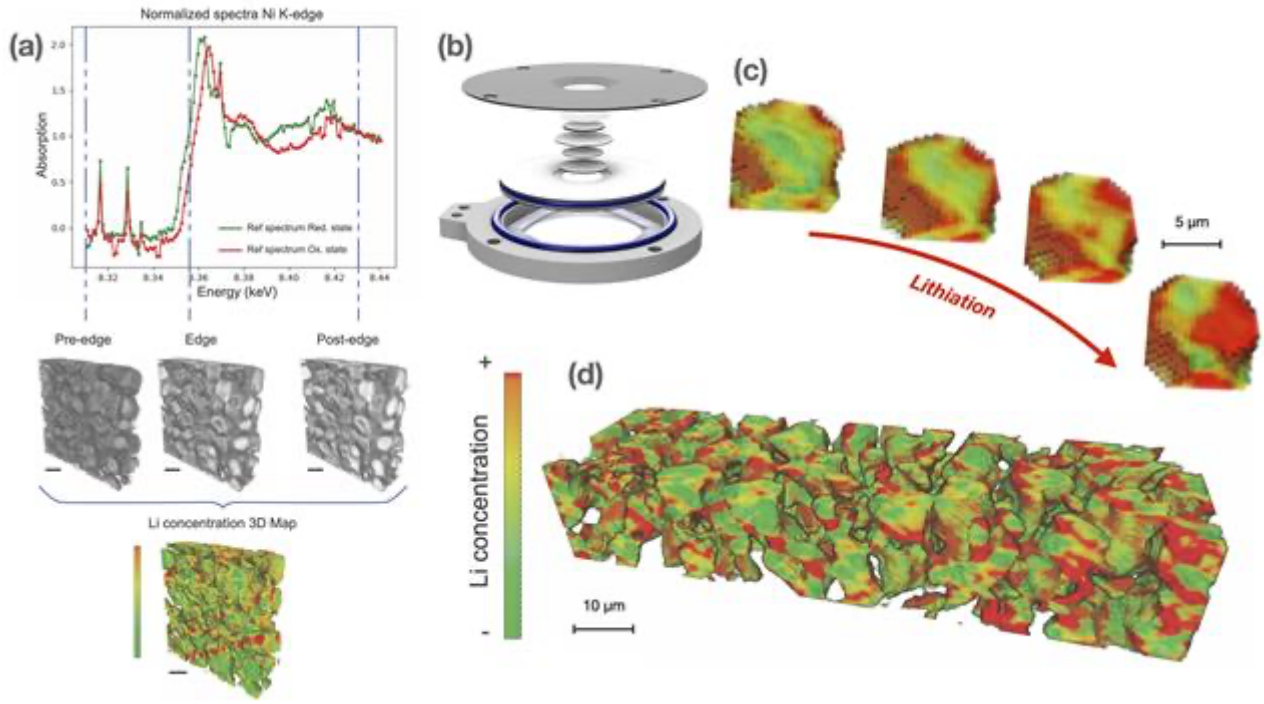

Keywords:

nano-XCT, operando experiments, lithiation dynamics

Reference:

[1] J. B. Goodenough, Energy Environ. Sci. 2014, 7, 14.
[2] Y. Yang, et al. Adv. Energy Mater. 2019, 9, 1900674.
[3] X. Lu et al. Nat. Commun. 2020, 11, 1.
[4] J. Nanda, et al. Adv. Funct. Mater. 2011, 21, 3282.
[5] J. Liu, M. Kunz, K. Chen, N. Tamura, T. J. Richardson, J. Phys. Chem. Lett. 2010, 1, 2120.
[6] K. Chen, et al. J. Phys. Chem. C 2019, 123, 3292.
[7] D. P. Finegan et al. Nat. Commun. 2020, DOI 10.1038/s41467-020-14467-x.
[8] Meirer, F. et al. Journal of Synchrotron Radiation 2011, 18 (5), 773–781.
[9] Wang, J. et al. Nature Communications 2016, 7, 1–7.
[10] Nguyen, T. et al. (2021). Advanced Energy Materials, 11(8), 2003529.
[11] Su, Z., et al. (2020). ACS Applied Energy Materials, 3(5), 4093-4102.
[12] Su, Z., et al. (2022). Chemistry-Methods, e202100051.
[13] Su, Z., et al. (2022). npj Computational Materials, 8(1), 1-1

721

Nanowire Triple-Junction GaInP/InP/InAsP Solar Cells Realized

Prof. Reine Wallenberg[1,2], Dr Lukas Hrachowina[2], Prof Magnus Borgström[2]
[1]national center for HREM, Lund University, Lund, Sweden, [2]NanoLund, Lund University, Lund, Sweden

PS-04 (1), august 26, 2024, 10:30 - 12:30

Background
Planar multi-junction solar cells, based on III-V semiconductors, matched to the solar spectrum, are today's world-record efficiency solar cells1. Multi-junction III-V nanowire (NW) solar cells with equal performance would require significantly less material and is more sustainable at lower cost than planar solar cells. The NW geometry allows more material combinations along the NW axis than for current multijunction solar cells. We report the design and proof-of-principle demonstration of axially defined GaInP/InP/InAsP triple-junction photovoltaic NWs optimized for light absorption exhibiting an open-circuit voltage (VOC) of up to 2.37 V. The open-circuit voltage amounts to 94% of the sum of the respective single-junction NWs.
Methods
Hexagonal Au seed particle arrays on 2 inch InP:S (111)B wafers were defined2 using displacement Talbot lithography, Au evaporation, and lift-off. We grew the NWs in a MOVPE reactor at 440°C. We used phosphine (PH3), arsine (AsH3), trimethylindium (TMIn), and triethylgallium (TEGa) as precursors, and hydrogen sulfide (H2S) and diethylzinc (DEZn) as n- and p dopants, respectively. Throughout NW growth, hydrogen chloride (HCl) was used to prevent tapering in situ. HAADF-STEM and XEDS was used to verify the composition and structure of the 12 different segments constituting the triple-junction solar cell, together with a LED-illuminated EBIC.
Results and conclusions
We used an EBIC set-up with a tungsten probe to electrically contact single NWs. The NWs can be excited by a LED source. For the triple-junction NWs, their voltage is the sum of the subcell voltages. We measured an average VOC of the triple-junction photovoltaic NWs of 94% of the sum of the VOC of single-junction photovoltaic NWs. The highest measured VOC of the triple junction photovoltaic NW, 2.37 V, corresponds to the same value as by adding the highest measured VOC of the single junctions.

REFERENCES:
1 J.F. Geisz, R.M. France, K.L. Schulte, M.A. Steiner, A.G. Norman, H.L. Guthrey, M.R. Young, T. Song, T. Moriarty, Six-junction III-V solar cells with 47.1% conversion efficiency under 143 Suns concentration, Nat. Energy 5 (2020)
2 L. Hrachowina, N. Anttu, M.T. Borgstr€om, Wafer-scale synthesis and optical characterization of InP nanowire arrays for solar cells, Nano Lett. 21 (2021). 7347e7353.
ACKNOWLEDGMENTS: Nano Lund, the K A Wallenberg Foundation and the Swedish Research Council

Fig. 1 Energy-dispersive X-ray spectroscopy line scans and STEM images of the whole NW (a) and the top junction (b). (c, d) EDXS line scans along the NWs from (a) and (b), respectively. A schematic drawing of the composition of the segments is inserted in (a) The arrows in (b, d) emphasize the position of the InP segment used in the Esaki tunnel diode.

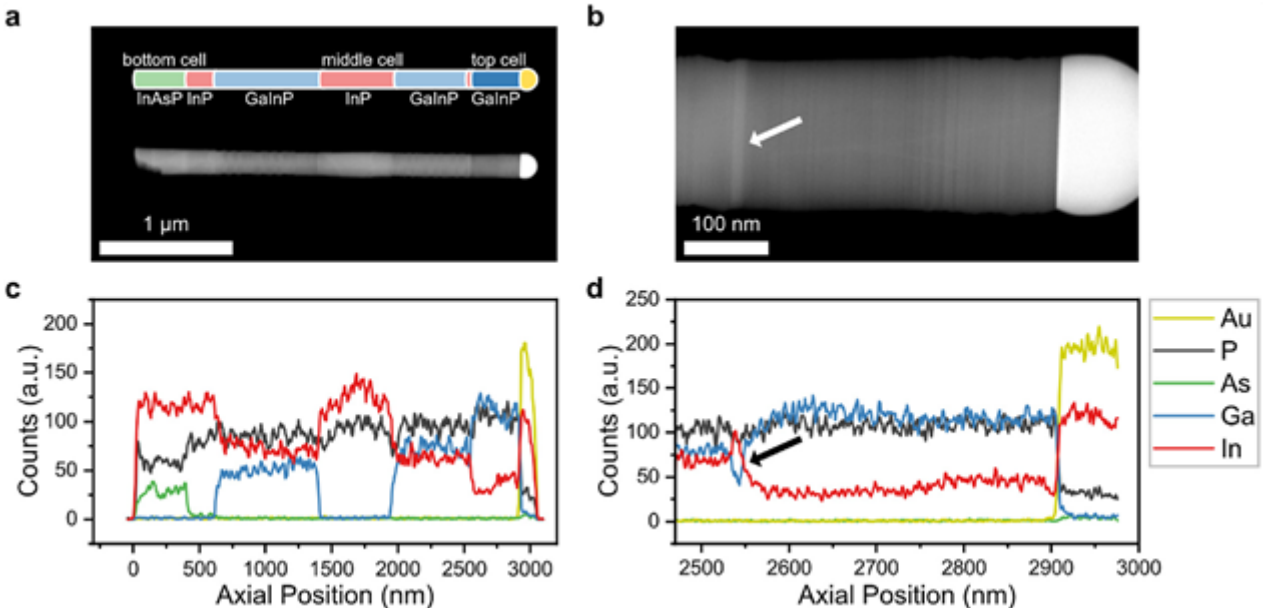

Keywords:

HREM, HAADF-STEM, Solar cell, EBIC

48

(In-situ) 3DED and other TEM Techniques Unravel (Ca,Sr)(Mn,Fe)O3-δ and LaxSr2-xMnO4-δ Structure-Property Relations in Redox Conditions

Daphne Vandemeulebroucke[1], Dr. Maria Batuk[1], Mr. Amirhossein Hajizadeh[1], Dr. Pascal Roussel[2], Dr. Myriam Wastiaux[2], Prof. Dr. Joke Hadermann[1]
[1]EMAT, University of Antwerp, Antwerp, Belgium, [2]UCCS, CNRS, University of Lille, Lille, France
PS-04 (2), Plenary, august 26, 2024, 14:00 - 16:00

Background
Many alternative energy applications involve inorganic crystalline solids exposed to redox conditions, e.g. solid oxide fuel cells (SOFCs) or chemical looping with oxygen uncoupling (CLOU). With the development of in-situ 3D electron diffraction (3DED) of solids at high-temperature in gas and vacuum conditions, great new potential is unlocked for unravelling structure transformations in such operational conditions, to understand the origins of e.g. high performance and degradation properties. Here, we investigated the influence of high-temperature reducing atmospheres on the structure of two such perovskite-based energy materials - CaMnO3-δ and LaxSr2-xMnO4-δ.

CaMnO3-δ is a perovskite with interesting properties as oxygen carrier in the CLOU process, i.e. a carbon capturing combustion technique that inherently separates expelled CO2 from air. The cycling stability and oxygen release temperature of this compound can be significantly improved by A or B site doping with e.g. Sr or Fe, but it has not yet been unravelled why. [1] [2]

Ruddlesden-Popper (RP) LaxSr2-xMnO4-δ are interesting electrode materials for symmetric solid oxide fuel cells (SOFCs) due to their electronic and chemical properties. Previously, they were reported from in-situ X-ray and neutron diffraction to remain stable upon heating to 700°C in H2 for $0 < x \leq 0.6$, although anomalously large atomic displacement parameters were found. Further, while all these structures had the same I4/mmm lattice, the x = 0.5 compound showed a higher conductivity in reducing environment (1.9 S cm −1), breaking the trend of the rest of the series (0.4, 0.5, and 0.8 S cm−1) which was not explained yet in literature. [3]

Methods
CaMnO3-δ, Ca0.75Sr0.25MnO3-δ, CaMn0.8Fe0.2O3-δ and LaxSr2-xMnO4-δ for x = 0, 0.25, 0.5, 0.75 and 1 were examined with in-situ and ex-situ 3DED, EDX, high-resolution HAADF-STEM and/or (mono STEM-) EELS. However, the investigation of oxides with in-situ TEM is not without obstacles. At temperatures above 700°C in reducing gas conditions, an extra silica layer is created in-situ around the studied oxide – as evidenced by EDX and EELS - due to a reaction coming from the Si3N4 of the heating chip. This shell can interfere with the reduction process, as shown from Mn valence determination by mono STEM-EELS. To overcome this problem, we performed a series of in-situ gas and vacuum experiments with LaxSr2-xMnO4-δ on graphene coated heating chips, in order to study the influence of various parameters and find the optimal conditions for in-situ TEM experiments on oxides in redox conditions, that can be directly linked to real-life energy applications.

Results
With in-situ 3DED in diluted H2 and in vacuum at 250°C-350°C, we captured the oxygen vacancy order in one of the intermediate oxygen deficient phases of CaMnO3-δ – i.e. CaMnO2.75 – and solved and refined its structure. We compared its structural transformations in H2 and vacuum high-temperature conditions with those of the doped Ca0.75Sr0.25MnO3-δ and CaMn0.8Fe0.2O3-δ to explain the differences in performance on the level of the atomic lattice.

Also, 3D electron diffraction reveals the previously unreported structure transformations of La0.25Sr1.75MnO4-δ and La0.5Sr1.5MnO4-δ to an incommensurate 2D and 1D modulated structure respectively, but the amount of order in the crystals differs. Moreover, high-resolution HAADF-STEM shows a difference in defect structure: where the x = 0.5 compositions exhibits many higher order RP n = 2 layer defects, this is not the case for the x = 0.25 material. Those structural differences allow to explain the higher conductivity for La0.5Sr1.5MnO4-δ than for La0.25Sr1.75MnO4-δ . [4]

Further, in-situ high-resolution HAADF-STEM (in vacuum) and 3DED (in gas) at 700°C also detect the formation of a perovskite phase on the surface of both materials. From EDX, the layer is observed to be La rich, which leads to differences in thermodynamics between the surface and the bulk structure. [4]

Conclusions

Despite the additional challenges of in-situ TEM on oxides at very high temperatures in gas, the combination of in-situ and ex-situ 3DED, high-resolution HAADF-STEM, EDX and (mono STEM)-EELS offered a lot of new structural information on (Ca,Sr)(Mn,Fe)O3-δ and LaxSr2-xMnO4-δ in redox conditions. For these samples, their increased performance as CLOU oxygen carrier on doping, and differences in SFOC anode conductivity, were respectively linked to their differences in oxygen vacancy order and/or differences in defect structure. This illustrates the benefits of a combination of various in-situ and ex-situ TEM techniques to gain new insights in the structure-property relations of redox-based energy materials.

Financial support is acknowledged from FWO I003218N, University of Antwerp BOF TOP 38689 and the European Commission NanED Grant number 956099.

Keywords:

3DED, in-situ, SOFC, CLOU, redox

Reference:

[1] Galinsky, N., et al. Appl. Energy 2015, 157, 358–367.
[2] Galinsky, N, et al. Appl. Energy 2016, 174, 80–87.
[3] Sandoval, M. V., et al. Int. J. Hydrogen Energy 2017, 42 (34), 21930–21943.
[4] Vandemeulebroucke, D., Batuk, M., Hajizadeh, A. and Hadermann, J. Chem. Mater. 2024, 36, 5, 2441-2449.

129

Exploring solid conversion products in lithium-sulfur batteries through cryo-TEM and machine-learning-supported small angle neutron scattering

Jean-marc Von Mentlen[1], Mrs. Ayca Senol[1], Mr. Thomas Demuth[3], Dr. Jürgen Belz[3], Dr. Alen Vižintin[4], Prof. Dr. Kerstin Volz[3], Prof. Dr. Vanessa Wood[1], Prof. Dr. Christian Prehal[2]
[1]ETH Zurich, Zurich, Switzerland, [2]Paris Lodron University Salzburg, Salzburg, Austria, [3]Phillips University Marburg, Marburg, Germany, [4]National Institute of Chemistry, Ljubljana, Slovenia
PS-04 (2), Plenary, august 26, 2024, 14:00 - 16:00

Background incl. aims
Lithium-sulfur batteries (LSB) have emerged as a promising candidate for future energy storage solutions, leveraging the abundance, cost efficiency, and low environmental footprint of sulfur as well as significant theoretical capacity. These batteries feature a sulfur-infiltrated, highly porous carbon cathode immersed in an organic liquid electrolyte and paired with a lithium-metal anode. Despite their potential, the broader application of Li-S batteries is hindered by challenges such as suboptimal sulfur/lithium sulfide mass loadings, diminished rate performance, and the depletion of active materials. This depletion primarily results from the formation of mobile polysulfides, which can irreversibly react at the lithium-metal anode. A central challenge is the insufficient understanding of the sulfur-to-lithium sulfide conversion process, critical to the battery's functionality. [1]
In recent years, small-angle neutron and X-ray scattering have become popular for investigating LSB. However, interpreting the scattering data is notoriously challenging heavily reliant on the selection and tuning of appropriate models, thus introducing the potential for user bias [2]. Conversely, electron microscopy offers model-free access to structural analysis and provides local chemical resolution. Nevertheless, challenges such as a small field of view, demanding sample preparation and sensitivity to air and beam exposure complicate the probing of such samples [3].
In this work, we leverage recent advances in cryo-vacuum transfer TEM holders to enable the structural and chemical analysis of highly sensitive cathode materials, such as lithium sulfide [3]. We integrate this local information with operando small-angle neutron scattering (SANS) experiments to model the evolution of the multiphase cathode structure during cycling. Utilizing the composition revealed by cryo-TEM, we interpret the operando SANS data using Plurigaussian Random Fields (PGRF) models — a stochastic approach that provides representative 3D structures spanning several hundred nanometers. Given the computational intensity of solving this inverse design problem through PGRF, we train a generative adversarial model to expedite the simulation process.

Method
A binder-free, sulfur-infiltrated carbon cathode was dried and grinded in a mortar after discharge. A lacey carbon grid was then dipped into the powder. Next, the sample was transferred under Argon atmosphere from the glovebox to the TEM using the MelBuild Double Tilt LN 2 Vacuum Transfer Holder. During measurement, the sample was cooled down to -165°C to reduce beam damage. The samples were investigated using a JEOL GrandARM (ETHZ) operated at 300kV and a JEOL JEM 2200FS at 200kV. EFTEM and EELS measurements were conducted on the 2200FS.
The SANS data were acquired at the D-22 beamline at the Institute Laue-Langevin (ILL) using a custom-built cell. The cell, housed in a PEEK body, featured aluminum current collectors serving both as electrical conductors and neutron transparent windows. It incorporated a copper foil current collector, a Li metal anode, a glassfiber separator, a carbon black cathode, and an additional aluminum current collector. The azimuthally averaged intensity curve was fitted using a PGRF model.

Results

The cryoTEM measurements confirm a two-phase discharge product: one crystalline and the other amorphous. Similar discharge products have previously been reported in in-situ TEM cells using ether-based Li2S6 catholytes [4]. EFTEM and EELS analyses of the discharge particles reveal that the crystalline phase consists of Li2S, while the amorphous phase comprises a lower-order polysulfide (LOPS). Both primary particles are smaller than 10 nm, with the LOPS being approximately half the size of the Li2S particles. For subsequent modeling, we selected Li2S2 as the LOPS, which has been identified as a byproduct in LSB.
Building on the two-phase discharge product, we chose a PGRF model to analyze the SANS data. PGRF models are ideally suited for generating a variety of hierarchical, three-phase structures. By using a deuterated solvent in our battery, we adjusted the electrolyte's contrast to match that of the carbon matrix in the cathode, effectively reducing the number of signal sources to three: carbon/catholyte, Li2S, and Li2S2. Given the computational intensity of calculating scattering curves based on PGRF, we trained a convolutional neural network to predict the scattering curve from the PGRF model's input parameters. This model predicts a normalized curve with a mean squared error below 10^-4 and achieves a computational speed increase of three orders of magnitude (20 s reduced to 2.5 s). This acceleration enables the use of computationally intensive fitting algorithms. We opted for a Bayesian Optimization approach, well-suited for navigating through convex parameter spaces like those of PGRF. The parameters derived from fitting the PGRF model provide insight into the structural evolution of the cathode during operation, supporting the hypothesized solution-mediated conversion mechanism [2]. This mechanism involves the disproportionation of Li2S2 and its subsequent direct electroreduction to Li2S.

Conclusion

This study highlights the synergy between cryoTEM and SANS in revealing the conversion mechanism of lithium-sulfur batteries (LSB), leveraging a cryo-vacuum transfer holder for detailed cathode analysis. By minimizing user biases and enhancing model selection accuracy, we've provided a clearer understanding of the cathode's structural evolution during operation. Our approach not only advances the field of energy storage by deepening insights into LSB conversion mechanisms but also sets a methodological standard for future research on conversion-type batteries

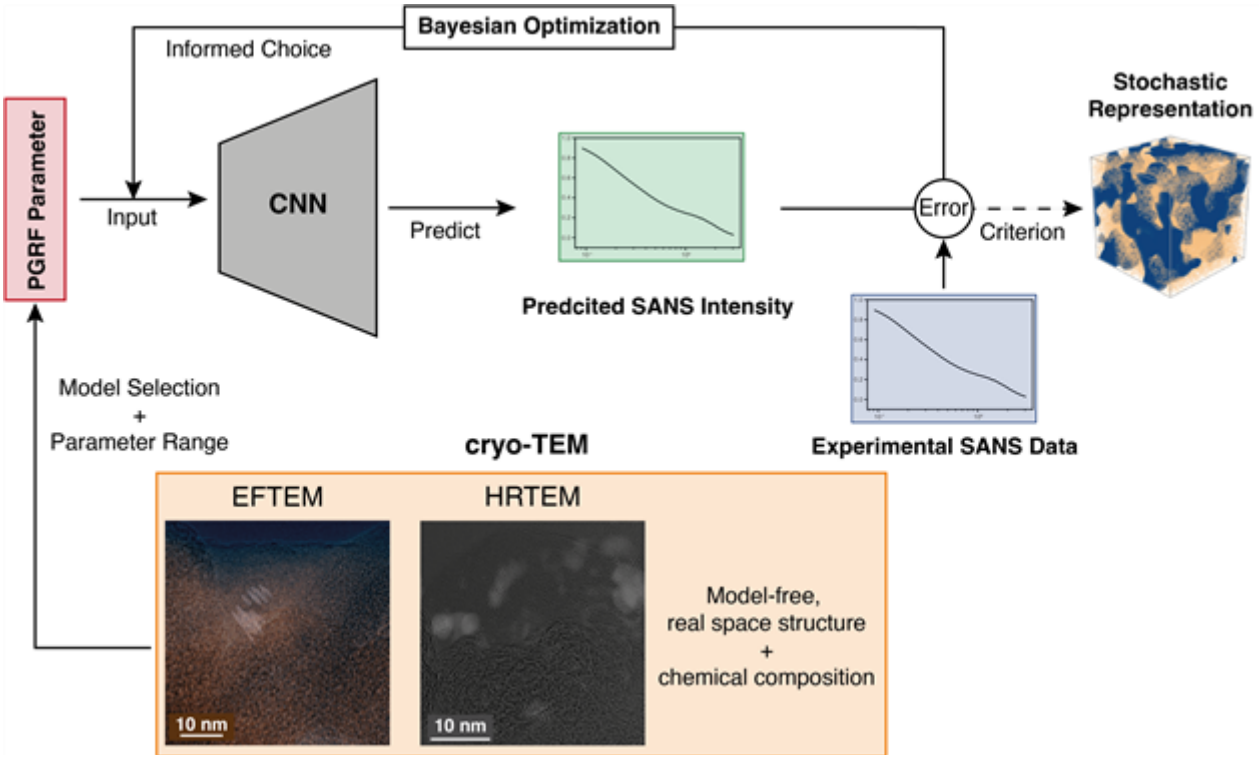

Keywords:

cryo-TEM, EELS, batteries, lithium-sulfur, machine-learning

Reference:

[1] Jan, W. et. al. Journal of Energy Storage 72-D, 108559 (2023)
[2] Prehal, C. et al. Nat Commun 13, 6326 (2022).
[3] Wang, X. et al. Joule 2, 2225-2234 (2018)
[4] Zhou, S. et al. Nature 621, 75–81 (2023)

195

Operando structural and chemical imaging of lithium battery interfaces

Sayantan Sharma[1,2], Dr. Luca Cressa[1], Dr. Tom Wirtz[1], Dr. Santhana Eswara[1]
[1]Advanced Instrumentation for Nano-Analytics (AINA), Materials Research and Technology Department, Luxembourg Institute of Science and Technology (LIST), Belvaux, Luxembourg,
[2]University of Luxembourg, Belval, Luxembourg

PS-04 (2), Plenary, august 26, 2024, 14:00 - 16:00

Background incl. aims
Lithium metal is a very promising anode material to develop batteries with higher energy density due to its high specific capacity and low redox potential. However, the widespread use of lithium as anode is hindered by the safety concerns stemming from the formation of dendritic structures at the electrode-electrolyte interfaces during battery operation [1]. Hence, understanding the fundamental mechanism behind the formation of these dendritic structures is crucial for the utilization of lithium metal in producing batteries with enhanced energy density and safety. Traditional ex-situ and in-situ analysis techniques are not sufficient to understand the transient processes involved in the nucleation and growth of these dendrites. Thus, operando techniques, which allow analysis while the battery is functioning, are essential for gaining deeper insights. The primary aim of this study is to devise a methodology for capturing the nanoscale structural and chemical changes occurring at the electrode-electrolyte interface during battery operation.

Methods
Our approach utilizes a dual-beam focused ion beam-scanning electron microscope (FIB-SEM) equipped with an in-house developed magnetic sector secondary ion mass spectrometer (SIMS) for operando structural and chemical imaging [2]. Secondary electron (SE) imaging helps to visualize the structural changes and SIMS imaging depicts the chemical alterations at the battery interfaces. Here SIMS is used as it is an ideally suited technique for high-sensitivity chemical analysis and imaging of all elements, including light elements like lithium. Thus, SIMS enables unequivocal detection of the lithium rich dendrites near battery interfaces. A special operando analysis setup has been developed through which the charging-discharging of the battery can be performed inside the FIB-SEM-SIMS instrument using an external potentiostat, while maintaining the necessary sample bias conditions to allow secondary ion extraction for simultaneous SIMS analysis.

Results
Using the FIB-SEM-SIMS instrument, all solid-state symmetrical lithium cells with garnet type solid electrolyte lithium lanthanum zirconium oxide (LLZO) were analyzed both before electrochemical cycling and after short-circuit [3]. Phases with darker contrast were identified in the gallium ion induced SE images of the electrolyte after short-circuit failure, SIMS imaging showed higher lithium-ion signal in those phases (Fig. 1e,1f). Thus, the presence of lithium rich dendrites in LLZO after short-circuit was confirmed by SIMS. The development of the operando setup enables us to perform SE and SIMS imaging of the battery interfaces during cycling. Therefore, it is now possible to detect and image the progression of lithium dendrite growth at different stages of cell operation. Furthermore, this operando setup allows direct correlation between the alterations in structure and chemistry of the electrode-electrolyte interface with the evolution of interfacial resistance by combining electrochemical experiments such as impedance spectroscopy with the SEM-SIMS analysis.

Conclusion

In summary, our operando FIB-SEM-SIMS setup allows real-time observation of the nanoscale processes at the interfaces linked with dendrite growth in solid-state lithium metal batteries. This helps in acquiring a more complete understanding about the phenomenon of dendrite formation in lithium metal batteries, paving the way for development of batteries with improved safety as well as electrochemical performance.

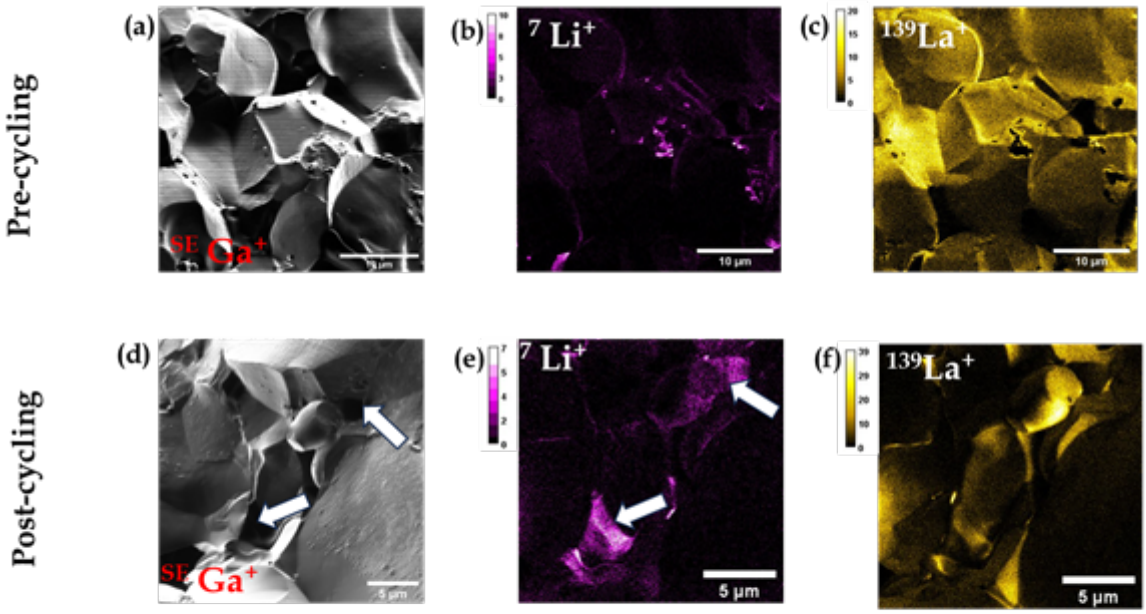

Figure 1. Gallium ion induced secondary electron image and SIMS elemental maps of $^{7}Li^{+}$ and $^{139}La^{+}$ in LLZO before cycling (1a,1b,1c) and after short-circuit (1d,1e.1f). White arrows in Fig.1d and Fig.1e indicate dendrites.

Keywords:

Operando imaging, lithium dendrites.

Reference:

[1] J.M. Tarascon and M. Armand, Nature 414, 359–367 (2001).
[2] O. De Castro et al., Analytical Chemistry, 94, 10754−10763 (2022).
[3] L. Cressa et al., Analytical Chemistry, 95, 9932–9939 (2023).
[4] The authors acknowledge funding from the European Union's Horizon Europe research and innovation program under grant agreement no. 101104032 (OPINCHARGE). The authors would also like to express their gratitude to Yanyan Sun of German Aerospace Center (DLR) for the LLZO samples.

444

In-situ TEM reduction of a solid oxide cell with NiO/YSZ and NiO/BZCY fuel electrode materials

Dr Svetlana Korneychuk[1,2,3], Cedric Grosselindemann[4], Laura-Alena Schäfer[5], Dr.-Ing. Mariya E. Ivanova[5], Hon.-Prof. Dr.-Ing. Norbert H. Menzler[5], Prof. Dr. Olivier Guillon[5], PD Dr.-Ing. André Weber[4], Prof. Dr. rer. nat. Astrid Pundt[1]
[1]IAM-WK, Karlsruhe Institute of Technology, Karlsruhe, Germany, [2]INT, Karlsruhe Institute of Technology, Karlsruhe, Germany, [3]KNMFi, Karlsruhe Institute of Technology, Karlsruhe, Germany, [4]IAM-ET, Karlsruhe Institute of Technology, Karlsruhe, Germany, [5]Forschungszentrum Jülich GmbH, Institute of Energy and Climate Research (IEK), IEK-1: Materials Synthesis and Processing, Jülich, Germany

PS-04 (2), Plenary, august 26, 2024, 14:00 - 16:00

Background
Increasing the durability of solid oxide cells is one of the main goals for achieving wider industrial application. The quality of the electrode plays a major role in the performance and durability of a fuel and electrolysis cells. Ni/YSZ or Ni/BZCY (BZCY stays for the state-of-the-art proton conducting ceramic material BaZr1-x(Ce,Y)xO3-d) electrodes of solid oxide cells are commonly reduced from NiO/YSZ or NiO/BZCY under hydrogen atmosphere at high temperatures, prior to operation. It is known from commissioning that e.g. reduction temperature and H2 pressure influence the initial performance of the fuel electrode by governing Ni particle size and shape. The reduction results in a significant change in microstructure. As specific microstructural properties are crucial to achieve high performance and durability of the cell, a comprehensive understanding of the reduction process is required.

Methods
With in-situ TEM we are able to observe the reduction of NiO in real time while exposing the sample to hydrogen gas and heat [1]. Using in-situ TEM atmosphere system from Protochips we studied the electrode reduction at the H2 pressures up to 1 atmosphere and temperatures up to 850 °C which fit the real working condition of a conventional solid oxide cell based on oxygen ion conductor as an electrolyte.

Results and conclusions
With this set-up we can observe the initial steps of NiO reduction, local change in oxidation state of Ni and formation of defects in Ni grains. Grain boundaries and triple junctions between NiO and YSZ or BZCY are determined as the starting points of the reduction process at lower temperatures. Closely reproducing the reduction conditions of the real cell, we demonstrate that NiO reduction mechanism is different from the previous findings. We also showed that the initial temperature of the reduction is crucial to achieve a high number of electrochemically active triple phase boundaries between e.g. Ni/YSZ and gas. In-situ results go in good agreement with ex-situ results obtained from a bulk cell reduced in a test bench described in Ref. [2].
Figure 1. Step-by-step reduction of NiO/YSZ material for fuel electrode. Ni becomes porous and nanocrystalline after the reduction. The grain size grows with temperature and pores disappear due to the Ni coarsening.

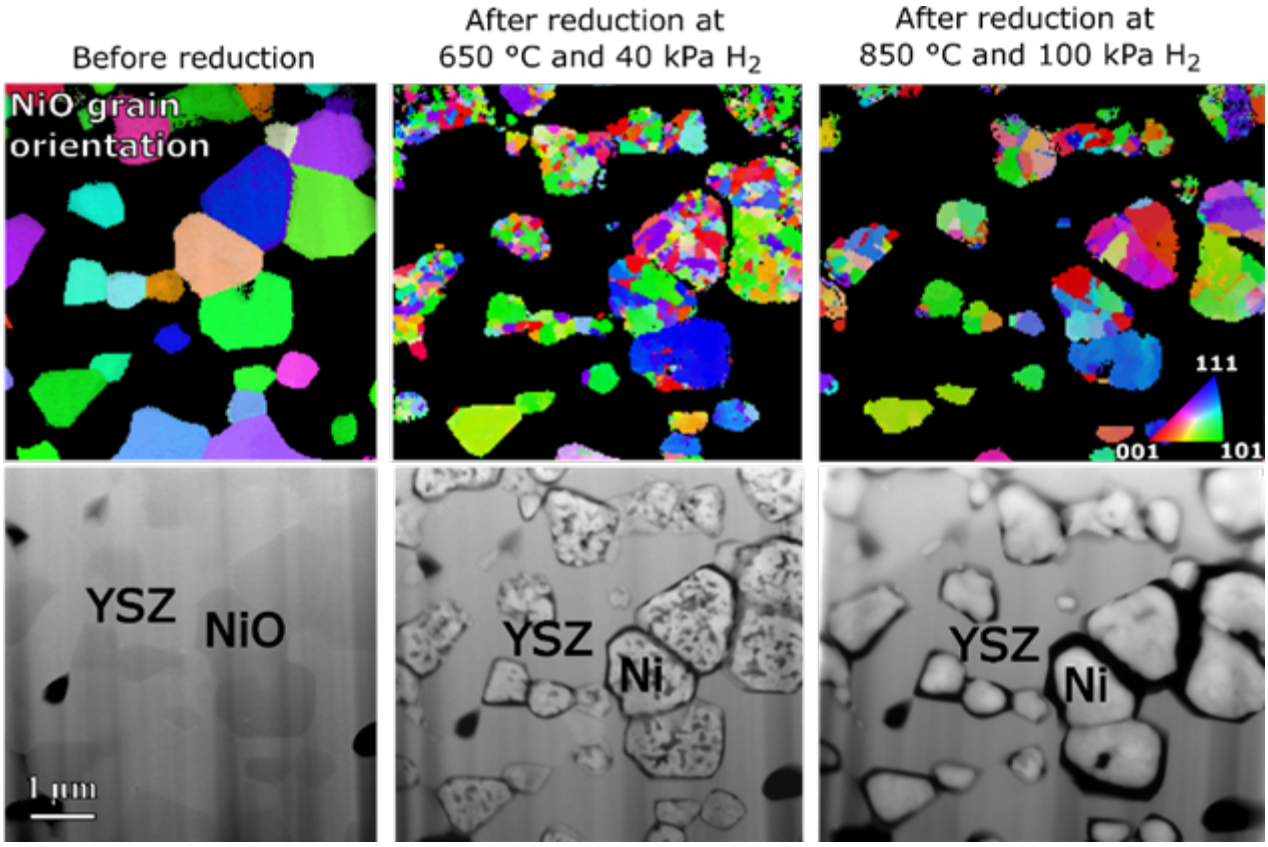

Keywords:

In-situ gas TEM, SOC, hydrogen

Reference:

[1] Korneychuk, S.; Grosselindemann, C.; Menzler, N.; Weber, A.; Pundt, Electrode. Rochester, NY October 17, 2023. https://doi.org/10.2139/ssrn.4604921.
[2] D. Klotz et al., Electrochim. Acta, 227, 110 (2017)

603

Operating a model Solid Oxide Fuel Cell in the Environmental Transmission Electron Microscope

Dr Matthieu Bugnet[1], Dr Thierry Epicier[2], Dr Cedric Frantz[3], Dr Stefan Diethelm[3], Dr Dario Montinaro[4], Dr Elizaveta Tyukalova[5], Dr Yevheniy Pivak[6], Prof Jan Van Herle[3], Prof Aïcha Hessler-Wyser[7], Prof Martial Duchamp[5], Dr Quentin Jeangros[7]
[1]CNRS, INSA Lyon, Université Caliude Bernard Lyon 1, MATEIS, UMR 5510 , Villeurbanne, France, [2]Université Claude Bernard Lyon 1, IRCELYON, UMR CNRS 5256, Villeurbanne, France, [3]Group of Energy Materials, Ecole Polytechnique Fédérale de Lausanne, Sion, Switzerland, [4]SolydEra S.p.A., Mezzolombardo, Italy, [5]Laboratory for In Situ & Operando Electron Nanoscopy, School of Materials Science, Nanyang Technological University, Singapore, Singapore, [6]DENSsolutions, Delft, The Netherlands, [7]Photovoltaics and Thin Film Electronics Laboratory, Ecole Polytechnique Fédérale de Lausanne, , Switzerland

PS-04 (2), Plenary, august 26, 2024, 14:00 - 16:00

Background incl. aims
Solid oxide fuel cells (SOFC) are a class of solid-state electrochemical conversion devices that produce electricity directly by oxidizing a fuel gas. They consist in an anode-cathode duet separated by a solid electrolyte, i.e., a material conducting oxygen ions. The anode is fed with hydrogen or other fuels whereas the cathode is in contact with air, meaning oxygen. Overall, a SOFC operates thanks to the combined action of two external stimuli: a gaseous environment and temperature. Owing to the recent advances in in situ and operando transmission electron microscopy (TEM), we have set up an experiment to operate a SOFC inside an environmental TEM to identify how the device microstructure determines its electrical properties. To do so, an elementary anode-electrolyte-cathode sandwich was prepared by focused ion beam (FIB) and mounted on a heating and biasing microelectromechanical (MEMS)-based specimen holder (DENSsolutions) and inserted in an Environmental TEM (FEI Titan ETEM), as shown in Figure 1 a,b.
Methods
Standard SOFC materials were investigated: the cathode was strontium-doped lanthanum manganite (LSM) co-sintered with yttria-stabilized zirconia (YSZ), the electrolyte was YSZ, and the anode a cermet of NiO co-sintered with YSZ. NiO was first reduced to Ni, leaving pores in the structure due to the volume loss and hence enabling the penetration of the fuel to the triple phase boundaries Ni/YSZ/porosity at the anode side. For practical reasons, we used a single chamber configuration to trigger the operation the cell: the anode and cathode were exposed simultaneously to the oxidant and reducing gases. Due to a difference in the catalytic activity between the electrodes, O2 should reduce at the cathode, while H2 should oxidize at the anode, thus leading to a voltage difference between the two terminals.
Results
The reduction of NiO was first performed under a forming gas N2:H2 in the ratio 20:1 under 15 mbar up to 750°C (N2 was constantly used as a mixing gas for safety reasons due to the need of mixing O2 and H2 in the single-chamber configuration). The O2 to H2 ratio was then increased to trigger the operation of the cell. A small quantity of O2 was introduced into the microscope, leading to a total pressure of about 16 mbar at 600°C. At this point, the variation of voltage between the anode and cathode was correlated to the gas composition and the anode microstructure (see Figure 1 c-g). The latter was analyzed by means of conventional and high-resolution imaging, diffraction, and EELS (electron energy-loss spectroscopy). The system was cycled several times by decreasing and re-increasing the O2 concentration in the gas flow, and correlations between microstructure, gas composition, and cell voltage were established, as it will be discussed at the conference. Results were further confirmed by macroscopic ex situ tests in an oven using the same materials [1].

Conclusion

The operation of a SOFC in a single chamber configuration was demonstrated using operando ETEM. Such operando experiments open numerous perspectives to investigate the root cause of failure pathways affecting SOFCs, like poisoning of active sites or coarsening of the Ni catalyst [2].

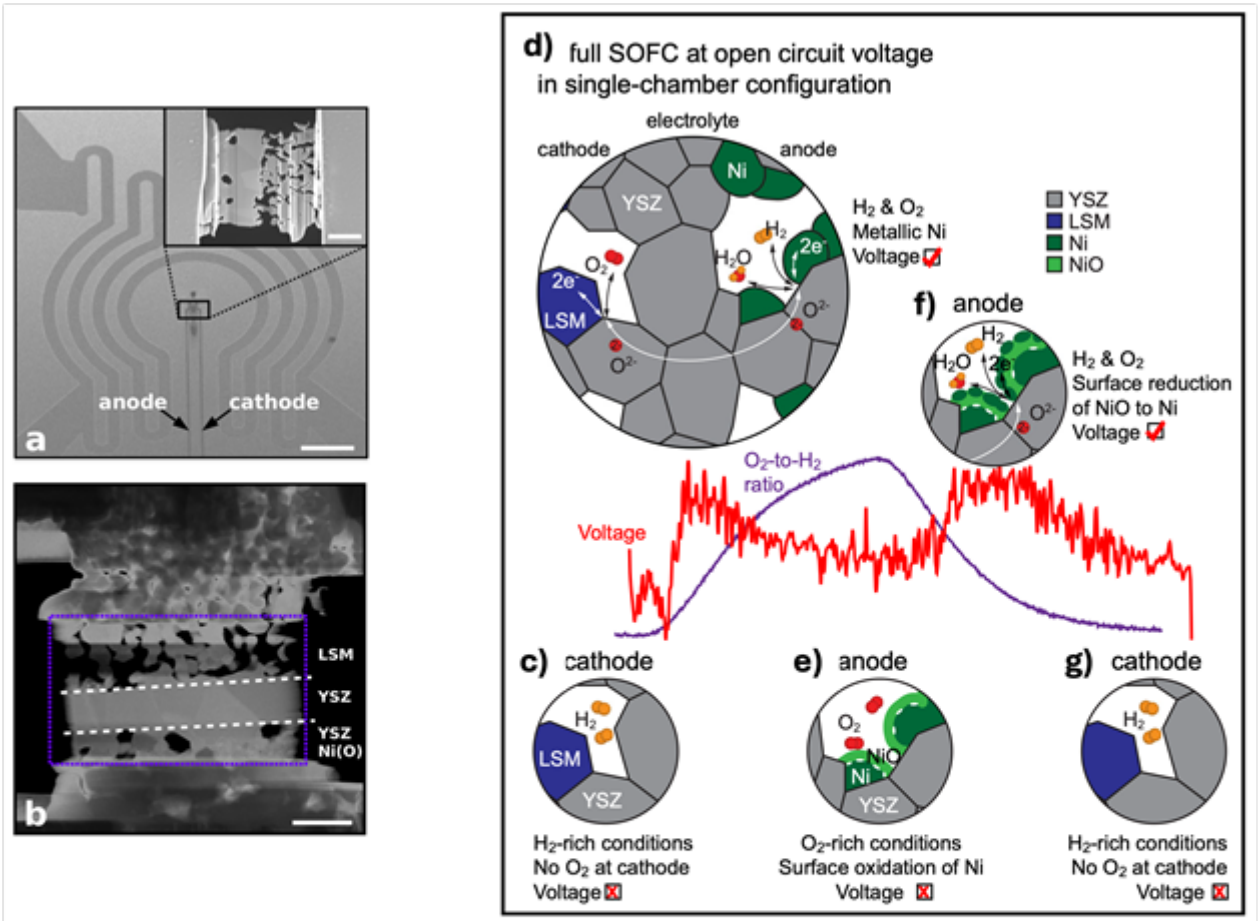

SOFC on MEMS chip. a) Secondary electrons SEM image of a biasing and annealing MEMS chip (DENSsolutions) for operando TEM, where the anode (Ni(O)-YSZ) and cathode (LSM) of the SOFC lamella (inset) are electrically connected to the biasing electrodes of the chip. Scale bar: 50 µm. b) STEM ADF of the electrically connected SOFC sample. Scale bar: 2 µm. **Schematic summary of the operation of the SOFC** in a single-chamber configuration as observed operando in the ETEM (c-g). a At low O2-to-H2 ratios, the absence of O2 prevents its reduction at the cathode. b When introducing O2, the cell starts to deliver a voltage synonym of its operation until (c) the surface of the Ni grains oxidises. d When decreasing the O2-to-H2 ratio, the surface of the NiO scale starts to reduce into Ni islands, re-initiating the oxidation of the fuel at the anode, which results in a voltage increase. e The process stops at low O2-to-H2 ratios (as in a). YSZ stands for yttria-stabilised zirconia, LSM for lanthanum strontium manganite.

Keywords:

SOFC, in situ, operando, ETEM

Reference:

[1] Q. Jeangros et al., Nature Communications 14 7959 (2023) https://doi.org/10.1038/s41467-023-43683-4

[2] The authors acknowledge the French microscopy network METSA for funding and the consortium Lyon-St-Etienne de microscopie for ETEM access. The FIB preparation was performed at the facilities for analysis, characterization, testing and simulations (FACTS, Nanyang Technological University). Additional support was provided by the INSTANT project (France-Singapore MERLION program 2019-2021) and the start-up grant M4081924 at Nanyang Technological University.

615

In-situ TEM Investigation of Degradation Process in Ni-Rich Cathodes.

Mr Ioannis Siachos[1,2], Dr Xiaodong Liu[1], Dr Annalena Genreith-Schriever[2,3], Dr Tingting Yang[4], Dr Penghan Lu[4], Prof. Rafal Dunnin-Borkowski[4], Prof. Clare Gray[2,3], Prof. Layla Mehdi[1,2]
[1]Department of Materials, Design & Manufacturing Engineering, University of Liverpool, Liverpool, UK, [2]The Faraday Institution, Harwell Campus, Didcot, Oxford, UK, [3]Department of Chemistry, University of Cambridge, Cambridge, UK, [4]Ernst Ruska-Centre for Microscopy and Spectroscopy with Electrons, Research Centre Juelich, 52425, Juelich, Germany

PS-04 (2), Plenary, august 26, 2024, 14:00 - 16:00

Background incl. aims
Lithium-ion batteries have become integral for energy storage in various applications, including electric vehicles, and portable electronics [1]. Cathode materials such as LiNi1−x–yMnxCoyO2 (NMC), LiNixCoyAl1−x−yO2 (NCA), LiCoO2 (LCO), and LiMn2O4 (LMO) are widely used [2]. However, challenges like fast capacity fade, high cost, and poor cycling performance persist. Layered LiNiO2 (LNO) shows promise but suffers from structural changes and oxygen evolution during cycling [3]. During cycling we can identify three distinct stages where, the layered O3 stacking sequence is reduced from trigonal structure with rhombohedral symmetry $R\bar{3}m$ to monoclinic C2/m, then into a layered mixture of O3 and O1 (H2-H3) stacking and further to a rocksalt phase ($Fm\bar{3}m$) [4]. Among all phases, the H2 to H3 transformation results in poor structural stability especially while operating at high voltages [5]. This study aims to investigate the degradation mechanism of LNO cathodes, focusing on its initial O3 stacking sequence.

Methods
The degradation dynamics of LNO cathodes were investigated using in situ electron microscopy, electron energy loss spectroscopy (EELS), and four-dimensional scanning transmission electron microscopy (4D-STEM). This degradation has been monitored in real-time, which traces for the structural changes taking place for Li+ diffusion and degradation taking place with the chemical composition. A constant potential of +4.3 V was applied and the first delithiation cycle was examined via in situ TEM. On the other hand, EELS contributed to valuable insights regarding the changes of chemical composition during cycling, while 4D-STEM aided in obtaining high-resolution images and analysis of diffraction in order to complete the characterization of structural transformations taking place within the material of the cathode.

Results
Observations revealed the layered structure of pristine LNO, with cation mixing layers rapidly forming new Ni-rich phases mixed with Li2O phase near the reaction front and pure NiO species further away. During the first delithiation cycle, expansion occurred as the particle was charged versus a Li metal source as the anode, resulting in increased c lattice parameters and phase transitions from H1 to monoclinic, then to H2 and H3 (representing collapse of the layered structure).

Conclusion
The study sheds light on the degradation mechanism of LNO cathodes with the O3 stacking sequence, elucidating structural and compositional changes during cycling. Future work will focus on comparing simulated and experimental phase reconstruction mechanisms from layered to spinel phases and investigating oxygen loss in LNO cathodes during cycling.

Keywords
Lithium-ion batteries, Ni-rich cathodes, degradation mechanisms, in situ TEM.

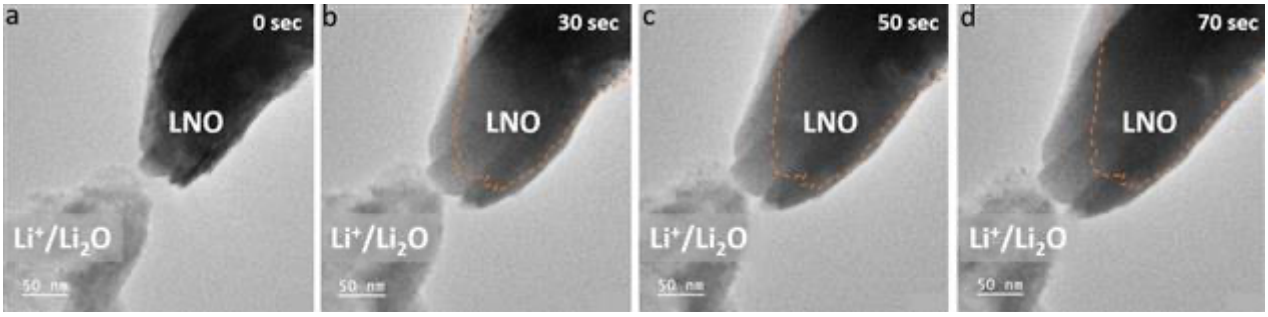

Keywords:

Lithium-ion, Ni-rich, degradation, in-situ TEM.

Reference:

[1] N Nitta et al, Materials Today 18 (2015), p. 252-264.
[2] M Radin et al, Advanced Energy Materials 7 (2017), p. 1602888.
[3] C Xu, Advanced Energy Materials 11 (2021), p. 2003404.
[4] I Seymour et al, Chemistry of Materials 27 (2015), p. 5550-5561.
[5] L de Biasi et al, ChemSusChem 12 (2019), p. 2240.

634

Atomic-resolution mapping of phonon modes across Magnéli structures in thermoelectric (Al,Nb)-doped TiO2

Dr Shihao Wang[1,2], Dr Demie Kepaptsoglou[1,3], Dr Jan Rusz[4], Dr Paul Zeiger[4], Dr Xiaodong Liu[5,6], Dr Robert Freer[6], Dr Quentin Ramasse[1,2]
[1]SuperSTEM Laboratory, STFC Daresbury Campus, Daresbury WA4 4AD, United Kingdom, [2]School of Chemical and Process Engineering, University of Leeds, Leeds LS2 9JT, United Kingdom, [3]Department of Physics, University of York, York Yo10 5DD, United Kingdom, [4]Department of Physics and Astronomy, University of Uppsala, P.O. Box 516, 75120, Uppsala, Sweden, [5]Department of Mechanical, Materials & Aerospace Engineering, University of Liverpool, Liverpool L69 3BX, United Kingdom, [6]Department of Materials, University of Manchester, Manchester M13 9PL, United Kingdom

PS-04 (2), Plenary, august 26, 2024, 14:00 - 16:00

Background incl. aims
Phonons play a critical role in many physical properties of a materials including their thermal and electrical conductivities. Changes in normal phonon mode frequencies occur in the presence of defects. In thermoelectric materials (TE), such defect-induced localised modification of the vibrational response is widely used to tailor the thermal conductivity [1]. In previous work [2,3] it was shown that atomic-level defect engineering resulted in the enhancement of the TE performance of (Al,Nb)-doped TiO2. The introduction of crystallographic shear (CS) structures leads to the reduction of lattice thermal conductivity, which is believed to occur through enhanced phonon scattering. Therefore, it becomes important to measure the spatial distribution and dispersion of the localized vibrational response across the CS structure, in order to gain insight into the heat-conduction process. Recent advances in scanning transmission electron microscopy (STEM) and electron energy-loss spectroscopy (EELS) have provided powerful and flexible tools to study phonons at high spatial resolution, down to single atom sensitivity [4]. In this work, we use STEM-EELS to probe the localised phonon response in CS structures at atomic resolution in the polar (Al,Nb)-doped TiO2.

Methods
EELS measurements were performed on a Nion UltraSTEM100MC ‘Hermes’ scanning transmission electron microscope, equipped with a Nion IRIS high energy resolution EELS spectrometer with a Dectris ELA direct electron detector. The acceleration voltage was 60 kV and the probe convergence semi angle was 31.5 mrad, resulting in a 1 Å probe size. The experimental optical geometry follows the conditions in Ref [4], in which the off-axis , or dark-field EELS (DF-EELS) geometry significantly reduces the contribution to the EELS signal of electrons having undergone delocalized dipole scattering, while promoting that of localized impact phonon scattering. This approach enables in principle single-atom sensitivity of phonon scattering.

Results
Fig. 1(a-b) shows a HAADF STEM image of the {120}-type CS structure in (Al,Nb)-doped TiO2 acquired along the [001] (rutile-equivalent) zone axis. The CS structure, which results in complex atomic lattice re-arrangements, is accompanied by the segregation of Al along the shear planes, with Al-rich columns preferentially occupying the Ti sites indicated by white arrows on Fig. 1b. Atomically resolved VEELS measurements performed across (Fig. 1(c-d)) reveal atomic scale variations localised at the CS structure boundaries. Changes in both the intensity and the frequency of the main modes are observed at the boundaries, with localised effects on the Al-rich columns. Results are discussed in context of the local structure and chemistry, determined at the same position through careful

chemical mapping, while phonon map simulations using the frequency-resolved frozen phonon multislice method [5] are used to rationalize the experimental findings.

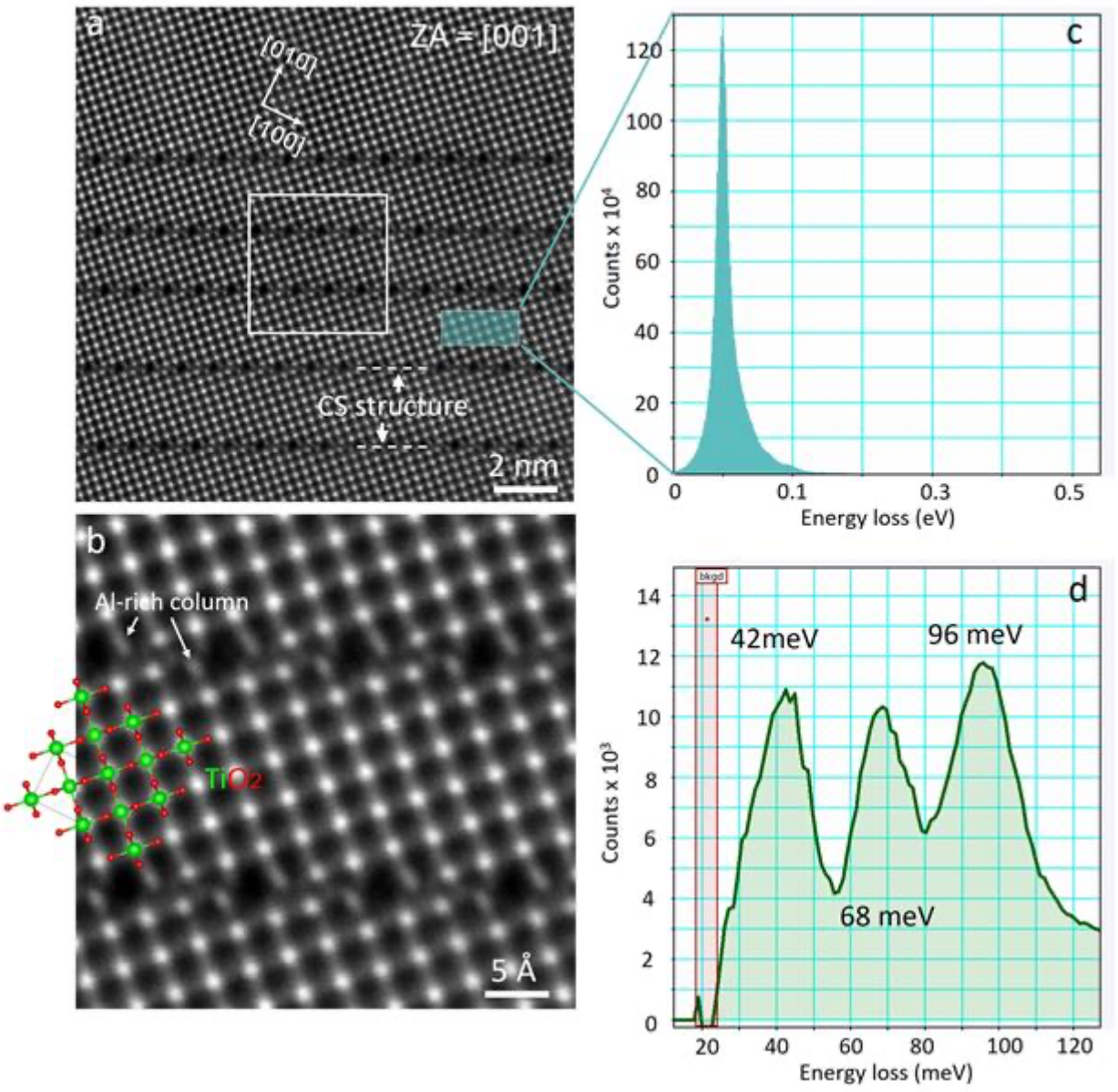

Keywords:

vibrational EELS, phonon, thermoelectric materials

Reference:

[1] D.G. Cahill, et al., Nanoscale thermal transport, J. Appl. Phys. 93 (2003) 793–818.
[2] X. Liu, et al., Controlling the Thermoelectric Properties of Nb-Doped TiO2 Ceramics through Engineering Defect Structures, ACS Appl. Mater. Interfaces. 13 (2021) 57326–57340.
[3] X. Liu, et al., High Power Factor Nb-Doped TiO2 Thermoelectric Thick Films: Toward Atomic Scale Defect Engineering of Crystallographic Shear Structures, ACS Appl. Mater. Interfaces. 15 (2023) 5071–5085.
[4] F.S. Hage, et al., Single-atom vibrational spectroscopy in the scanning transmission electron microscope, Science. 367 (2020) 1124–1127.
[5] P.M. Zeiger, J. Rusz, Efficient and Versatile Model for Vibrational STEM-EELS, Phys. Rev. Lett. 124 (2020) 25501.

699

Unveiling degradation mechanisms in layered Li-rich cathode materials using combined operando neutron diffraction and 4D-STEM

Dr. Tingting Yang[1], Maolin Yang[2], Zhongyuan Huang[2], Dr. Rui Wang[3], Peng-han Lu[1], Prof. Rafal Dunin-Borkowski[1], Dr. Lei Jin[1], Prof. Yinguo Xiao[2]
[1]Forschungszentrum Juelich, Juelich, Germany, [2]Peking University Shenzhen Graduate School, ShenZhen, China, [3]Department of Engineering, University of Cambridge, Cambridge, UK
PS-04 (2), Plenary, august 26, 2024, 14:00 - 16:00

Background incl. aims
Layered Li-rich nickel-cobalt-manganese (LRM) oxides are promising materials for applications as cathodes in next-generation high-capacity power batteries.[1] However, the commercialization of LRMs is challenging due to their cycling instability, which originates from their intrinsic structural characteristics and deterioration processes.[2] Until now, neither their structures, which can comprise two-phase nanocomposites or only single-phase solid solutions, nor their degradation pathways, have been clarified. It is noteworthy that existing studies are based on assumptions and inferences regarding the structure under specific conditions and do not truly reflect the actual structural evolution of LRM cathodes under operational conditions.[3-5] Moreover, due to the lack of systematic research on typical failure structures in LRM cathodes, the structural evolution throughout the entire lifecycle of LRM cathodes remains obscured. Therefore, it's of great importance to reveal the actual evolution process of the structure and the degradation mechanism of LRM cathodes unfer operational conditions comprehensively. The aim is to unveil initial lattice structure and the complete structural evolution process, encompassing transition metal rearrangement, phase structure evolution, defect structure growth, and ultimate structural failure, throughout the entire lifecycle of rich lithium manganese cathodes, with the hope of providing insights for the design of LRM materials.
Methods:
This study employs in operandon neutron diffraction technology with characteristics such as sensitivity to light elements and resolution of TMs. the study combines advanced pression-assisted 4D-STEM technology with comprehensive phase analysis capabilities, supplemented by atomic-resolution aberration-corrected electron microscopy (HAADF-STEM), focusing on both short and long-range structures of LRM cathode materials.
Results:
In this work, We prepared a LR-NCM | graphite full cell and carried out both in operando neutron diffraction and low dose and precession-assisted 4D-STEM to map spatially-averaged structural evolution in real time over a large field of view and visualize light (O, Li) and heavy (TM) atoms simultaneously with atomic spatial resolution before, during and after cycling. Our work provides detailed insights into dynamic nanostructure evolution and local structural interactions through multiscale characterizations. The structure of pristine LRM is demonstrated to be a solid solution based on C2/m symmetry, resembling a thin layer of spinel. In the initial cycling, irreversible extraction of Li ions from the transition metal layers leads to the formation of vacancies within the layers, causing irreversible structural transformations within the material. The in operando neutron diffraction technique further tracks the formation of oxygen vacancies after the first discharge. Despite surface coating with a spinel layer to prevent oxygen loss, the effectiveness is limited. In subsequent extended cycles, continuous loss of excess Li ions and migration of TMs within the layers

result in the irreversible transformation of the internal structure from a lithium-rich phase to a conventional layered phase. This transformation leaves numerous vacancies within the layers, leading to the formation of internal nanoscale defects. These defects obstruct the channels for Li-ion transport within the layers, consequently causing a decline in material performance.

Conclusion:

Our work provides a new perspective on material failure mechanisms, emphasizing the importance of intrinsic modification methods in stabilizing the internal structure of layered high-energy cathodes, beyond conventional surface modifications.

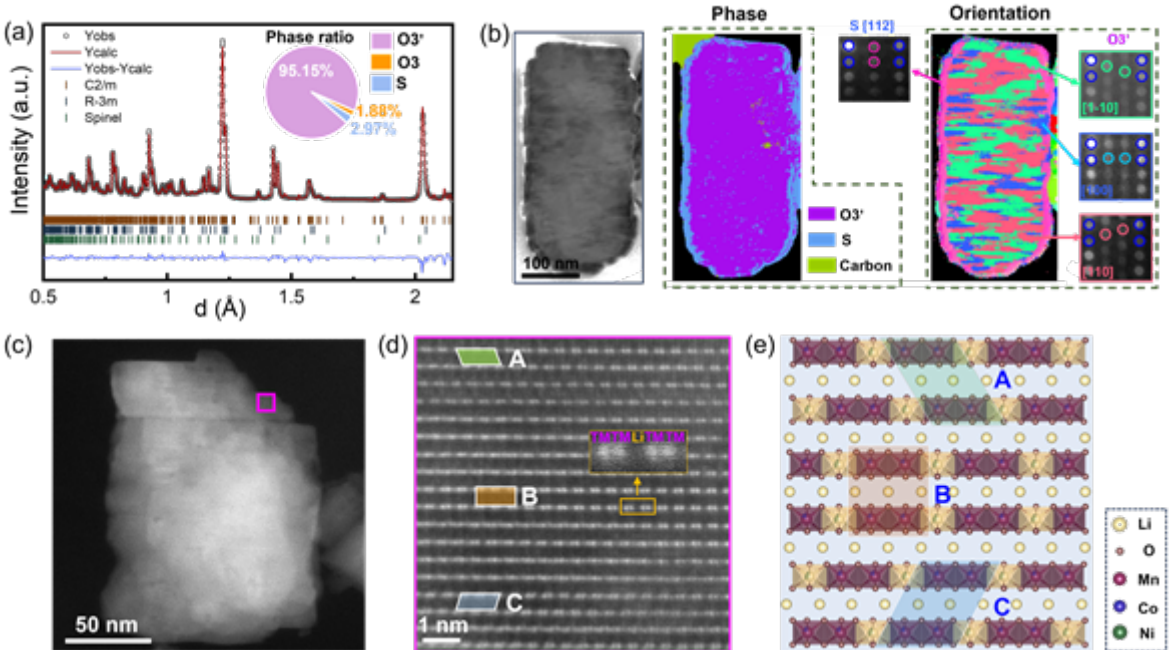

Keywords:

Degradation-mechanism, Li-rich cathode, neutron-diffraction, 4D-STEM

Reference:

[1] P. Rozier, J. Tarason, J. Electrochem. Soc. 162 (2015) A2490−A2499.
[2] L. Côrrea, E. Ortega, A. Ponce, et.al, arXiv preprint arXiv:2301.10286 (2023).
[3] R.A. House, G.J. Rees, M. Perez-Osorio, et.al, Nat. Energy 5 (2020), 777-785
[4] J.Huang, B.Ouyang, Y. Zhang, et.al, Nat. Mater. 22 (2023), 353-361.
[5] P. Pearce, A. Perez, G. Rousse, et.al, Nat. Mater. 16 (2017), 580-586.

157

Unique in-situ characterization workflow of Cathode Components using AFM-in-SEM

Veronika Hegrova[1], Mr. Radek Dao[1], Dr. Vojtech Schanilec[1], Dr. Jan Neuman[1]
[1]NenoVision s. r. o., Brno, Czech Republic

PS-04 (3), Plenary, august 27, 2024, 10:30 - 12:30

Background incl. aims
As the demand for efficient and sustainable energy storage solutions grows, a lot of effort is dedicated to comprehending the battery components' functionalities. Not only exploring new configurations but also new materials are essential for improved efficiency, safety, lifetime, etc. of the new-generation lithium-ion batteries [1]. However, such materials require precise sample surface preparation and handling to avoid unwanted reactions or surface changes which then influence understanding of the battery component features.
Methods
In this work, we focus on the in-situ study of Cathode Active Materials (CAM) and present a unique measurement workflow that preserves the sample surface from oxidation without compromising sample preparation quality, moreover, enabling valuable insights into chemical and electrical properties. The CAM tape samples are prepared in a glovebox on a proper holder, cross-sectioned using Broad Ion Beam (BIB) polishing, and further moved to the Atomic Force Microscope in a Scanning Electron Microscope (AFM-in-SEM) for electrical and chemical characterization. The sample transfers between all instruments are realized using a safe sample transfer system under a controlled environment, so the sample is never exposed to air or humidity, and thus, the surface remains clean and preserved from chemical reactions.
Results
With such a workflow, we studied Nickel-Cobalt-Manganese (NCM) tape with solid electrolyte, see Fig. 1. We determined the electronic conductivity using Conductive AFM (C-AFM) and distinguished the individual elements using Energy Dispersive X-ray Spectroscopy (EDS), all under in-situ conditions. We see that the NCM grains are well conductive, while the solid electrolyte remains non-conductive, which is correct, as the solid electrolyte only has an ionic conductivity (the dark part of Fig. 1c). The most conductive seems to be the secondary particles interface (the brightest part of Fig 1c), which perfectly correlates to the carbon additive observed in EDS map (Fig. 1a). Such precision would be unlikely possible or very challenging without the in-situ analysis.
Similarly, we observed a CAM tape with different grains, Nickel-Cobalt-Aluminum (NCA) and NCM, in a liquid electrolyte. The connection of the EDS map with electronic C-AFM shows that the conductivity of the grains differs 1000 times. From understanding such grains and their conductivity, the difference should be much lower. As we see in the SEM image, the NCM grain had probably been delaminated from the collector, and the conductive connection with the NCM particle was established via the inter-particle interface through the NCA particle.
Conclusion
These results emphasize the need for advanced measurement workflow and instrumentation, which could greatly help in understanding the cycling effects, durability, or lifetime of both primary and secondary particles of battery components. The above-mentioned characterization workflow is convenient, time-efficient, and suitable for a proper understanding of failure analyses and quality control of the battery components. Our findings were obtained using AFM LiteScope, which is compact enough to be used in SEM, in this case, Helios 5 Hydra DualBeam, CleanMill for fine polishing, and CleanConnect for sample transfer [2].

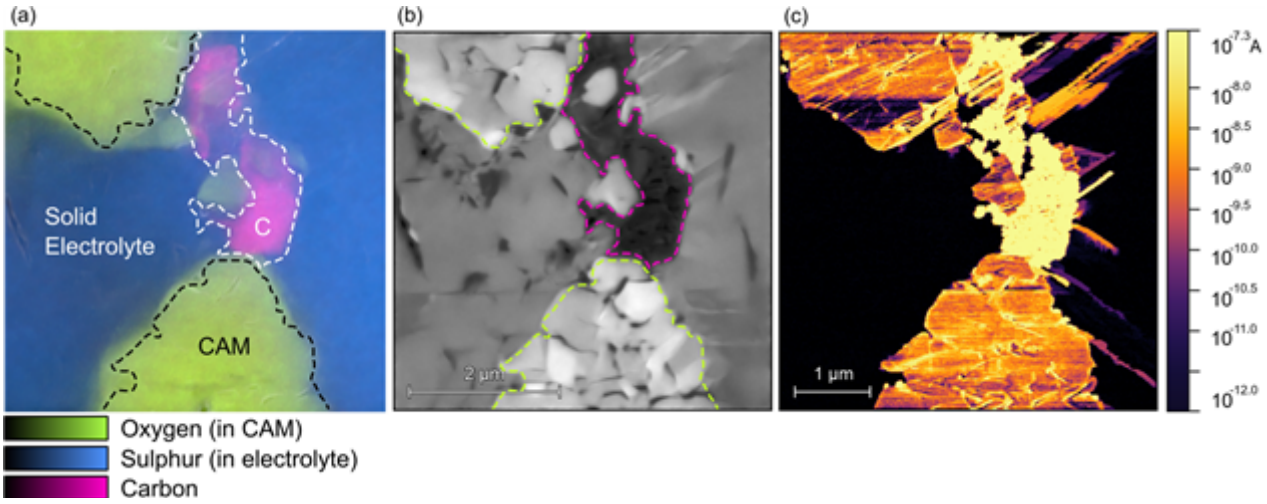

Keywords:

in-situ, batteries, AFM, SEM, conductivity

Reference:

1. Itani, Khaled, and Alexandre De Bernardinis. "Review on New-Generation Batteries Technologies: Trends and Future Directions." Energies 16.22 (2023): 7530.
2. We would like to thank Libor Novák and Petr Zakopal from Thermo Fisher Scientific for their assistance with sample surface preparation.

437

Unraveling the original dissolution mechanism of LiFePO4 when treated for recycling

Dr. Adrien Boulineau[1], Julie Poulizac[1,2], Dr. Emmanuel Billy[1], Pr. Karien Masenelli-Varlot[2]
[1]Univ. Grenoble Alpes, CEA, LITEN, Grenoble, France, [2]Univ. Lyon, INSA Lyon, UCBL, CNRS, MATEIS, Villeurbanne, France

PS-04 (3), Plenary, august 27, 2024, 10:30 - 12:30

Background incl. aims
This presentation aims at demonstrating the original mechanism involved during the acid leaching treatment of the very common material used in Li-ion batteries, LiFePO4. Such treatment is the basis of the hydrometallurgical process used for recycling the material and the understanding of the chemical reactions involved is critical to optimize the recycling process. To date and to our knowledge, such a mechanism established thanks to advanced TEM experiments among which operando liquid TEM and STEM EELS for phase mappings has never been highlighted.

Methods
We first carried out operando liquid TEM experiments to follow the evolution of the shape of the particules and to see if the dissolution process was monotonous or composed of severals growth and dissolution steps. Ex situ characterisations on materials residues recovered from partial dissolutions, including HRTEM imaging and STEM-EELS experiments, were then performed. They enabled the identification of the phases and their localisation. All the results are finally correlated and confronted to global chemical and structural analyses by the means of ICP-MS and XRD experiments.

Results
Operando liquid TEM experiments are demonstrating a monotonous dissolution process without any reprecipitation or growth of particles. Moreover as already reported by us [1], it was possible to show the kinetic observed operando was comparable with the one deduced from ex-situ dissolution experiments. Ex-situ XRD analyses are evidencing a rather quick formation of crystallites composed by the FePO4 phase with still the presence of the pristine LiFePO4 one. Discriminating both phases is a challenge but STEM-EELS and HRTEM analyses enabled to prove the coexistence of both phases into the same particles and they demonstrate that a core-shell type or shricking-core mechanism does not occur as it is usually observed during such reactions.

Conclusion
During this talk we are presenting the original dissolution mechanism that is based on the tranformation from monocristalline LiFePO4 particles toward polycrstalline FePO4 ones separated by LiFePO4 residues. We demonstrate the evolution occurs into the same particules without any nucleation of new particules. Then, this is the level of pH that is governing the continuous dissolution process or its interruption. This study is of importance since it allows process optimization. It is also of great interest on a fundamental aspect since we demonstrate the generation of particles where the LiFePO4 and FePO4 phases coexist. Such phenomenon is not really expected when we know the bahavior of the material that is always presenting monophased particles when used in a li-ion battery [2,3].

Keywords:

Operando-liquid-TEM, HRTEM, EELS, LiFePO4.

Reference:

[1] J. Poulizac, A. Boulineau, E. Billy, K. Masenelli-Varlot, Microscopy and Microanalysis, Volume 29, Issue 1, February 2023, Pages 105–117.
[2] C. Delmas, M. Maccario, L. Croguennec, F. Le Cras, F. Weill, Nature materials 7, issue 8, pages 665-671.
[3] V. Srinivasan, J. Newman, J. Electrochem. Soc., 2004, 151,A1517–A1529.

616

Identification of Chemical Segregation and Surface Twinning Structures in Electro-deposited Al Dendrites

Dr Xiaodong Liu[1], Dr Fatemehsadat Rahide[2], Dr Tingting Yang[3], Dr Penghan Lu[3], Dr Sonia Dsoke[2,4,5], Dr Helmut Ehrenberg[2], Professor Rafal E Dunin-Borkowski[3], Professor Layla Mehdi[1,6]
[1]Department of Materials, Design & Manufacturing Engineering, University of Liverpool, Liverpool, UK, [2]Institute for Applied Materials, Karlsruhe Institute of Technology, Eggenstein-Leopoldshafen, Germany, [3]Ernst Ruska-Centre for Microscopy and Spectroscopy with Electrons, Research Centre Juelich, Juelich, Germany, [4]Department of Sustainable Systems Engineering, Albert-Ludwigs-University of Freiburg, Freiburg, Germany, [5]Fraunhofer Institute for Solar Energy Systems, Department of Electrical Energy Storage, Freiburg, Germany, [6]Albert Crewe Centre, University of Liverpool, , UK

PS-04 (3), Plenary, august 27, 2024, 10:30 - 12:30

Background incl. aims
Lithium-ion batteries (LIBs) dominate the industry, but limited lithium supplies and safety concerns with their electrolytes push the search for alternatives. Rechargeable aluminium batteries (RABs) are promising among post-lithium battery chemistries, which exhibit considerable potential as candidates for future applications due to the low cost of component materials and excellent theoretical energy density. Most research on aluminium batteries (AlBs) has focused on enhancing cathode materials [1] and ionic liquid electrolytes [2], overlooking attention to Al anodes [3]. It is crucial to note that the inherent metallic nature of aluminium increases susceptibility to dendrite formation during reversible plating and stripping processes [4]. Dendrites pose safety risks by breaching separators, leading to anode disintegration and cell failure. Uneven Al deposition, resulting in dendrite formation, can cause cell short circuits, particularly under repeated cycling at high capacities [5]. Therefore, it is of great importance to obtain in-depth understanding of the Al dendrite growth mechanism to increase battery safety. Multiple approaches were adopted to restrain the Al dendrite growth and identify the dendrite growth mechanism. Whilst most studies are preferred to reveal the mechanisms from the perspective of electrochemistry, electron microscopy is able to provide more straightforward approaches from crystallographic perspectives to understand the dendrite growth mechanism.

Methods
Chronoamperometry (CA) was performed to electroplate Al on Al foil from the [EMImCl]/AlCl3 electrolyte. The electrodeposited Al dendrite morphology was observed by a ThermoFisher Helios 5CX FEG FIB-SEM. The grain growth and orientation of the dendrite were determined by Transmission Kikuchi Diffraction (TKD) techniques, using an Oxford Instrument Symmetry S3 Electron Backscatter Diffraction (EBSD) detector. The scanning transmission electron microscopy (STEM) and corresponding EDX elemental analysis were carried out using a ThermoFisher Scientific Spectra 300 aberration-corrected microscope, operated at 200kV. Samples for STEM were fabricated by the ThermoFisher Helios 5CX FIB.

Results
In this work, we employed Focused Ion Beam-Transmission Kikuchi Diffraction (FIB-TKD) and STEM techniques, to investigate the crystallographic structure of the Al dendrite and the chemical species formed during the Al-dendrite growth. Figure 1 shows a tree-shaped Al dendrite, with clear primary dendrite feature and secondary dendrite arms. The corresponding STEM EDX and FIB-TKD maps from the cross sections parallel and perpendicular to the growth direction enable us to identify the chemical segregation inside the dendrite and the grain growth along the dendrite. In combination

with the detailed aberration-corrected STEM images and the corresponding spectroscopy study, we are able to determine the detailed chemical species inside the dendrite arms and thereby investigate how they affect the Al dendrite growth, including growth orientation and preference.

Conclusion

This investigation provides new understanding of Al dendrite growth and offers insight into the reaction mechanism between the Al and electrolyte, which could guide the future development of new rechargeable Al batteries.

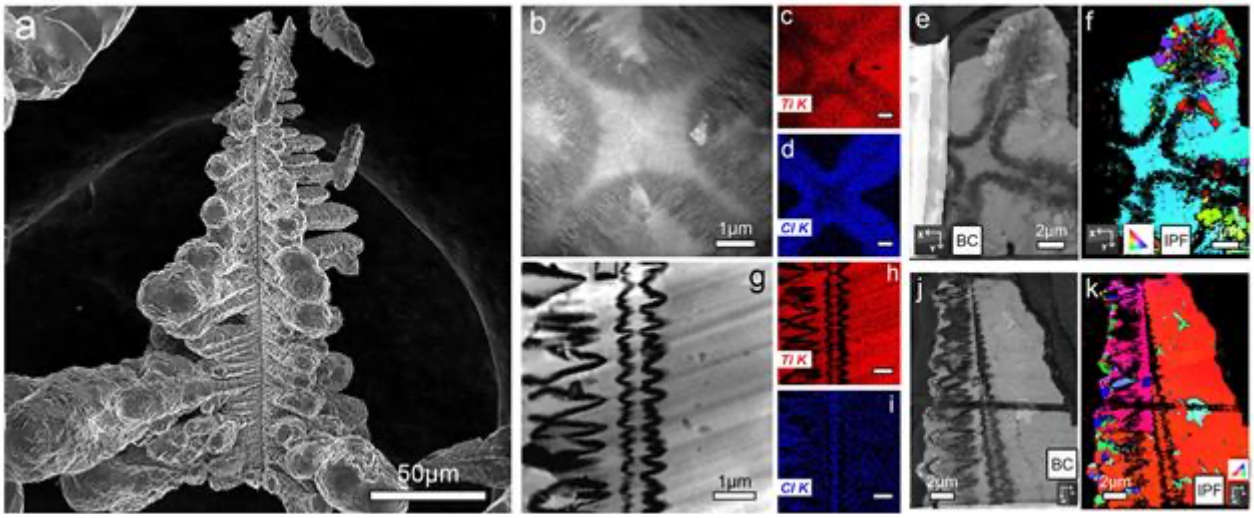

Keywords:

Dendrite; Aluminium battery; TEM; TKD.

Reference:

[1] G.A. Elia et al. Advanced Materials, 28(2016), p. 7564–7579.
[2] M. Angell et al. PNAS, 114(2016), p. 834–839.
[3] M. Jiang et al. Advanced Materials, 34(2022), p. 2102026.
[4] E. Berretti et al. Materials, 9(2016), p. 719.
[5] J. Zheng et al. Nature Energy, 6(2021), p. 398–406.

622

Stability insights of MnO2 electrocatalysts from identical location and in-situ electrochemical liquid cell electron microscopy

Dr. Raquel Aymerich Armengol[1], Lau Morten Kaas[1], Alba Bech Larsen[1], Marika Birkedal Norby[1], Christian Danvad Damsgaard[1,2], Peter Christian Kjærgaard Vesborg[1], Jakob Kibsgaard[1], Stig Helveg[1]
[1]Center for Visualizing Catalytical Processes (VISION), Technical University of Denmark (DTU), Kongens Lyngby, Denmark, [2]Nanolab, Technical University of Denmark (DTU), Kongens Lyngby, Denmark

PS-04 (3), Plenary, august 27, 2024, 10:30 - 12:30

Background incl. aims
Electrocatalysts require high activity as well as long-term stability to ensure their practical and economic viability. Nevertheless, although critical, the stability consideration is oftentimes overlooked in research[1]. For instance, manganese dioxides are considered promising electrocatalysts to substitute expensive noble metals due to their high abundance, low price and oxygen evolution reaction (OER) activity. However, their electrochemical and structural stability during operation is still controversial[2]. Herein, we will address the stability of MnO_2 using identical location (IL-EM) and electrochemical liquid phase electron microscopy (ec-LPTEM), which offer an excellent platform to investigate the electrocatalysts performance in-situ[3].

Methods
The structure and morphology evolution of the MnO_2 electrocatalysts are characterized using SEM and (S)TEM imaging and associated spectroscopy techniques such as EDS and EELS in ex-situ, in identical locations and in-situ in ec-LPTEM. This combination approach allows the dynamic study of structural changes within the liquid as well as the effects of longer electrochemical operation.

Results
Our results address the debated existence of a stability window for the operation of MnO_2 catalysts for the acidic OER. Measurements based on IL-EM and ec-LPTEM are presented on the specific potential range and conditions of operation within the stability of the catalyst. Beyond the stability window, the structural evolution of the catalyst from its synthesis will be directly correlated through time-resolved imaging to the electrochemical stability during OER operation to resolve mechanisms governing the catalyst instability.

Conclusion
We present a thorough study addressing the growth and electrochemical and structural stability of MnO_2 electrocatalysts for the acidic OER using IL-EM and ec-LPTEM. Such results are key for the design of durable non-noble electrocatalysts.

Keywords:

IL-(S)TEM, ec-LPTEM, in-situ, electrocatalysis, stability

Reference:

0 The Center for Visualizing Catalytic Processes is sponsored by the Danish National Research Foundation (DNRF1462)
1 Hochfilzer et al., ACS Energy Lett. 2023, 8, 3, 1607–1612
2 Li et al., Angew. Chem. Int. Ed. 2019, 58, 5054.
3 Shen et al., Acc. Chem. Res. 2023, 56, 21, 3023–3032

662

Analyzing Lithiation Dynamics in LiFePO4 Cathode : Insights from TEM Experiments and Phase Field Modeling

Ahmed Yousfi[1], Justine Jean[1], Kevyn Gallegos Moncayo[1], Florent Magaud[1], Guillaume Boussinot[2], Arnaud Demortière[1]
[1]Laboratoire de Réactivité et Chimie des Solides(LRCS)/Centre National de Recherche Scientifique(CNRS)/Université de Picardie Jules Verne(UPJV)/RS2E, Amiens, France, [2]Access e.V Institute, Rheinisch-Westfälische Technische Hochschule (RWTH) Aachen University, Aachen, Germany

PS-04 (3), Plenary, august 27, 2024, 10:30 - 12:30

Lithium-ion batteries have revolutionized the field of portable electronics and electric vehicles by providing efficient and compact energy storage solutions. Despite advancements, several challenges continue to persist, such as limited battery lifespan, capacity degradation, and safety concerns. To address these issues and gain deeper insights into the underlying mechanisms, we present a comprehensive study involving an electrochemical liquid cell for in situ transmission electron microscopy (TEM) experiments. The utilization of the Dark Field technique (Figure 1) in this device enables us to directly observe the lithiation/delithiation process [1]. Through electron diffraction, we can track the modification of lattice parameters induced by the lithiation process.

In this study, we can observe the dynamic evolution of the delithiation interface between the LiFePO4 (LFP) and FePO4 (FP) phases inside a single crystal. This real-time monitoring provides valuable insights into the fundamental processes occurring during charge and discharge cycles. Additionally, we aim to evaluate the local displacement field extracted from the 4D-STEM ACOM (Acquisition of Crystal Orientation Maps) datasets [2-4]. Indeed, the lithiation process induces modifications in the lattice parameters of the FePO4 host, necessitating the calculation of the symmetric strain tensor at the LFP/FP interface and the estimation of the elastic free energy density. By integrating 4D-STEM data treatments and analysis, we can accurately characterize the strain distribution and its influence on the phase transformation dynamics.

To gain a comprehensive understanding of the lithiation/delithiation dynamics and further elucidate the underlying mechanisms, we employ phase field model to simulate the diffusion phenomena. The phase-field model has proven to be a powerful tool for studying phase transformations and microstructure evolution in materials. Here, we use an Allen-Cahn type phase-field approach to investigate the phase transition from LiFePO4 to FePO4 cathode crystals in the presence of Li-ion chemical potential difference with the surrounding liquid electrolyte. The solid-solid phase boundary between LFP and FP phases modeled as a diffuse interface of finite width [5], and its motion is implicitly governed by the phase-field variable. We numerically solve a set of partial equations describing the temporal evolution of the phase-field variable and the chemical potential [6, 12]. By incorporating the real particle morphology, obtained by TEM imaging, and considering the smoothed boundary method (SBM) [10], our phase field model provides a more realistic representation of the lithiation/delithiation dynamics within LiFePO4 crystals.

Initially, we employ a simple 2D model incorporating the chemical free energy and the interfacial free energy with a double-well potential approach [7]. By studying the kinetics of the lithiation/delithiation process within the LFP particle, which follows a one-dimensional Li-ion diffusion path, we observe two distinct regimes known as Surface Reaction Limited (SRL) and Bulk Diffusion Limited (BDL), as described in [8]. Our simulations are obtained by varying a kinetic

parameter l in our equations, this parameter is inversely proportional to the net rate of insertion R that we find in [11].
Furthermore, we extend our model by incorporating the elastic free energy to consider its influence on the phase growth direction and shape during the LFP/FP phase transition [9] within a realistic LiFePO4 single particle morphology. The elastic properties are adjusted using strain maps based on 4D-STEM data treatments and adaptative diffraction image registration.

In conclusion, this research explores the Li-ion insertion (or extraction) mechanisms into (or from) LiFePO4 crystals using in situ TEM experiments combined with phase-field simulations. The correlation between the phase-field model and the 4D-STEM results provides valuable insights into the complex dynamics of phase transformations and microstructure evolution, contributing to the understanding of key factors affecting the performance and lifetime of Li-ion batteries. Our approach contributes to the elucidation of the intricate process that drives the dynamics of lithiation inside individual cathode materials during the electrochemical process.

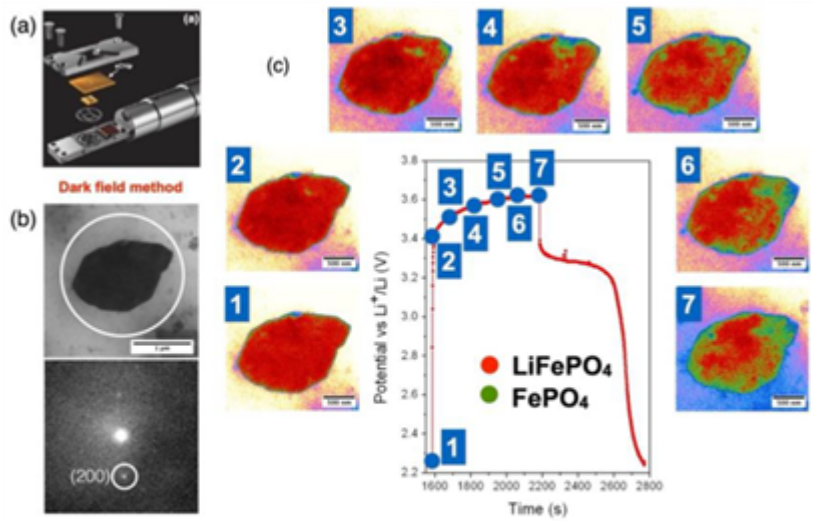

Figure 1: (a) In situ liquid electrochemical TEM cell. (b) TEM image of LFP single crystal surrounded by a liquid electrolyte. Electron diffraction pattern with (200) spot selected for the Dark Field imaging. (c) In situ monitoring of delithiation process in Li_xFePO_4 using Dark Field image (TEM).

Keywords:

Phase-field model, Allen-Cahn, LiFePO4, 4D-STEM

Reference:

[1] O. M. Karakulina, et al. J. Nano letters, 18(10) (2018), p. 6286-6291
[2] A. Bhatia, et al. Small Methods, 6 (2022), p. 2100891
[3] N. Folastre, et al. Microscopy and Microanalysis, 27 (2021), p. 3446-3447
[4] A. Gomez-Perez, et al., Microscopy and Microanalysis, 27 (2021), p.2234-2235
[5] M. Fleck, et al. Computational Materials Science, 153 (2018), p. 288-296
[6] N. Moelans et al. Computer Coupling of Phase Diagrams and Thermochemistry, 32 (2008), p. 268-294
[7] S. Daubner, et al. Physical Review Materials, 5 (2021), p. 035406
[8] L. Hongn, et al. Npj computational materials, 5 (2019), p. 118
[9] M. Tang, et al. The Journal of Physical Chemistry, 115 (2011), p. 4922-4926.
[10] Yu Hui-Chia, et al. Modelling Simul. Mater. Sci. Eng. 20 (2012) 075008 p. 41.
[11] G. K. Singh, et al. Electrochemica Acta, 53 (2008), 7599-7613
[12] A. Yousfi et al., Microscopy and Microanalysis, 29, (2023), 678-679

772

Microstructural Influence on Sodium Filament Growth in All Solid-state Batteries

Dr. Ziming Ding[1], Dr. Yushu Tang[1], Till Ortmann[2], Dr. Janis Kevin Eckhardt[2], Dr. Marcus Rohnke[2], Dr. Georgian Melinte[1], Prof. Dr. Christian Heiliger[2], Prof. Dr. Jürgen Janek[2], Prof. Dr. Christian Kübel[1,3]
[1]Institute of Nanotechnology (INT), Karlsruhe Institue of Techonology (KIT), Karlsruhe, Germany, [2]Institute for Physical Chemistry and Center for Materials Research, Justus Liebig University Giessen, Giessen, Germany, [3]Karlsruhe Nano Micro Facility (KNMF), Karlsruhe Institute of Technology (KIT), Germany

PS-04 (3), Plenary, august 27, 2024, 10:30 - 12:30

Background incl. aims
All solid-state batteries (ASSBs) using metal anode (e.g. lithium and sodium) are projected to possess high energy and power density and avoid the fire risk of liquid electrolyte counterparts. However, few commercial ASSBs working at room temperature are reported due to sluggish kinetics and severe solid-solid interfacial problems. Among various interfacial problems, the dendritic growth potentially leading to cell failure cannot be yet avoided through the high elastic modulus of solid electrolytes (SEs) as initially expected for ASSBs. Apart from the mechanical property of grain boundaries (GBs), their electronic properties are also expected to be responsible for lithium filamentary dendrite growth and penetration in the SEs. Although this intergranular growth mechanism in inorganic SE based lithium ASSBs is well studied, there is still much to be learned for sodium ASSBs. Especially, anisotropic Na+ ion transport presented in grain bulk of the well-known Na superionic conductor (NaSICON) (e.g. Na3Zr2Si2PO14) even with 3D transport path, not to speak of Na-β''-alumina with layered crystal structure and 2D transport path. Its contribution to the overall Na+ ion transport and the sodium filament growth, for instance, at GBs is still unclear.
Methods & Results
Due to the outstanding stability to Na metal, we used polycrystalline Na-β''-alumina SE (Ionotec. Ltd, UK) as a model material to investigate the microstructural impact on the sodium filament growth. A transmission electron microscopy (TEM) suitable Cu | Na-β''-alumina | Au(Pt) multilayer system was prepared with a focused ion beam (FIB) (FEI Strata 400S) equipment. The electric bias was applied on this system through a scanning tunneling microscopy (STM) nanotip (ZEPtools Technology Company) as schematically illustrated in Figure 1a - b. Na+ ion transport can be prompted by the biasing from the Na-β''-alumina towards the Au/Pt layer and cathodic deposition of sodium occurred at the interface between Na-β''-alumina and the Au/Pt layer in a transmission electron microscope (ThermoFischer Scientific Themis Z). Time-series scanning transmission electron microscopy (STEM) imaging (Figure 1c – f) was used to record the morphological changes e.g. filament growth at the interface between the SE and electrode as well as at the GB. In addition, to build a direct correlation between the filament growth and microstructure, automated crystal orientation mapping (ACOM) by precession electron diffraction-assisted 4D STEM (Figure 1g) was conducted across the polycrystalline Na-β''-alumina specimen. It revealed randomly oriented crystals distributed in the polycrystalline Na-β''-alumina mostly connected by random HAGBs, but hardly any coincidence site lattice boundaries have been observed. Furthermore, since the Na+ ion transport can be different in the grains due to the distinctive orientation of the Na+ ion conduction planes and the external electric field, the GB behavior can also be different as the schematic illustration in Figure 1h for corresponding types. In this case, the filament growth occurred at the GB, which can block the ion transport due to the anisotropic character as shown in Figure 1g.
In addition, significant electron beam effects have been excluded by blank beam reference experiments and sodium filament formation has further been confirmed by post-mortem secondary ion mass spectrometry (SIMS) studies. Moreover, the observed microstructure has been used to

simulate the anisotropic Na+ ion transport in the Na-β''-alumina. This helps to understand sodium filament formation and how a critical filament network might form leading to the failure of the battery.

Conclusion

In our study, the relationship between the microstructure and sodium filament growth as well as Na+ ion transport was explored through a crystal orientation analysis. Moreover, sodium filament growth occurred at random HAGBs. The anisotropic ion transport can contribute to the Na+ ion transport blockage of GBs. This blockage at GBs seems to facilitate formation of sodium filaments. Therefore, the microstructure including GB types and orientation should be taken into account for optimizing oxide based SE performance both in terms of sodium filament formation as well as overall ionic conductivity.

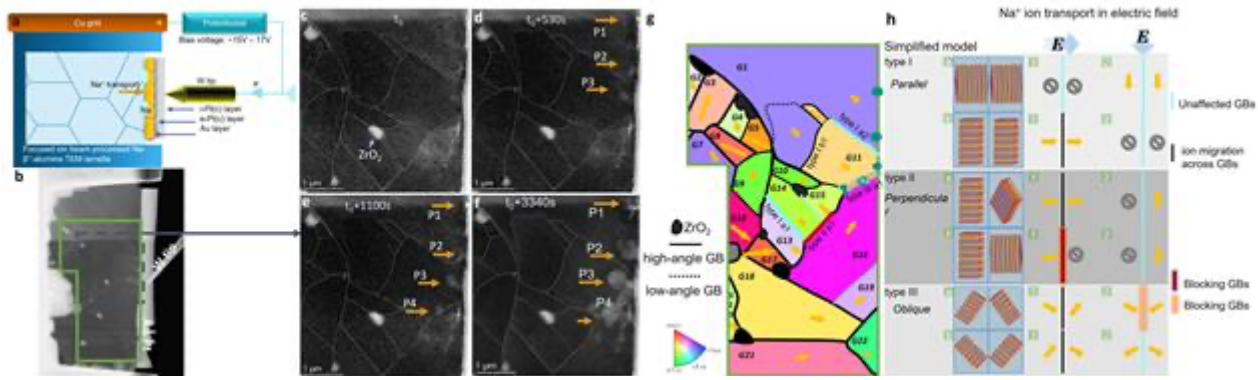

Keywords:

solid electrolytes, microstructure, filament growth

154

Oxidation states of IrOx characterised by EELS and ED-PDF

Dr. Trung-Dung Tran[1,2], Mr. Dogan Ozkaya[1,2]
[1]Johnson Matthey Technology Centre, Reading, UK, [2]ePSIC, Diamond Light Source, Didcot, UK
PS-04 (4), Plenary, august 27, 2024, 14:00 - 16:00

Background incl. aims
The global interest in hydrogen as a primary fuel has been fostering fundamental research of IrOx (Iridium oxide) - the most stable catalyst known for water-electrolysis to produce hydrogen. The presence of Ir(IV)/Ir(III) redox coupling is crucial for Oxidation Evolution Reaction (OER) activity of IrOx while metallic Ir only plays a little role in the aspects of stability and conductivity [1,2]. However, spatial distribution of Ir(III) with respects to Ir(IV) in IrOx catalysts has never been demonstrated previously. This kind of distribution would not only be a clear picture showing how Ir(III) can work together with Ir(IV) in an active and stable catalyst but also provide guidance for chemical engineering in tuning the oxidation state configuration for higher performance-to-mass ratio of the catalyst material.

Methods
In this talk, we will present the oxidation states of IrOx characterised by STEM-based EELS and Electron Diffraction based Pair Distribution Function (ED-PDF). The EELS method is based on measuring the profiles of electronic excitations from 5p and 4f to 5d and above the Fermi level (O and N edges). The EELS experiments were designed to minimise the effect of thickness variation (that can alter the plasmonic background) while improving signal/noise and energy resolution for detailed electronic-structure profiles.
Beside EELS, Electron diffraction pair distribution function (ED-PDF) [3] is another capable technique for characterisation of Ir-O bonding and IrOx atomistic structures, especially amorphous IrOx [4].

Results
O&N-edge profiles for different Ir oxidation states are shown in Figure 1(a). As shown in Figure 1(b), the microscopic distribution of Ir(IV), Ir(III) and Ir-metal can be mapped thanks to the differences seen in the corresponding O&N-edge profiles. Complementary to the Ir O&N-edges, EELS of O K-edge can give information about the atomistic structures of different IrOx phases. Figure 1(c) shows that amorphous IrOx, hollandite-type IrOx and the rutile-type structure of IrO2 can be distinguished clearly by the hybridisation profile in the O K-edges.
Ir-oxide (both amorphous and crystalline) and Ir-metal can also be characterised by ED-PDF. Figure 1(d) shows different distribution profiles of interatomic distances (particularly Ir-O bonds and Ir-Ir metallic bonds) for rutile-type IrO2, amorphous IrOx and Ir-metal.

Conclusion
This work shows the powerful capability of EELS and ED-PDF for characterisation of IrOx. The importance of EELS combined with EDPF will also be discussed in the presentation.

Figure 1. (a) EELS O&N-edges of different Ir oxidation states; (b) EELS mapping of Ir(IV), Ir(III) and Ir(0)-metal; (c) EELS O K-edge of amorphous IrOx, hollandite-type IrOx and rutile-type IrO2; (d) ED-PDFs of amorphous IrOx, rutile-type IrO2 and Ir-metal.

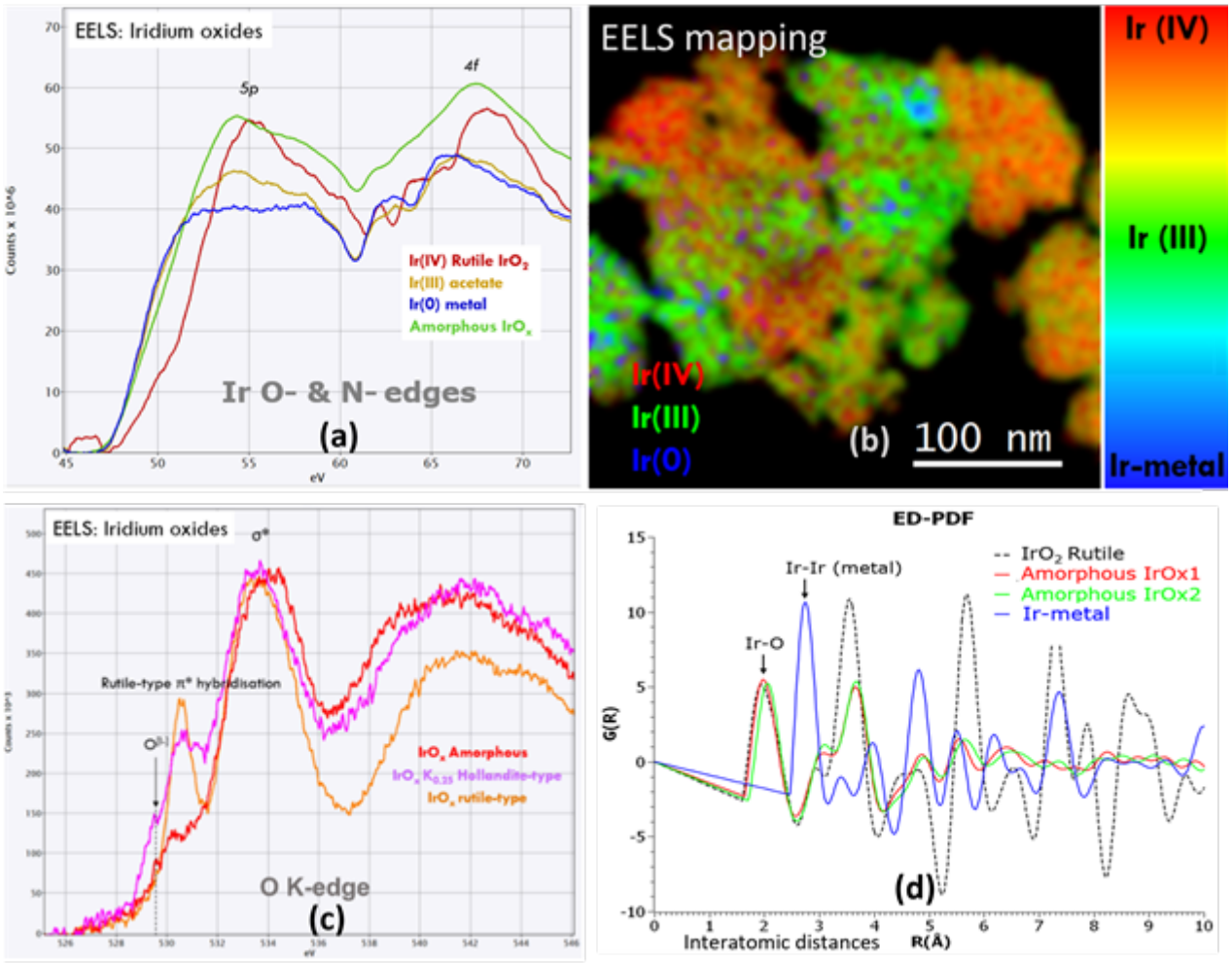

Keywords:

EELS, oxidation state, ePDF, IrOx

Reference:

1. Pfeifer V. et. al., 2016, Chem. Sci., 7(11), 6791.
2. Siracusano S. et. al., 2017, J. Power Sources, 366, 105.
3. Tran D. T. et. al., 2017, J. Appl. Cryst., 50, 304.
4. Willinger, E. et. al., 2017, J. Am. Chem. Soc., 139(34), 12093.

296

Electron Microscopy of Novel Lithium Alloy Anodes for Solid State Batteries

Dr Ed Darnbrough[1], Mrs Myra Ng[1], Dr Sreejith Olakkil Veedu[1], Prof David Armstrong[1], Prof Chris Grovenor[1], Prof Pete Nellist[1]
[1]University of Oxford, Oxford, United Kingdom

PS-04 (4), Plenary, august 27, 2024, 14:00 - 16:00

Background incl. aims
All-solid-state lithium-ion batteries offer higher capacities and improved safety compared with batteries that make use of a liquid electrolyte in part because of their potential to utilise a lithium metal anode and a solid ceramic electrolyte. Changing to a solid-state electrolyte removes many of the safety concerns surrounding lithium-ion batteries that are associated with the volatile and flammable liquid electrolytes currently used. An initial lack of understanding of the mechanical and diffusion properties of lithium metal means attempts to use pure lithium metal as the negative electrode (anode) have failed at the high currents and rates required for powering electric vehicles (EV). In this work we aim to solve these issues through alloying lithium to produce anodes with novel microstructures that can achieve the currents and rates required for EV application. Understanding how these new materials function as anodes requires characterisation of the behaviour of lithium entering and exiting the material, requiring microscopy up to atomic resolution with spectroscopy [1]. We study three lithium alloy systems (Li-Ca Li-Sr, and Li-Ba) for which no transmission electron microscopy has so far been reported in the literature.
The overarching aim of this work is to develop a deep understanding of the materials properties and mechanisms behind the premature short-circuiting and failure of solid-state batteries. A proposed route for initiating dendrite growth that leads to short-circuit failure is a non-uniform electric current at the anode-electrolyte interface caused by void formation during stripping [2]. We propose an alloy anode material as a solution that on stripping will retain full interface contact between the anode and electrolyte during cycling thus stopping void formation at the interface between the electrode and electrolyte. This is achieved by producing an anode from a two-phase material consisting of the lithium metal, to be cycled, and a lithium intermetallic that remains as a three-dimensional scaffold to provide both electrical and ionic contact between the current collector and the solid electrolyte throughout cycling. This concept was shown to be viable by Jia et al [3] electrochemically cycling the Li-Ca system with a liquid electrolyte. However, development of these alloys requires a full understanding of the mobility and bonding of lithium through the distinct phases and the microstructures produced by manufacturing and how those change with cycling.

Methods
A combination of plasma focused ion beam milling and scanning electron microscopy energy dispersive x-ray characterisation are used for the identification of the two-phase material on a larger scale and to identify regions of interest for the production of transmission electron microscopy lamella. Given the air sensitive nature of these materials, anaerobic sample preparation and transfer was used between instruments. Transmission electron microscopy and electron diffraction are used confirm the creation of the desired phases. Like most battery materials these lithium containing phases and the lithium metal that surrounds them are highly beam sensitive. Preliminary data shows that the pure lithium metal phase loses crystallinity (as observed by disappearance of electron diffraction spots and directly imaged lattice planes) when illuminated with a dose rate greater than 6 e/A2/s.

Results

Energy dispersive X-ray spectroscopy shows the material as cast has two distinct phases one containing the group two element and one without. Standard EDX spectroscopy cannot detect lithium meaning that the composition of alloys cannot be determined at this step and additional techniques are required for phase characterisation. Transmission electron diffraction from extracted lamella shows that the anode materials formed have two distinct crystallographic phases, in each case containing a lithium metal phase and a lithium intermetallic. The three intermetallic phases studied range in complexity from large face centre cubic (Li23Sr6 F m -3 m) to large hexagonal (CaLi2 and Li4Ba P 63/m m c). The microstructure varies dependent on the alloying element and the local composition during solidification with the width and homogeneity of the scaffold phase reducing with reduced group two element concentration. Preliminary cycling data shows that the material is capable of working as an anode and characterisation shows that the intermetallic scaffold remains after lithium has been stripped from the electrode. The graphic shows that the removal of the lithium metal is observed to be preferential to the conversion of the intermetallic and voids form first in the metal regions closest to the electrolyte. In the graphic the voids are highlighted in red at the top of the anode after a partial strip furthest from the stainless-steel current collector interface denoted in green. In each of these PFIB cross section images the dark regions are lithium metal and the light regions left behind are the LiCa2 intermetallic. Electron diffraction from lamella produced from these cycled anodes shows that the calcium containing regions have not changed phase compared with that observed in the uncycled material.

Conclusion

This work acts as the first step towards producing an anode for all solid-state batteries that is resistant to failure during cycling due to loss of ionic and electronic pathways at the interface. The knowledge gained here will direct future anode development that will be the foundation of successful creation of a commercially viable all-solid-state battery for electric vehicles.

Acknowledgements

This research was funded in part, by the UKRI Faraday Institution [SOLBAT FIRG026]. For the purpose of Open Access, the author has applied a CC BY public copyright licence to any Author Accepted Manuscript version arising from this submission. The authors acknowledge use of characterisation facilities within the David Cockayne Centre for Electron Microscopy, Department of Materials, University of Oxford, alongside financial support provided by the Henry Royce Institute (Grant ref EP/R010145/1).

Graphic caption:

i) pristine as cast lithium calcium two-phase anode, ii) partially stripped material, iii) fully stripped anode. The dark phase in each image is lithium metal and the light phases are lithium calcium intermetallic (the material below the green line is the stainless-steel current collector).

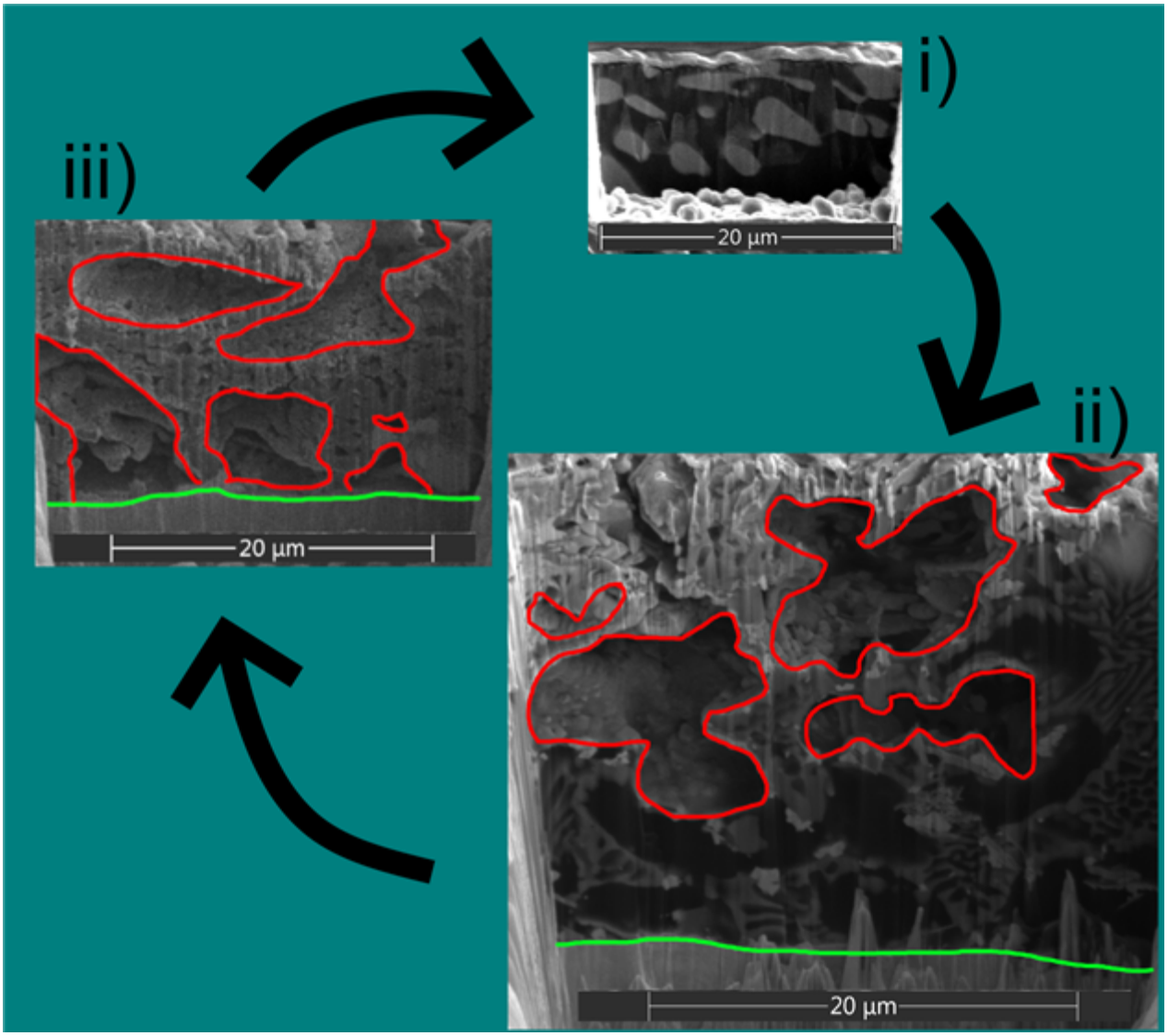

Keywords:

lithium alloy anodes, solid-state batteries

Reference:

[1] - Xu, Y., et al. (2020). Atomic to Nanoscale Origin of Vinylene Carbonate Enhanced Cycling Stability of lithium Metal Anode Revealed by Cryo-Transmission Electron Microscopy. Nano Letters, 20(1), 418–425.
[2] - Ning, Z et al. (2023). Dendrite initiation and propagation in lithium metal solid-state batteries. Nature, 618(7964), 287–293. https://doi.org/10.1038/s41586-023-05970-4
[3] - Jia, W et al. (2019). A dual-phase Li–Ca alloy with a patternable and lithiophilic 3D framework for improving lithium anode performance. Journal of Materials Chemistry A, 7(39), 22377–22384. https://doi.org/10.1039/C9TA08798B

306

Mitigating radiation damage in beam sensitive battery materials by adapting scanning parameters

Mme. Hannah Nickles Jäkel[1], Mr Eric Gautron[1], Mr Maurice Peeman[2], Mr Philippe Moreau[1], Ms Patricia Abellan[1]
[1]Nantes Université, CNRS, Institut des Matériaux de Nantes Jean Rouxel, IMN, 44000 Nantes, France, [2]Thermo Fisher Scientific, Eindhoven, Netherlands

PS-04 (4), Plenary, august 27, 2024, 14:00 - 16:00

Background incl. aims
Electron-beam sensitivity of battery materials hinders the full potential of high-resolution STEM-EELS insights on battery failure mechanisms. It is therefore important to understand how electron beam induced alterations can be minimized. Beam damage mitigation in STEM can be achieved by adjusting electron probe properties such as beam size, current and acceleration voltage, by changing dwell time, but also by changing the scan pattern and thus, exploiting the spatial component of beam damage (1). For the latter, many different approaches have shown great promise. Alternative scanning techniques, such as leapfrog scanning, which explores the effect of increasing pixel spacing (2), or sparse scanning, which irradiates only a percentage of pixels (3), can reduce damage compared to conventional raster scanning. Since beam damage is a process that is highly dependent on the type of material being irradiated, damage mitigation techniques require material-specific investigations to ensure effective adaption of the scanning parameters. Here we are interested in Li-containing battery materials, where for LiF, for example, radiolysis is more dominant than knock-on damage (4). Methodical experiments are necessary to understand how irradiation conditions like acceleration voltage, electron dose, and scan pattern can be optimized for specific electron beam sensitive battery materials.

Methods
In order to determine the optimum acceleration voltage, damage cross-sections for different acceleration voltages are calculated for various battery materials. To gain a better understanding of the damage mechanisms involved, damage is systematically induced on Li-containing battery materials and monitored with STEM-EELS ((S)TEM Themis Z 3G). The effect on materials damage of conventional scan patterns is compared to different “alternative” scan patterns.

Results
The calculated damage cross-sections show, that avoiding knock-on damage by imaging below a threshold voltage is not applicable for (S)TEM measurements of lithium-containing battery materials. STEM-EELS observations provide insights on the degradation of LiF to metallic Li, being consistent with radiolysis being the dominant damage mechanism. EELS spectra of LiF over radiation time show that the LiF bulk plasmon peak and the Li K-edge for LiF at 61 eV decrease, while the bulk plasmon peak for metallic Li appears at 7 eV. Lastly, scanning variations give insights on damage delocalization in battery materials. Damage imposed by conventional scanning is compared to different alternative scan patterns, by quantifying electron beam induced alterations in image intensity.

Conclusion
With the gained understanding for radiation damage in specific battery materials, optimized acceleration Voltage and scan pattern can be chosen to reduce electron beam induced alterations. Optimized scanning parameters enable higher imaging flexibility and could provide new insights into battery failure mechanisms.(5)

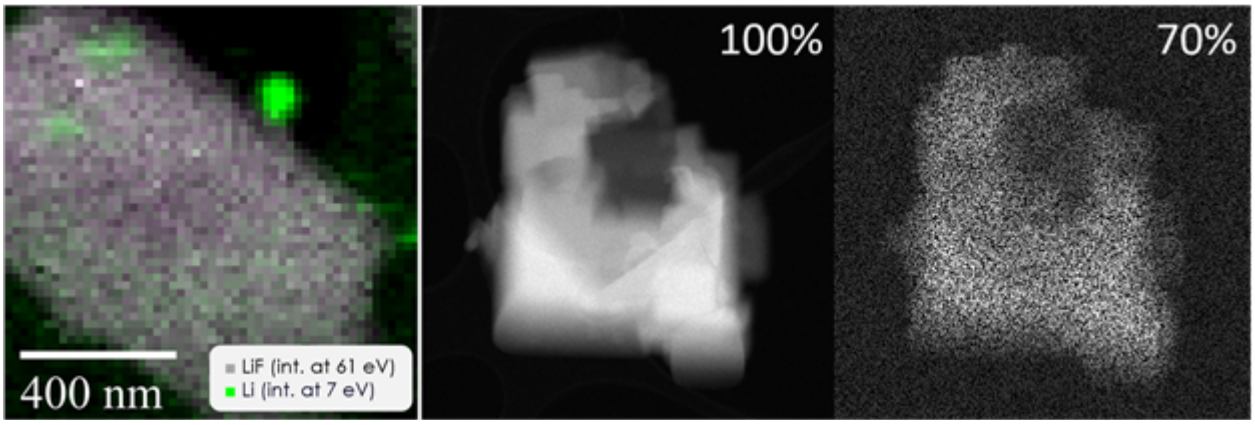

Keywords:

beam-damage, scan pattern, battery materials

Reference:

(1) Boniface, M. (2017). Nanoscale evolution of silicon electrodes for Li-ion batteries by low-loss STEM-EELS, Ph.D. thesis in Material Physics. Université Grenoble Alpes.
(2) Egerton, R. F. (2017). Scattering delocalization and radiation damage in STEM-EELS. Ultramicroscopy, 180, 115–124.
(3) Nicholls, D., Lee, J., Amari, H., Stevens, A. J., Mehdi, B. L., & Browning, N. D. (2020). Minimising damage in high resolution scanning transmission electron microscope images of nanoscale structures and processes. Nanoscale, 12(41), 21248–21254.
(4) Hobbs, L. W. (1987). Electron-beam sensitivity in inorganic specimens. Ultramicroscopy, 23(3), 339–344.
(5) Acknowledgements: The authors thank the OPINCHARGE project, which received funding from the European Union's Horizon Europe research and innovation programme under grant agreement No 101104032. We acknowledge Battery2030+ for their support to the OPINCHARGE project. Measurements were performed using the IMN's characterization platform, PLASSMAT, Nantes, France.

533

Investigating the formation of surface reconstruction layers in Ni-rich cathode materials using STEM

Lara Ahrens[1,2], Kilian Vettori[3], Dr. Shibabrata Basak[4], Prof. Dr. Rüdiger-A. Eichel[4], Prof. Dr. Joachim Mayer[1,2]
[1]Central Facility for Electron Microscopy (GFE), RWTH Aachen University, Aachen, Germany, [2]Ernst Ruska-Centre for Microscopy and Spectroscopy with Electrons, Forschungszentrum Jülich, Jülich, Germany, [3]Physical-Chemical Institute, Justus-Liebig-University, Gießen, Germany, [4]Institute of Energy and Climate Research (IEK-9), Forschungszentrum Jülich , Jülich, Germany
PS-04 (4), Plenary, august 27, 2024, 14:00 - 16:00

Background incl. aims
Lithium-ion batteries (LIB) are a key technology towards an emission-reduced transportation sector, in particular for electrical vehicles (EVs). One of the most promising cathode materials for LIBs are Ni-rich NMC cathode materials (LixNiyMnzCo1-y-zO2, with x > 0, y > 0.6). The main benefits of Ni-rich cathodes are an increased capacity, a high energy density and lower cost compared to conventional LIBs, which are needed to push the mileage limit and to make EVs more affordable. Although the advantages are great, Ni-rich NMC suffers from thermal and structural instabilities leading to a shorter life time and server capacity fading. The main degradation mechanisms occurring in NMC are: formation of surface reconstruction layer, formation of cathode-electrolyte interface (CEI), degradation of electrolyte and cracking of particles. [1,2]
This study focuses on the formation of surface reconstruction layer, specifically on the phase transition from layered structure (space group R-3m) to rocksalt phase (space group Fm-3m). [3] In the rocksalt phase the transition metals occupy the Li-positions and thus block the Li-diffusion paths. [4] A core-shell model describes the growth of this surface reconstruction layer, in which the degradation starts at the top of the surfaces and propagates into the bulk. [4] The aim of this study is to observe the phase change from layer structure to rocksalt structure and provide an answer to the questions: Does the rocksalt layer grow over time while the cell is kept under the harsh conditions of 4.5V and if so, is a trend in thickness growth of the rocksalt layer measurable?

Methods
A set of coin-half-cells against lithium was kept at high voltage of 4.5V for over 30 days. Every 2 days an electrochemical impedance spectroscopy (EIS) measurement was conducted. Afterwards, the cells were dissembled and the cathode sheets were rinsed with solvent. Using FIB-SEM allowed to cut very thin lamellas out of the cycled cathode sheets. However, preparing the sample for analysis presents several challenges. Firstly, the organic binder that surrounds the NMC particles melts faster under the ion-beam, leading to instabilities. Secondly, powder samples tend to redepositing and curtaining due to the pores in between. Finally, NMC is sensitive to the ion-beam, requiring lower voltages to be applied to reduce the amorphous layer on top. STEM was used to image the surface area of the particles down to atomic scale. Since the electron beam affects the NMC material and can lead to a phase transition from layered to rocksalt structure, it is very important to control the dose of the electron beam. [5] In addition, EEL spectra were acquired to provide a better understanding of the degradation process by monitoring the valance states of the transition metals. Moreover, further analytical methods such X-ray photoelectron spectroscopy (XPS) and secondary ion mass spectrometry (SIMS) were applied to investigate e.g. CEI formation.

Results

The EIS measurements showed an exponentially growing charge transfer resistance (Rct) which is an easily accessible indicator for degradation. Looking at the particles at atomic scale, the formation of rocksalt was present as depicted in Figure 1. The transition from layered to rocksalt appeared gradually and a typical transition region was visible. Interestingly, the variation of the thickness of rocksalt layer varied significantly within a lamella and even within one particle. It could be observed that the surrounding of the surface influenced the tendency to form rocksalt. A comparable, continuous trend in the growth of the surface reconstruction layer, as the Rct suggested, was not evident globally. However, the maximum thickness of degraded surface increased over time.

Conclusion

HRSTEM coupled with EELS provided a great insight into the rocksalt formation. The study indicates that while the core-shell model is generally a valid approximation for describing surface reconstruction in Ni-rich NMC, the real world is more complex. Therefore, it is crucial to comprehend the conditions under which a rocksalt structure is formed. Furthermore, understanding the time-correlation of different degradation mechanisms is crucial to improve battery materials.

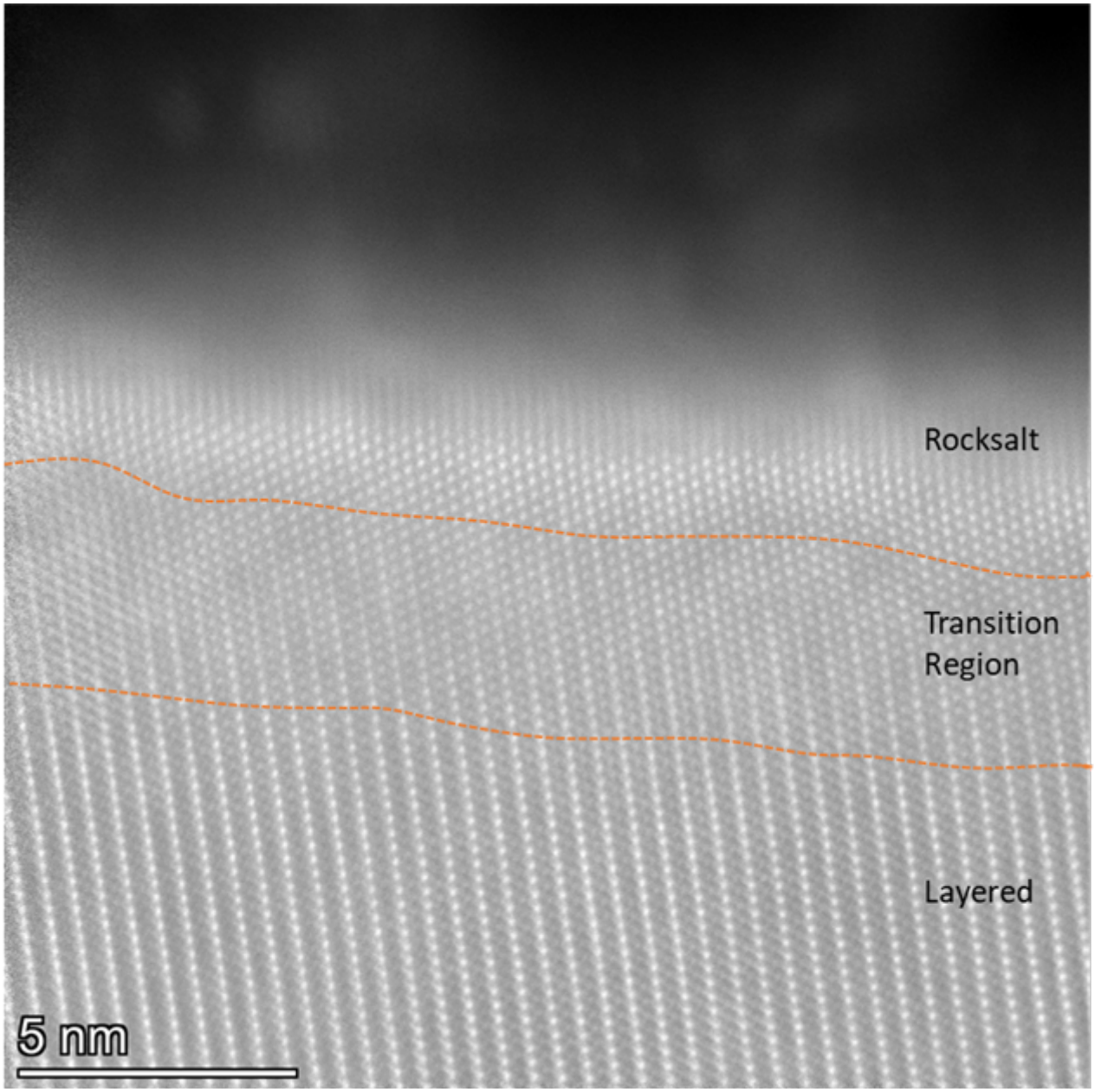

Keywords:

Li-ion batteries, degradation, high voltage

Reference:

[1] Dose et al., ACS Energy Lett. 10, 3524–3530 (2022).
[2] Jiang et al., Adv. Energy Mater. 48, 2103005 (2021).
[3] Bak et al., ACS Appl. Mater. Interfaces 6, 24, 22594–22601 (2014).
[4] Jung et al., Adv. Energy Mater. 4, 1300787 (2014).
[5] Lin et al., Sci Rep 4, 5694 (2014).

587

PFIB-preparation and STEM-characterization of electrochemically plated lithium at the interface to the solid electrolyte Li6PS5Cl

Franziska Hüppe[1], Juri Becker[2], Dr. Jürgen Belz[1], Dr. Shamail Ahmed[1], Dr. Till Fuchs[2], Dr. Burak Aktekin[2], Prof. Dr. Jürgen Janek[2], Prof. Dr. Kerstin Volz[1]
[1]Department of Physics, Philipps-Universität Marburg, Marburg, Germany, [2]Institute of Physical Chemistry and Center for Materials Research, Justus-Liebig-Universität Gießen, Gießen, Germany
PS-04 (4), Plenary, august 27, 2024, 14:00 - 16:00

Solid-state batteries are of particular interest when it comes to safe high-energy storage as they potentially enable the usage of lithium anodes. Theoretically, a lithium metal anode has a more than 10 times higher specific charge capacity than graphite [1], which is typically used as anode material in commercially available lithium-ion batteries. But, industrial production of highly reactive lithium metal anodes is challenging. One approach is to electrochemically deposit lithium in a so-called anode-free cell. The lithium is plated between a current collector and the solid electrolyte during charging. In the half-cell assembly investigated throughout this study, the current collector consists of stainless steel and the solid electrolyte of argyrodite-type Li6PS5Cl. The latter is a promising solid electrolyte candidate due to its high ionic conductivity, but comes along with a solid electrolyte interphase (SEI) formation when in contact with lithium metal [2]. Therefore, the characterization of interfacial side reactions at the micro- and nanoscale is crucial.

Scanning transmission electron microscopy (STEM) offers structural insights at atomic resolution. Still, it comes with a challenging sample preparation that is further complicated by moisture and ion beam sensitivity of the battery materials. Furthermore, lithium metal and sulfide electrolytes like Li6PS5Cl require cryogenic conditions during ion- and electron-beam exposure to withstand the beam doses. The plasma focused ion beam (PFIB) system Helios 5 Hydra CX is capable of an inert-gas transfer from and to the glove box as well as sample preparation at temperatures around -190 °C. In the PFIB, the sample is thinned to electron-transparency (< 100 nm), from where it is transferred to the glove box and mounted in a sealed transfer holder (Mel-Build) for further investigation in a STEM (JEOL JEM-2200FS). Low-dose electron imaging and STEM-EDX (energy dispersive X-ray spectroscopy) at cryogenic temperatures are performed.

The lamella preparation of the highly sensitive lithium metal and Li6PS5Cl requires adapted preparation steps: low ion currents to preserve the Li | Li6PS5Cl interface as well as eliminating tungsten deposition. Usually, tungsten deposition is used to protect the sample during thinning and to attach the sample to the manipulator needle for lift-out and attachment of the lamella to the copper TEM grid. The high mobility of ions in Li6PS5Cl makes it impossible to distribute the tungsten atoms of the precursor gas locally. Hence, a complete gas-free workflow is needed. The manipulator needle is attached to the lamella gas-free using redeposition of the needle material. Also, the lamella is attached to the copper grid using redeposition of the grid. The steel current collector serves as a protection layer during thinning.
The thinned lamella is investigated in the STEM. A cryo-STEM EDX map and spectrum are depicted in Figure 1. The dark blue area (Figure 1b) encircles Li6PS5Cl with its characteristic peak relation of phosphorus, sulfur, and chlorine, as seen in the corresponding EDX spectrum (dark blue graph Figure 1c). Between lithium and Li6PS5Cl is a roughly 200 nm thick SEI, colored in light blue in Figure 1b, showing chlorine enrichment in the EDX map (Figure 1a) as well as in the corresponding EDX spectrum (light blue graph Figure 1c). Lithium is not detectable using EDX, as it’s characteristic X-rays have too low energy and are absorbed by the detector’s window.

The preparation of electrochemically plated lithium and Li6PS5Cl using the PFIB is highly complex and requires the absence of air as well as cryogenic conditions. Nonetheless, the effort is necessary to gain structural and chemical information on the SEI. An approximately 200 nm thick chlorine-rich layer between plated lithium and argyrodite-type Li6PS5Cl is already observed. Further measurements like STEM-EELS (electron energy loss spectroscopy) to detect lithium and TEM-PED (precession electron diffraction) for structural information need to be carried out.

Figure 1

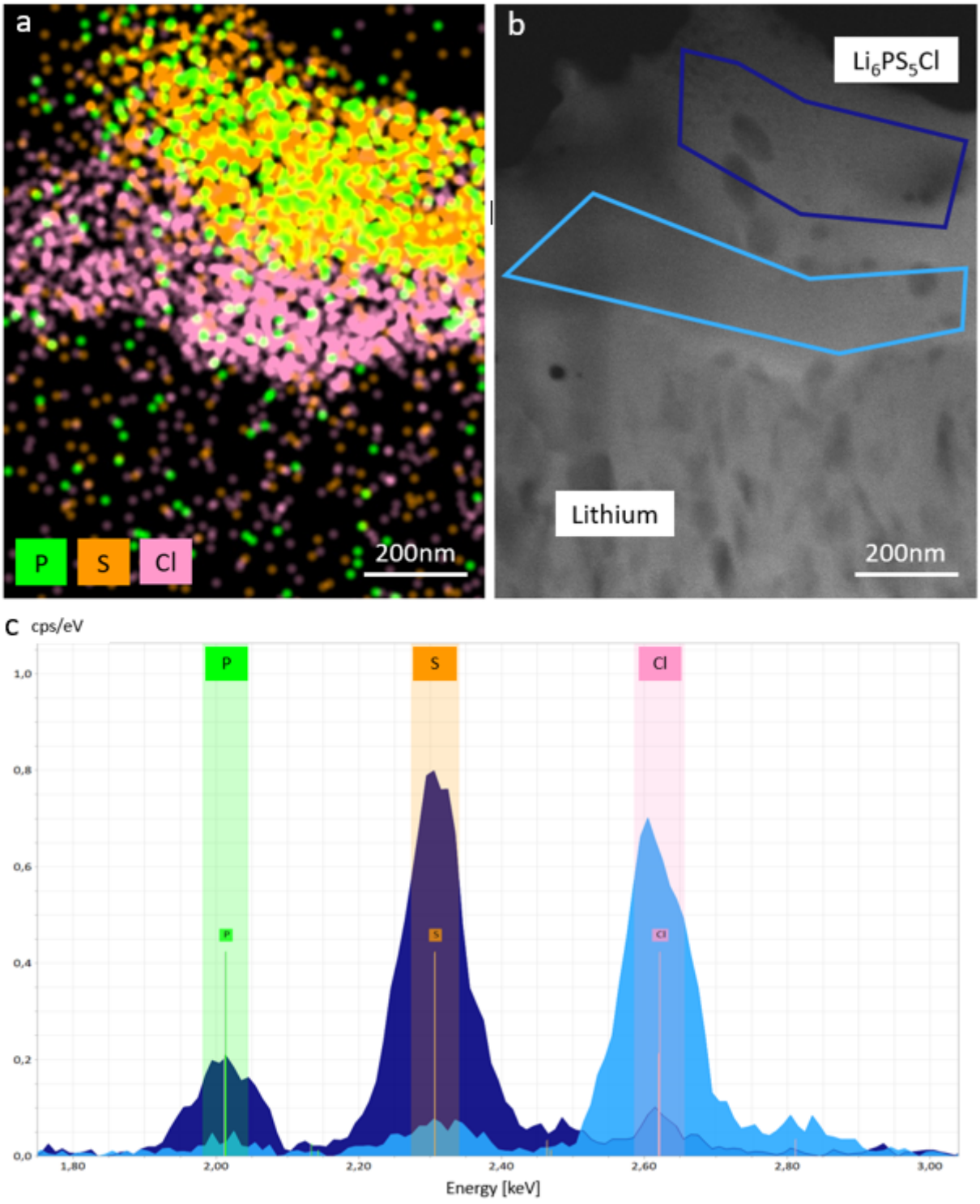

Keywords:

Plasma-FIB, Battery, Inert-gas-transfer, Anode-free-cell

Reference:

[1] W. Xu et. al.: Energy & Environmental Science, 2014, 7, 513
[2] Y. Nikodimos et. al.: Energy & Environmental Science, 2022, 15, 991

619

Defect engineering of core-shell systems based on 2D transition metal dichocalgenides

Juan José Quintana González[1], Antonio Jesus Medina Olivera[1], Dr Ramon Manzorro[1], Dr Cédric Pardanaud[2], Dr Rong Sun[1], Dr Ana Belén Hungría[1], Dr Laura Cubillana Aguilera[3], Dr Jose María Palacios Santander[3], Dr Juan Carlos Hernández Garrido[1], Dr Luc Lajaunie[1]
[1]Department of Inorganic Chemistry, Faculty of Sciences. University of Cadiz, Puerto Real, Spain, [2]Aix-Marseille Université, CNRS, PIIM UMR 7345, Marseille, France, [3]Department of Analytical Chemistry, Faculty of Sciences. University of Cadiz,, Puerto Real, Spain

PS-04 (4), Plenary, august 27, 2024, 14:00 - 16:00

Background
One of the biggest challenges facing the development and profitability of new ways to obtain H_2 by water splitting method is to find new materials for Hydrogen Evolution Reaction (HER) electrocatalysis that are not based on Pt, with the aim to obtain electrodes which are both performant and sustainable. The synthesis of TMD(Transition metal dichalcogenide)-based materials is one of the most promising strategies. MoS_2-Au hybrid systems have shown high HER activity, and the plasmonic properties of gold makes it an interesting proposal in photoelectrocatalysis. In this work, we report the synthesis and complete physical and chemical characterization of both Au@MoS_2 and Au@Mo(W)S_2 core-shell nanostructures. In addition, we have studied the influence of thermal reduction treatment in hydrogen atmosphere to increase the activity of these systems via a precise control of the number of shell layers and associated defects.

Methods
Electrochemical HER behavior of the samples was determined by using linear sweep voltammetry (LSV), cyclic voltammetry (CV) and vhronoamperometry, the last one in combination with a light source to study the plasmonic properties. The measurements were carried out in a three-electrode standard set-up in acid conditions (H_2SO_4 0.5M) by using a Biologic potentiostat/galvanostat (SP-150e) with platinum, Ag/AgCl and glassy carbon electrodes as a counter, reference and work electrodes. Structural characterization was performed in a double-corrected Transmission electron microscope (FEI Titan Cubed) in combination with in-situ TEM studies of the evolution of the sample under thermal hydrogen conditions carried out in environmental gas-cell (Climate Holder, DENS Solutions). Other complementary techniques, such as XPS and Raman spectroscopies, were performed to give a complete insight on the structure and chemistry of the samples.

Results
Au@Mo(W)S_2 systems with different W/Mo ratios (including W/Mo=0) were synthesized. TEM analyses highlight the presence of W atoms in the shell layers of the nanostructures. Moreover, a reduction in the number of shell layers additional thermal treatment can be observed by applying a thermal treatment in reducing conditions, as evidenced by both ex situ and in situ TEM studies. The incorporation of such defects induce to a change in the electrochemical properties of the material: low W/Mo ratios enhance the HER activity with respect to the pure Mo sample. However, the thermal treatment affects differently each sample: the best activity being observed for the pure Mo sample heated at 800°C whereas the ternary Au@Mo(W)S_2 samples show an improvement at lower temperature, highlighting thus the interplay between heteroatoms and structural defects on the HER properties. Moreover, plasmonic properties of the sample was evidenced, by both light-assisted electrochemical studies and low-loss STEM-EELS analyses.

Conclusion

This work provide a complete overview on both the integration of W hetetoatoms and the incorporation of structural defects by thermal treatment into 2D-based core-shell structures. The detailed structural and electrochemical characterization of these processes allow us to link the structural and electrochemical properties as well to fine-tune the chemistry of theses systems.

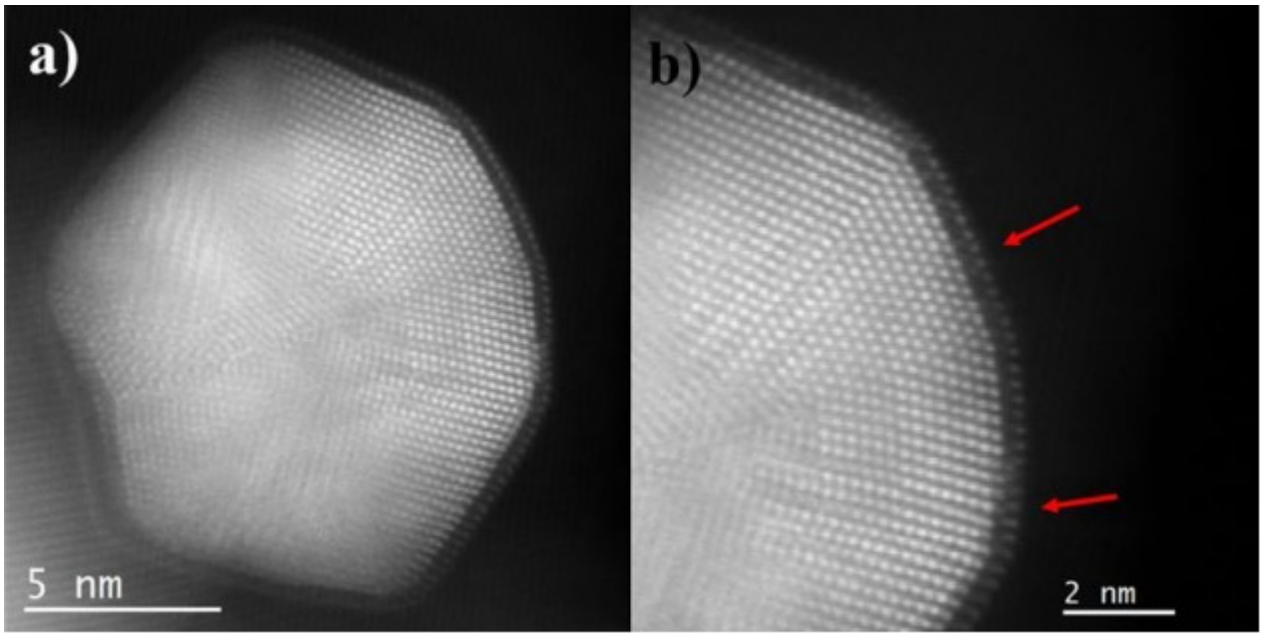

Keywords:

TMD core-shell plasmonic-material HER

Reference:

[1] J.J. Quintana Gonzalez et al., Int. J. Hydrogen Energy. 51, 371-382 (2024)
[2] A.R. Baz-Ziv et al., ACS Appl. Ener. Matter. 2, 8, 6043-6050 (2019)

867

From design to « operando » experiments in the SEM: application to battery studies

Dr Neelam Yadav[1], Mrs Melissa HERMANN ALba[1], Dr Morcrette Mathieu[1,2], Dr Carine Davoisne[1,2]
[1]LRCS, UMR CNRS 7314, Amiens, France, [2]Réseau sur le Stockage Electrochimique de l'Energie (RS2E), FR CNRS 3459, , France

PS-04 (4), Plenary, august 27, 2024, 14:00 - 16:00

In batteries, electrochemical reactions take place at the interfaces (electrodes-electrolyte, etc.), inducing more or less reversible change such as poor ion transport, dendrite formation, electrochemical degradation and chemo-mechanical degradation[1]. Among the new-generation systems under development, all-solid-state batteries (ASSBs) are no exception to this rule. Understanding the phenomena at interfaces that lead to premature battery ageing is therefore crucial to understanding and finding ways of improving the battery. Thanks to the emergence of in-situ and operando techniques, these complex, constantly evolving interfaces can now be studied by live, battery-scale observations using SEM[2].
To carry out this type of study, we have developed a simple electrochemical cell (Figure 1) that can be used to operate all-solid state lithium metal batteries inside the SEM. The use of lithium metal, which is an air-sensitive compound, led us to fabricate a sealed box enabling the battery to be transferred between the glovebox and the SEM (and vice versa). Morphological (secondary and backscattered electron imaging) and chemical (X-ray energy dispersive spectroscopy) changes at solid-state interfaces could thus be monitored in real time and during battery operation.
In this study, we focused on sulfide-based solid electrolyte (SE) particle size distribution and its impact on electrochemical performance. A batch of Argyrodite (Li6PS5Cl (LPSCl)) was sieved to obtain two batches of particles range (0,5-20µm and 50-150µm). The AASBs were prepared using the two particles size distribution while keeping the anode (lithium metal), cathode (active material: NMC) composite formation and the fabrication process constant.
From the two particles sized distribution, the one with the large particles have better electrochemical performance. From morphological point of view at the cathode composite electrode, the formation of a cathode electrolyte interface is visible in the different batteries but is more developed in the case of small sized particles. In the solid electrolyte, the type of cracks differs with relatively strait feature for small particles and sinuous one for large one. At the anodic interface, a lost in contact between the SE separator and the lithium is observed and increased with the cycling process with a higher impact for the small particles (Figure 2.a and b). By investigating further, the formation of dendrites with different morphologies are visible at the anodic interfaces (Figure2.c).
We categorized the observed changes into three modes: (i) electrical failure by the formation of lithium dendrites of different morphologies following the ES going up to short circuit in the case of small particles, (ii) mechanical failure by the formation of cracks in the electrolyte whose shape and propagation strongly depend on the distribution particles size and (iii) electrochemical failure with the formation of solid electrolyte interphases on the surface of the active material. The main obstacles for the use of lithium metal are related to the propagation of lithium dendrites and thus to the mechanical instability of solid electrolytes.

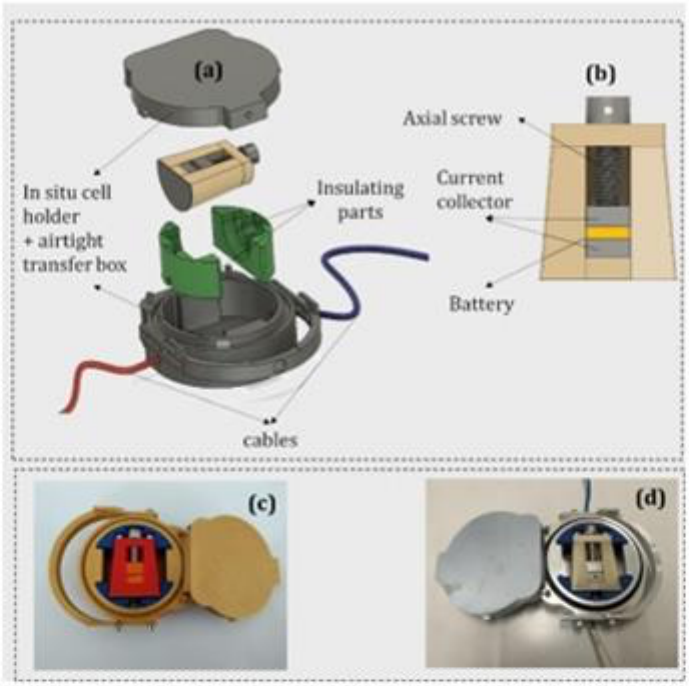

Figure 1: development step of the electrochemical cell for SEM "operando" studies

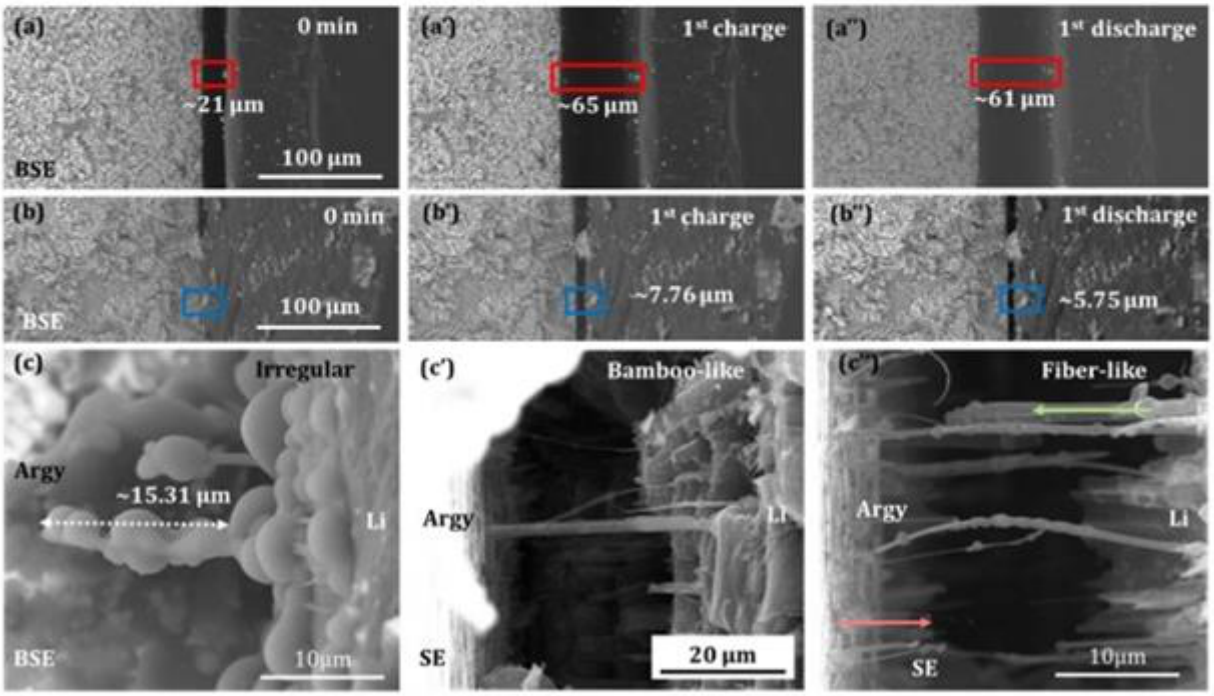

Figure 2: The depiction of loss of contact in small SE particles at (a) 0 min (a') 1st charge and (a") 1st discharge in large SE particles at (b) o min (b') 1st charge and (b") 1st discharge. Morphologies observed for large particles: These are at the end of the 10th cycle. (c) Irregular shape (c') Bamboo-like (c") fibre-like.

Keywords:

SEM, operando cycling, battery

Reference:

[1] S. Wang, H. Xu, W. Li, A. Dolocan, and A. Manthiram, "Interfacial Chemistry in Solid-State Batteries: Formation of Interphase and Its Consequences," J. Am. Chem. Soc., vol. 140, no. 1, pp. 250–257, 2018.

[2] M. Nagao, A. Hayashi, M. Tatsumisago, T. Kanetsuku, T. Tsuda, and S. Kuwabata, "In situ SEM study of a lithium deposition and dissolution mechanism in a bulk-type solid-state cell with a Li2S–P2S5 solid electrolyte," Phys. Chem. Chem. Phys., vol. 15, pp. 18600–18606, 2013.

1126

Mapping Li in thin-films and heterostructures by EELS and ptychography: case of Li7La3Zr2O12 and LiCoO3

Dr Adam Kerrigan[2], Dr Connor Murril[2], Dr Demie Kepaptsoglou[1,3], Dr Chris Allen[4], Dr Mohsen Danaie[4], Dr Frederick Allars[4], Prof Vlado Lazarov[1,2]
[1]School of Physics, Engineering and Technology, University of York, York, UK, [2]The York-JEOL Nanocentre, University of York, York, UK, [3]SuperSTEM Laboratory, SciTech Daresbury, Daresbury, UK, [4]Electron Physical Science Imaging Centre, Diamond Light Source Ltd., Oxford, UK

PS-04 (4), Plenary, august 27, 2024, 14:00 - 16:00

Background incl. aims
Improving upon the current generation of lithium-ion batteries requires a fundamental understanding of electrochemical and structural/chemical changes due to work-cycles of the electrodes/electrolyte heterostructure. Multiple mechanisms exist for cell degradation, whether this be through structural fatigue in the bulk of the electrodes or via formation of solid electrolyte interfaces (SEIs). With resolutions achievable below 1 Å in aberration corrected transmission electron microscopy (TEM), structural analysis of grains, grain boundaries, as well as interfaces between electrode (LiCoO2, LCO) and electrolyte (Li7La3Zr2O12, LLZO) as well as formed current induced SEIs is possible on atomic scale. Determining the structural characteristics of the boundaries and interfaces will allow us to build atomistic models for calculating the electronic properties for lithium diffusion. The observation of defects and interfacial composition down to atomic resolutions is fundamental to understanding the specific characteristics changing the efficiency of lithium-ion movement through the device. By combining ptychography and high resolution EELS we demonstrate that Li can be uniquely traced through the grown films, and more importantly at the grain boundaries that delimitate higher with lower regions of Li.

Methods
The thin films were grown by pulsed laser ablation (PLD) on several substrates including Al2O3, GGG and SrTiO3. STEM-EELS was done using Nion UltraSTEM100MC – Hermes Scanning Transmission Electron Microscope (STEM), operated at 60kV. The instrument is equipped with a cold field emission source, with energy spread of around 6meV.
The electron energy loss spectroscopy (EELS) spectrum images (SI) were acquired with a probe with an energy spread of 150 meV with a collection half-angle of 22 mrad. The HAADF-STEM imaging and 4D STEM imaging was done by aberration corrected JEOL Grand ARM at 300keV.

Results
Single layer films of LCO, annealed at various temperatures, have been imaged in HAADF-STEM with regions of rhombohedral, spinel and cubic phases identified. As temperature increases during the annealing process the films show a reduction in rhombohedral phase grains and an increase in number of cubic grains. This fits with the assumption that the spinel and cubic phases are the stabilisation of an increased reduction in lithium content, respectively. Grain boundaries between the three phases of the deposited films have been studied via EELS in order to map the Li content and potential channels between the nanograins. Further to this electron ptychography was performed showing the Li position in the grains and across boundaries, corroborating the spectroscopic data.

Heterostructures of LCO and LLZO grown on GGG substrates have also been studied via STEM, EDS and EELS datasets to understand the details of both electrode and electrolyte as well as features appearing at the interface. Interfacial decomposition appears most dependant on temperature, with the scale of intermixing greatly reduced when subjecting heterostructures to applied bias. LCO will

grow crystalline on LLZO (LCO/LLZO) allowing a crystalline electrode/electrolyte interface to form, whereas the electrolyte remains amorphous when deposited on top of crystalline LCO (LLZO/LCO). However, LLZO/LCO structures promote the formation of $LaCoO_3$ interfacial layers and crystallites of cobalt-containing structures growing through into the LLZO layer. These contribute to a complex system formed during thermal decomposition and intermixing occurring at the solid-state interface.

Conclusion

The position of Li atoms, within three phases of differing Li content, in LCO have been imaged. This insight can help engineer LCO films with optimal Li transport properties, and provide insiights of the effect of annealing in crustalisation process of these thin films and heterostructures. LCO and LLZO interfaces have been grown and studied via STEM-HAADF, and STEM-EELS. The orientation of the substrate only allows for crystalline LCO/LLZO interfaces whilst LLZO/ LCO heterostructures have an intermixing $LaCoO_3$ layer and large crystallites that pierce into the LLZO film.

The combined approach of imaging and spectroscopy have been shown to be rather beneficial in determining the structure and Li content in the thin films and heterostructures of Li based oxides used as electrolyte and electrodes.

Keywords:

STEM-EELS, Li batteries, Ptychography

22

Seeing the nanoscale dynamics in gas-based processes by using in-situ TEM

Tanmay Ghosh[1,3], Ms Tjiu Weng Weei[1], Mr. Khakimjon Saidov[2,3], Mr. Antoine Pacco[5], Mr Harold Philipsen[5], Mr Utkur Mirsaidov[2,3,4], Mr Zainul Aabdin[1]
[1]Institute of Materials Research and Engineering, A*STAR (Agency for Science, Technology, and Research), Singapore 138634, Singapore, Singapore, [2]Center for Advanced 2D Materials and Department of Physics, National University of Singapore, Singapore 117546, Singapore, Singapore, [3]Center for BioImaging Sciences and Department of Biological Sciences, National University of Singapore, Singapore 117557, Singapore, Singapore, [4]Department of Materials Science and Engineering, National University of Singapore, Singapore 117575, Singapore, Singapore, [5]imec, Kapeldreef 75, Leuven, B-3001, Belgium, Leuven, Belgium

Poster Group 1

Functional nanostructures are often transformed through gas-based processes such as restructuring, oxidation, and sublimation. This process is called plasma-less gas-phase etching and is particularly important to achieve damaged-free sub-10-nm metal recess to facilitate the integration of metal interconnects with upcoming logic or memory components, crucial for advancing future microelectronic devices towards higher performance and miniaturization. The process involves gas-phase oxidation and subsequent sublimation where the liquid phase etching usually struggles due to poor diffusion in deep and narrow trenches. Furthermore, it provides precise depth control and reduced sidewall damage, making it advantageous over plasma-based or liquid chemical etching for metal recess or etching narrow trenches in microelectronics. However, understanding the detailed dynamic pathways of these transformation processes in gas environments is lacking, yet it is crucial for optimizing such etching techniques. In this work, we tracked the details of a densely packed 32-nm-wide Mo-metal lines recess by using the gas-phase in-situ TEM method. Specifically, the nanoscale modifications in the densely packed 32-nm-wide Mo-lines induced by the gas environments were observed in real-time. In this talk, I will discuss some of this research exploring the previously unknown intermediate steps of the restructuring of Mo-lines under a gas environment. The obtained dynamic insights possess a great impact on the development of semiconductor nanodevices.

Keywords:

In-situ TEM, Nanoparticles, Metal interconnects

30

Analyses of Observed Speciation of Cobalt in NMC cathodes Using Laboratory X-ray Absorption Spectroscopy (XAS)

Andreas Bergner[1], Simon John[1]
[1]Quantum Design GmbH, Pfungstadt, Germany

Poster Group 1

We report the X-ray Absorption Spectroscopy (XAS) investigation of four samples of NMC electrodes using QuantumLeap™ H2000. Co XANES show three isosbestic points. Principal component analysis (PCA) and Iterative Target Transform Factor Analysis (ITTFA) reconstruction of the experimental X-ray Absorption Near Edge Structure (XANES) show that two of the samples contain two unique species of Co. In the remaining samples, the speciation of Co can be described by the linear combinations of the two distinct species, validating QuantumLeap's synchrotron-like performance.

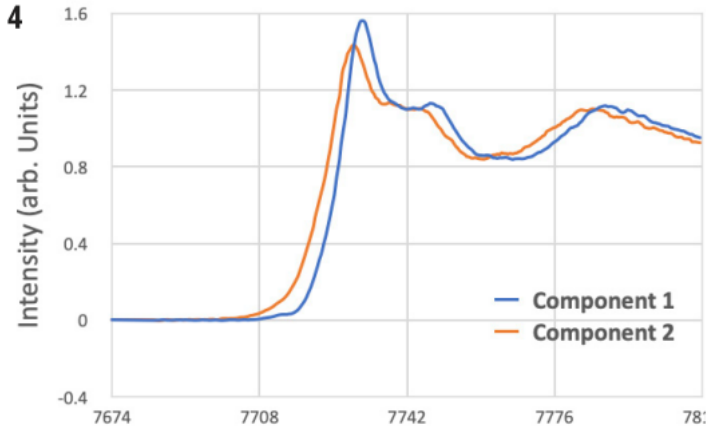

Figure 4: ITTFA reconstructed experimental two principal XANES components (component 1 in blue and component 2 in orange) of cobalt investigated in the series of NMC electrode samples.

Keywords:

XAS ITTFA XANES battery NMC

31

Observing Lithium Ion Battery Bonds During Charge Cycling Using Laboratory XAS

Andreas Bergner[1], Simon John[1]
[1]Quantum Design GmbH, Pfungstadt, Germany

Poster Group 1

X-Ray Absorption Spectroscopy (XAS) analyses of measurement results obtained with QuantumLeap H2000 of Lithium ion NMC batteries are presented. For the set of samples analyzed, Mn is largely electrochemically inactive and the octahedral coordination is retained. The Mn-O and Co-O bond lengths are shown to change minimally with cycling whereas the Ni-O bond suffers from Jahn-Teller distortion.

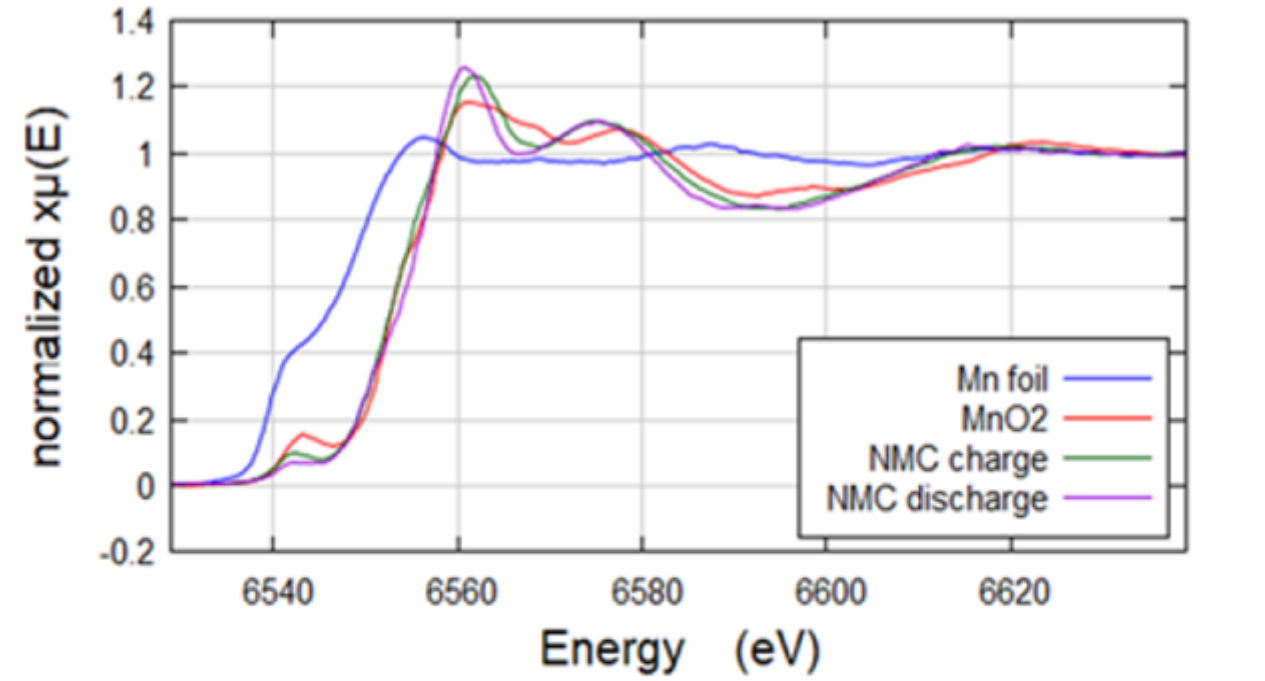

Figure 1: Mn-K edge of NMC electrodes fully charged and discharged. Comparison of the MnO2 model and Mn foil oxidation states shows that Mn in NMC are in an oxidation state of ~4+. The absorption edge energy does not change much showing that Mn acts as a spectator during cycling.

Keywords:

XAS battery lithium EXAFS x-ray

39

Understanding strain and composition effects in fuel cell catalysts using advanced electron microscopy and DFT

Alessandro Zanre[1], Dr. Aaakash Varambhia[2], Dr. Dogan Ozkaya[2], Dr. Xiaonan Luo[3], Prof. Sergio Lozano-Perez[1], Prof. Rebecca J. Nicholls[1], Prof. Peter D. Nellist[1]
[1]Department of Materials, University of Oxford, , United Kingdom, [2]Johnson Matthey Technology Centre, , United Kingdom, [3]Contemporary Amperex Technology Co., Limited, , P. R. China

Poster Group 1

Background and aims
Hydrogen fuel cells are an important technology for decarbonising road transport and shipping. Their efficiency is limited by the oxygen reduction reaction (ORR), which requires catalysts to achieve acceptable performance for the cell. The state of the art ORR catalysts are Pt-X nanoparticles, where X is another transition metal. These nanoparticles have a core-shell structure, consisting of an alloyed Pt-X core surrounded by a Pt rich shell. They perform much better as ORR catalysts than pure Pt nanoparticles, however the origins of this activity enhancement are not fully understood. The main factors that are hypothesised to be responsible are ligand effects, where chemical differences between Pt and X modify the electronic properties of the catalyst surface, and strain effects, where changes in nanoparticle size and shape induced by the size mismatch between Pt and X lead to changes in electronic structure. Core-shell nanoparticles have been observed to have a high degree of strain at the surface which affects the d band structure at the nanoparticle surface, which is crucial in determining O binding strength and ORR catalytic activity. Complex strain states with a significant shear component have been observed in the outer layers of core-shell nanoparticles via atomic resolution scanning transmission electron microscopy (STEM); while the effect of volume changing normal strains on catalytic activity has been widely studied, those of shape changing shear strains have been largely overlooked in the literature. Our key aim in this work is to use computational modelling to understand the electronic properties of experimentally observed nanoparticle structures, and the effect of these properties on catalytic activity, as a step towards better understanding the structure-property relationship and improving fuel cell catalyst design.

Methods
Microscopy: Alloyed Pt-Co core-shell fuel cell catalyst nanoparticles on C have been provided by Johnson Matthey. Atomic resolution high angle annular dark field STEM (HAADF-STEM) with EDX and EELS has been performed on these nanoparticles to understand their structure and composition at the atomic level. Column positions relative to a reference grid which is fitted to a nanoparticle structure have been used to measure variations in strain across its extent. The compositional information allows the elastic strain to be distinguished from lattice parameter changes arising from different local alloy compositions.

Computation: DFT calculations have been performed using CASTEP 22.11 on pure Pt to measure the effect of normal and shear strains on the d band centre. All calculations were performed with the PBE functional. Equilibrium bulk and slab structures were first obtained by geometry optimisation. Strain states representative of those seen in STEM images of catalyst nanoparticles were then applied and the d projected PDOS and d band centre of these strained structures were calculated and compared.

Results
Atomic resolution HAADF-STEM measurements of catalyst nanoparticles have shown that the outer layers exhibit both normal and shear strains relative to the reference structure that was fitted to the

nanoparticle. DFT calculations have shown that the shear strains typically observed in catalyst nanoparticles are unlikely to have a significant effect on their electronic properties.

Conclusions

The ability to reliably map strain at the atomic scale for nanoparticles is an important step in linking structure to activity, and ultimately determining the optimal surface structure for ORR catalysts. The independence of electronic properties on small shear strains suggests that unit cell volume is a key descriptor of catalytic activity.

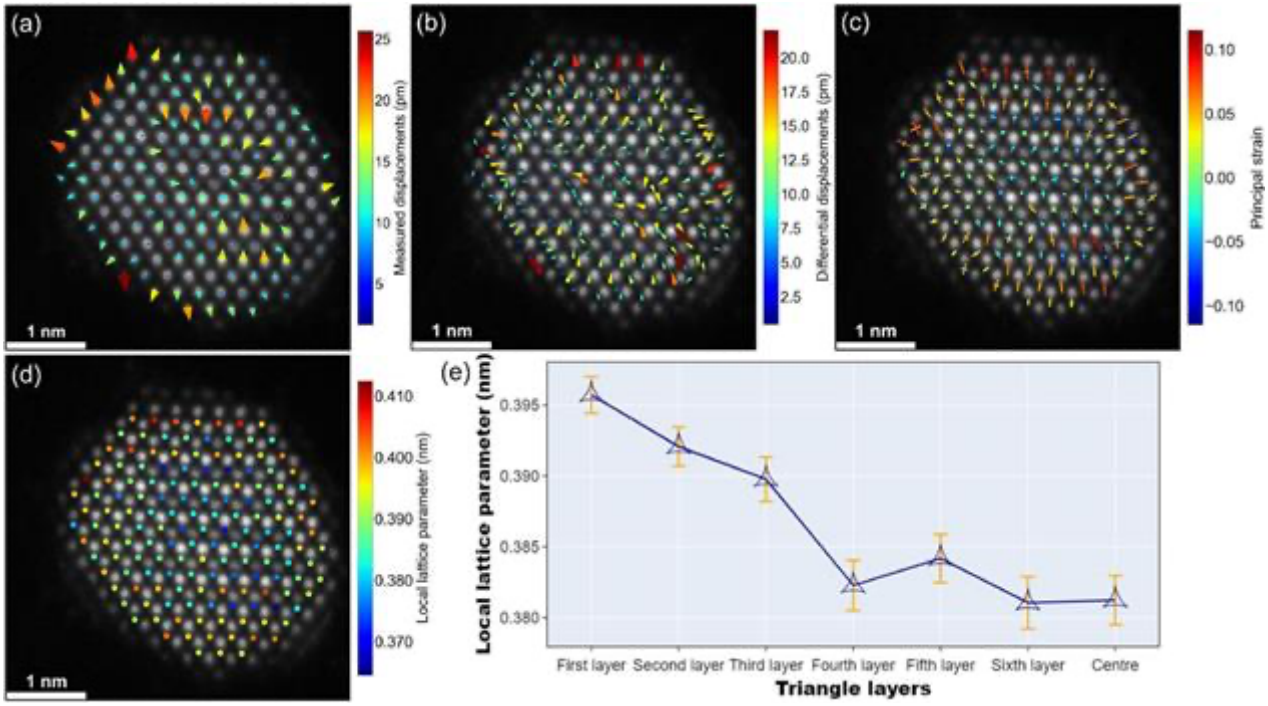

Keywords:

HAADF-STEM, DFT, catalysis, strain

Reference:

Luo, X. et al. (2022), Ultramicroscopy, 239, 113561

65

Quantification of Lithium in State-of-the-Art low Voltage STEM

Pr. Raynald Gauvin[1], Mr. Nicolas Brodusch[1], Mrs. Stéphanie Bessette[1]
[1]Mining and Materials Engineering,McGill University, Montréal, Canada

Poster Group 1

Background incl. aims
This paper will present new achievements and challenges in performing quantitative EDS and EELS maps of lithium-based materials in a state-of-the-art low-voltage scanning transmission electron microscope. With the energy revolution coming because of global warming, Lithium-Ion Batteries of higher energy densities and much lower cost must be developed to allow the transition of fuel-based vehicles to be replaced with electrical vehicles. This will only become a reality if we can quantify lithium at the Nanoscale to see where it becomes lost during the electrochemical cycling of the batteries.
Methods
State-of-the-art results acquired with the Hitachi SU-9000 dedicated STEM will be presented. This microscope has EELS capabilities that allow Li detection [1], being the first to be sold by Hitachi High-Technologies. It is also equipped with the Extreme EDS system from Oxford Instruments that can detect the K line of lithium [2]. The SU-9000 has a resolution of 0,22 nm in bright field STEM without aberration correctors and this allows lattice imaging. A cryogenic specimen holder allows to analyze Li based materials at 77 K.
Results
Figure 1-a shows an EELS spectrum of Li2FeSiO4 taken with the Hitachi SU-9000 at 30 keV. Even if X-ray emission was not detected with the EDS detector for this material for the same reasons stated above for Li2CoSiO4, the ionization edges are visible for Fe, Li, and Si. This shows the strong advantage of EELS over EDS (or WDS) for Li quantification. This is seen in figure 1-b which shows a Li EELS edge-to-background ratio map of an Al-Li 2099 alloy recorded with the three-detectors system on the Hitachi SU-9000 at 30 keV. This map shows the round δ’ precipitates (Al3Li) of 5 to 20 nm and the T1 plates (AlCuLi) that have thicknesses between 1 to 2 nm. Results obtained with a cryo-holder to evaluate possible minimization of beam damage will be presented.
Conclusion
It is not always possible to detect Li with EDS because its 3S electron can be bonded with another atom. EELS is superior to EDS since it is always possible to detect the ionization edge if the beam damage can be minimized with a cryo-holder. The downside of EELS is the need for a transparent specimen.

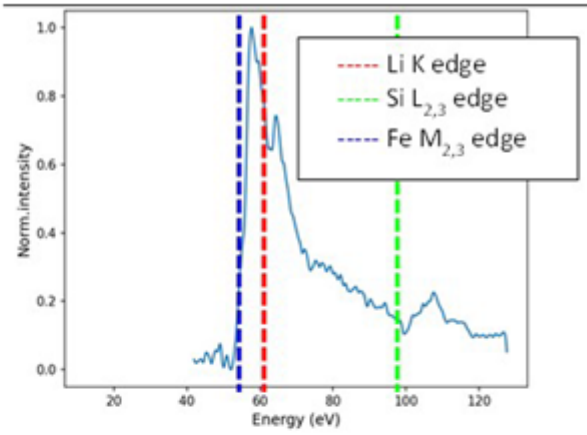

Figure 1-a

EELS spectrum of Li_2FeSiO_4 taken with the Hitachi SU-9000 at 30 keV.

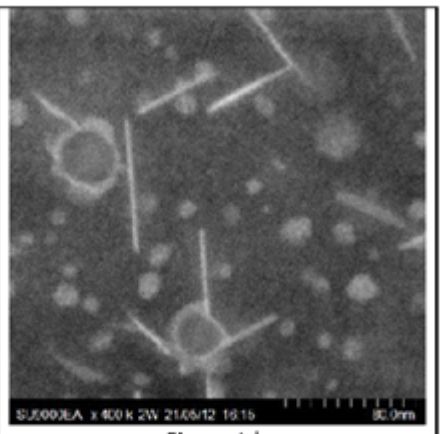

Figure 1-b

Li EELS edge-to-background ratio map of an Al 2099 alloy taken with the Hitachi SU-9000 at 30 keV.

Keywords:

Electron Energy Loss Spectroscopy, Lithium

Reference:

[1] N. Brodusch, H. Demers, A. Gellé, A. Moores, R. Gauvin (2019), Ultramicroscopy, 203, pp.1-36.
[2] P. Hovington, V. Timoshevskii, S. Burgess, H. Demers, P. Statham, R. Gauvin, K. Zaghib (2016), Scanning, 38, 6, pp. 571 – 578.
[3] R. Gauvin et al. (2021), Microscopy and Microanalysis, 27, pp. 1868-1869.

134

Structure analysis on the nm scale: The amorphous LiNbO3 coatings for solid state batteries

Johannes Haust[1], Dr. Jürgen Belz[1], Dr. Shamail Ahmad[1], Mrs. Narges Adeli[1], Mrs. Franziska Hüppe[1], Mrs. Yiran Guo[2], Mr. Linus Erhard[3], Dr. Jochen Rohrer[3], Dr. Anna-Lena Hansen[2], Dr. Valeriu Mereacre[2], Prof. Dr. Karsten Albe[3], Prof. Dr. Kerstin Volz[1]
[1]Philipps University Marburg, Marburg , Germany, [2]Karlsruhe Institute of Technology, Karlsruhe, Germany, [3]Technical University of Darmstadt, Darmstadt, Germany

Poster Group 1

Background
To enhance the chemical stability of a cathode active material (CAM) in a Li ion solid state battery (SSB) a protective coating is applied. Such a coating should have - in addition to the chemical stability - a high Li ion conductivity. LiNbO3 is one material having these properties, which is already successfully applied in SSBs [1,2]. Its ionic conductivity depends strongly on the structure, amorphous LiNbO3 has higher ionic conductivity than crystalline one. This leads to the need of detailed knowledge of the structure and the morphology of the material when applied as thin coating in a battery cell and the correlation of these properties with the electrochemical performance [1].

Methods
In this work we use three different LiNbO3 coatings calcinated at 80°C, 350°C and 550°C on LiNi0.6Co0.2Mn0.2O2 (NCM622) as CAM. To get insights on the structure of the coatings various scanning transmission electron microscopy techniques (STEM) like high angle and virtual annular dark-field imaging (HAADF & VADF), energy dispersive X-Ray spectroscopy (EDS), electron energy loss spectroscopy (EELS) and scanning precession electron diffraction (SPED) were used. To further elucidate the amorphous structure of the coating the reduced pair distribution function (rPDF) [3,4], which contains information about nearest neighbor distances in the material, is calculated from the SPED diffraction patterns. These structural results are then correlated to the electrochemical performance of a battery cell with the respective coated CAM.

Results
HAADF and EDS images show that for the samples calcinated at 350°C and 550°C the coating forms a homogeneous layer covering the entire NCM622 particles. In contrast to that the coating covers only a few parts of the NCM622 particle for the sample calcinated at 80°. SPED measurements show that in the case of 550°C calcination temperature the coating is crystalline whereas for lower calcination temperatures such as 350°C and 80°C the coating is amorphous. Further quantification of the structure of these two amorphous samples through the rPDFs reveals distinct differences in the inter atomic distances. These structural differences of the three samples also influence their electrochemical performance. The battery cell with the coated CAM calcinated at 350°C shows a higher capacity after around 300 cycles compared to the cell with the uncoated CAM. For the cells with the coated CAM calcinated at 550°C and 80°C the capacity during cycling is inferior to the cell with the uncoated CAM.

Conclusion
Correlations between structural results of LiNbO3 coating on NCM622 calcinated at different temperatures to the electrochemical performance of the material in a battery cell show that the best performance is achieved by an amorphous coating covering the whole NCM622 particles. This is achieved at a calcination temperature at 350°C. Higher temperatures lead to a crystalline structure of the coating. Lower temperatures lead to a different amorphous structures as well as an only partial

coverage of the coating. 550°C and 80°C calcination temperature of the coated CAM lead then to a poorer electrochemical performance of the battery cell.

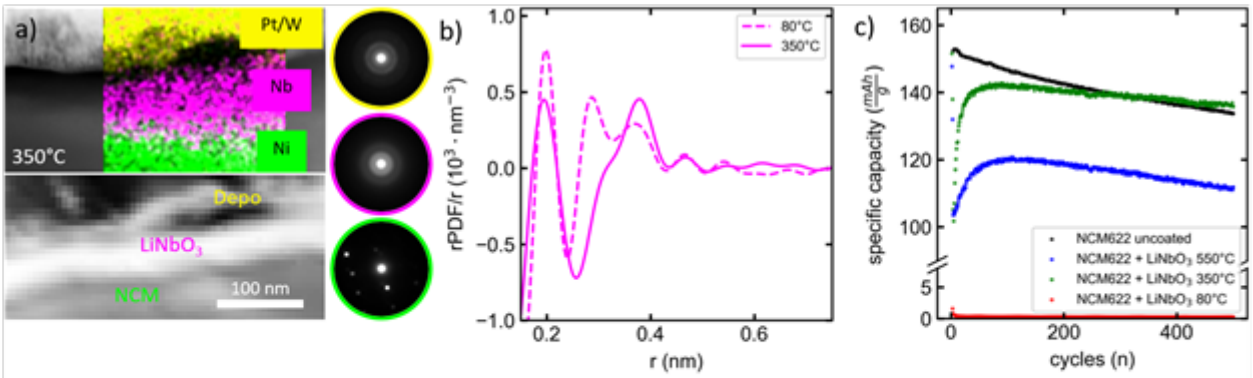

Figure 1 a) top STEM HAADF image of NCM622 coated with $LiNbO_3$ calcinated at 350°C and EDS maps as inset. bottom VADF image of a SPED 4d dataset of the same sample. PED patterns of the NCM, $LiNbO_3$ and the Pt/W depo right show the amorphous nature of the coating. b) rPDF of the diffraction patterns of the $LiNbO_3$ coating with 80°C and 350°C calcination temperature underlining the different amorphous structures of the two samples. c) Electrochemical performance of a battery cell with NCM622 uncoated as well as coated with $LiNbO_3$ calcinated at different temperatures. The cell with the coated CAM calcinated at 350°C shows after around 300 cycles the best performance.

Keywords:

SPED EPDF AMORPHOUS BATTERY COATING

Reference:

1. Weber, D. et al., Eur J Inorg Chem 33 (2020), 3117–3130
2. Walther, F. et al., Chem. Mater. 33 (6) (2021), 2110–2125
3. Tran, D. T. et al., Journal of applied crystallography 50 (Pt 1), 50 (2017), 304–312
4. Ehrhardt, K. M. et al., Chem. Mater. 33 (23) (2021), 8990–9011

166

In situ TEM/EELS and spatially resolved XAS/XRF analysis of CuO electrocatalyst for CO2 reduction

Dr Manfred Erwin Schuster[1], Dr Gea T. van de Kerkhof[2], Dr Angela E. Goode[1], Dr Urša Podbevšek[1]
[1]Johnson Matthey, Sonning Common, United Kingdom, [2]Diamond Light Source, Didcot, United Kingdom

Poster Group 1

Background
Electrochemical devices such as fuel cells and electrolysers enable chemical and energy transformations that are required to help achieve net-zero targets by 2050. One of the emerging technologies is electrochemical reduction of CO2 into value-added products, such as carbon monoxide, formic acid and ethylene. [1] The best performing cathode catalyst for producing ethylene and other C2+ products in a CO2 electrolyser is oxide-derived copper (OD-Cu), which is metallic coper formed in situ via reduction of a copper oxide-based electrode in the electrolyser. The activity of OD-Cu tends to be significantly higher than that of similar Cu catalysts that have been reduced ex situ prior to being incorporated into the electrolyser, which suggests that additional or superior active sites are generated during the in situ electrochemical reduction [2]. In addition, the catalyst can experience significant structural changes under CO2 electroreduction conditions [3]. Obtaining structure-performance relationships of copper requires in situ characterization, which is due to the surface oxidation and possible restructuring the metal experiences when exposed to open circuit potential and air during disassembly of the electrochemical cell. In situ characterisation imaging techniques such as XAS and XRF are therefore a crucial step to capture the active catalyst formation and the morphology dynamics under electrochemical conditions. These techniques suffer from lower spatial resolution, which limits the level of understanding of the underlaying dynamics for reactions involving gases or liquids. This motivated our investigation of the hypothesis that specific conditions of thermal reduction experiments can led to the Cu structures formed under electrochemical conditions. In this way, a higher spatially-resolved analysis could be done by extrapolation from gas-phase investigation.
Methods
In this work we present in-situ TEM gas phase thermal reduction experiments of CuO samples and correlate them with in-situ liquid phase electrochemical reduction of CuO samples carried out on the i14 nanoprobe beamline (Diamond Light Source). Synchrotron-based spectroscopy techniques, such as X-ray absorption spectroscopy (XAS) and X-ray fluorescence spectroscopy (XRF) are very powerful methods to study the chemical nature of the catalyst under relevant conditions [4]. Combining the i14 nanoprobe beamline(down to 50 nm resolution) with aberration corrected electron microscopy (Å resolution) allows to use spatially resolved XRF imaging to study morphology and dynamics in a liquid biasing environment and link it to gas-phase experiments on the nanoscale.

Results/Conclusion
We will show the benefit of combining these techniques to reveal the effect of the thermal reduction on the CuO particles (morphology / oxidation state) through a combination of in-situ STEM imaging and EELS versus the electrochemical reduction as revealed by the in-situ liquid cell i14 XRF/XANES experiment (Figure 1). We will also address the challenges with liquid biasing experiments such as beam-induced damage, especially to the ionomer that is commonly present in catalyst layers (e.g. Nafion), and challenges involved with sample preparation.

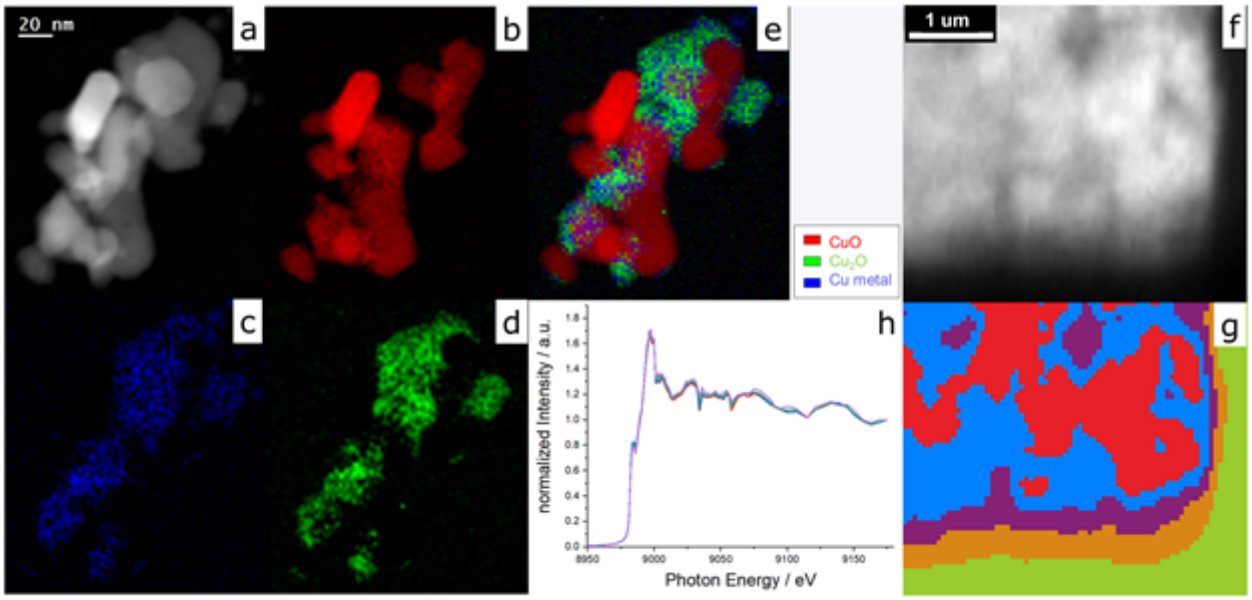

Figure 1: a) STEM HAADF image, Cu L edge EELS map of CuO b), Cu metal c), Cu_2O d) and RGB map of Cu oxidation states at 600°C e); 9.2keV XRF map f), XANES cluster map g) and extracted XANES spectra h) during liquid cell experiment

Keywords:

CO2-reduction, Cu, in-situ, TEM-synchrotron,

Reference:

[1] Stephens, I. E. L. et al.; J. Phys. Energy 4, 042003(2022).
[2] Li, C.; Ciston, J.; Kanan, M.; Nature 508, 504–507(2014).
[3] Amirbeigiarab, R., Tian, J., Herzog, A. et al.; Nat Catal 6, 837–846(2023).
[4] Lin, SC., Chang, CC., Chiu, SY. et al.; Nat Commun 11, 3525,(2020)

183

Materials characterization of recycled batteries (black mass): automated quantitative phase classification in 3D

Ria Mitchell[1], Mr Andy Holwell[1], Dr Richard Taylor[1], Dr Eddy Hill[1]
[1]Carl Zeiss Microscopy Ltd, Cambourne, UK

Poster Group 1

Background incl. aims
Recovery of valuable raw materials from spent batteries (e.g., Cu, Al, Fe, Mn, Ni, Co, Li, P, etc), is important in the shift away from environmentally damaging raw material extraction. The black mass production process starts with the collection and disassembly of the battery. The procedure that follows is akin to the processing of a mineral ore. The disassembled components are shredded to produce the black mass powder, containing the valuable metals. Most processes then treat the black mass with reagents to separate the individual metals. The efficiency of any such process depends on the knowledge of the composition of the black mass, of any impurities it may contain, and how said impurities interact with the reagents to passivate the recovery of the metals. Therefore, the efficient recovery of metals from black mass is dependent on the detailed understanding of its composition. Here, we present novel bulk phase analytical techniques for the 3D characterization of black mass. The use of automated phase classification via X-ray microscopy highlights details of the chemistry and morphology of its constituents non-destructively in 3D, therefore improving the characterization process immeasurably.

Methods
We present a combined workflow using 3D X-ray imaging via a ZEISS Xradia 620 Versa X-ray Microscope (XRM), and advanced reconstruction techniques to enhance contrast, reduce noise, and resolution recovery using the ZEISS Advanced Reconstruction Toolbox (ART). Finally, we use an automated 2D and 3D quantitative phase classification approach in the Scanning Electron Microscope (SEM) and XRM using Mineralogic 2D and 3D, respectively. This combination of approaches in a correlative workflow contribute towards our better understanding of the black mass.

Results
We identify a variety of components of different densities, including foils, separators, and both liberated and non-liberated cathodes containing electrode particles (Figure 1). To enhance the data further, we use modules of the Advanced Reconstruction Toolbox: firstly, ZEISS DeepRecon Pro software, a machine-learning based reconstruction option for advanced de-noising and enhanced contrast. Reconstructing data in this way allows us to collect fewer projections meaning scans are faster and more samples can be imaged. In the black mass, there is a marked improvement in the quality of the data: noise is significantly reduced, and contrast is improved so individual electrode particles are identified with more clarity. Secondly, we apply ZEISS DeepScout software. DeepScout is an AI powered method to upscale scans to a larger field of view whilst preserving high resolution, a form of Resolution Recovery. We increase the field of view by over 2x, enabling us to observe electrode particles at high resolution over a larger area. Both approaches lead to segmentations and quantification representative of a larger sample area without compromising resolution. To quantify the different components within the black mass, we use two complementary approaches: ZEISS Mineralogic 3D and 2D. Mineralogic 3D classifies materials in the 3D XRM data using deep learning to execute automated mineralogy and phase identification. The materials classifier uses the XRM data histogram following DeepRecon Pro reconstruction and identifies two types of battery (LFP and NMC) and two types of foil (Al and Cu), as well as graphite and Al polymer separator. Therefore, we can quantify each of these components and visualize them in 3D to identify the location of valuable

retrievable elements in the black mass. This is further supported by complementary analyses via ZEISS Mineralogic 2D. This is obtained using an SEM with the assistance of the chemical SEM-EDS data, allowing for quantitative phase analyses rather than singular chemical elements alone. In this approach we are also able to quantify the different phases, and understand the location and quantities of recoverable elements such as lithium, manganese, cobalt, aluminum, copper, and iron. Both results indicate that in fact two different battery types are present in this sample, as well as two different types of foil when it was thought that the foils were removed during an earlier part of the black mass production process.

Conclusion

Our results show that it is easily possible to identify and quantify recoverable phases from black mass, which will help towards the battery recycling process. These advanced characterization techniques are imperative to ensure the black mass production process is reliable and exact in a world where valuable constituent recovery from batteries will become essential going into the future.

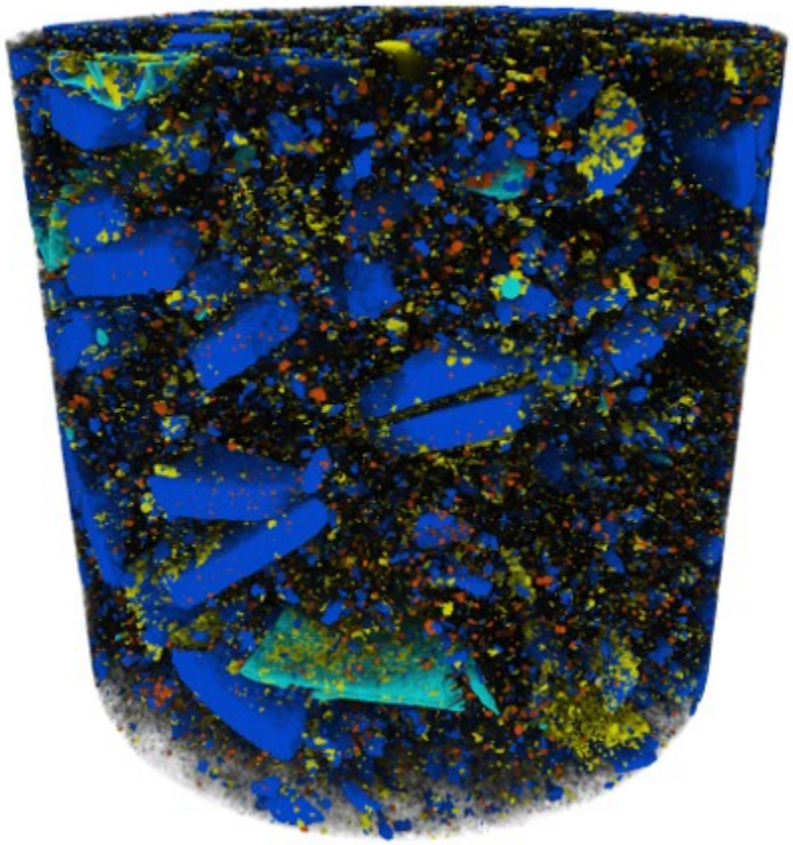

Keywords:

battery recycling, automated mineralogy, tomography

187

Combining in-situ synchrotron and electron microscopy techniques to study NiFe catalysts for CO2 methanation

Dr Manfred Erwin Schuster[1], Dr Pilar Ferrer[2], Dr Rosa Arrigo[3]
[1]Johnson Matthey, Sonning Common, United Kingdom, [2]Diamond Light Source, Didcot, United Kingdom, [3]University of Salford, Manchester , United Kingdom

Poster Group 1

Background
Nickel-based catalysts on various supports have been widely studied for CO2 methanation due to higher activity, nickel's natural abundance, and relative low cost. However, most Ni-based catalysts suffer from deactivation due to carbon deposition, oxidation, sintering, and chemical poisoning. Recently, significant progress has been made in the exploitation of novel/modified Ni-based catalysts for CO2 methanation. As far as the support is concerned, the effect of various supports (CeO2, ZrO2, TiO2, MgO and mixed oxides) on Ni-based catalysts was studied with the goal to increase metal dispersion as well as induce an electronic effect for improving the selectivity towards methane over CO. In our collaborative study we investigated the effect of promoters of both support and active metal on hydrotalcite derived Ni/Al2O3 catalysts. From our catalyst screening experiments, we were able to select TiO2 as best support modifier and Fe as an active metal promoter. Amongst the prepared novel catalysts for CO2 methanation Ni-Fe/Al2O3 and Ni/CeO2-TiO2-ZrO2-Al2O3 were found to be exceptionally active and relatively more stable than commercially available catalysts (Ni/Al2O3). We apply multi-length-scale structural characterization in operando to these systems to gain mechanistic insights of general validity.

Methods
In this contribution we will combine in-situ TEM gas phase experiments with in-situ hard X-ray experiments to reveal the changes of the electronic structure the catalysts undergo under reduction and methanation conditions. We will present a comparative analysis of the following systems: Ni/Al2O3, Ni-Fe/Al2O3, Ni/CeO2-Al2O3 and Ni/CeO2-TiO2-ZrO2-Al2O3. In-situ TEM experiments will be complimented by in-situ gas phase experiments carried out on the i14 nanoprobe beamline utilizing an adapter which allows us to study the sample under the same experimental conditions [1]. This capability allows us to carry out multilength scale in-situ experiments by combined TEM and nanoprobe XANES, thereby linking dynamics observed on a nm- scale with those at the um scale. Mass spectrometer data acquired during the experiments will be used to correlate structural changes with catalytic activity.

Results
Figure 1 shows, as an example, the changes Ni-Fe/Al2O3 undergoes from its fresh form, during reduction at 500°C in H2/He and during reaction conditions at 300°C in a mixture of CO2, H2 and He. The distribution of Ni metal and oxide species as well as the changes in Fe oxidation state as function of the experimental conditions are obtained by in situ EELS mapping. Two regions can be identified: Metallic Ni nanoparticles are exsolved during the hydrogenation step (blue square in Figure 1 a, c), which contain a small amount of Fe; Highly dispersed NiO species are collocated with Fe(II)/Fe(III) species (black and red squares in Figure 1a, c and corresponding EELS spectra in Figure 1 e)). In addition, operando XANES unveil the presence of metallic Ni and Fe species, more so in the core of the particle (Figure 1 f, g).

Conclusion

The comparative analysis of these systems allows to clarify the role of the heteroatoms on the electronic structure of Ni. We will show that similarly to Fe, Ce acts as a sacrificial O-scavenger, maintaining Ni in a metallic state during the methanation thereby favouring methane formation over CO. We will also clarify the role of TiO2 in preserving a high dispersion of Ni.

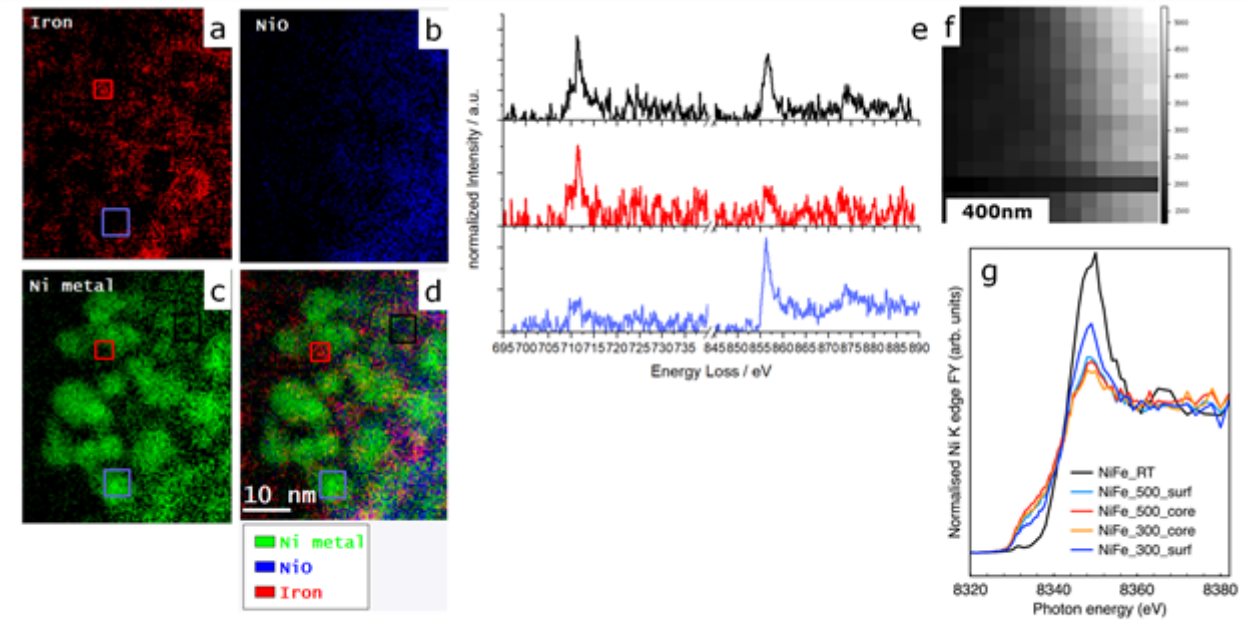

Figure 1: in-situ TEM EELS a) Iron L edge, b) NiO, c) Ni metal L edge EELS map, d) RGB EELS map of Iron, NiO and Ni metal species; e) extracted EELS spectra from ROIs within d) acquired at 300°C in reaction conditions; in-situ hard X-ray 8.5 keV XRF map f) and extracted Ni XANES spectra g) acquired at 300°C in reaction conditions

Keywords:

in-situ, TEM-synchrotron, multilengthscale, CO2-methanation, catalysis

Reference:

[1] J. Synchrotron Rad. 2022, 29, 431-438.

189

Identifying transient defects in exsolution of nanoparticles by semi-quantitative ABF STEM imaging

Andreas Rosnes[1,3], Mr. Holger von Wenchstern[1,3,4], Mr. Jonathan Polfus[2,3], Mr. Øystein Prytz[1,3]
[1]Department of Physics, University of Oslo, Oslo, Norway, [2]Department of Chemistry, University of Oslo, Oslo, Norway, [3]Center for Material Science and Nanotechnology, University of Oslo, Oslo, Norway, [4]Felix-Bloch-Institut, Universität Leipzig, Leipzig, Germany

Poster Group 1

Background

Exsolution enables direct growth of transition metal nanoparticles embedded in metal oxide supports, which are attractive for various electrochemical and catalytic applications for energy conversion and storage. In exsolution, the transition metal is first incorporated into the metal oxide matrix, and exsolve as metal nanoparticles under reducing conditions by diffusion, reduction, nucleation and growth. Foreign cations in perovskites usually substitute the A- or B-site depending on their relative size with respect to the host species. Small transition metals are thus commonly expected to prefer the B-site. However, the exsolution process is observed to be relatively fast, which is unexpected based on the low diffusivity of the B-site with strong covalent bonds to the oxygen octahedra. In similar perovskite systems, it has been suggested that small transition metals favor an interstitial position with square planar coordination adjacent to A-site vacancies [1], as illustrated in fig (a). In this work, the Ni position in A-site deficient La-doped $SrTiO_3$ in the initial stages of exsolution is explored using semi-quantitative STEM. The knowledge obtained will support the development of a microscopic model of the exsolution phenomenon, which can be applied for optimized process strategies for energy conversion and storage applications based on the anchored nanoparticles.

Method

Powders with nominal stoichiometry $La_{0.2}Sr_{0.7}Ti_{0.9}Ni_{0.1}O_3$ were synthesized by solid-state reaction. Exsolution of nickel metal particles were performed by reduction under 5% H_2 in Ar atmosphere at 800 °C for 30 minutes. The relatively large difference in atomic number (Z) between O (Z=8) and Ni (Z=28) is exploited in the STEM images by projecting the matrix along the <100> orientation to isolate the potential interstitial Ni position on the oxygen column. A FEI Titan G2 60-300 instrument with a DCOR Cs probe corrector was operated at 200 kV with a convergence angle of 33.1 mrad to obtain an ABF image from collection angles of 8-34 mrad, suitable to image the lighter element columns. The Z-dependency was identified using the multislice method as implemented in the abTEM package [2] by simulating STEM images with the experimental conditions for a thickness-defocus series of an ideal $SrTiO_3$ structure, and for an atomic model with an interstitial Ni and A-site vacancies. The experimental column intensities were determined by fitting 2D Gaussians using the Atomap package [3]. A statistical-model based approach based on Akaike and Bayesian Information Criterion (AIC, BIC) was utilized for fitting the intensity histogram to identify the most likely independent intensity contributions. The semi-quantitative approach proposed by Aarholt et al. [4] was adopted to identify the point defect from the relative intensities of the columns.

Results

As a rule of thumb, the intensity of ABF images is proportional to Z^a with a = 1.3 which originates from a balance between elastic and thermal scattering that are most dominant for lighter and heavier atoms, respectively.[5] However, changes in collection angle, thickness, defocus, and atomic number may alter this Z-dependency. By simulating a thickness-defocus map of ABF images of the ideal <100>-orientated $SrTiO_3$ structure with the employed collection angles, a linear Z-dependency is

identified from the ratio between the intensities of the Ti- and Sr-columns, as seen in fig 1(b). From the simulated ABF image of the atomic models with interstitial Ni located on the O-column in fig (c), a split in a histogram of integrated intensities of the columns is expected to be observed in the experimental ABF image.
In fig (d), the experimental ABF image of the exsolved sample on the <100> orientation is presented with the inset illustrating the location of the 2D Gaussians fitted to the atomic columns. A statistical-model approach based on the integrated classification likelihood is adopted to avoid under- and overfitting the histogram of intensities, and to avoid biased interpretations. From fitting an increasing number of Gaussians, one calculates a score based on maximizing the log-likelihood function of the fit while penalizing the number of components and their complexity, which in our case, was done according to AIC and BIC. The log-likelihood function has a negative pre-factor, meaning a lower score indicates a higher likelihood of a valid physical description of the experimental data by the model. Both criteria agree on a three-component model for the optimized fit of the histogram of the integrated intensities of the 2D Gaussians of the O-column, seen in fig (e) and (f). There is, however, no guarantee of a physical validity of the model despite a good fit, but from the interpretation of the ratio of the mean value of component 2 and 3, the ratio becomes 1.23 ± 0.14 which results in an average Z of 9.83 ± 1.11 given a linear Z-dependency and interpreting component 2 as the O-column. The calculated value of 1 Ni for every 10 O provides an average Z of 9.82. While the absolute quantification of the number of Ni on the O-columns is challenging, the results indicate the presence of a foreign species on the columns which may be Ni. The first component can be interpreted as O-columns with a high number of oxygen vacancies generated due to the reducing environment.

Conclusion

A semi-quantitative approach utilizing the open-source packages abTEM and Atomap was adopted to identify the defect position of Ni in A-site deficient La-doped $SrTiO_3$ upon exsolution under reducing atmospheres. Simulated multislice images show a linear Z-dependency for the experimental conditions used. The intensity distribution of the O-columns in the experimental ABF image is best modelled using three Gaussians. The component of highest intensities holds a relative mean value to the main component that agrees with a calculated intensity ratio for the presence of Ni using linear Z-dependency. The interstitial defect position of Ni is expected to play an important role in the diffusion step of the exsolution process.

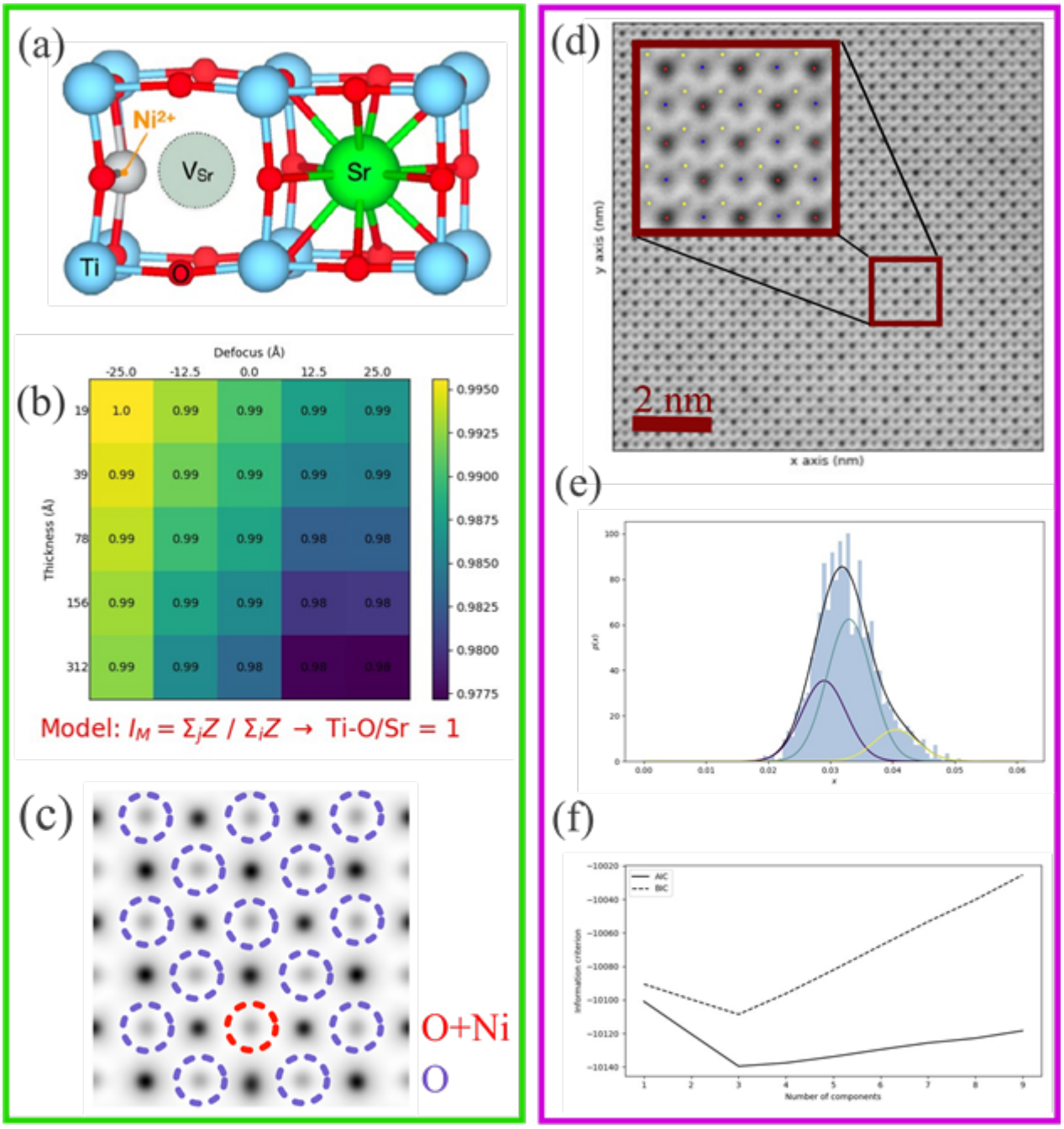

Fig: (a) Atomic model of interstitial Ni adjacent to an A-site vacancies in SrTiO3. (b) Quantification of relative intensity of Ti-O/Sr for a thickness-defocus map shows a linear Z-dependency. (c) <100> ABF STEM image of atomic model with the defects. (d) Experimental ABF STEM image with magnified image of fitted gaussians on the Sr- (red), Ti- (blue), and O-column (yellow). (e) Histogram of intensity from integration of 2D gaussians fitted to the experimental O-columns with the three optimized components identified using the (f) plot of the Akaike and Bayesian Information Criterion.

Keywords:

Point defects, Quantitative STEM, Open-source

Reference:

1. Polfus et al. J. Mater. Chem A. 2016;May 24;4(21):8105–12.
2. Madsen J, Susi T. Microscopy and Microanalysis. 2023 Jul 22;29(Supplement_1):680–680.
3. Nord M et al.Adv Struct Chem Imag. 2017 Dec;3(1):9.
4. Aarholt T, Frodason YK, Prytz Ø. Ultramicroscopy. 2020 Feb;209:112884.
5. Findlay SD et al. Ultramicroscopy. 2010 Jun 1;110(7):903–23.

210

A crystallographic aspect of Li metal anodes: Understanding the functionality of lithium-ion all-solid-state batteries

Dr Pawel Nowakowski[1], PhD Cecile Bonifacio[1], Mrs Mary Ray[1], Mr Paul Fischione[1]
[1]Fischione Instruments, Export, USA

Poster Group 1

Background

Enabling the use of Li metal as an anode in all-solid-state batteries (ASSB) promises higher energy density and safer operation when compared to current Li-ion batteries due to the integration of nonflammable solid-state electrolyte. Increasing demand for safe electrical energy storage, especially in the transportation sector, has resulted in rapid and continuous growth of ASSB research [1].
It is undeniable that both cathode and anode microstructure have a direct impact on battery cell performance. The coulombic output, charge and discharge rates, and life cycle depend on grain size, boundary characteristics, and crystal orientation (texture). The small grain size tends to increase electrical resistivity, which degrades battery performance. High-angle grain boundaries are the most resistive due to corresponding strain fields, which are the result of high dislocation densities. Crystal orientation can promote intercalation, prohibit intercalation, or increase instability [2]. For example, closely packed crystallographic planes (grain facets) are favorable for higher ion mobility. Considering the many microstructural parameters and relationships between them, it is critical to evaluate the best candidate for Li metal anode before battery fabrication.
However, there is little work reported on the microstructural characterization, which allows for the evaluation and comparison of various lithium metal sources.
Li is highly sensitive to oxygen, nitrogen, water, and carbon dioxide, which makes sample preparation for microstructural characterization impossible in ambient atmosphere. Lithium is also a very soft material, and its crystallographic structure can be easily damaged by mechanical interaction. The inherent characteristics of lithium metal demand a controlled environment workflow from sample preparation to structural investigation in a scanning electron microscope (SEM). In the past few years, considerable effort has been devoted to developing accurate sample transfer technology [3].
We demonstrate a workflow that allows the evaluation and comparison of different lithium anode sources. The workflow consists of cryogenic broad Ar ion beam milling sample preparation, cryogenic sample transfer to the SEM, and microstructural characterizations. We will discuss the challenges of cryogenic observations in the SEM. All results are supported by energy dispersive X-ray spectroscopy (EDS) and backscatter electron diffraction (EBSD) measurements.

Methods

All samples [pure Li metal ribbons, Sigma-Aldrich] were prepared using a broad Ar ion beam milling system [TrionMill, Fischione Instruments]. The samples were transferred from the ion mill to a Ga FIB system [Scios DualBeam, Thermo Fisher Scientific] using cryo transfer [Actively Cooled Transfer device, Quorum Technologies Ltd. / Fischione Instruments]. The Scios DualBeam is equipped with a PP3004 airlock and PP3005 SEM/FIB cryo stage [Quorum Technologies Ltd.] All SEM analytical measurements were done using an X-Max 150 mm2 EDS detector coupled with Aztec software [Oxford Instruments] and e-FlashFS EBSD detector combined with Esprit software [Bruker Nano Analytics].

Results and conclusions

Three lithium sheets (Li-1, Li-2, and Li-3) were compared. Figure 1 shows the inverse pole figure (IPF) color-coded EBSD maps for the three samples. The average grain size is 100 µm, 150 µm, and 1150 µm (Li-1, Li-2, and Li-3, respectively). Figure 2 represents corresponding pole figures. Note that multiple maps acquired from different sample regions were used for average grain size and texture determination for each sample. Sample L1-1 is characterized by {110}<001> texture, sample L1-2 has strong rotated cube texture {100}<011> in the rolling (RD), transverse (TD), and normal (ND) reference directions, while sample Li-3 represents random texture. If one of these materials was integrated as an anode material to ASSB, the normal direction would be aligned with the Li+ mobility direction between the anode and cathode.

The {110} crystal facets have the lowest surface energy and the closely packed atom arrangement for body-centered cubic lithium structure; these characteristics contribute to high Li diffusivity, which improves cycling stability and battery lifetime [4]. Large grains are more desirable for high coulombic output, while small grains are not [5]. Therefore, larger grain sizes combined with a {110}<001> texture would be the best choice for a Li metal anode because it is likely to provide the best battery performance.

Accurately evaluating lithium anode microstructure is critically important to developing superior battery performance.

Fig. 1. Inverse pole figure, color-coded EBSD maps acquired from sample Li-1 (a), sample Li-2 (b) and Li-3 (c).

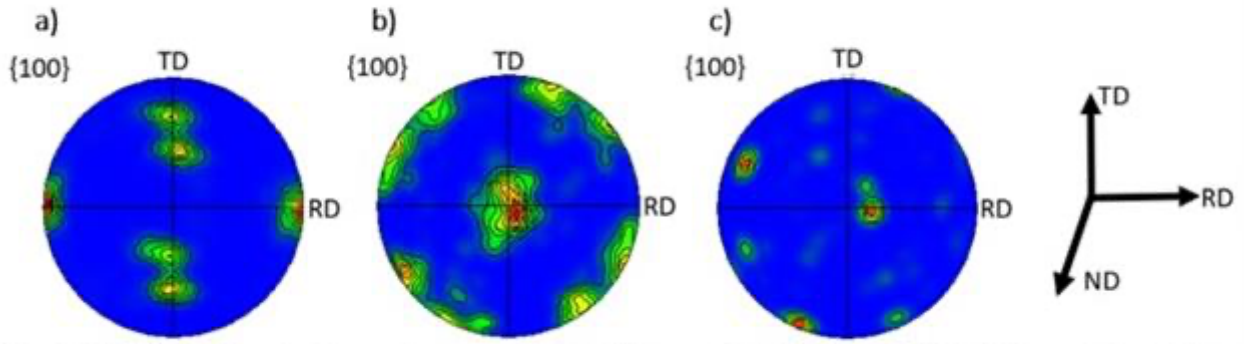

Fig. 2. EBSD {100} pole figures from sample Li-1 (a), sample Li-2 (b) and Li-3 (c). Presented statistics were calculated over at least four maps per each sample acquired from different sample regions.

Keywords:

Li-ion battery, texture, microstructure, BIB

Reference:

1. B. Stéphanie, et al., International Energy Agency, http://iea.li/nzeroadmap (accessed on Jan 31, 2023).
2. A. Quinn, et al., Cell Reports Physical Science, 1, 8 (2020).
3. N. Stephant, et al., Micron, 110 (2018).
4. R. Hendriks, et al., ACS Applied Energy Materials, 1, 12 (2018)
5. B.L. Mehdi, et al., Scientific Reports, 6, 1 (2016).

230

New Workflows and Innovations for Maximizing Relevance of In Situ TEM Results for Liquid-Based Applications

Mrs. Jennifer Mcconnell[1], Dr. Madeline Dressel Dukes[1], Dr. Nynke Krans[1], Dr. Yaofeng Guo[1], Dr. Tim Eldred[1], Dr. Kate Stephens[1], Franklin Walden[1], Patrick Wellborn[1], Dr. David Nackashi[1], Dr. John Damiano[1]
[1]Protochips, Morrisville, United States of America

Poster Group 1

Background
Over the last 20 years, in situ (scanning) transmission electron microscopy [(S)TEM] has become an established experimental technique, driving innovation in material design and supporting new applications-based research strategies [1]. Its unique combination of ultra-high resolution imaging/analysis and relevant in situ sample environments has opened a new window into understanding material performance and degradation over time [2-3]. The goal of in situ TEM research is understanding the relationship between the structure of a material and its resulting function. Once commercial in situ TEM systems became available, a new set of experimental challenges revealed themselves: creating reproducible sample preparation that does not alter material behavior, understanding how to properly scale an experiment from bulk to nanoscale, keeping accurate records of the tens or hundreds of changing parameters utilized during an experiment, understanding electron beam effects, and managing/visualization of large amounts of data. While the ability for the in situ TEM system to produce pertinent environmental conditions is incredibly important to the relevance of the results, it is equally important to have a reliable means of streamlining all steps of the experimental workflow surrounding the in situ TEM experiment itself. Here we describe recent advancements supporting the entire in situ TEM workflow, from sample preparation to in situ conditions to data publication, that increase the reproducibility and relevance of the results while also providing compliance with FAIR principles [4]. Examples to be discussed are related to the global push for more efficient, cost-effective, and environmentally friendly means of energy storage and generation: batteries, electrocatalyst, and nanomaterial chemistry and growth.
Methods
All results discussed use Protochips in situ TEM solutions equipped with AXON machine vision software. Protochips in situ solutions are flexibly designed to create the most relevant in situ environments for a variety of materials in different research areas while being optimized for important analytical techniques such as EDX, EELS, iDPC, 4D-STEM, and others. Sample supports are MEMS-based silicon chips, called E-chips, that are designed and fabricated in-house at Protochips with input from scientific experts in the community. Functional measurements are done with high-sensitivity, low-noise potentiostats and highly sensitive source measuring units (SMUs). Liquid-phase electrochemical experiments are performed with Poseidon AX Liquid Cell system and newly added capabilities will be shown, such as standard reference electrodes, flow management E-chips, and others. The electron beam is calibrated and dose/dose rate are measured and recorded using the AXON Dose module. Stabilization of dynamic samples is done live with automated physical drift correction from the AXON Synchronicity module. Visualization and export of results are done offline with the AXON Studio module.
Results
Data from a wide array of research areas such as liquid-based batteries, electrocatalysts, nanomaterial synthesis chemistry, and corrosion will be discussed. The in situ TEM workflow involves multiple different facets: sample preparation onto E-chips, experiment optimization outside the TEM, data collection of dynamic materials, production of in-situ conditions that are relevant to the material's operational or native environment, and alignment of structural data (TEM) with functional

data (mass spectrometry, cyclic voltammetry, etc.) for trend identification (Fig. 1). Each part of the integrated workflow will be discussed, describing the recent innovations that support proper scaling from bulk to nanoscale, accelerating productivity in and outside the lab, and fostering collaboration and discovery with local and global collaborators. Utilizing these new innovations will significantly improve experimental reproducibility, strengthen the relevance of results to applications-focused communities and enable more publications in application-specific journals, as well as lower the learning curve to in situ TEM for new researchers.

Conclusions

In situ TEM is clearly gaining traction as an important technique for application-focused research strategies alongside traditional bulk, macro, and mesoscale techniques. Relevant in situ TEM results can provide the most direct window towards innovations for improved materials. Increasing the relevance of the results not only lies in creating new environmental capabilities and in situ stimuli, but in innovations for all the steps involved in the scientific workflow. From reproducible sample preparation to data management and visualization, the entirety of the workflow needs to be considered when planning for and incorporating in situ TEM into applications-based research.

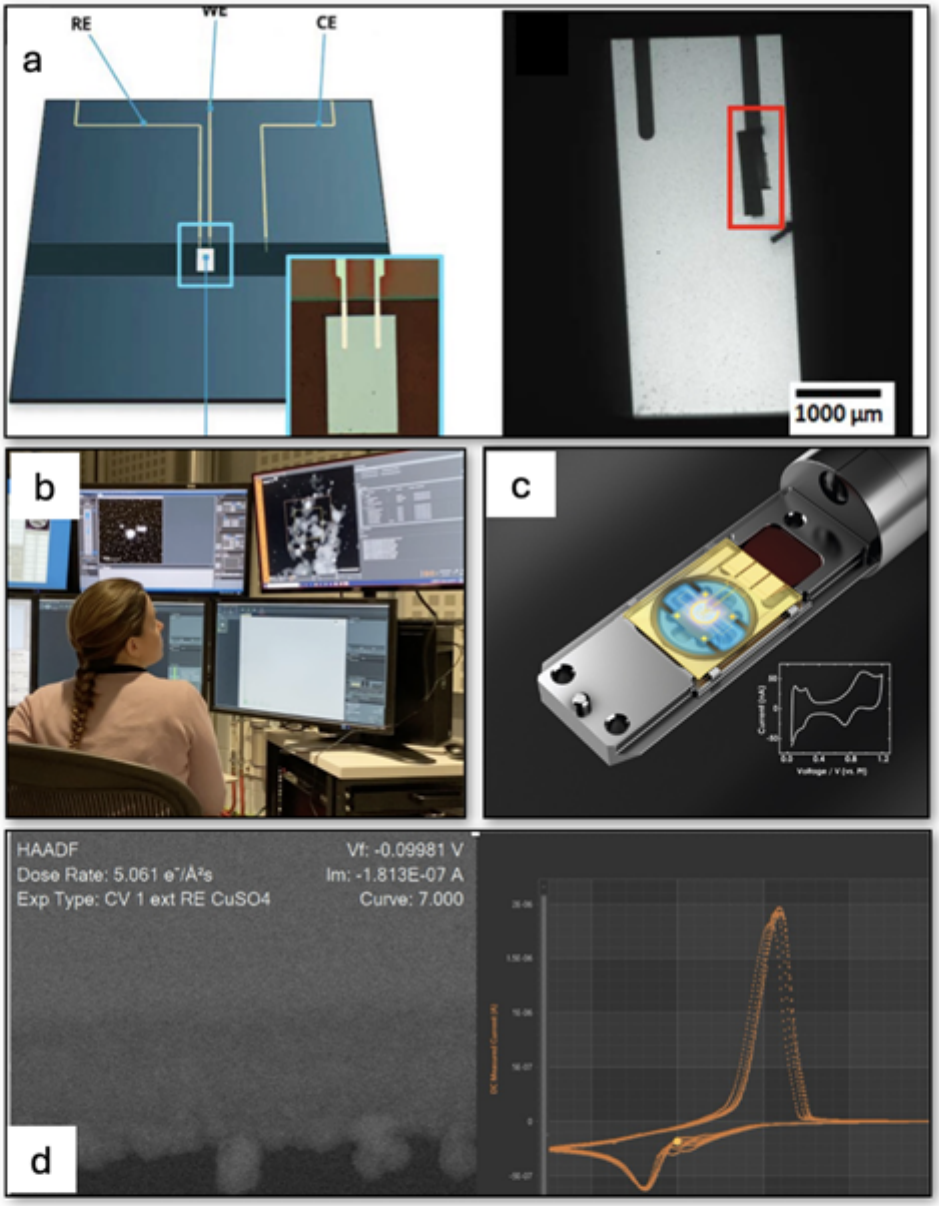

Fig. 1. Representative images from each step of the in-situ TEM workflow: sample preparation, data collection, analysis of materials in situ, and publication. a) sample preparation onto MEMS-based E-chips, in this case FIB lamella preparation onto E-chips for battery-related investigation [5], b) collection of in-situ data using AXON modules for live physical stabilization and parameter recording and alignment, c) in situ analysis, in this case, electrochemical analysis with Protochips Poseidon AX system, and d) publication using AXON Studio for data visualization, trend analysis, and ultimately video generation for reports and publications regarding electrochemical investigation of dendrite growth. Structural and functional data are automatically aligned and reported side-by-side.

Keywords:

innovation, new technology, in situ,

Reference:

[1] ACS Nano 2022, 16, 10, 15503–15511
[2] Nature 2023 614,7947, 262-269
[3] ACS Nano 2023, 17, 20, 20434–20444
[4] Scientific Data 2016, 3, 160018
[5] Small Methods 2022, 6, 2100891

236

Electron Channeling Contrast Imaging (ECCI) of Ion Battery Cathode Materials

Ph.d. Candidate Meysam Naghizadeh[1], Dr. Chisu Kim[2], Pr. Raynald Gauvin[1]
[1]Department of Mining and Materials Engineering, McGill University, Montréal, Canada, [2]Center of Excellence in Transportation Electrification and Energy Storage Hydro Québec, Varennes, Canada

Poster Group 1

The microstructural characterization of ion battery cathode materials is often studied by transmission electron microscope (TEM) due to its high spatial and angular resolution which enables precise analysis of the battery materials. However, TEM studies present several challenges that might hinder their suitability for numerous potential applications. The conventional processes of preparing thin foils for TEM analysis, such as twin jet electropolishing, are time consuming and expensive. Moreover, when high-energy electron beams interact with the specimen in TEM, the studied sample may experience damage through various mechanisms, including knock-on displacement, radiolysis, and heating, leading to changes in the microstructure and properties of materials, particularly those sensitive to beams [1,2]. Here, another interesting approach for bulk specimens is presented that offers both a high spatial resolution and a large field of view at relatively low accelerating voltages: the use of ECCI in a field emission scanning electron microscope (FESEM). ECCI is an imaging method that relies on the change of backscattered electron (BSE) intensity caused by differences in the angle between the incoming electron beam and the crystallographic orientation of the lattice planes in crystalline samples. When the incoming electrons are parallel (or very close to parallel) to the lattice planes, low BSE intensity and hence a darker area can be anticipated, while with the increase in the angle, higher intensity and a brighter area are expected. ECCI technique allows us to figure out how the specimen's crystallographic orientation changes, along with identifying features like grain boundaries and cracks, as well as individual lattice defects such as dislocations [3,4].
In this study, the microstructural evolution of two different layered Li-ion based (composed of secondary particles) and Na-ion based (composed of primary particles) cathode materials in their pristine state was investigated. High resolution secondary electron (SE) and ECC images were acquired with the use of Hitachi SU8000 dedicated FESEM at a relatively low accelerating voltage of 4 kV. For this purpose, cross-sectional samples were prepared using a Hitachi IM4000 ion milling machine.
Figures 1a and b show the SE and ECC cross-sectional images of a Li-ion based cathode polycrystalline secondary particle. The secondary particle comprises many single crystalline primary particles. Primary particles are simply like the 3-dimensional grains found in conventional polycrystalline metallic materials with different crystal orientations. As can be seen in Figures 1a and b, the primary particles cannot be well recognized in the SE image (Figure 1a), while in the ECC image they are completely clear with very well-defined grain boundaries thanks to the ECCI technique (Figure 1b). Furthermore, the imperfections between the primary particles such as voids and pores are more evident with sharp edges in the ECC image compared to the SE image.
The SE and ECC cross-sectional images of a Na-ion based cathode single crystalline primary particle are represented in Figures 1c and d. The SE image displays the primary particle with an irregular shape without any distinguished lattice features (Figure 1c). However, the ECC image depicts the same particle with two clearly visible features shown by yellow arrows: I) coincidence site lattice boundary (CSLB) and II) intragranular crack along the CSLB as a preferential site for crack initiation (Figure 1d). In an earlier study by the authors [5], the presence of CSLBs in the same specimen has been shown with the aid of Hitachi SU9000 scanning transmission electron microscope (STEM). Conclusively, this work unraveled the unique role of ECCI technique as a perfect microanalysis tool for reasonably priced and rapid investigation of the cathode battery materials.

Figure 1. a) SE and b) ECC cross-sectional images of a Li-ion based cathode polycrystalline secondary particle. c) SE and d) ECC cross-sectional images of a Na-ion based cathode single crystalline primary particle.

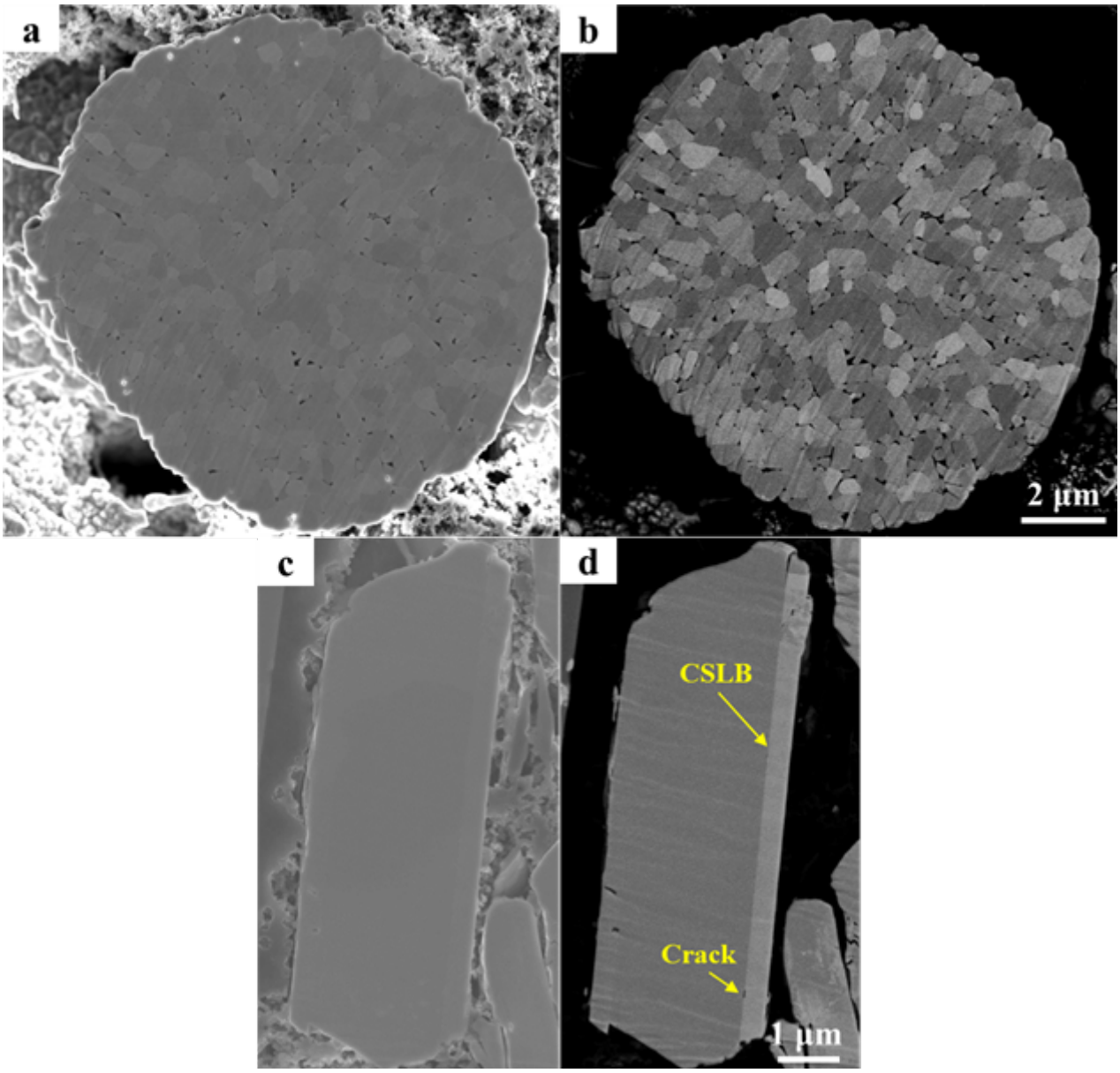

Keywords:

ECCI, Battery, Cathode, Grain Boundary

Reference:

[1] Y. Wen et al., NPG Asia Materials, 9 (2017), e360.
[2] J. Cui et al., Advanced Materials, 33 (2021), 2000699.
[3] S. Kaboli et al., Microscopy and Microanalysis, 19 (2013), pp. 1620-1631.
[4] D.C. Joy et al., Journal of Applied Physics, 53 (1982), pp. R81-R122.
[5] M. Naghizadeh et al., Microscopy and Microanalysis, 29 (2023), pp. 1331-1332.

287

STEM, PED and EELS: A powerful combination for the investigation of cathode-active-materials for batteries

Thomas Demuth[1], Dr. Michael Malaki[1], Dr. Shamail Ahmed[1], Dr. Philipp Kurzhals[2,3], Dr. Andreas Beyer[1], Prof. Dr. Jürgen Janek[2], Prof. Dr. Kerstin Volz[1]
[1]Materials Science Center (WZMW) and Department of Physics, Philipps Universität Marburg, Marburg, Germany, [2]Institute of Physical Chemistry & Center for Material Research, Justus-Liebig-University, Gießen, Germany, [3]BASF SE, New Battery Materials and Systems, Ludwigshafen, Germany

Poster Group 1

Background incl. aims

With the ever-increasing demand for high-capacity and high-power energy storage systems, solid-state batteries and their components are subject of intense research [1].The Cathode Active Material (CAM) is the main component contributing to the battery's specific energy as well as its cost [2]. State-of-the-art CAMs are transition metal oxides of the form Li (Ni_(1-x-y) Co_x Mn_y) O_2 [3]. To increase the specific energy and simultaneously decrease the cost of the CAM, high Ni contents above 95% are desired [4]. However, these Ni-rich CAMs suffer from rapid capacity fade due to degradation during cycling, forming a rock-salt-like NiO phase [5]. To detect and understand these degradation processes at the micro- and nanoscale, we investigate $LiNiO_2$ (LNO) sintered at different temperatures as a model system for Ni-rich CAMs utilizing transmission electron microscopy techniques. Here, we demonstrate the effectiveness of combining direct imaging, diffraction, and spectroscopy for investigating LNO secondary particles across various length scales. High Angle Annular Darkfield Scanning Transmission Electron Microscopy (HAADF STEM) can provide high-resolution images at atomic resolution. However, the data acquisition is locally confined to an area of a few hundred nanometers and the differentiation between similar structures of different phases may not always be unambiguous. Complementary, Precession Electron Diffraction (PED) offers detailed information about the phase and orientation of entire CAM particles with a local resolution in the nanometer range, but this information relies on previous knowledge about the expected phases as input. Thus, unknown inter- and mixed phases cannot be identified, which necessitates validation by other measuring techniques. Electron Energy Loss Spectroscopy (EELS) provides insight into the elements present in the CAM and their bonding environment, which effectively complements PED and STEM measurements.

Methods

The lamellae for TEM investigation were prepared by focused ion beam milling with a JEOL JIB 4601F dual-beam system. A beam of Ga ions with varying energies from 30 kV to 5 kV was employed to thin the samples to a thickness below 100 nm. HAADF STEM images as well as the EELS spectra were recorded on a double Cs-corrected JEOL JEM 2200FS microscope operated at 200 kV. The PED data sets were recorded on a JEOL JEM 3010 operated at 300 kV. Scanning and precession of the beam were realized by employing the NanoMEGAS ASTAR and Topspin System.

Results

During our investigation of LNO primary particles using STEM, we observed several regions that cannot unambiguously be assigned to either the layered $LiNiO_2$ phase or the degraded rock-salt-like NiO phase solely based on the high-resolution HAADF STEM images. One example is depicted in the attached Figure. On the bottom, the layered LNO phase in (210) orientation is easily recognizable. In the center of the micrograph, a structural transformation occurs, resulting in a different structure on the top. However, from the HAADF STEM image alone it is unclear whether it is the layered phase in (211) orientation or the NiO phase in (210) orientation, as both structures exhibit nearly identical

atomic positions of transition metals, which are mainly detected in HAADF STEM. In this context, a PED dataset, which correlates recorded diffraction patterns with computed diffraction patterns of the expected phases, can provide valuable information regarding the phase and orientation of the measured particle. A PED orientation map of the investigated primary particle is presented in the attached Figure. Regions of the same color exhibit the same crystallographic phase and orientation. The diffraction patterns of the layered phase better match than those of the NiO phase, confirming that the layered LNO phase is not degraded but is present in a different orientation. However, in addition to the two prominent orientations highlighted in green and orange on the PED orientation map, a thin purple region appears at the surface of the particle close to the vacuum, matching the NiO rock-salt phase. Since the sample's thickness affects which diffraction spots appear in the PED pattern, it is essential to verify whether the recorded pattern results from the presence of a different phase or from a thickness effect at the grain's edge. Moreover, the PED algorithm always matches one of the pre-input phases with the recorded data, leaving uncertainty regarding whether the proposed phase truly exists in the sample or if it resembles one of the matched phases but is actually a new, unknown phase. In this regard, spectroscopic methods such as EELS can complement PED measurements. As EELS is sensitive to the oxygen bonding environment, LNO and NiO exhibit different O EELS signatures. Particularly, the oxygen pre-peak at 527 eV is characteristic of transition metal layer oxides and absent in NiO, serving as a reliable indicator for phase determination. In the observed LNO particles, the O pre-peak is evident in the bulk but absent at the surface of the investigated grain, consistent with the PED results. Representative EEL spectra from both bulk and surface regions are provided in the Figure. By combining locally resolved STEM measurements with PED datasets of the entire secondary particle and spectroscopic measurements, we conclude that degradation of the pristine layered LNO particles occurs not only at the surface of the secondary particle but also at the grain boundaries of the primary particles within the secondary particle. The degree of degradation correlates with the sintering temperature, whereas a higher sintering temperature leads to more severe degradation.

Conclusion

We combined the results of HAADF STEM, PED, and EELS measurements of LNO secondary particles sintered at different temperatures as a model system for the investigation of degradation processes in Ni-rich CAMs. These techniques complement each other exceptionally well, providing a comprehensive understanding of the material's properties beyond what can be achieved through individual measurements alone.

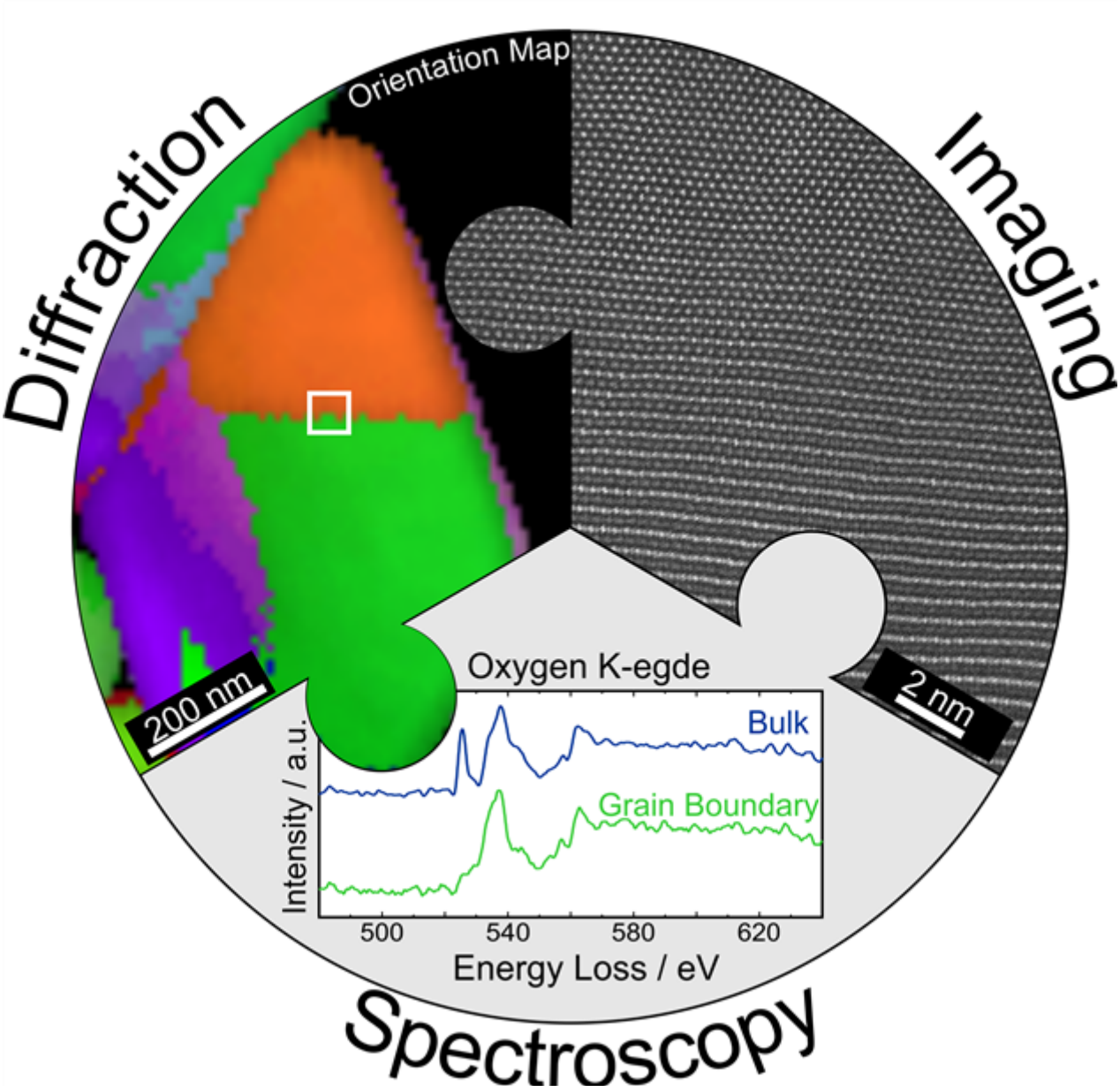

Keywords:

STEM, PED, EELS, CAM, Battery

Reference:

[1] Roitzheim et al, ACS Appl. Energy Mater. 2022, 5, 6913−6926
[2] Minnmann et al., Adv. Energy Mater. 2022, 12, 2201425
[3] Kurzhals et al., J. Electrochem. Soc., 2021, 168, 110518
[4] Bianchini et al., J. Mater. Chem. A, 2020, 8, 1808
[5] Ahmed et al., Adv. Energy Mater. 2020, 2001026

290

A Real Space Understanding of Short Range Order in Disordered Rocksalt Cathodes

Dr Emma Hedley[1], Mr Liquan Pi[2], Prof. Peter G. Bruce[2,3,4], Prof. Peter D. Nellist[2]
[1]Monash University, Melbourne, Australia, [2]University of Oxford, Oxford, United Kingdom, [3]Faraday Institution, Didcot, United Kingdom, [4]The Henry Royce Institute, Oxford, United Kingdom

Poster Group 1

Background

Disordered rocksalts (DRS) have a rocksalt structure, with the disordered nature relating to compositional disorder, predominately on the cation sublattice, which generally contains lithium and some combination of transition metals. In some instances, disorder can also be present in the anion lattice when fluorine is added to the composition.
They have emerged recently as an alternative to layered cathode structures in Li-ion batteries. These materials have attracted commercial and scientific interest because of their potential to enable fully cobalt-free, high-energy density cathodes [1]. DRS cathodes do not have a well-defined layered structure through which lithium can move in and out of the material as in most well-established commercial materials. Instead, lithium is understood to percolate through the material by hopping from one octahedral site to the next, via the tetrahedral interstitials. The energetics of the tetrahedral interstitials are proposed to be related to the surrounding ions [2]. This process can only occur when a network of such sites is formed on a length scale matching the particle size. Short-range order (SRO) and its inherent correlation with local arrangements of atoms play a critical role in determining the ability of lithium to migrate reversibly through the material [3]. This study aims to demonstrate the capability of STEM imaging methods to provide insights into the local arrangements of atoms associated with the SRO.

Methods

The presence of highly structured diffuse scattering in electron diffraction patterns, such as that observed in Figure 1a, has been widely used to indicate the presence of SRO in these materials [3]. Still, to the best of our knowledge, no precise understanding of the nature of this ordering has been achieved. Diffuse scattering of a similar nature has been observed in other materials understood to contain SRO; and is widely discussed as being related to correlations of lattice sites associated with polyhedral geometries, such as the octahedral cluster depicted in Figure 1b. These polyhedra are understood to correspond to three-dimensional loci in reciprocal space, from which the electron diffraction of a particular reciprocal lattice plane can be understood as the intersection of the lattice plane with the three-dimensional loci, illustrated in Figure 1c [4]. However, electron diffraction does not give precise local information about the distribution of the ordering within a particle nor does it identify the composition of the correlated clusters. The Z-contrast nature of annular dark field (ADF) imaging is demonstrated to be sensitive to the SRO by the presence of the diffuse scattering features in the Fourier transform of ADF images (Figure 1d and 1e).

Results

In this study, we develop a method of understanding these features by suppressing contrast from the Bragg reflections in the lattice from ADF images which show intensity variations in neighbouring atomic columns. Extending on this, we demonstrate a real-space method based on calculating the inverse Fourier transform of the square modulus of the Fourier transform, which we refer to as a correlograph, to identify the nature of the correlations in real space, as demonstrated in Figure 1f. The inset region in Figure 1f shows the correlograph and identifies both positive and negative correlations on a filtered image where the lattice contrast has been suppressed.

Conclusions

The method proposed in this study allows distinct differences in the SRO to be interpreted from the ADF images that arise from composition variations. These differences in terms of the homogeneity of the SRO and composition of the clusters can't be distinguished from the diffraction data alone. This method enables us a new understanding of the SRO and, in turn, a link between the structural units of the SRO and the ability of the materials to sustain lithium percolation.

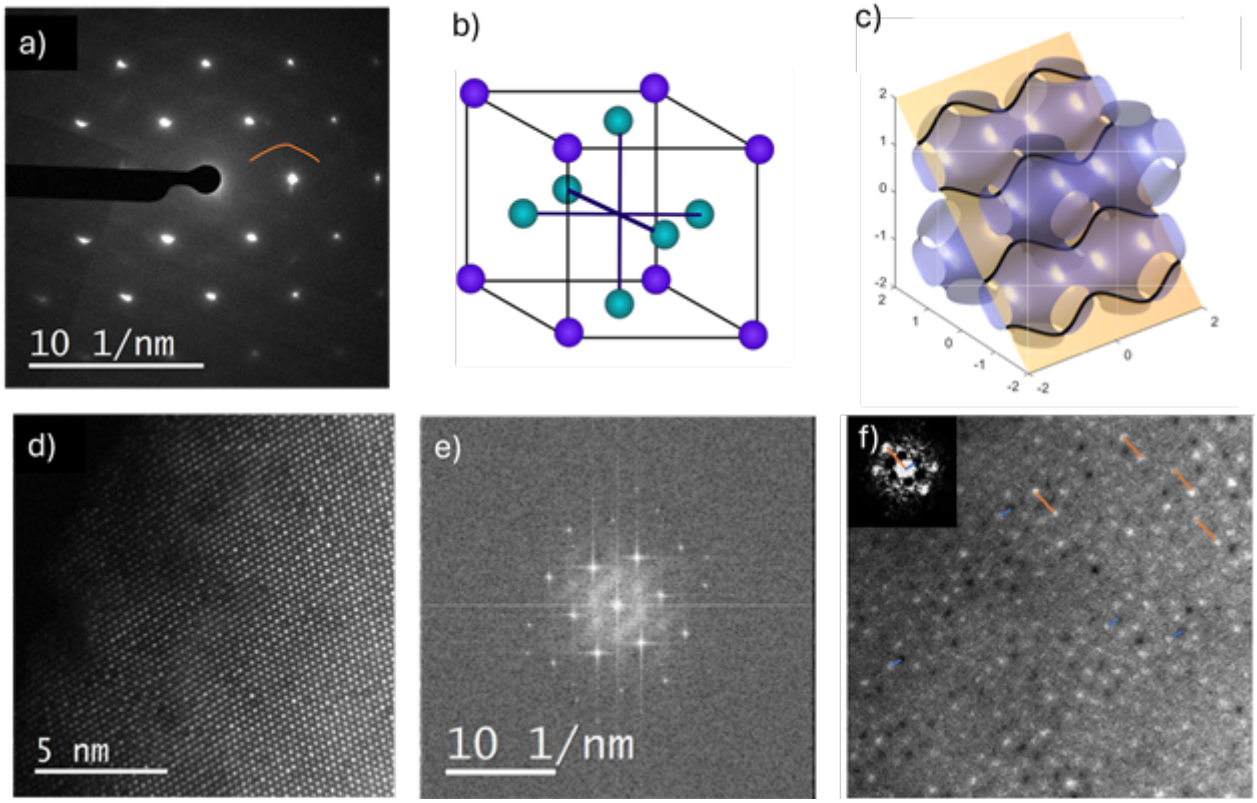

Keywords:

Disordered-Rocksalts
STEM
Energy-Materials
ADF

Reference:

1. Z. Lun et al., Nature Materials, 2021, 20, 214–221
2. . Urban, J. Lee, and G. Ceder, Advanced Energy Materials, 2014, 4, 400-478
3. H. Ji et al., Nature Communications, 2019, 10, 592
4. R. De Ridder, G. Van Tendeloo, and S. Amelinck, Acta Crystallographica, 1976. 32, 2216–224

297

Unveiling the Optoelectronic and Thermal Properties of SnSe Polycrystals via EELS

Francesco Salutari[1], Dr. Sharona Horta[2], Mr. Marc Botifoll[1], Dr. Maria Chiara Spadaro[1,3,4], Dr. Maria Ibañez[2], Dr. Jordi Arbiol[1,5]
[1]Catalan Institute of Nanoscience and Nanotechnology (ICN2) , Campus UAB, Bellaterra, 08193 Barcelona, Spain, [2]Institute of Science and Technology Austria (ISTA), AM Campus 1, 3400 Klosterneuburg, Austria, [3]Department of Physics and Astronomy "Ettore Majorana", University of Catania, via S. Sofia 64, Catania 95123, Italy, [4]CNR-IMM, via S. Sofia 64, Catania 95123, Italy, [5]ICREA, Pg Lluis Companys 23, 08010 Barcelona, Spain

Poster Group 1

Tin Selenide (SnSe) has become a globally focused research topic in the field of thermoelectricity thanks to its low thermal conductivity and high electrical transport performance, which combined result in remarkable thermoelectric efficiencies. In its crystalline form, SnSe suffers from poor mechanical properties, rigid controlled crystal growth conditions and high production costs [1]. This has led the research to focus instead on SnSe polycrystals which, although less performing with respect to their crystalline counterpart, have great potential for significant efficiency enhancement [2]. A potential strategy to overcome the performance degradation, mainly related to the higher thermal conductivity of Tin oxide (SnOx) which percolates in the material through the grain boundaries, is by selective doping [3]. Here, we prove the effectiveness of Na doping in limiting the formation of SnOx and substituting the oxide at the grain boundaries in form of coherent precipitates through Scanning transmission Electron Microscopy (STEM). The ultralow spatial resolution imaging (~1Å) achieved with the aberration corrected STEM Spectra 300, combined with EDX spectroscopy, allows to map the elemental distribution at the grain boundary with atomic resolution, highlighting the presence of Na confined within the boundary.
The effect of the Na inclusions on the electronic and vibrational properties of SnSe polycrystals is further investigated through Low-Loss EEL Spectroscopy. Monochromated operation on the beam accelerated at 60kV, combined with low beam currents (~70pA) and convergence and collection semi-angles of 30 and 20 mrad, respectively, allow to collect the forward-scattered and higher momentum transfer signals in the first Brillouin Zone. From here, the information on the bandgap together with the plasmonic and phonon signals can be extracted for each probe position. In the specific, bandgap fitting across the doped grain boundary is supported by a customized Python algorithm [4], which highlights the decrease in the pure SnSe bandgap value due to the Na inclusions, in accordance with the DFT calculations. Further investigation on the vibrational signals within the low range of the EELS spectrum is performed to evidence the phonon modes that appear when in proximity of the grain boundaries. The specific vibrational-modes mapping will in the future enable the acquisition of phonon dispersion at grain boundaries, interfaces, edges, and various nature defects unlocking a powerful tool for thermoelectric performance evaluation at the atomic scale.

Keywords:

Thermoelctricity, EELS, Bandgap, Phonon modes

Reference:

1. Progress in Materials Science 97 (2018): 283-346; Nanoscale Adv., 2021, 3(2), 326–332
2. Nature Materials 20.10 (2021): 1378-1384; Nanoscale, 2020, 12(44), 22534-22540
3. Advanced Functional Materials 26.37 (2016): 6836-6845.
4. Nature Communications 13.1 (2022): 4089.

334

Effect of preparation and oxygen evolution catalysis on CoNiFe oxide electrocatalysts revealed by STEM-EELS

Dr. Nils Rockstroh[1], Ms. Trang Pham[1], Mr. Carsten Kreyenschulte[1], Ms. Annette-Enrica Surkus[1], Mr. Robert Francke[1]
[1]Leibniz Institute for Catalysis e.V. (LIKAT), Rostock, Germany

Poster Group 1

Background incl. aims
Hydrogen is considered as a competent and green energy carrier that can be obtained by water electrolysis [1]. However, this process is mainly limited by the water oxidation half reaction, the OER (oxygen evolution reaction). Therefore, substantial efforts for this reaction focus on the development of catalysts that are comprised of abundant metals, and which simultaneously fulfil the requirements of high current densities, low overpotential, high mass activity and excellent stability. Here, such a system is presented using CoNiFe oxide in alkaline oxygen evolution. The effect of the synthesis procedure as well as the influence of the catalytic conditions on the material are investigated by STEM coupled with EELS and EDX.

Methods
The catalysts were investigated by a probe corrected JEOL JEM-ARM200F (Schottky emitter) equipped with a Gatan Enfinium ER EELS and a JEOL JED-2300 EDX spectrometer having a silicon drift detector (dry SD60GV). A rather high beam current was applied to keep the acquisition time low. The FWHM of the zero-loss peak (ZLP) was about 1.2 eV and the DualEELS mode was applied. The spectra were recalibrated at each pixel by the position of the ZLP.

Results
CoNiFe (2:2:1)/M, synthesized under an oxygen-deficient atmosphere (1 vol% air in Ar), shows the best catalytic performance. Synthesis of CoNiFe (2:2:1) under a reductive atmosphere (CoNiFe (2:2:1)/H; 5% H2 in Ar) or oxygen-rich conditions (CoNiFe (2:2:1)/A; air) leads to less active catalysts. While CoNiFe (2:2:1)/M and CoNiFe (2:2:1)/A show a quite uniform distribution of the incorporated metals, CoNiFe (2:2:1)/H shows enrichment of metallic Ni containing nanoparticles on the bulk. More pronounced differences can be observed in the EEL spectra, in particular at the O K edge. Whilst CoNiFe (2:2:1)/A shows a pronounced pre-edge feature at about 528 eV, it is only barely noticeable and slightly shifted to higher energy losses in CoNiFe (2:2:1)/H and CoNiFe (2:2:1)/M. Additionally, CoNiFe (2:2:1)/M exhibits a feature at about 545 eV, which was not present in the other materials. This behaviour is also observed in the spectral regions (L edges) of Co, Ni, and Fe. All M L edge features of CoNiFe (2:2:1)/A ressemble that of oxidized metals M [2-4]. In contrast, CoNiFe (2:2:1)/H and CoNiFe (2:2:1)/M show both, reduced and oxidized states of the contained metals. In CoNiFe (2:2:1)/H, metallic Ni was observed, with Co and Fe remaining oxidic. In addition to metallic Ni, CoNiFe (2:2:1)/M exhibits also partially reduced Co. The incomplete reduction of the metal centers in CoNiFe (2:2:1)/M and CoNiFe (2:2:1)/H is also reflected by the presence of an oxygen signal.
The most active catalyst CoNiFe (2:2:1)/M was also investigated after electrolysis in the absence of nafion. The observed decrease of the ECSA (electrochemically active surface area) was also reflected by a denser appearance of the particles and a decreased size of the crystallites constituting these particles (see graphic). The composition of the material has also changed considerably with a non-uniform distribution of the constituting elements. Some regions lack almost completely Ni and exhibit a reduced contents of iron, leading to a cobalt enriched material. The EEL spectra at the O K edge ressemble those of the fresh catalyst, while the L edges of Co and Fe point towards the presence of these metals in their oxidized forms.

Conclusion

STEM-EELS is a powerful method to investigate changes of electrocatalysts at the nm scale. The different preparation procedures of CoNiFe (2:2:1) yield materials with differently oxidized metals which can be observed by EELS. While CoNiFe (2:2:1)/A exhibits completely oxidized metals, metallic Ni is present in CoNiFe (2:2:1)/H and non-oxidic Ni and Co are present in CoNiFe (2:2:1)/M. After electrolysis in the presence of CoNiFe (2:2:1)/M the signal shape at the O K edge is retained, however, the material is lacking some Ni. STEM-EELS is thus able to detect changes at a very low concentration of the analyte that may escape the eye of bulk analysis methods.

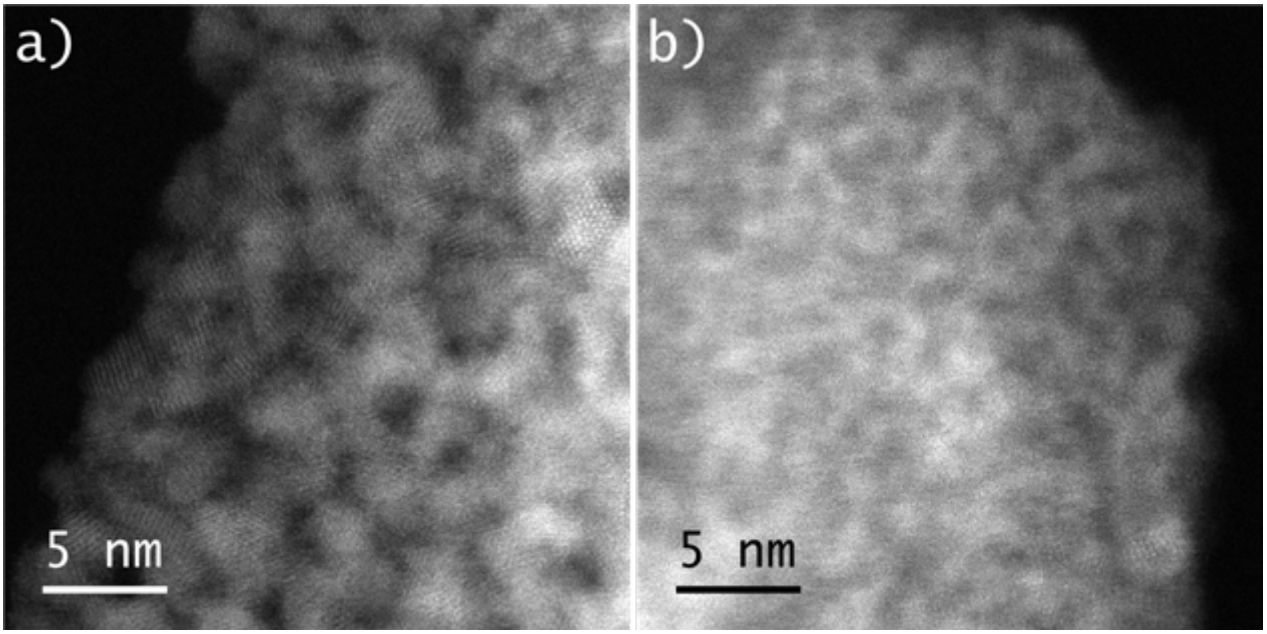

Keywords:

STEM, EELS, OER, oxide, catalysis

Reference:

[1] N. Armaroli, V. Balzani, ChemSusChem 2011, 4, 21-36.
[2] P. Müller, M. Meffert, H. Störmer, D. Gerthsen, Microsc. Microanal. 2013, 19, 1595-1605.
[3] B. Rellinghaus, S. Stappert, E. F. Wassermann, H. Sauer, B. Spliethoff, Eur. Phys. J. D 2001, 16, 249-252.
[4] B. Mo et al. At. Spectrosc. 2022, 43, 53-59.

359

Towards 3D quantitative imaging in FIB-SEM for applications in battery materials

Stephanie Bessette[1], Prof. Raynald Gauvin[1]
[1]McGill University, Montreal, Canada

Poster Group 1

Background incl. aims
The development of more efficient and safer battery materials stems from the commitment to green energy initiatives. To fully understand the failure mechanisms of newly developed battery materials at the micrometer level and below, scanning electron microscopy is a technique of choice. Focused ion beam (FIB) combined with SEM broadens the characterization capabilities of electron microscopy by revealing sub-surface microstructure and phase distributions. The technique permits quantitative analyses from the reconstruction of volumes from collected 2D SEM datasets. Moreover, the collection of Energy-dispersive X-ray spectroscopy (EDS) and Electron Backscatter Diffraction (EBSD) maps from the generated x-rays and EBS patterns can help explain further the chemical and structural stability of the materials in 3D. Degradation over time during cycling can originate from alterations of the microstructure of particles, such as the apparition of cracks due to volume expansion, changes in grain morphology or activity at grain boundaries. This work aims to obtain quantitative information on the distributions of the different phases of lithium-based cathodes from field-emission (FE)-SEM datasets of 2D images, including porosity. Porosity is a critical parameter in battery design, since it directly affects electronic and ionic diffusion processes [1,2] and therefore battery performance. An interest will be given towards the changes in the phase distributions as a result of cycling, therefore pristine (uncycled) and cycled specimens will be compared including EDS and EBSD data.
Methods
Hitachi Ethos NX5000 FIB-SEM microscope located at the Facility for Electron Microscopy Research at McGill University will be used to prepare volumes using the slice and view technique of pristine and cycled cathodes. SE and BSE images will be acquired simultaneously at low voltage (2kV) during the slice and view routine to ensure the characterization of the fine pore structure from the small probe interaction volume. Ultim Max 100 SDD detector and Symmetry S2 EBSD (up to 4500 patterns per second collection) from Oxford Instruments will be used with 20 keV at given slices to collect chemical and crystalline information on the cathodes. Dragonfly software from Comet [3] is used to segment the 2D image datasets into 3 semantic phases (porosity, active material (particles) and binder (carbon)) using Deep Learning methods. Watershed algorithms are used to differentiate the labeled voxels in the phases and separate nearby voxels into individual elements for pore and active material to obtain statistical data on each phase.
Results
A preliminary dataset was obtained from a pristine lithium based cathode using Ga FIB milling with 3.5nA current with a slice thickness of 40nm. A total of 441 frames were collected with in-lens BSE(U) and BSE(L) detectors using simultaneous acquisition and a pixel size of 50nm. A volume of 19,6µmx20,5µmx17,5µm of the sample was reconstructed after registration of the slices and cropping. A U-net neural network was trained on a subset of the total stack manually segmented using thresholding on the mixed BSE U+L images, with 20% of the data retained for validation. It was found that 51,9% of the volume constitutes of carbon binder, 37,2% Li-based active material and 10,9% porosity. Histograms of the pore and active material populations were constructed after single particle separation with the watershed algorithm. Following fractal geometry theory from Mandelbrot[4], the probability distribution of particles P is linked to the fractal dimension D with P(r>R)=AR^(-D). Deriving the equation to get the probability density ρ(R), the fractal dimensions D of

both subsets can be extracted using the equation D=1/(m-1), knowing the radius R is expressed proportional to the volume V^(1/D) and m is the slope of the fitted straight line obtained from taking the logarithm of both sides of the derived equation. The fractal dimension of the pores yields D=0.60 and the active material is found to have D=0.99.

Conclusion

Preliminary image analysis using a FIB-SEM dataset on a pristine cathode showed the distributions of active material, carbon binder and pores. A neural network was trained to segment the cathode's phases and object analysis was used to study the pristine cathode. It was determined that the fractal dimension D of the pore medium in the cathode is 0.60, while the active material particles, containing Li, is set at 0.99. In both cases, the fractal dimension value is lower than one and therefore indicate that objects composing the phases are disconnected. Analysis of cycled specimens will enable us to observe the behavior of percolation pathways over time. The newly installed Ultim Max 100 SDD detector and Oxford Instrument's Symmetry S2 EBSD will be used to generate 3D volume reconstructions on pristine and cycled Li-based cathodes in addition to the image segmentation and quantitative results obtained from EM datasets. The addition of 3D chemical and crystalline information will give new insights into the effect of charge-discharge cycles on the distribution of phases and permit the observation of defects in 3D that can help explain battery failure mechanisms.

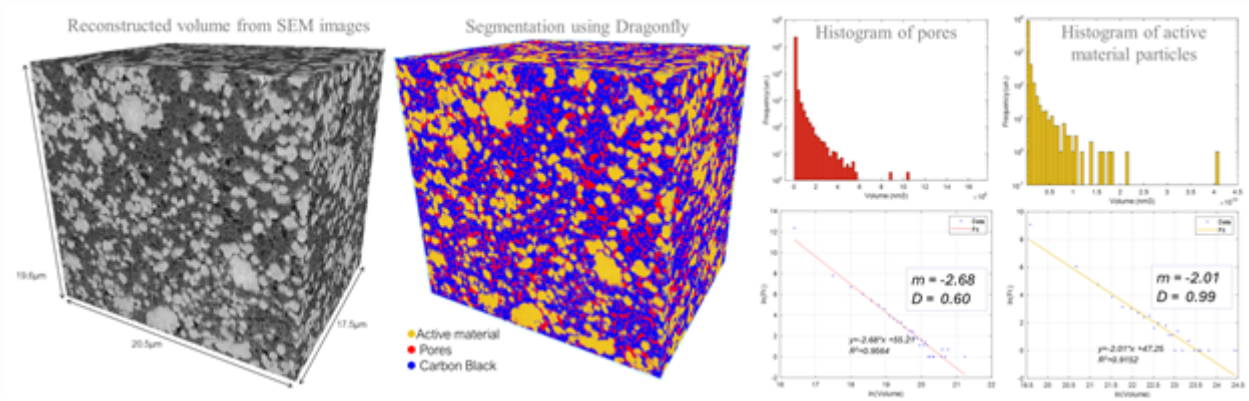

Keywords:

FIB-SEM, 3D-EDS,3D-EBSD, quantitative imaging, battery

Reference:

[1] Chen, Y.H.; Wang, C.W.; Zhang, X.; Sastry, A.M. Porous cathode optimization for lithium cells: Ionic and electronic conductivity, capacity, and selection of materials. J. Power Sources 2010, 195, 2851–2862

[2] Beuse, T.; Fingerle, M.; Wagner, C.; Winter, M.; Börner, M. Comprehensive Insights into the Porosity of Lithium-Ion Battery Electrodes: A Comparative Study on Positive Electrodes Based on LiNi0.6Mn0.2Co0.2O2 (NMC622). Batteries 2021, 7, 70.

[3] Dragonfly. 2022, Comet Technologies Canada Inc.: Montreal, Canada.

[4] Mandelbrot, B. The Fractal Geometry of Nature. Revised ed., W.H. Freeman, 1982.

391

Characterization of Solid Electrolyte-free Si anodes for all-solid-state batteries (ASSBs) using Cryo-STEM

Dr. Shamail Ahmed[1], Dr. Hanyu Huo[2], Mrs. Franziska Hüppe[1], Dr. Jürgen Belz[1], Prof. Dr. Jürgen Janek[3], Prof. Dr. Kerstin Volz[1]
[1]Structure and Technology Research Laboratory, Philipps University of Marburg, Marburg, Germany, [2]The Bruce Group, University of Oxford, Oxford , United Kingdom, [3]Institute of Physical Chemistry, Justus Liebig University Giessen, Giessen, Germany

Poster Group 1

Background:
Solid-state lithium-ion batteries (ASSBs) hold great promise for delivering higher energy density and safer performance than conventional lithium-ion batteries. Lithium metal is a highly studied choice for the anode due to its high energy potential. However, its use in ASSBs is hindered by the issue of dendrite formation and growth. Conversely, silicon offers a capacity that is tenfold greater than that of graphite, presenting itself as a cost-effective and promising substitute for lithium metal.[1] Unfortunately, the potential of Si as an active anode material hasn't been fully tapped in ASSBs. Recently, solid electrolyte (SE) free Si anodes have been found to have improved performance compared to their SE-containing counterparts;[2] however, there is still considerable room for improvement. One of the ways to enhance these electrodes is to have detailed insights into the microstructure concerning various electrochemical treatments.

Methods:
Si particles (mixed with 0.5 wt % of polyvinylidene fluoride binder) are first pressed to form a pellet. This electrode is cycled against an In/InLi counter electrode using LPSCl as an SE. We utilize cryo aberration-corrected scanning transmission electron microscopy (AC-STEM) to characterize the microstructure of SE-free Si anodes after the 1st cycle. Since ASSB samples are air and moisture-sensitive, the cells are dissembled in an Ar-filled glove box, and the Si electrodes are retrieved. The sample is transferred from the glove box to a plasma FIB (PFIB) in an argon atmosphere. It is prepared at approximately -190 °C using an Ar-ion beam from the Helios 5 Hydra CX PFIB to thin and polish the specimen. Afterward, the samples are moved back into the argon atmosphere of the glovebox. The sample is then mounted onto a double-tilt Atmos Defend Holder from Melbuild within the glove box. This holder is capable of transporting the sample from the glovebox to the S/TEM under an argon atmosphere, reaching temperatures of about -170 °C during measurements. At the S/TEM, the samples are measured at roughly -170 °C employing multiple techniques, such as HR-S/TEM, energy dispersive X-rays spectroscopy (EDXS), electron energy-loss spectroscopy (EELS), four-dimensional STEM nano-beam diffraction and precession electron diffraction (4D STEM NBD/PED), etc., under cryogenic conditions.

Results:
Figure 1(a) is a STEM high-angle annular dark field (HAADF) image of pristine Si particles. The cloudy contrast on the edges of the particles shows SiOx particles (confirmed vis EDXS, not shown here). Figure 1(b) is a cryo-STEM HAADF image of the bulk electrode after the 1st cycle. A massive microstructure transformation is observed with Si particles showing an amorphous structure (confirmed by PED, not shown here). Figure 1(c) is a cryo-STEM HAADF image of the region marked in Figure 1(b), showing a unique texture of the Si amorphous structure, commonly found after 1st cycling. A cryo-STEM HAADF tomography has also been performed in this region, showing a sheet-like structure (not shown here). Figure 2 shows Li and Si cryo-STEM EELS maps of a selected region

after the 1st cycle. SiOx consumes a considerable amount of irreversible Li at the surface of the Si particles.

Conclusion:
Though the detailed analysis of the samples after subsequent electrochemical treatments is still underway, the drastic evolution of the Si electrode structure after 1st cycle is critical to finding the lithiation behavior of novel SE-free Si electrodes for ASSBs.

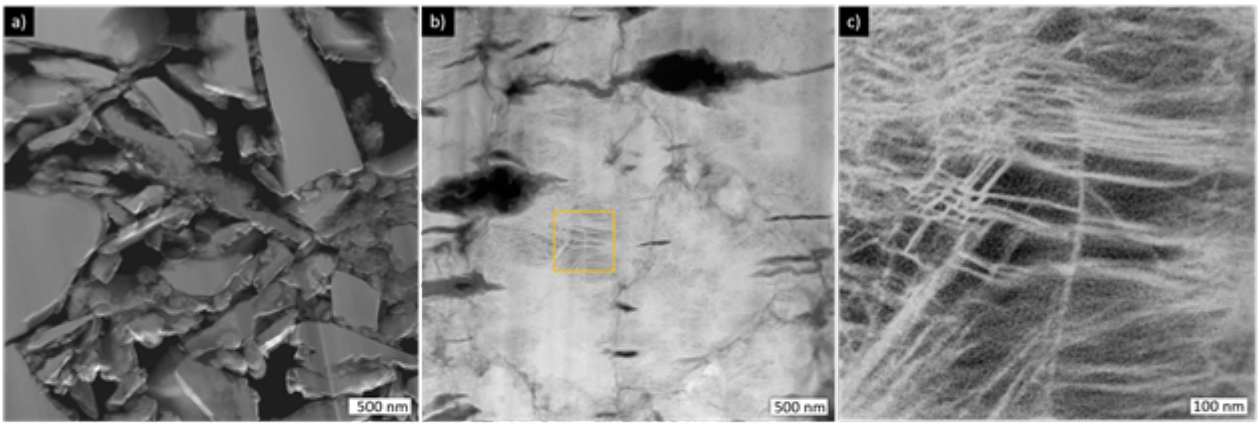

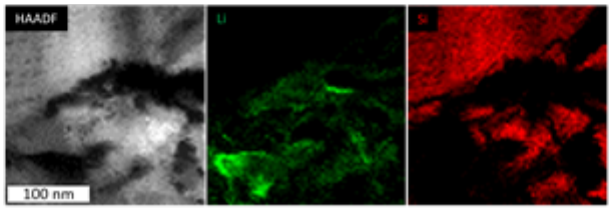

Keywords:

Si-anode, STEM, Cryo, EELS, HAADF

Reference:

References:

[1] I. Na, H. Kim, S. Kunze, C. Nam, S. Jo, H. Choi, S. Oh, E. Choi, Y. B. Song, Y. S. Jung, Y. S. Lee, J. Lim, ACS Energy Lett. 2023, 1936.

[2] H. Huo, M. Jiang, Y. Bai, S. Ahmed, K. Volz, H. Hartmann, A. Henss, C. V. Singh, D. Raabe, J. Janek, Nat. Mater. 2024, 1.

404

Defects and alloy ordering in Pt-Cu nanoparticulate electrocatalysts

Ana Rebeka Kamsek[1,2], Dr. Francisco Ruiz-Zepeda[1], Anja Logar[1,3], Dr. Marjan Bele[1], Prof. Dr. Goran Dražić[1], Prof. Dr. Nejc Hodnik[1,3]
[1]Department of Materials Chemistry, National Institute of Chemistry, Ljubljana, Slovenia, [2]Faculty of Chemistry and Chemical Engineering, University of Ljubljana, Ljubljana, Slovenia, [3]University of Nova Gorica, Nova Gorica, Slovenia

Poster Group 1

Background incl. aims
Proton exchange membrane fuel cells are an alternative to fossil fuel-powered engines in the mobility and energy sector. They use hydrogen as fuel and do not directly generate greenhouse gas emissions. However, the cost of the electrocatalyst for the oxygen reduction reaction (ORR) still poses an issue, as it commonly contains scarce platinum. Currently, supported Pt-alloy nanoparticles are commonly used to lower the amount of Pt but retain good ORR performance. Despite numerous studies on structure-property relationships of such electrocatalysts, the effects of selected structural features on the catalytic activity and stability remain unexplored. Ensembles of supported metallic alloy nanoparticles typically vary in size, shape, composition, crystal structure, presence of defects, and other structural subtleties, all of which impact catalytic performance. Therefore, advanced characterization methods are needed to obtain average and local information about the catalyst structure to correlate it to its properties [1]. The study aims to provide an accurate description of the presence and type of defects and crystal ordering in carbon-supported platinum-copper nanoparticles and an insight into how advanced microscopy complements electrochemical methods in terms of answering questions about the structure-property relationship.
Methods
Various analogs of carbon-supported platinum-copper nanoparticles were synthesized using a wet impregnation method and subsequent thermal annealing in a tube furnace using specified temperature-time profiles and atmospheres. X-ray diffraction, scanning transmission electron microscopy (STEM), 4D-STEM, and electrochemical measurements were used to characterize the samples. Simulated X-ray and electron diffraction patterns and images were used to interpret experimental results. 4D-STEM datasets were collected for individual nanoparticles of a selected sample. Virtual detectors were used to construct real-space images from the 4D dataset, and clustering and matrix factorization were used to segment the dataset and determine commonly occurring patterns that can be associated with specific structural features within the catalyst.
Results
The platinum-copper alloy with a composition close to $PtCu_3$ crystallizes as an ordered or disordered alloy, depending on the annealing temperature. For analogs that were annealed in a reductive atmosphere at a temperature at a transition between the two well-known phases, diffraction patterns revealed the presence of periodic anti-phase boundaries, separating ordered alloy crystallites. The modulated unit cell was previously reported for a bulk material, but not in the context of nanomaterials. Based on differences in column intensities, an anti-phase boundary was observed in real space on an atomically resolved STEM micrograph, where the expected column intensities were confirmed with STEM image simulations, as seen in the Figure. The presence of anti-phase boundaries has not proven itself critical in determining the catalytic activity of the investigated material. For an analog, exhibiting a mix of the ordered and disordered alloy phases, a 4D-STEM investigation of individual nanoparticles provided diffraction patterns containing information on the local crystal structure. The data analysis enabled the discovery of notable features within the data without explicitly specifying what diffraction signal they should cause. In the case of platinum-copper

nanoparticles, it revealed a spatial distribution of the signal, associated with the ordered alloy phase, which is one of the factors previously shown to govern the catalytic activity towards the ORR.

Conclusion

The investigation resulted in a quantitative description of periodic anti-phase boundaries in platinum-copper nanoparticles following a specified thermal annealing protocol [2]. Simulated data for both powder diffraction patterns, as well as STEM images, helped explain experimental results. 4D-STEM proved itself useful in providing local crystal structure information, which can be inferred from the dataset in an unsupervised way. This imaging modality can bring added value to studies, probing the complex structure-property relationships of nanoparticulate electrocatalysts.

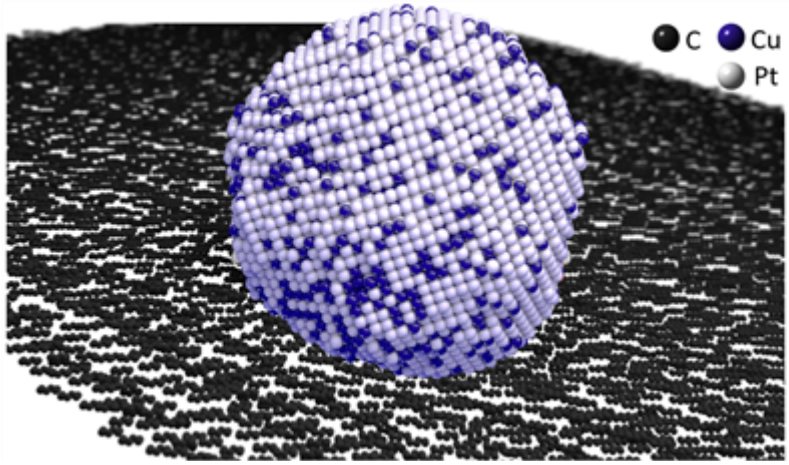

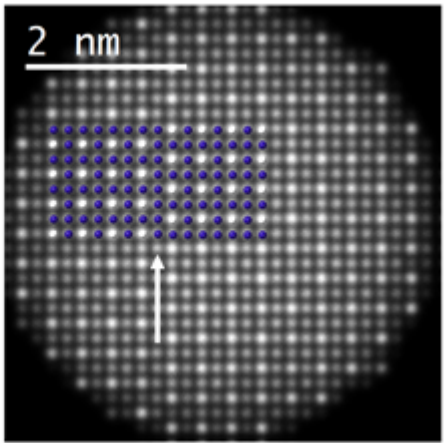

Keywords:

electrocatalysis, nanoparticles, crystal structure, 4D-STEM

Reference:

[1] A. R. Kamšek, F. Ruiz-Zepeda, A. Pavlišič, A. Hrnjić, N. Hodnik. Curr. Opin. Electrochem. 35 (2022) 101052.

[2] A. R. Kamšek, A. Meden, I. Arčon, P. Jovanovič, M. Šala, F. Ruiz-Zepeda, G. Dražić, M. Gaberšček, M. Bele, N. Hodnik. Mater. Today Nano. 23 (2023) 100377.

543

Towards Quantitative Liquid Phase Electrochemistry for Understanding Electrochemical Processes

Shibabrata Basak[1], Junbeom Park[1], Hongyu Sun[2], Hugo Pérez Garza[2], Eva Jodat[1], André Karl[1], Rüdiger-A Eichel[1]
[1]Institute of Energy and Climate Research, Fundamental Electrochemistry (IEK-9), Forschungszentrum Jülich GmbH, Jülich, Germany, [2]DENSsolutions B.V., Delft, The Netherlands

Poster Group 1

Background incl. aims
Liquid phase transmission electron microscopy (LPTEM) has emerged as a powerful tool, presenting enormous potential for understanding the electrochemical processes behind electrolysis, batteries, and other technologies [1]. However, obtaining high-resolution structural and chemical information during these electrochemical processes remains a challenge due to the issue of liquid thickness. While utilizing a monolithic MEMS-based nanoreactor with integrated electrodes can be a potential solution, it too faces limitations from an electrochemical perspective. To ensure proper ion conduction to mirror processes occurring in macroscopic cells, LPTEM studies require a thicker liquid layer, which directly contradicts the need for high-resolution information. On the other hand, obtaining high-resolution information through post-mortem studies, by disassembling a typical two-chip nanoreactor, too is not a viable solution due to possible changes due to absence of the native liquid environment. Furthermore, ideally high-resolution information is required at different stages of in situ experiments. These necessitate the ability to dynamically control the liquid thickness. novel method that enables high-resolution and analytical electron microscopy studies within a liquid flow cell [2].

Methods
Smart micro electrical mechanical systems (MEMS) and holder designs have enabled us to control liquid flow and thickness, allowing us to create a stable and reproducible environment that is ideal for investigating the electrochemical processes of interest [2,3]. In particular thanks to the on-chip flow capability, the liquid in the field of view can be efficiently reduced by flowing gas, which is termed “purging” [4]. This purging method enables the acquisition of high-resolution TEM images, chemical composition and valence analysis through energy-dispersive X-ray spectroscopy (EDX) mapping and electron energy-loss spectroscopy (EELS). In addition, the purging approach is both reversible and reproducible, which therefore enables the alternation between a thick and a thin liquid configuration. This provide us the necessary dynamic control over the liquid thickness to perform the electrochemical experiments in a thick liquid configuration and then perform anlytical studies including 4D STEM at the thin liquid configuration to enable the best resolution without changing the state of the sample. This coupled with simple image processing that has allowed us to extract 3D information from the in-situ image series and a step towards live 4D STEM provides the pathway to developing new and more efficient energy technologies.

Results
Dendrite growth during cycling is one severe problem to harm durability and safety of energy applications, so many efforts have been studied to inhibit the dendrite growth. One example case is aqueous zinc (Zn) based battery chemistry, including redox flow battery, which has recently generated significant interest as an alternative battery technology for stationary applications beyond Li-ion batteries. The main driving force is the high volumetric capacity of aqueous zinc batteries, low cost, safety, and abundance of Zn metal. Despite these advantages, alongside electrode passivation, anode shape change, and H2 evolution, the problems of Zn dendrite growth cause premature battery

failure and safety hazards, severely limiting the progress and further commercial exploitation of aqueous Zn batteries. Direct visualization of dendrites under operando conditions can lead to an in-depth understanding and the development of the most effective mitigation routes toward achieving a compact plating and smooth stripping of Zn during battery cycling, which is a prerequisite for battery safety, longevity, and viability. Thus we apply the developed method for dynamic control of liquid thickness and image processing to gain 3D growth along with crystallographic orientation information of the Zn deposits during electrodeposition using 0.1 M ZnSO4. Figure 1. Showcase dendrite formation and extracted 3D information from the in-situ image series.

Conclusion

The 3D visualization of electrodeposition at the nanoscale enabled us to study how different electrolyte additives affect growth across all three planes (XY, YZ, and XZ) and thus establish a workflow that researchers can utilize to optimize electrolytes to promote compact deposition and mitigate unwanted features like dendritic growth for Zn and other battery chemistries and electrodeposition processes in general.

Figure Caption

Figure 1: Investigation of Zn dendritic growth during plating in static 0.1M ZnSO4. (a-c) STEM images obtained at 7th, 8th and 9th seconds. (d) The plated Zn volume vs. time. (e-g) Processed images show the Zn dendritic growth between 7-8, 8-9, and 9-10 seconds. A color map on (g) represents the thickness [µm] at that second.

Acknowledgments

S. Basak, J. Park, E. Jodat, A. Karl, and R.-A. Eichel acknowledge the funding provided by the BMBF (German Research Foundation) through the project DERIEL (03HY122C).

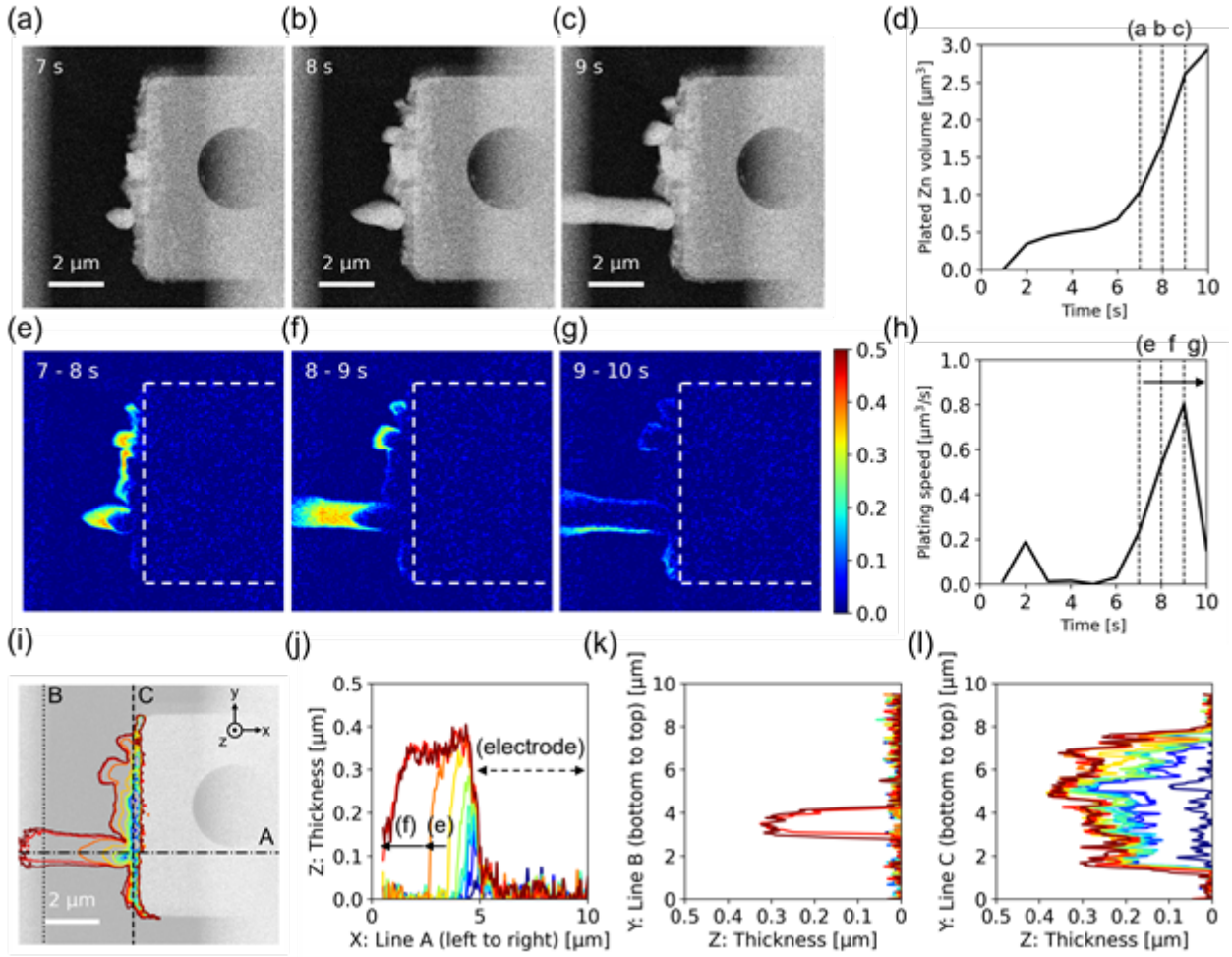

Keywords:

liquid phase TEM, 4DSTEM, 3D

Reference:

[1] S. Basak et al., Chem. Phys. Rev. 3, 031303 (2022).
[2] N. Cheng et al., Nanotechnology, 33 (44), 445702 (2022).
[3] J. Park et al., Advanced Engineering Materials, (2024).
[4] Y. Pivak et al., Microscopy, 72 (6), 520–524 (2023).

562

Scale-bridging microscopic characterization of complex energy devices enabled by novel cross-sectional preparation routines

Marco Hepp[1], Charles Ogolla[1], Dominik Stepien[2], Dominik Bresser[2], Benjamin Butz[1], Tristan Zemke[1]
[1]Micro- and Nanoanalytics Group, University of Siegen, Siegen, Germany, [2]Helmholtz Institute Ulm, Ulm, Germany

Poster Group 1

Background incl. aims
Energy devices like batteries, fuel cells and solar cells are assembled from multiple functional components with different material properties. To gain a fundamental understanding of structure property relations, to systematically contribute to performance enhancement and to unravel device degradation and failure mechanisms, high quality cross-sections of entire devices or of as large regions as possible are required for complementary microscopic analysis.

Methods
Since many devices not only consist of different classes of materials but also of liquid and/or air sensitive components, working under cryogenic and/or inert conditions is essential to conserve their pristine state. To enable scale-bridging cross-sectional characterization of those devices all the way down to the atomic level, we utilize different preparation tools. A novel self-built cryo-cutter allows us to produce cross-sections of entire devices like pouch-cells in a one-step process and thus to investigate the inner structure in their pristine state by OM from the macroscopic scale to the optical resolution limitations. For characterization down to the atomic scale (cryo)ultramicrotomy is employed to generate high-quality and large-area cross-sections, e.g., of PEM-FCs and even highly reactive battery electrodes not only for investigation by OM/SEM (microtomic blockface) but also for (atomic resolution) TEM, as high-quality thin samples with thicknesses below 50 nm are provided.

Results
In this contribution, we demonstrate the scale-bridging capabilities of those preparation techniques applied to various devices and their components in conjunction with advanced (electron) microscopic and spectroscopic methods. Examples include devices like batteries (Fig. 1 a) and components thereof (Fig. 1 b) as well as complex fuel cells.

Conclusion
The applied techniques and developed routines are ideally suited to investigate even complete devices, individual components as well as materials. Aspects range from interfaces of individual layers and components in terms of their morphology and contact to the systematic identification of their composition and chemical bonding states.

Acknowledgement
Part of this work was performed at the DFG-funded Micro-and Nanoanalytics Facility (MNaF) of the University of Siegen (INST 221/131-1) utilizing its major TEM instrument FEI Talos F200X (DFG INST 221/93-1, DFG INST 221/126-1) and sample preparation equipment

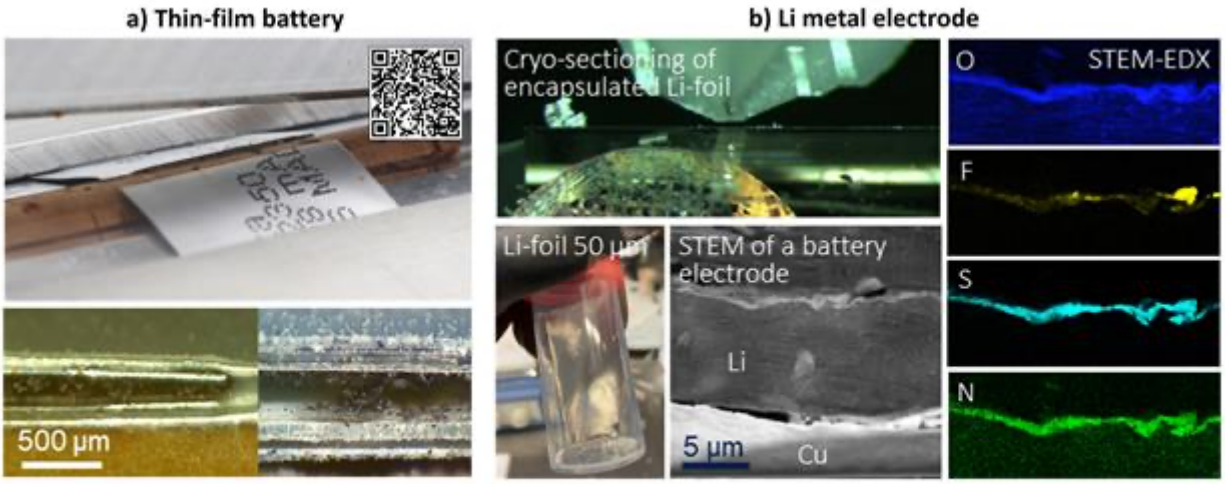

Fig 1: a) Cross-sectional preparation of commercially available Li/MnO_2 thin-film battery by self-developed cryo-cutter tool, b) Cryo-ultramicrotomy of lithium metal electrode for battery solid electrolyte interphase research

Keywords:

energy devices, ultramicrotomy, batteries, cryo

644

Scale-Bridging Analysis of Hierarchical Mesoporous Transition Metal Foams

Jonas Frohne[1], Dr.-Ing. Julian Müller[1], Dr. Jean Marie Vianney Nsanzimana[1], Charles Otieno Ogolla[1], Prof. Benjamin Butz[1]
[1]Micro- and Nanoanalytics Group/University of Siegen, Siegen, Germany

Poster Group 1

Mesoporous materials have attracted tremendous attention in recent decades due to their unique property portfolio and potential applications in various fields such as energy storage, catalysis and sensoring. Mesoporous copper for example has proven suitable as a material for large-scale production due to its properties, cost efficiency and excellent accessibility. Mesoporous transition metals comprise an enormous surface area, high electrical conductivity, improved catalytic activity, and long-term mechanical stability. Those properties are strongly influenced by the material's morphology specifically the pore size, pore distribution as well as connectivity. The chemical composition of the surface particularly governs the material's catalytic properties.
Dealloying as a technique utilises the differences in the galvanic series. A porous structure is created by selectively etching out an element of an alloy. Dealloying has been established as a facile method to tailor hierarchical porous structures with extensive pore networks of varying sizes dependent on the depth and location in the material. It is, therefore, a robust, scalable and cost-effective approach for the synthesis of mesoporous transition metals and their alloys [1].

In this study, dealloying is applied under various process parameters to investigate their influence on the porous structures formed using a copper-manganese alloy sample. The dealloying process is conducted under acidic conditions (hydrochloric acid). To unravel structure formation dependent on the various process parameters, e.g., pore size and distribution, morphology of pores, composition etc., advanced 3D imaging techniques including micro-computed tomography (µCT), focused ion beam (FIB), and transmission electron microscopy (TEM) tomography are employed along different length scales. To gain a deeper understanding of how morphology and composition influence catalytic activity and stability, we evaluated the performance of mesoporous copper foams as electrodes for the hydrogen evolution reaction (HER).

The resulting structures exhibit systematic channel networks and variations in pore size depending on depth and location in the material. We found that even small changes in the synthesis process can have a significant impact. For example, very small concentrations (≤1 at%) of other elements may lead to strongly altered morphologies with, e.g. an order of magnitude smaller pores and higher overall mechanical stability; moreover, the catalytic properties and overall morphology were affected.

We successfully have fabricated mesoporous copper for HER reaction. Multiscale analysis of the structures of the dealloyed material from the millimetre to the nanometre range facilitate the understanding of structure formation and unravels the complex structure-property relationship. The project, therefore, contributes to the detailed understanding of the impact of the various reaction parameters of the dealloying process to the structures formed, and subsequently their impact on the performance of the material.

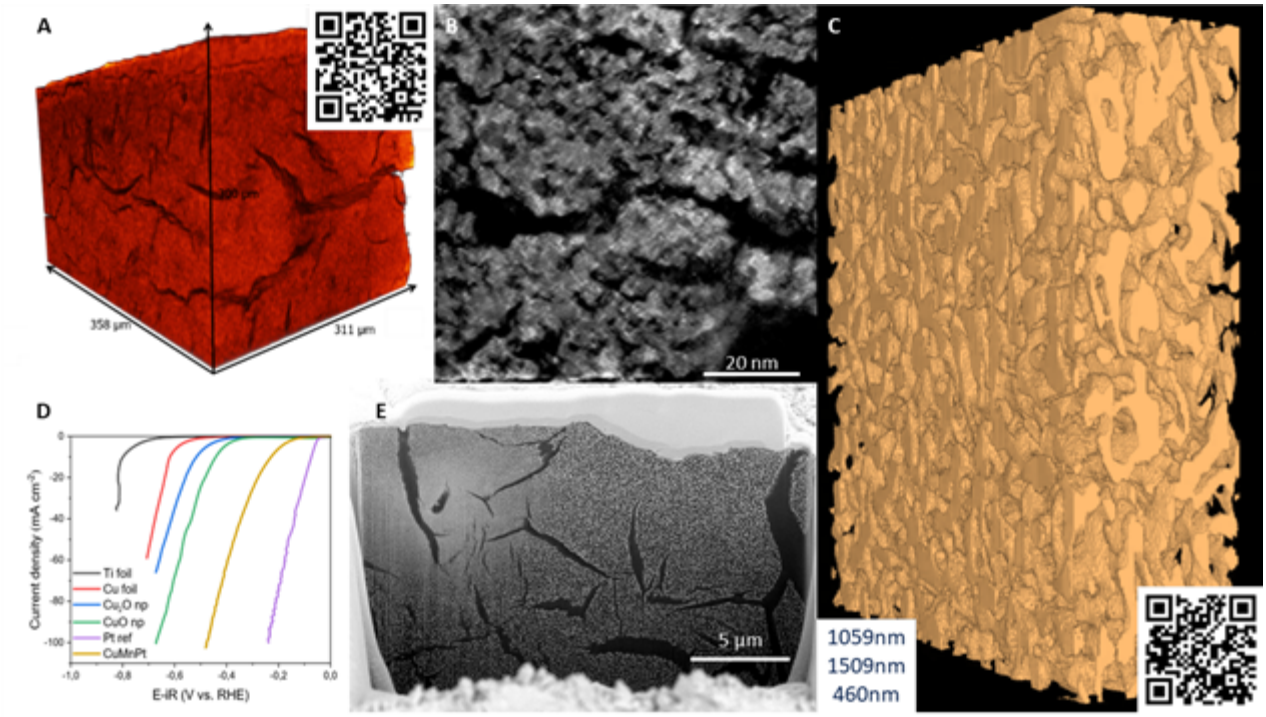

Figure 1. (A) 3D rendering of the mesoporous copper foam obtained from micro-computed tomography (µCT). (B) Representative 2D slice from TEM tomography of a modified foam after 20 iterations of algebraic reconstruction technique (ART) algorithm. (C) 3D rendering of the foam from FIB-SEM tomography. (D) HER measurements with mesoporous copper-based electrodes. (E) FIB cross-section of a mesoporous copper foam with good visible cracks.

Keywords:

Dealloying, Nanostructured-material, Hierarchical, Scale-bridging-analysis, Catalyst

Reference:

[1] McCue, I., Benn, E., Gaskey, B., & Erlebacher, J. (2016). Dealloying and Dealloyed Materials. Annual Review of Materials Research, 46(1), 263–286.

700

In-Situ insights into Multivalent Metal Energy Storage: A model system for calcium sulfur batteries

Marco Kögel[1], Prof. Jannik C. Meyer[1,2]
[1]NMI Natural and Medical Sciences Institute at the University of Tübingen, Reutlingen, Germany,
[2]Institute of Applied Physics, University of Tübingen, Tübingen, Germany

Poster Group 1

As we globally realize large-scale electrical energy storage coupled with the rapid increase in global electromobility, the challenge of securing a consistent supply of critical raw materials utilized in lithium-ion batteries (LIB) continues to grow. Consequently, the search for alternative systems delivering comparable energy densities has become an important topic. Multivalent metals, renowned for their long-term stability, emerge as promising candidates in this regard.

The combination of calcium and sulfur represents a potent alternative, attributed to their abundant availability and recent research delineating the appreciable stability of their electrolyte system. [1] Nevertheless, to enhance fabrication efficiency, performance, and stability, a deeper understanding of the electrochemical dynamics at the anode surface, where the electrolyte interfaces with calcium, is essential. The work in the Casino project [2] aims for an understanding and optimization of key aspects towards its application.

The electrochemistry happens at the surface between the electrodes and electrolyte system. Understanding the details is what makes improvements possible. A novel in-situ model system is developed to mimic the behavior of the macroscopic symmetric Ca-Ca battery system while allowing atomic-level observations. Direct transfer of 2D materials enables the formation of liquid pockets and therefore high-resolution studies. [3,4] Calcium and electrolyte solution is encapsulated between 2D materials, and In-situ investigations are employed combined with EELS and EDX to uncover key mechanisms.

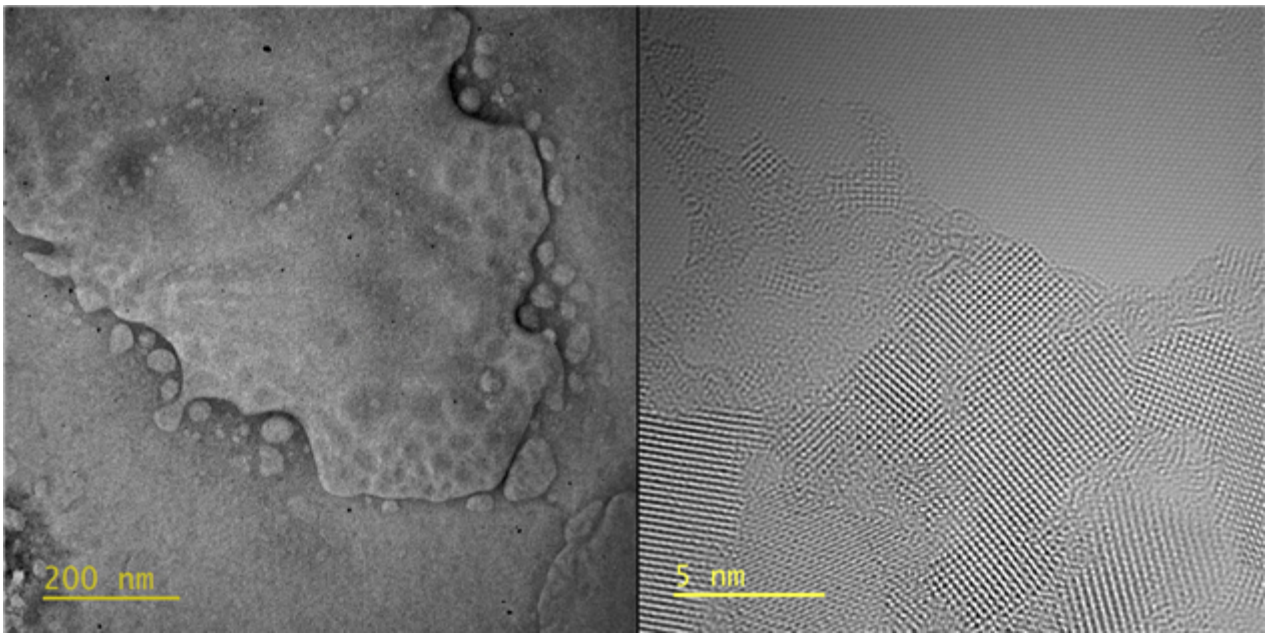

Keywords:

in-situ TEM, Multivalent Batteries

Reference:

The project was financially supported by the Bundesministerium für Bildung und Forschung (BMBF), under project CaSino, Grant number (Förderkennzeichen) 03XP0487D.

[1] Li, Z et. al., Energy Environ. Sci. 12, 3496–3501 (2019)
[2] https://www.dlr.de/tt/en/desktopdefault.aspx/tabid-14027/7108_read-80787/ , https://www.nmi.de/projekte-1/projektdetail/casino
[3] Jong et al., Science, 335(6077):61–64, 4 2012.
[4] Martin Textor and Niels de Jonge, Nano Letters 2018 18 (6), 3313-3321

714

Understanding the effect of Al:ZnO coating on the structural and chemical stabilities of LiNi1/3Mn1/3Co1/3O2 electrode

Ardavan Makvandi[1,5], Dr. Michael Wolff[2], Dr. Sandra Lobe[2], Bastian Heidrich[3], Dr. Martin Peterlechner[1,5], Dr. Christoph Gammer[4], Dr. Sven Uhlenbruck[2], Prof. Martin Winter[3,6], Prof. Gerhard Wilde[1]

[1]Institute of Materials Physics, University of Münster, Münster , Germany, [2]Forschungszentrum Jülich GmbH, Institute of Energy and Climate Research, Materials Synthesis and Processing (IEK-1) Jülich Aachen Research Alliance: JARA-Energy, Jülich, Germany, [3]MEET Battery Research Center, Institute of Physical Chemistry, University of Münster, Münster , Germany, [4]Erich Schmid Institute of Materials Science, Austrian Academy of Sciences, Leoben, Austria, [5]Laboratory for Electron Microscopy, Karlsruhe Institute of Technology, Karlsruhe, Germany, [6]Helmholtz Institute Münster, IEK-12 Forschungszentrum Jülich GmbH, Münster , Germany

Poster Group 1

LiNi1/3Mn1/3Co1/3O2 (NMC-111) is one of the most promising cathode materials in Li-ion batteries. However, structural and chemical instabilities of the electrode / electrolyte interface at high charge cut-off voltages lead to capacity fading. It is necessary to study the structure and chemistry of electrodes and electrode / electrolyte interfaces in Li-ion batteries since the interfaces determine the local Li-ion transport kinetics and the electrochemical performance. Surface modification using metal oxides is one of the best approaches to suppress capacity fading. In this work, a systematic study on the degradation mechanism of an uncoated NMC-111 powder electrode was presented. Moreover, the effect of an Al-doped ZnO (Al:ZnO) coating layer on the chemical and structural stabilities of NMC-111 electrode cycled at high charge cut-off voltages was analyzed using scanning electron microscopy, analytical transmission electron microscopy, and X-ray photoelectron spectroscopy. The objective of this work is to study the effect of electrode / electrolyte interface on the degradation mechanism and also the effect of coating layer on the stability of electrode / electrolyte interface. The coating layer was applied to commercial NMC-111 powder using a microwave-assisted sol-gel synthesis method. High-resolution TEM imaging, STEM imaging, nano-beam electron diffraction (NBD), electron-energy-loss spectroscopy (EELS), and energy dispersive X-ray spectroscopy (EDX) were carried out using a FEI Titan Themis G3 60-300 TEM. Cross-sectional TEM samples were prepared using a ZEISS cross-beam 340 FIB-SEM. In the case of uncoated NMC-111 electrode, cation mixing, pitting corrosion due to hydrofluoric acid attacking the electrode surface, and an irreversible phase transformation from a trigonal layered to a rock-salt phase occurred, leading to capacity fading. While, in the case of Al:ZnO – coated NMC-111 electrode, cation mixing, pitting corrosion, and the irreversible phase transformation were mitigated. Therefore, the rate capability and capacity retention were improved since the coating layer protected the electrode surface from the direct electrolyte exposure.

Keywords:

EELS, TEM, EDX, NBD, SEM

Reference:

Makvandi, A., Wolff, M., Lobe, S., Heidrich, B., Peterlechner, M., Gammer, C., Uhlenbruck, S., Winter, M., Wilde, G. Al-doped ZnO-Coated LiNi1/3Mn1/3Co1/3O2 Powder Electrodes: The Effect of a Coating Layer on The Structural and Chemical Stability of The Electrode / Electrolyte Interface. Adv. Mater. Interfaces 11, 2300668 (2024).

725

Ultra-fast and facile synthesis of cathodes for rechargeable batteries using an organic syntehsis route

Dr Saul Rubio[2], Mr Julio E. de la Rosa-Melian[1], Dr Francisco J. Garcia-Garcia[1], Dr Eva M. Perez-Soriano[1], Dr Cristina Arevalo[1], Dr Isabel Montealegre-Melendez, Dr Ana M Beltrán[2], Dr Juan G. Lozano[1]

[1]Departamento de Ingeniería y Ciencia de los Materiales y del Transporte, Escuela Técnica Superior de Ingeniería, Universidad De Sevilla, Sevilla, Spain, [2]Departamento de Ingeniería y Ciencia de los Materiales y del Transporte, Escuela Politécnica Superior, Universidad De Sevilla, Sevilla, Spain

Poster Group 1

The development of new promising cathode materials for lithium-ion batteries and sodium-ion batteries must go hand-in-hand with the development of new, more efficient, and more environmentally friendly synthesis routes. Several strategies have been reported in the literature to try to overcome the current limitations that prevent a broader deployment of promising cathode materials for intercalation batteries. Among them, the synthesis of electrode materials via an emulsion procedure demonstrated to be beneficial to obtain materials with controlled morphology [1].

In particular, a novel synthesis route [2], which involves the use of metal acetates, water, and oleic acid to form an emulsion is specially promising since only organic precursors are used, and the side reaction products are not contaminant,which makes it significantly more environmentally friendly. Here we present a structural and electrochemical characterisation of the cathodes synthesised using a modification of the aforementioned route. This modification reduces the mixing times of all the precursors required down to a few minutes, which is a very significant improvement compared with the tradicional sol-gel or ball-milling routes used at the laboratory levels. Furthermore, the modification makes this route very easily upscalable at the industrial level.

We have synthesised a large variety of promising cathodes for the families of lithium-ion and sodium-ion batteries. Transmission electron microscopy and related techniques were used to evaluate the quality of the particles fabricated using this novel synthesis route, and the results are compared with particles fabricated using the more stablished synthesis methods. The particle size and distribution were characterised by means of conventional transmission electron microscopy, while X-ray energy dispersion spectroscopy maps in scanning-transmission electron microscopy (STEM) was used to visualize the elemental distribution in individual particles. Aberration-corrected STEM corroborated that the expected atomic structure had been achieved in individual particles.

In a subsequent step, the particles were analysed at the fully charged and several-times cycled states to visualize the atomic rearrangements and chemical changes that may lead to battery failure. In those cases, the electron dose was carefully controlled to avoid irreversible beam damage, especially in the charged particles. Additionally, multi-frame acquisition followed by non-rigid registration and averaging was used to further reduce the damage due to exposure to the electron beam.

All the results obtained using the ultra-fast synthesis route described here are in very good agreement with those obtained for the same materials using the more conventional sol-gel or mechanical dry-mixing methos, whereas the times involved are considerably reduced.

Keywords:

Cathodes, Li-ion, Na-ion, STEM, Organic

Reference:

[1] A. Pan, D. Choi, J.-G. Zhang, S. Liang, G. Cao, Z. Nie, B. W. Arey, J. Liu, J. Power Sources, 2011, 196, 3646.
[2] F. J. García, R. Klee, P. Lavela, M. R. D. Bomio, J. L. Tirado. ChemElectroChem, 2020, 7, 3528.

729

Visualization of binder mixtures in hard carbon composite electrodes using OsO4 and uranyl acetate staining

Gregor Neusser[1], Tom Philipp[1], Sven Daboss[1], Clarissa Read[2,3], Paul Walther[2], Christine Kranz[1]
[1]Institute of Analytical and Bioanalytical Chemistry, Ulm University, Ulm, Germany, [2]Central Facility for Electron Microscopy, Ulm University, Ulm, Germany, [3]Institute of Virology, Ulm University Medical Center, Ulm, Germany

Poster Group 1

Background and aims

Aqueous processable binders, such as a sodium carboxymethyl cellulose (CMC) - styrene butadiene rubber (SBR) mixture are crucial constituents in composite battery electrodes ensuring good adhesion properties, high elasticity as well as improved cyclability and thermal stability (Alvira et al. 2022). The uniform distribution of the binder, active material, and conductive carbon is a prerequisite. Inhomogeneous distribution that may occur during the fabrication and processing of the electrode, such as coating, drying, and calendaring can lead to segregation, delamination or solidification which directly influence the overall battery performance (Jaiser et al. 2016). Therefore, its crucial to assess the distribution of the constituents, particularly the binder as agglomeration or segregation of the binder during longer cycling may lead to capacity loss.
The aim of the study is the visualization of CMC and SBR binder components next to hard carbon (HC) and conductive nano carbon particles using osmium tetroxide (OsO4) and uranyl acetate (UA) staining. OsO4 stains the double bonds present within SBR (Lee et al. 2022), whereas UA reacts with the carboxy groups (Stoeckenius 1961) of the CMC. As CMC is soluble in water, the sample preparation techniques must be adapted. In this study, we applied the embedding procedure introduced by Eswara-Moorthy et al., where Pt is deposited within a several µm deep volume of the sample using a 30 kV electron beam. This method avoids mechanical polishing using aqueous solutions and provides excellent contrast within the sample.

Methods

HC electrodes were prepared by doctor blading of a water-based slurry consisting of 80 wt.% HC, 10 wt.% SuperP, 5 wt.% Na-CMC and 5 wt.% SBR. The sample was first stained with OsO4 vapour by placing the sample in a sealed container together with a couple of droplets of 4 % aqueous OsO4 solution for 6 days, whereby the droplets were replenished after 3 days. In a second step, a droplet of 2 % uranyl acetate dissolved in ethanol was placed on the sample, removed after 30 min, and the sample was then rinsed with ethanol. The samples were investigated using a Helios Nanolab 600 and a Quanta 3D FEG (both Thermo Fisher Scientific Inc., USA). To achieve better contrast, avoid shine through artefacts, and reduce curtaining effects during FIB milling, the samples were embedded in Pt using electron beam induced deposition (EBID) with methylcyclopentadienyl trimethyl platinum as precursor and an electron beam operated at 30 kV, 32 nA. EDX mapping was conducted using an Element EDX detector attached to the Quanta and Apex standard software package (both EDAX Inc., Germany). The microscope was operated at 6 kV and 16 nA with a dwell time of 50 µs and 64 frames.

Results

Compared to the non-stained sample, secondary electron (SE) images of FIB cross-sections of the EBID Pt embedded region of the stained sample show reasonable contrast between the binder, HC particle and Pt (Fig.1 a & b). The contrast is sufficient to easily segment the 3 phases in FIB-SEM tomography data sets. It is also possible to distinguish between the binder matrix and conductive carbon nano particle within the binder. Although pores larger than approximately 1 µm in diameter were not completely filled with Pt, the delicate structure of the binder phase was well preserved.

Regions containing binder material are completely embedded and therefore provide volumes suitable for FIB-SEM tomography studies due to the enhanced contrast. EDX maps reveal the successful staining of both components, SBR with OsO4 and CMC with UA (Fig1. d & e). However, it should be noted, that remnants of the UA staining procedure may occur within the sample, but UA particles can be clearly distinguished. They appear brighter than the binder components in the SE images (e.g., Fig1 c & d, marked with red star) and in EDX measurements, as they contain less C but significant amounts of Na.

Conclusion

In this contribution, we show the potential of OsO4 and UA staining of SBR and CMC binder mixtures to reveal the 3D distribution of the binder phase within HC composite electrodes. EBID Pt embedding results in improved contrast and avoids artefacts as well as protect the delicate binder structures. The here described sample preparation method is suitable for FIB-SEM tomography studies and EDX mappings of FIB cross-sections, as the Pt surrounding the binder also limits the extend of the excitation volume compared to epoxy resin embedding. As both binder components react with different staining agents, namely CMC with UA and SBR with OsO4, both components can be tracked individually using EDX. For TEM-tomography studies EBID Pt embedding may not be suitable and should be replaced by classic epoxy resin embedding.

Fig.1: SE images and EDX maps of FIB cross-sections of EBID Pt embedded HC composite electrodes, red arrows point at binder components, hard carbon particles are exemplarily marked with “HC” a) SE image of non-stained electrode; b) SE image of the stained electrode with the stained binder components revealing clear difference in grey value relative to the HC particle and Pt embedding; c) SE image of ROI for EDX mapping; d) Os distribution; e) U distribution, red star marks possible UA remnant from the UA staining step.

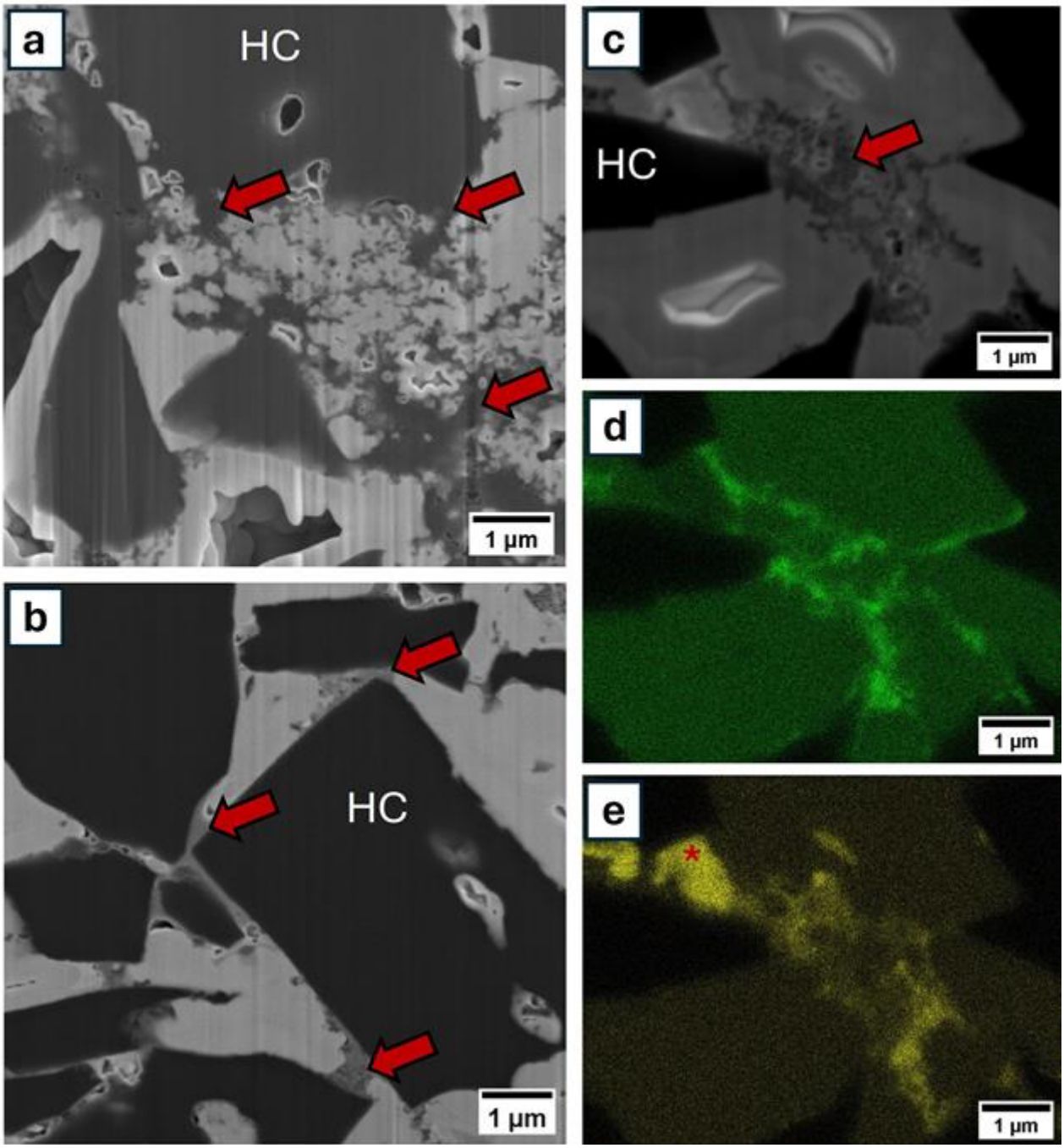

Keywords:

OsO4/UA staining, FIB-SEM-tomography, SBR-CMC binder

Reference:

Alvira D, Antorán D, Manyà JJ. Assembly and electrochemical testing of renewable carbon-based anodes in SIBs: A practical guide. Journal of Energy Chemistry. 2022;75:457-477. doi: 10.1016/j.jechem.2022.09.002

Jaiser S, Müller M, Baunach M, Bauer W, Scharfer P, Schabel W. Investigation of film solidification and binder migration during drying of Li-Ion battery anodes. Journal of Power Sources. 2016;318:210-219. doi: 10.1016/j.jpowsour.2016.04.018

Lee J-H, Kim J, Jeong MH, Ahn KH, Lee HL, Youn HJ. Visualization of styrene-butadiene rubber (SBR) latex and large-scale analysis of the microstructure of lithium-ion battery (LIB) anodes. Journal of Power Sources. 2023;557:232552. doi: 10.1016/j.jpowsour.2022.232552

Stoeckenius W. Electron microscopy of DNA molecules “stained” with heavy metal salts. Journal of Biophysical and Biochemical Cytology. 1961;11(2):297-310. doi: 10.1083/jcb.11.2.297

Eswara-Moorthy SK, Balasubramanian P, van Mierlo W, et al. An In Situ SEM-FIB-Based Method for Contrast Enhancement and Tomographic Reconstruction for Structural Quantification of Porous Carbon Electrodes. Microscopy and Microanalysis. 2014;20(5):1576-1580. doi:10.1017/S1431927614012884

731

Toward 3D imaging of the PEMFC electrode microstructure

Dr Laure GUETAZ[1], Mr Mamadou Sangare[1], Dr Thomas David[1], Dr Zineb Saghi[2], Dr Arnaud Morin[1], Dr Joël Pauchet[1]
[1]Université Grenoble Alpes, CEA, LITEN, Grenoble, France, [2]Université Grenoble Alpes, CEA, LETI, Grenoble, France

Poster Group 1

Background incl. aims
Proton Exchange Membrane Fuel Cells (PEMFCs) are being developed mainly for transport applications. Significant progress has been made over the last decade, leading to the commercialization of the first generation of fuel cell cars. More recently, R&D efforts have shifted to heavy-duty vehicles, where PEMFCs are more competitive with Li-ion batteries. However, their cost and durability are still the two barriers limiting the expansion of this market. To overcome these obstacles, we still need to optimise the components and structure of the electrodes and better understand their degradation mechanisms.
PEMFC electrodes are a nano-porous material composed of carbon particles (30 nm) supporting platinum nanoparticles (3 nm) - the catalysts of electrochemical reactions - and linked together by ionomer (proton conducting polymer).
Scanning and transmission electron microscopies (SEM and TEM) are widely used for investigating the microstructure of PEMFC electrode. They have played a significant role in the improvement of electrode components and the understanding of their main degradation mechanisms. However, the currently available descriptions of the electrode microstructure do not allow yet to unambiguously identify the key microstructural parameters that limit gas and proton transport within the electrode. These factors are crucial as they govern PEMFC performance, especially at high current densities, and are therefore the subject of numerous studies, using either fine electrochemical measurements or modeling approaches.
The aim of our work is to provide an improved description of the electrode microstructure in 3D to give quantitative information on its porosity, Pt nanoparticle (NP) spatial distribution and ionomer distribution. For this purpose, we are developing 3D characterization techniques applied to the PEMFC electrodes, such as electron tomography and 3D FIB-SEM.

Methods
The studied cathode electrode was prepared using TEC10E50E catalyst from Tanaka that is 50 wt % loading of Pt deposited on high-specific area carbon (HSAC), and Nafion D2020 as the electrode ionomer. The Pt loading of the electrode is 0.2 mgPtcm-2 and the ionomer/carbon ratio is 0.8.
The electrode was analyzed using electron tomography and 3D FIB-SEM.

Results
As a first step, electron tomography analyses were performed on the Pt/HSAC powder to determine the distribution of Pt NPs which can be located either on the carbon surface (outer NPs) or inside the carbon porosity (inner NPs)[1-2]. Our strategy is to record tilt image series by using two annular detectors: i) a high angle annular detector avoiding Pt NP diffraction contrast for the 3D image reconstruction of Pt NPs (without diffraction artifact) and ii) a lower angle annular detector that enhances carbon contrast for the 3D image reconstruction of the carbon phase. These two segmented images were then combined (Figure 1), allowing the calculation of the NP size histogram but also of the volume and the surface area of the two NP populations (inner and outer NPs).
On the second step, the porosity of the electrode was analyzed by 3D FIB/SEM. A volume of around 10 X 10 x 5 µm3 was imaged with a cubic voxel size of 5 × 5 × 5 nm3. The solid phase (carbon, Pt NPs

and ionomer) segmentation was based on a composite image created from two electron detectors (secondary and backscattered electrons) and using a machine learning software. Quantitative data such as the total porosity and the pore size distribution were extracted from this volume. Figure 2a shows a 2D slice of this segmented volume where the solid phase is in black and the porosity in white.

In order to analyze the electrode porosity with a higher spatial resolution, electron tomography experiment was also performed on a 150 nm thick slice of the electrode cut by ultramicrotomy after being embedded in an epoxy resin. The tilt image series were recorded with a pixel size of 0.5 nm and a field of view of 2 x 2 µm2. The 2D slice of the reconstructed volume (Figure 2b) shows that the largest solid agglomerates detected on the 3D FIB/SEM image can be identified as an agglomeration of numerous carbon particles. The challenge now is to quantify the porosity created between these carbon particles, which cannot be detected by 3D FIB-SEM.

Finally, the distribution of the ionomer was analyzed within the electrode similarly to [3]. For this analysis, a 150 nm slice of the electrode was cut by cryo-ultramicrotomy without embedding in epoxy resin as described in [4]. TEM images show that the ionomer is not homogeneously distributed on the surface of the entire carbon particles but is often observed in the concave surface created between the carbon particles (Figure 3). These observations suggest a ionomer distribution in agreement with the heterogeneous ionomer coating model proposed by Inoue et al. [5]. We also suggest that a part of the ionomer could be localized in the small pores located inside the large carbon agglomerates described in the previous paragraph. This could explain why the ionomer is so difficult to detect on TEM images.

Conclusion

The different 3D electron microscopy techniques make it possible to obtain information on the distribution of the different components of the PEMFC electrode. This 3D description of the electrode can then be incorporated into recent models that calculate electrochemical performance as a function of microstructural parameters, in an attempt to identify the key parameters that limit cell performance. Similar studies are also being carried out on aged electrodes after the fuel cell operation.

This work has been done in the frame of the FURTHER-FC project. This project has received funding from the Fuel Cells and Hydrogen 2 Joint Undertaking (now Clean Hydrogen Partnership) under Grant Agreement No 875025. This Joint Undertaking receives support from the European Union's Horizon 2020 Research and Innovation program, Hydrogen Europe and Hydrogen Europe Research.

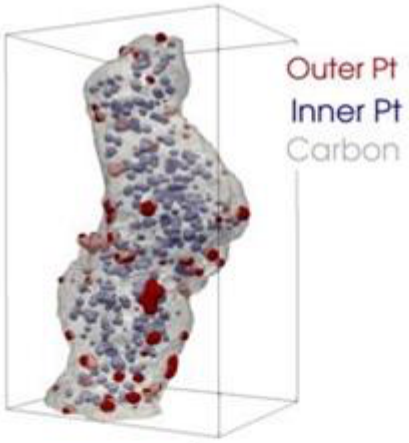

a)

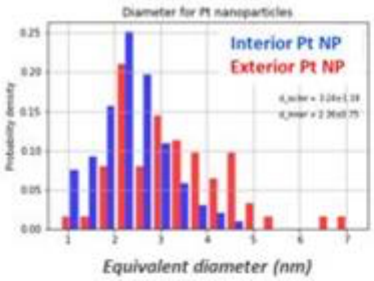

b)

***Figure 1**: a) 3D view of the Pt/HSAC powder obtained from electron tomography experiment and after segmentation (C in grey, inner Pt NPs in blue and outer Pt NPs in red). The parallelogram is 80 x 80 x 110 nm³. **b)** Histograms of the two population Pt NP size*

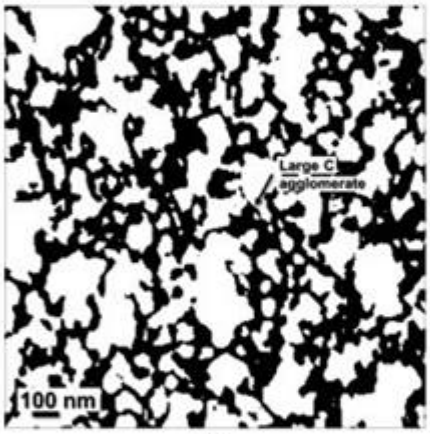

a)

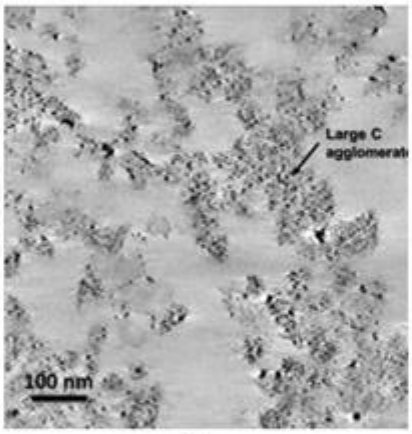

b)

***Figure 2**: Electrode 2D slices extracted from **a)** segmented volume obtained by 3D FIB/SEM and **b)** from reconstructed 3D image obtained from electron tomography experiment.*

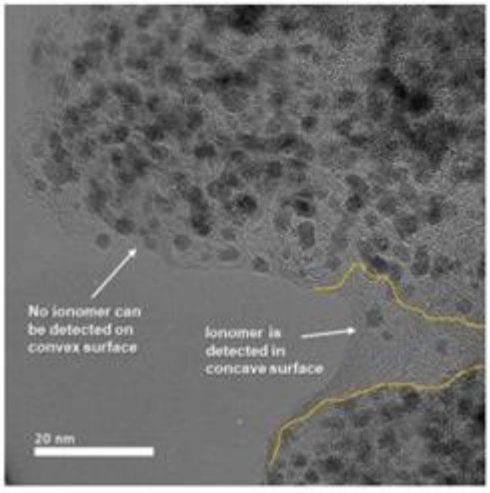

***Figure 3**: HRTEM image showing that the ionomer is not homogeneously distributed on the surface of the entire carbon particles but is often observed in the concave surface created between the carbon particles.*

Keywords:

PEMFC, Electrode, e-tomography, 3D FIB-SEM

Reference:

[1] T. Ito et al., Electrochemistry, 79 No. 5 (2011), 374
[2] B. T. Sneed et al., ACS Appl. Mater. Interfaces, 9, (2017), 29839
[3] R. Girod et al., Nature Catalysis, 6, (2023), 383.
[4] M. Barreiros Salvado et al., J. of Power Sources, 482, (2021), 228893
[5] G. Inoue Intern. J. Hydr. Energy , 41, (2016), 21352.

737

Investigating solar degradation mechanisms of the Ta3N5 photoelectrode by in-situ transmission electron microscopy

Dr. Annett Thøgersen[1], Dr. Øystein Dahl[4], Dr. Shima Kadkhodazadeh[2], Dr. Michael Seifner[2], Msc. Martin Fleissner Sunding[1], Dr. Ingeborg-Helene Svenum[4], Dr. Mathieu Grandcolas[1], Professor Thomas Willum Hansen[2], Dr. Ingvild Julie Thue Jensen[1], Dr. Athanasios Chatzitakis[3]
[1]SINTEF, Oslo, Norway, [2]DTU, Lyngby, Denmark, [3]UiO, Oslo, Norway, [4]SINTEF, Trondheim, Norway

Poster Group 1

Background incl. aims

Photoelectrochemical water splitting is a clean and renewable method to directly convert green energy carrier from solar light into hydrogen. Ta3N5 is a promising photocatalytic material for use as a photoanode, with suitable bandgap (2.2 eV), and with the conduction band (CB) and valence band (VB) energy levels appropriately straddling the water redox potentials [1]. By applying only 1.23 V of overpotential, the photocurrent density under 1 Sun illumination reaches the theoretical limit of approx. 13 mA.cm2 [2, 3]. However, during operation when the photoelectrode is exposed to water, sunlight, and biasing conditions, photocorrosion has shown to occur. This reduces the stability of the device significantly and degrades the material by oxidizing the surface. In order to utilize this material as a stable and efficient photoanode, it is important to understand and prevent the solar degradation process. We have previously investigated the stability of the electronic band structure of Ta3N5 using operando ambient pressure X-ray photoelectron spectroscopy (AP-XPS) at the HIPPIE beamline at the MAX IV synchrotron in Lund using the “dip and pull” setup for pure Ta3N5 as well as NiOx coated materials and found Fermi-level pinning to occur, and a significant improvement was made by stabilizing the surface. We then wanted to investigate the dynamic structural changes that occur to Ta3N5 during the degradation process when Ta3N5 is exposed to water vapor, biasing conditions, and light.

Methods

Ta3N5 thin films on glass substrates were made with pulsed vapor deposition of metal Ta, following a nitridation process. Some samples were also made with a protective NiOx coating. The ex-situ characterization work was done using a FEI Titan G2 transmission electron microscope (TEM), DCOR Cs probe corrector, Super-X EDS detector, and Gatan GIF Quantum 965 electron energy loss (EELS) Spectrometer at SINTEF in Oslo. While the in-situ TEM characterization was carried out using an environmental transmission electron microscope a Titan E-Cell 80-300ST TEM at DTU. The TEM sample was made with a focused ion beam and connected to a heating and biasing chip with a diode placed on top of the extra contacts.

Results

During the degradation process, an amorphous layer is formed at the surface. The surface layer formation is highest when combining water, light, and biasing of the sample. The process seems to first make small nanocrystals of Ta3N5. After some time, they are amorphized, and new nanocrystals are formed. This process continues till we have a stable uniform surface layer.

Conclusion

The surface degradation process creates an amorphous layer, and is most pronounced when combining water, light, and bias. The degradation first makes small nanocrystals of Ta3N5, for then to amorphized them separately.

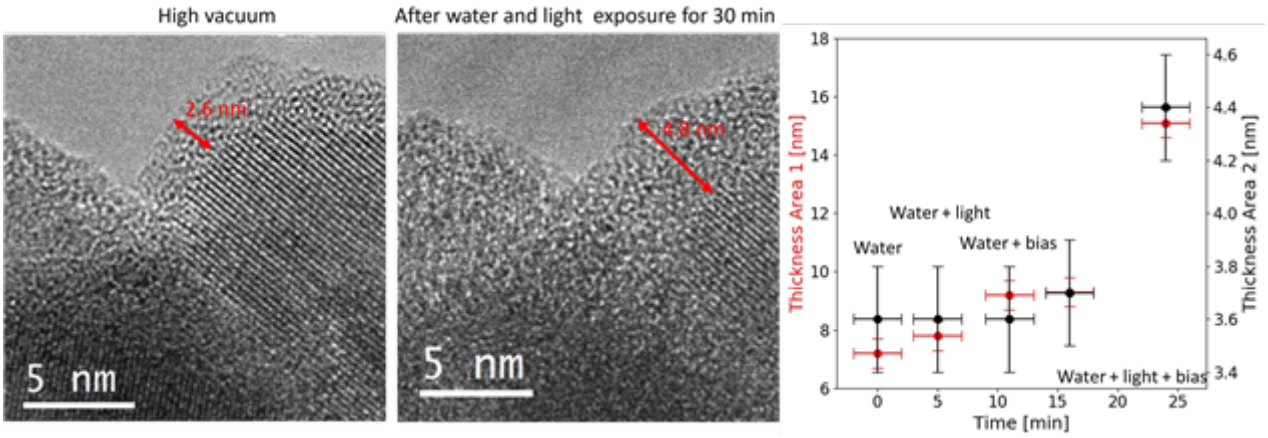

Keywords:

Degradation, TEM, operando, Ta3N5, Hydrogen

Reference:

Reference:
[1]: Xu, Chatzitakis, Jensen, Grandcolas, Norby. Photochem. Photobiol. Sci. 18 (2019) 837
[2]: Xu, K.; Chatzitakis, A.; Backe, P. H.; Ruan, Q.; Tang, J.; Rise, F.; Bjørås, M.; Norby, T. Applied Catalysis B: Environmental 2021, 296, 120349.
[3]: Liu, G.; Ye, S.; Yan, P.; Xiong, F.; Fu, P.; Wang, Z.; Chen, Z.; Shi, J.; Li, C. Energy & Environmental Science 2016, 9 (4), 1327-1334

785

Insights on the disordered nature in amorphous-based anode materials from Electron Pair Distribution Function

Dr. Anuj Pokle[1], Marte Orderud Skare[2], Shihui Feng[3], Dr Cheuk Wai Tai[3], Dr Asbjørn Ulvestad[2], Prof Xiaodong Zou[3], Prof Øystein Prytz[1]
[1]Department of Physics and Center for Materials Science and Nanotechnology, University of Oslo, Oslo, Norway, [2]Department of Battery Technology, Institute for Energy Technology, Kjeller, Norway, [3]Department of Materials and Environmental Chemistry, Arrhenius Laboratory, Stockholm University, Stockholm, Sweden

Poster Group 1

In the field of material science, the ability to determine structures at high spatial resolution is paramount for understanding their properties. While traditional X-ray and electron diffraction techniques have been successful in determining crystalline structures, the need for new techniques is evident. Conventional methods fall short in providing detailed structural information for disordered structures, such as those found in nanostructured and amorphous materials, making our research on the disordered nature of anode materials all the more significant.

The pair distribution function (PDF) method based on X-ray and neutron diffraction is widely employed for providing quantitative information in amorphous materials [1]. Nonetheless, understanding medium-range structural order in amorphous materials is non-trivial, where the position of atoms cannot be assigned by any equation based on translation vectors. Electron Diffraction (ED) related PDF (ePDF) in Transmission Electron Microscope has the advantage of investigating ordering locally. However, ePDF-based analyses may be affected by dynamical effects, altering the scattering intensities.

This work aims to expand the developed methodology to battery materials research by employing electron diffraction data to obtain PDF coupled with low-loss electron energy loss spectroscopy [2]. This will enable us to delve into the role of volume expansion during lithiation in silicon-carbon-based anode materials, which is a crucial aspect of the electrode's functioning.

Keywords:

S/TEM, ePDF, EELS, batteries

Reference:

1. Zeng, L., Tran, D. T., Tai, C.-W., Svensson, G. & Olsson, E. Atomic structure and oxygen deficiency of the ultrathin aluminium oxide barrier in Al/AlOx/Al Josephson junctions. Sci Rep 6, 29679 (2016).
2. Tran, D. T., Svensson, G. & Tai, C.-W. SUePDF: a program to obtain quantitative pair distribution functions from electron diffraction data. J Appl Cryst 50, 304–312 (2017).

808

Operando Environmental TEM observations of SOEC Ni-YSZ fuel electrode dynamics

Mr. Magnus Björnsson[1], Mr. Søren Simonsen[1], Mr. Ming Chen[1]
[1]Department of Energy Conversion and Storage, The Danish Technical University, Kgs. Lyngby, Denmark

Poster Group 1

Power-to-X is emerging as a key player in the decarbonization of our energy infrastructure and at its core is electrolysis. The most efficient electrolysis technology is Solid Oxide Electrolysis Cells (SOEC) [1] however, large scale implementation has been halted by the concerns regarding loss of efficiency caused by degradation. The most important degradation process occurs in the Ni-Yttria stabilized zirconia (YSZ) fuel electrode. The driving factors are changes in Ni particle morphology and wetting angle, which are suggested to be correlated to the local SOEC operating conditions [2, 3]. Previous studies which have set out to investigate changes to the Ni morphology during SOEC conditions have only done so using post-mortem analysis where the sum of all the experimental parameters are observed. This makes it difficult to identify the correlation between the local test conditions and the morphological changes to the Ni particles.

To study the dynamic electrode processes occurring under standard SOEC operating conditions, we apply a newly developed operando electrochemical environmental transmission electron microscopy (ETEM) method [4, 5]. The method is adapted so that it allows us to follow the morphological changes of Ni particles in Ni-YSZ fuel electrodes, enabling us to map the degradation as a function of operating conditions. The aim of this project is to bring SOEC technology ahead by determining a so-called safe operational window which can limit, or possibly eliminate, the detrimental and irreversible degradation of Ni-YSZ fuel electrodes.

Sample preparation is carried out with a Zeiss FIB-SEM dual-beam which enables micromachining of bulk samples. The prepared samples are placed on a MEMS-chip from DENSsolutions which is capable of simultaneous heating and biasing. The finalized samples are imaged using a TITAN ETEM which allows the samples to be subjected to a reactive gas environment. Our method presents a novel way of studying the dynamic processes occurring in Ni-YSZ fuel electrodes as a function of real-life operating conditions. This will allow us to determine a safe operational window in which the most severe degradation can be avoided. This will ensure longer operating lifetimes of SOEC and make the technology more desirable in terms of large-scale implementation and ultimately advancing the decarbonization of our energy infrastructure.

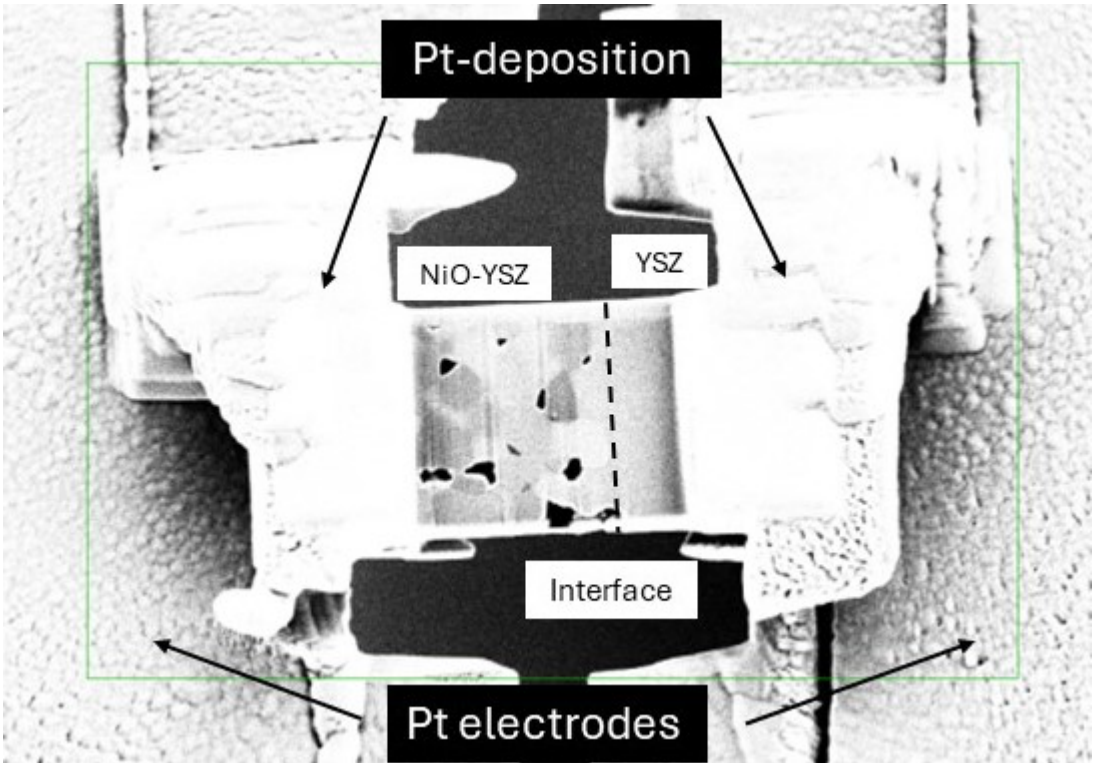

Keywords:

Power-to-X, FIB-SEM, ETEM, Ni-wetting

Reference:

[1] A. Hauch, R. Küngas, P. Blennow, A. B. Hansen, J. B. Hansen, B. V. Mathiesen, and M. B. Mogensen, Science, vol. 370, 10, 2020.

[2] Y. Wang, C. Wu, B. Zu, M. Han, Q. Du, M. Ni, K. Jiao, J. Power Sources. 516, 2021.

[3] M. Trini, A. Hauch, S. De Angelis, X. Tong, P.V. Hendriksen, M. Chen, J. Power Sources. 450 (2020) 227599.

[4] Z. Ma, C. Chatzichristodoulou, F.M. Chiabrera, K.S. Mølhave, S.B. Simonsen, ACS Energy Letters, 9 (2024) 2007-2012

[5] Z. Ma, C. Chatzichristodoulou, W.L. Dacayan, K.S. Mølhave, F.M. Chiabrera, T.E.L. Smitshuysen, C.D. Damsgaard, S.B. Simonsen, Small Methods (2024)

820

Transmission electron microscopy studies of ferroelectric ZrO2 thin films

Phd Student Marian Cosmin Istrate[1], Dr Corneliu Ghica[1], Dr Jose Pedro Basto Silva[2]
[1]National Institute of Materials Physics, 105 Bis Atomistilor, 077125, Magurele, Romania, [2]Physics Center of Minho and Porto Universities (CF-UM-UP), University of Minho, Campus de Gualtar, 4710-057, Braga, Portugal

Poster Group 1

INTRODUCTION

The discovery of ferroelectricity in zirconia and hafnia [1] based thin films revolutionized the research in the field of ferroelectrics and paved the way for their integration into real applications. However, the wake-up phenomenon associated with the presence of non-polar phases and/or defects in the films still hinders the reliability of the device operation. Therefore, new strategies for achieving ferroelectric single-phase orthorhombic zirconia and hafnia based thin films are welcomed.

EXPERIMENTAL/THEORETICAL STUDY

8-nm thick ZrO2 thin films were grown by ion-beam sputter deposition (IBSD) onto 0.7 wt% Nb-doped SrTiO3 substrates with (001), (011) and (111) orientations.
Cross-sectional TEM samples were made by first mechanical thinning followed by Ar+ ion milling on a Gatan PIPS machine at 4 kV acceleration voltage and 6 degrees beam incidence angle. TEM observations were performed using a probe-corrected analytical high-resolution JEMARM 200F electron microscope operated at 200 kV.

RESULTS AND DISCUSSIONS

We note the Figure inserted in the graphic area by Figure 1. Fig. 1(a), (b) show HRTEM images of a ZrO2/(011)Nb:STO thin film. The ZrO2/(011)Nb:STO structure with (111) and planes of the o-phase are indexed. The FFT pattern shown in Fig. 1(c) corresponds to an area delimited by the red square inside the ZrO2 layer in Fig. 1(a). It contains a well-defined pattern of spots, proving a high crystalline quality of the ZrO2 film in terms of grain size and preferential crystallographic orientation. The main FFT peaks were measured, indexed and assigned to the (13-1), (111) and (02-2) planes of the orthorhombic structure of ZrO2 in the [-211] zone axis orientation. [2]

CONCLUSIONS

The HRTEM investigations indicate that substrate orientation control proves to be an efficient way to manipulate the phase of the as-grown ZrO2 thin films. We also studied ZrO2 films grown on (001)Nb:STO and these second set of films showing mixed orthorhombic and monoclinic phases. Macroscopic ferroelectric measurements of the phase pure, orthorhombic (111)ZrO2 films showed a remnant polarization of ~14 µC/cm2 and a coercive field of ~1.4 MV/cm. Also, piezo force microscopy measurements showed that polar domains could be written/read and reversibly switched with a phase change of 180°.

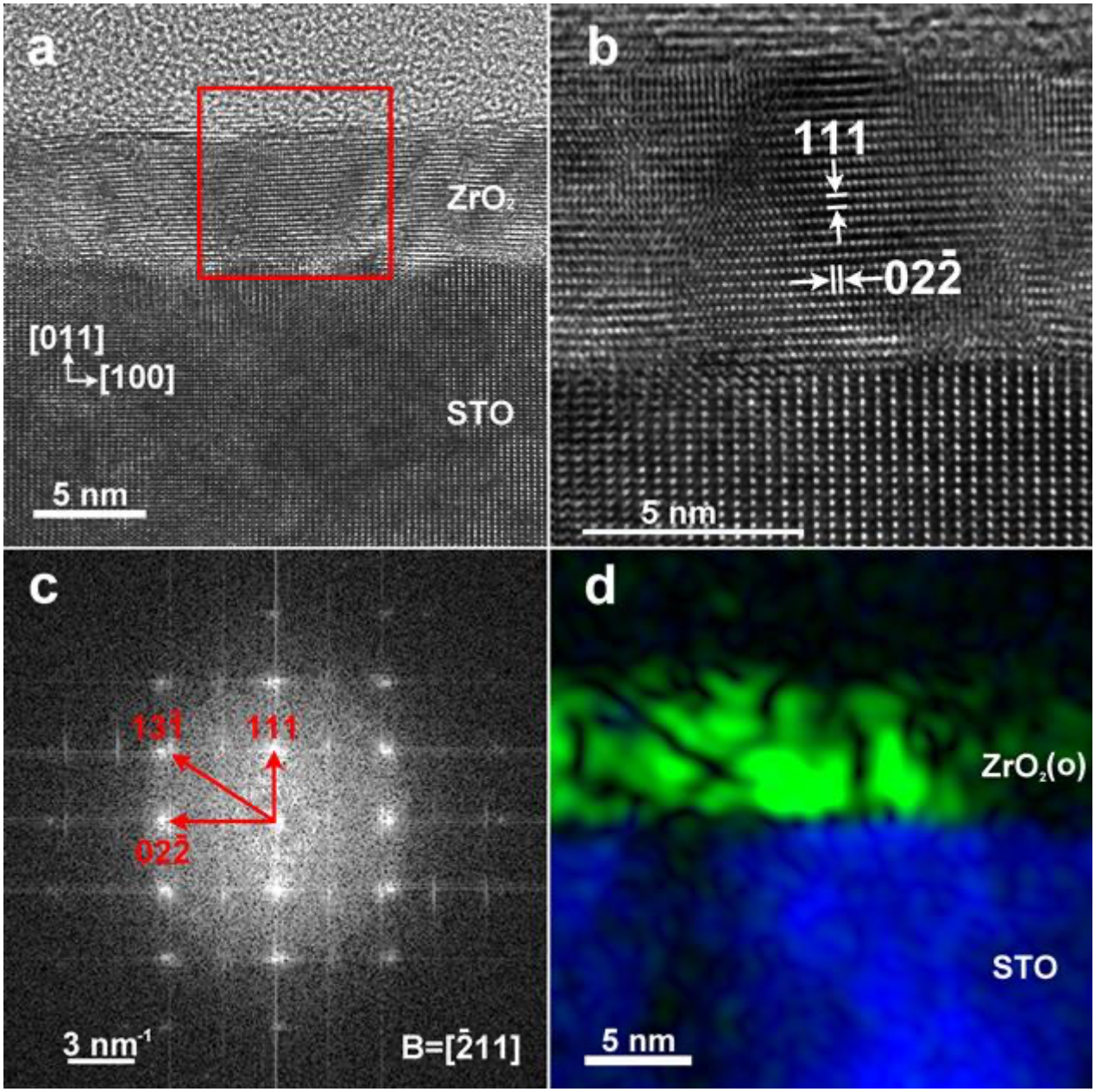

Keywords:

HRTEM, Ferroelectric, Thin film

Reference:

1. T. S. Boescke, J. Mueller, D. Braeuhaus, U. Schroeder, and U. Boettger, Appl. Phys. Lett. 99, 102903 (2011)
2. José P.B. Silva, Marian C. Istrate, Markus Hellenbrand, Atif Jan, Maximilian T. Becker, Joanna Symonowicz, Fábio G. Figueiras, Veniero Lenzi, Megan O. Hill, Corneliu Ghica, Konstantin N. Romanyuk, Maria J.M. Gomes, Giuliana Di Martino, Luís Marques, Judith L. MacManus-Driscoll, Ferroelectricity and negative piezoelectric coefficient in orthorhombic phase pure ZrO2 thin films, Applied Materials Today, Volume 30, 2023, 101708, ISSN 2352-9407,

821

Characterization of the structure and chemistry of solid electrolyte

Dr Kyung Song[1], Dr Abin Kim[2], Professor Byungwoo Kang[2]
[1]Korea Institute of Materials Science , Changwon, Republic of Korea, [2]Pohang University of Science and Technology , Pohang, Republic of Korea

Poster Group 1

Background incl. aims
Solid-state Li metal batteries (SSLMBs) have been of great interest for electric vehicles due to their high energy density and safety features. Garnet-type $Li_7La_3Zr_2O_{12}$ (LLZO) solid electrolyte (SE) is a promising candidate due to its high ionic conductivity and stability with Li metal. While its preparation and electrical properties have been extensively studied, research on air handleability and Li metal wettability has been relatively limited. Addressing Li_2CO_3 formation on LLZO surfaces is critical because the formed Li_2CO_3 hinders the electrical properties, creates poor interfaces, and reduces metal wettability [1]. We developed a Li_2CO_3-proof LLZO (AH-LLZO) SE that is stored and handled in humid air without compromising electrical properties and simultaneously shows excellent Li metal wettability.
Methods
To understand the air-handling ability of LLZO, we performed characterization of structure and chemistry using SEM, XPS and STEM-EELS.Two samples were prepared by a simple solid-state reaction. One sample (C-LLZO) has a known composition ($Li_7La_3Zr_2O_{12}$) with a large excess amount of Li to compensate for the expected Li loss during high temperature treatment, and the other sample (AH-LLZO) contains excess Al and the same large amount of excess Li.
Results
SEM-EDS analysis reveals a distribution of Al both in the bulk and at the grain boundary of AH-LLZO. Some Al segregates into the grain boundary, while some is doped into the bulk. Elemental profiles of the Al $L_{2,3}$- and La $N_{4,5}$-edge via STEM-EELS further confirm that the Al in present both regions. The grain shows an almost constant amount of Al, but a sharp increase at the grain boundary suggests an Al-rich environment, possibly $LiAl_5O_8$-related phases, which is the most stable Li-deficient Al-rich phase [2]. High-resolution XPS confirms the absence of carbon-related peaks at a depth of 100 nm from the AH-LLZO surface which is clearly distinguished from C-LLZO, which exhibits a strong carbonate peak. To confirm the detailed surface structure, we performed STEM-EELS analysis across LLZO grain boundary for two LLZO. Consistent with the XPS results, AH-LLZO does not have any carbonrelated peaks in the grain or at the grain boundary, indicating that there is no Li_2CO_3 propagation into the core via the grain boundary. In contrast, C-LLZO exhibits carbon signals inside the grain boundary, suggesting that Li_2CO_3 formation/propagation in the bulk through the grain boundary can be occurred [3]. The EELS peaks for the oxygen at the grain boundary are similar to the oxygen binding energy of Al-rich Li-Al-O-related compounds such as $LiAl_5O_8$. This Li-Al-O-related phase at both the surface and the grain boundary blocks against water or carbonate infiltration, leading to the suppression of the Li_2CO_3 formation/propagation.
Conclusion
The presence of excess Al and Li without charge/site balance in the LLZO causes a distinctive microstructure with Al-doped LLZO grains and Li-Al-O phases at the grain boundary/surface. In the Al-doped LLZO grain, the preferential occupation of Al at 96h sites can reduce the LiOH formation and then suppress Li_2CO_3 formation. The Li-Al-O-related phases on the surface and at the grain boundary, particularly the $LiAl_5O_8$-like phase, act as a hydrophobic barrier, blocking water adsorption.

Keywords:

Solid electrolyte, LLZO, STEM-EELS

Reference:

[1] Kim, A.; Kang, J.-H.; Song, K.; Kang, B. ACS Appl. Mater. Interfaces 2022, 14 (10), 12331−12339.
[2] Mo, S.; Zhang, B.; Zhang, K.; Li, S.; Pan, F. Phys. Chem. Chem. Phys. 2019, 21 (25), 13758−13765.
[3] Kim, A.; Song, K.; Kang, B. ACS Energy Lett. 2024, 9, 1976-1983.

824

Correlative study of hematite-based photoanodes for solar water splitting by transmission electron and X-ray microscopies

Léon Schmidt[1], Bilal Meddas[2], Walid Baaziz[1], Dana Stanescu[2], Stefan Stanescu[3], Ovidiu Ersen[1]
[1]IPCMS CNRS / Université de Strasbourg, Strasbourg, France, [2]SPEC CEA Saclay / CNRS, Gif sur Yvette, France, [3]Synchrotron SOLEIL, Saint-Aubin, France

Poster Group 1

Background incl. aims
In the framework of hydrogen production as means for renewable energy storage, titanium-doped hematite (Ti:α-Fe_2O_3) nanorods have received renewed interest for potential use as a photoanode in photoelectrochemical cells, owing to their high theoretical photoelectrochemical activity, absorption spectrum compatible with sunlight, as well as the abundance of its constituents, allowing cost- and resource-efficient production of hydrogen by solar water splitting (SWS) [1].

In a previous work [2], a two-step synthesis for this material was developed. First, using $FeCl_3$ and $TiCl_3$ precursors, the deposition by aqueous chemical growth (ACG) of an intermediate phase, Ti-doped akageneite (Ti:β-FeOOH) on a glass/FTO substrate was carried out. This step is followed by the annealing of the intermediate phase in a controlled oxygen and nitrogen atmosphere to yield the final Ti-doped hematite photoelectrode structure.

Both synthesis steps are very sensitive to various parameters, which can change the outcome of the final iron oxide structure and its efficiency for the SWS process. Parameters such as the pH of the initial precursor solution, age of the $TiCl_3$ precursor, time and temperature of the thermohydrolysis process as well as of the annealing process, and annealing atmosphere, may all have an impact on the structure and the properties of the final material [3].

Herein, we study the as-obtained hematite nanostructures to characterize their morphology, crystalline structure, chemical composition and electronic properties, as a function of the various synthesis parameters. A correlative approach combining transmission electron microscopy (TEM), yielding images with high spatial resolution, with synchrotron-based scanning transmission X-ray microscopy (STXM) exhibiting chemical sensitivity, in the aim to extract morphological and structural features from the former, electronic structure and chemical coordination from the latter.

Furthermore, we relate the results obtained by these microscopy techniques with photoelectrochemical (PEC) results, to establish a structure-function relationship and thus to be able to optimize the synthesis of the photoanodes for yielding higher efficiency in the hydrogen production process.

Finally, in situ environmental TEM was used to study the annealing step under varying gas atmospheres to elucidate the transition mechanism as a function of gas composition, time and temperature.

Method
To characterize the Ti:α-Fe_2O_3 structures, a correlative approach combining TEM and STXM was implemented. Samples were recovered by scratching the surface of the hematite/FTO glass substrate, retrieving the hematite powder to be placed on either Cu grids or SiN membranes, both of which can be analyzed in TEM and STXM successively. In STXM, the samples were measured at the

absorption edges of Ti L2,3 (450-470 eV), O K (520-560 eV) and Fe L2,3 (700-740 eV), to provide localized XAS spectra describing the chemical state and coordination of the atoms of interest.
In TEM, conventional and high-resolution images were acquired in classical TEM and in STEM (BF and HAADF) to obtain morphological and structural information, corroborated by electron diffraction data and EDX spectroscopy maps, the latter to be compared with the chemical information obtained by STXM. Also, in situ environmental TEM experiments were carried out using a sealed cell-based holder inside the microscope in which a controlled gas atmosphere and temperature can be applied to the sample, allowing to monitor changes in morphology and chemical composition in real time.
PEC measurements were carried out in a dedicated PEC cell, using the hematite-based photoanode as working electrode, a Pt foil as counter electrode and an Ag/AgCl reference electrode, under a back-side illumination of 1 sun (0.1 W/cm²).

Results

For the first step, it was found that using an aged $TiCl_3$ precursor leads to the formation of mixed phase compounds, composed of both hematite (α-$Fe_2(III)O_3$), i.e. only Fe3+ cations in the structure, and a reduced phase, identified as magnetite ($Fe_3(II, III)O_4$), containing both Fe2+ and Fe3+, in the final products. In contrast, samples prepared with a fresh $TiCl_3$ precursor, only pure hematite was obtained (as shown in Fig. 2), which is the active phase for PEC and therefore the targeted result.
A comparative study changing the composition of the annealing gas, using various ratios of O_2/N_2, ranging from 0% to 100% has shown that the partial reduction of the sample is independent from the gas composition, meaning that this phenomenon is independent of the annealing environment but rather inherent to the specific sample composition. In fact, STXM-XANES measurements on the aged precursor revealed a change in its oxidation state, from Ti(III) to Ti(IV). The Ti(IV) cations incorporated in the akaganeite structure causes the reduction of Fe(III) to Fe(II) by charge compensation, yielding a partially reduced hematite structure after annealing, independently of the gas atmosphere.
These results were confirmed by in situ TEM measurements, showcasing a similar mechanism for the annealing independent of gas composition for samples prepared with the aged precursor, confirming the hypothesis that the reduction behavior originates from precursor ageing.
PEC measurements revealed that the photocurrent Jph of the samples prepared with aged precursor were, on average, lower than samples prepared with a fresh precursor, which was linked to the presence of the reduced phased in the former samples.

Conclusion

In this work, we have showcased the impact of the precursor aging, which, despite the low concentration of the dopant (< 1 at. %), plays a tremendous role on the reduction of targeted hematite phase and thus the efficiency for the solar water splitting application.
Further work is also currently being carried out to understand the influence of other important parameters, particularly the pH of the precursor solution, for which preliminary results showed that it directly impacts the length of the nanorods, yielding to varying PEC efficiencies.

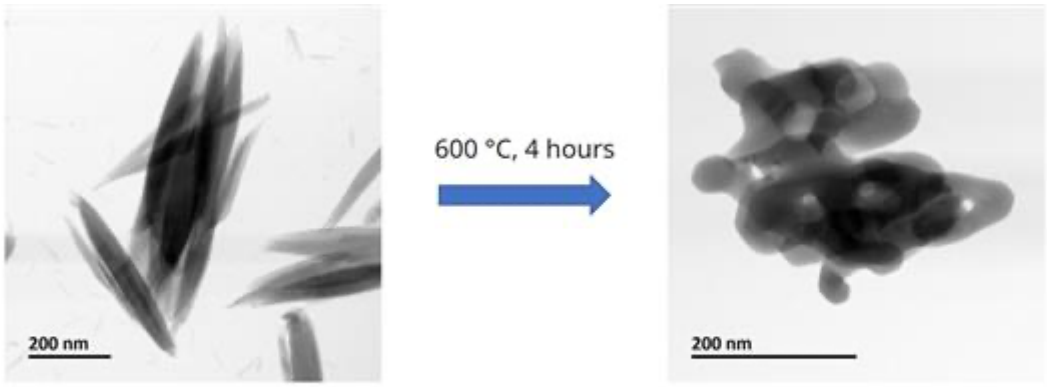

Figure 1: BF-STEM micrographs of as-retrieved akaganeite sample (left) and annealed hematite sample (right), synthetized with a fresh Ti precusor

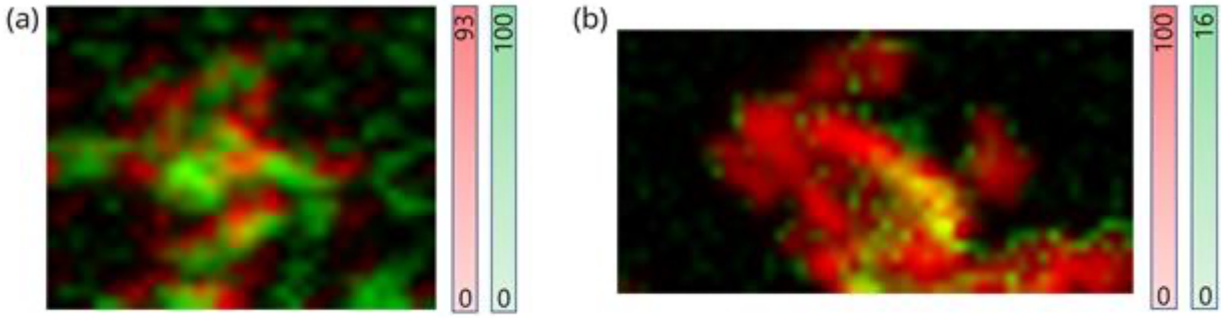

Figure 2: Red-green composite STXM image of the final hematite sample prepared with (a) aged and (b) fresh Ti precusor. Red pixels indicate regions fitting to a hematite reference spectrum, green pixels to a magnetite reference spectrum

Keywords:

Correlative, TEM, STXM, photoelectrochemistry, hydrogen

Reference:

[1] K. Sivula, F. Le Formal, and M. Grätzel, ChemSusChem. 2011, 4, 4.
[2] D. Stanescu et al., J. Mater. Chem. A. 2020, 8, 39.
[3] S. Stanescu et al., ACS Appl. Mater. Interfaces. 2023, 15, 22.

842

Structural Probing of Charging Mechanism in LiNiO2 at High Voltage using Microscopy and Spectroscopy

Dr Jun Chen[1], Dr Mikkel Juelsholt[2], Dr Robert House[1], Prof Peter Bruce[1]
[1]Department of Materials, University of Oxford, Oxford, United Kingdom, [2]Department of Chemical Engineering. Columbia University, New York, United States

Poster Group 1

Background

The demand of high-energy lithium-ion batteries boosts the interest in increasing Ni content in cathodes and raising charge cutoff voltage. LiNiO2 is a critical archetypal material for high energy density Li-ion batteries, forming the basis of Ni-rich cathodes in use today. Unfortunately, LiNiO2 suffers from a number of problems at high states of charge which have been linked with oxygen redox. Substantial efforts have been made to understand the structural transitions that take place when Li is extracted from LiNiO2, but there remains considerable debate over its structural mechanisms, in particular the extend of Ni oxidation and oxygen participation when charging at high cutoff voltage. [1,2]

Methods

We use polycrystalline LiNiO2 powder to make composite electrodes into Li coin cells. After charging and discharging to specific states of charge, we disassemble the cell for following characterizations. We use the annular dark-field scanning transmission electron microscopy (ADF-STEM) to directly examine structural changes at the atomic level. We employ combined neutron and synchrotron X-ray powder diffraction analysis that takes account of the stacking faults, and quantified the Ni vacancies formed when the material is charged across the voltage plateau. High resolution resonant inelastic X-ray scattering (RIXS) at the O K-edge is used to detect the molecular O2 that could be formed associated with O-redox. Ni L-edge and O K-edge X-ray absorption spectra are collected to probe the chemical state changing in LiNiO2. Chemical analysis by inductively coupled plasma-optical emission spectroscopy (ICP-OES) is used to check if there is Ni dissolution into the electrolyte after cycling.

Results

The atomic-resolution showed the surface densification and cation mixing evolution near surface region of LiNiO2 over charging to high cut-off voltage (Fig. 1a). When charging acrossing the 4.2V plateatu vs. Li+/Li, the particles form core–shell nature, with a Ni-rich, Ni1.75O2 rocksalt-like shell approximately of 5 nm thickness at the top of charge. The refinement of neutron and synchrotron X-ray powder diffraction demonstrates 8% Ni vacancies form in the originally fully dense transition metal layer at 4.2 V (Fig. 1b). Chemical analysis by ICP shows that the Ni absent from the bulk does not leave the particles. While in principle there is sufficient Ni3+/4+ oxidation capacity to account for all the Li+ removed on charge without O2- oxidation, high resolution RIXS at the O K-edge confirms the presence of trapped molecular O2, on charging across the plateau, which is accommodated Ni vacancy clusters. Ni L-edge XAS measurements in fluorescence yield mode implies the average oxidation state of Ni of less than +4, coexisting with the presence of O-redox at the top of charge (Fig. 1c,d).

Conclusion

Our results reveal that the structural instability in LiNiO2 is more extensive than previously thought. As illustrated in Fig. 1e, beyond the 4.2 V vs. Li+/Li plateau, Ni accumulates at and near the surface of the particles, forming a Ni-rich shell approximately 5 nm thick; enhanced by loss of O2 from the surface. This shell has composition of Ni1.75O2 shell a Ni oxidation state of +2.3. The oxidation of

O2− across the 4.2 V plateau forms O2 trapped in the particles and is accompanied by the formation of 8% Ni vacancies on the transition metal sites of previously fully dense transition metal layers. The overall Ni oxidation state of the particles measured by XAS in fluorescence yield mode after charging across the plateau to 4.3 V vs. Li+/Li is approximately +3.8; however, taking account of the shell thickness and the shell Ni oxidation state of +2.3, this indicates a Ni oxidation state in the core closer to +4 for compositions beyond the plateau.

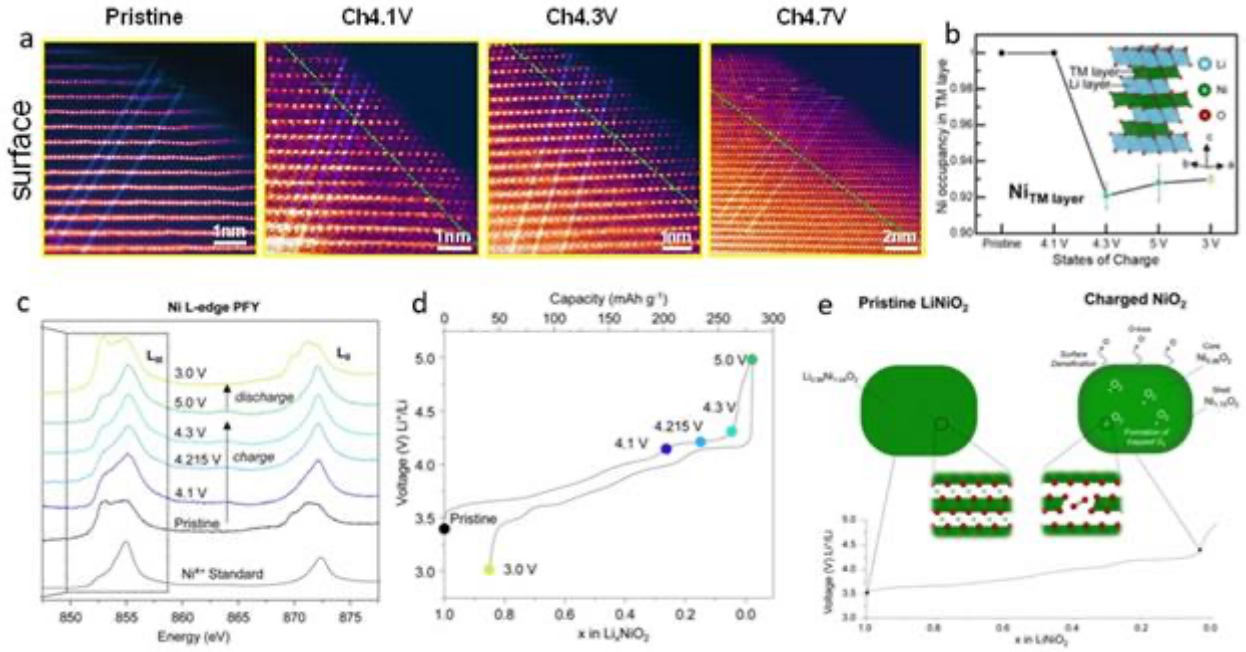

Keywords:

LiNiO2, charging mechanism, electron microscopy

Reference:

[1] Li, N. et al. Unraveling the Cationic and Anionic Redox Reactions in a Conventional Layered Oxide Cathode. ACS Energy Letters 4, 2836-2842 (2019).

[2] Genreith-Schriever, A. R. et al. Oxygen hole formation controls stability in LiNiO2 cathodes. Joule 7, 1623-1640, (2023).

904

Investigation on photocorrosion of TiO2 during photoelectrochemistry process by electron microscopy together with operando ICP-MS

Dr. Yiqun Jiang[1], Dr. Martin Rabe[1], Dr. Ilias Efthimiopoulos[1], Prof. Christina Scheu[1], Dr. Siyuan Zhang[1]
[1]Max-Planck Institut für Eisenforschung GmbH, Düsseldorf, Germany

Poster Group 1

Background incl. aims
With the growing environmental deterioration and ever-increasing energy demand, exploring a renewable and clean energy for human development has been regarded as a promising research subject. Hydrogen is one of the most desirable energy carriers. Fujishima and Honda discovered that hydrogen can be generated from water splitting on a TiO_2 photoelectrode under UV light illumination.[1] TiO_2 is considered to be stable since its redox potential has been calculated to be more positive/negative relative to the water oxidation/reduction potential. This means that photogenerated charge carriers would participate in driving the desired water splitting reactions rather than oxidizing or reducing semiconductor photoelectrodes.[2] Nevertheless, it is reported that there is degradation of performance and alterations in surface morphology of TiO_2 under UV light irradiation. Understanding the dynamic catalyst behaviour during electrochemical application plays a key role in developing improved catalysts.

Methods
We applied scanning electron microscopy (SEM), aberration-corrected transmission electron microscopy (TEM), X-ray diffraction (XRD), x-ray photoelectron spectroscopy (XPS) and Raman spectroscopy together with operando inductively coupled plasma mass spectrometry (ICP-MS) coupled with illuminated scanning flow cell to investigate photoelectrochemical (PEC) corrosion pathways of TiO_2 semiconductor photoelectrodes. TiO_2 nanotube array was utilized as our model system to conduct the quantitative study in understanding the effect of the PEC conditions on its photostability. PEC measurements were performed on a Reference600 potentiostat (Gamry) with a three-electrode PEC cell in 0.1 M of $HClO_4$ solution as the electrolyte. The electrolyte was pumped through the PEC cell into ICP-MS for time-resolved analysis of the amount of dissolved titanium ions.

Results
The XRD pattern indicates that all peaks agree well with the tetragonal rutile phase (SG, $P4_2/mnm$; JCPDS No. 21-1276) which is further confirmed by Raman spectrum. X-ray photoelectron spectroscopy (XPS) analysis was performed to study the chemical components and the states of Ti and O in the TiO_2 nanocomposites. The XPS spectra reveal that the dominant elements are Ti, O of the TiO_2 composites. The peaks located at about 458 and 464 eV are corresponding to Ti 2p3/2 and Ti 2p1/2, respectively. SEM (Figure a, b) show that the prepared TiO_2 exhibits nanotube morphology with a thickness of 2.1 µm and an average diameter of 150 ± 20 nm. TiO_2 nanotube grows along with the direction [001] as demonstrated from TEM images (Figure c,d) and high-resolution TEM (HRTEM) image confirms that the surface is (110) facet. From operando ICP-MS setup (Figure f), we can measure the dissolution of TiO_2 during PEC process. Through this method, the operation parameters of PEC on photoelectrodes can be controlled to elucidate sufficiently by quantifying dissolved metal ions of photoelectrode surface in the electrolyte during the whole PEC process in real time.

Conclusions
In summary, our work demonstrates that electron microscopy characterization together with operando ICP-MS plays an important role in investigating the intrinsic mechanism of the improved

PEC performance and photostability of TiO_2. The technique will be strongly needed in our future research and offers significant guidance in (photo)electrochemistry field.

Keywords

TiO_2, electron microscopy, photocorrosion, photoelectrochemistry

Graphic

Figure 1. SEM images (a, b), TEM images (c, d), HRTEM image (e) and operando ICP-MS setup (f).

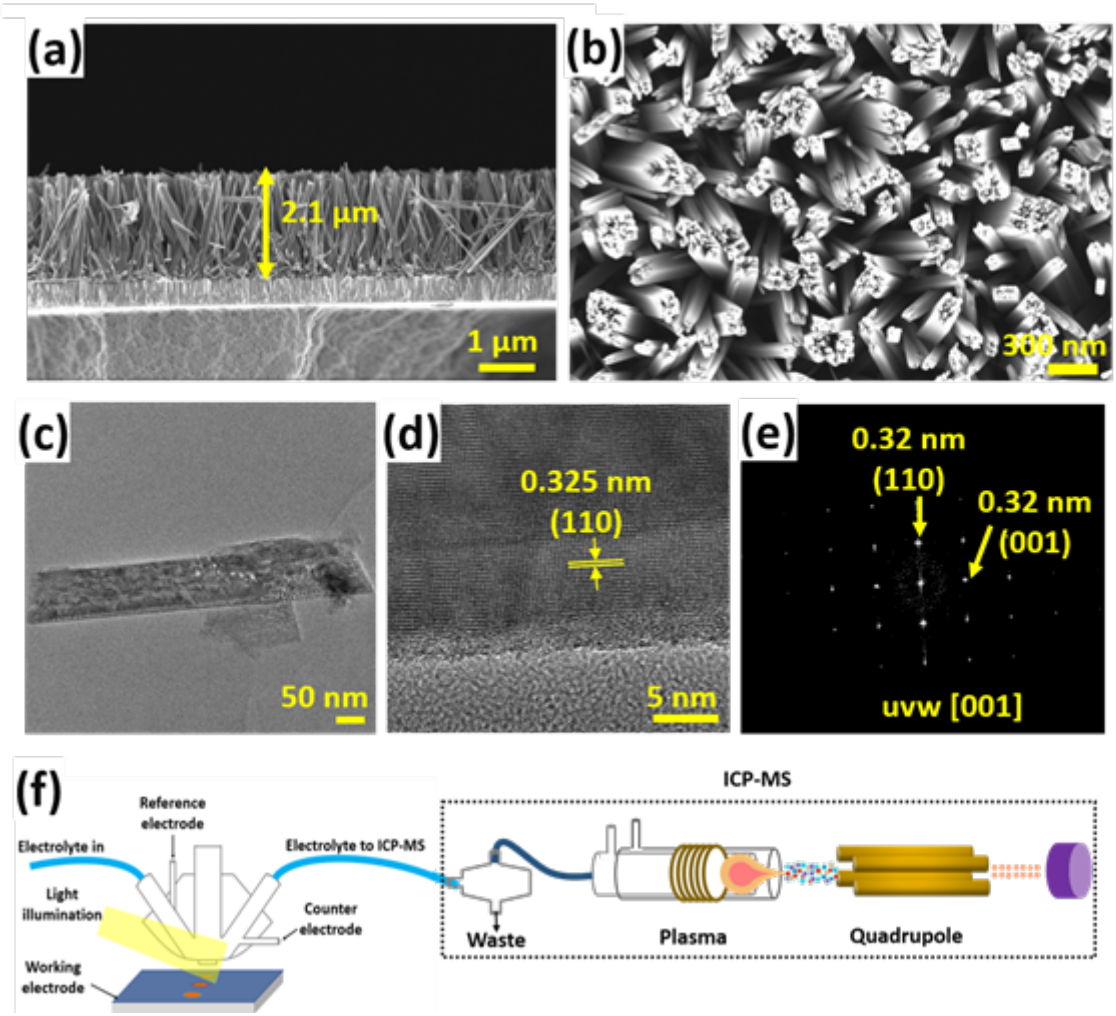

Keywords:

TiO_2, electron microscopy, photocorrosion, photoelectrochemistry

Reference:

[1] Fujishima, A. and K. Honda, Electrochemical Photolysis of Water at a Semiconductor Electrode. Nature, 238(1972) 37-38.

[2] S. Chen, L.-W. Wang, Thermodynamic Oxidation and Reduction Potentials of Photocatalytic Semiconductors in Aqueous Solution, Chemistry of Materials, 24(2012) 3659-3666.

921

In-situ HAADF-STEM observation of phase transformation in microencapsulated Al-Cu-Si alloy

Dr Melbert Jeem[1], Dr Norihito Sakaguchi[1], Dr Takahiro Nomura[1]
[1]Faculty of Engineering, Hokkaido University, Sapporo, Japan

Poster Group 1

Background incl. aims
The increasing relevance of latent heat storage through phase change materials (PCMs) in advanced thermal energy storage technologies is underscored by challenges such as deformation during thermal cycling. This issue is typically mitigated by encapsulating PCMs to create microencapsulated PCMs (MEPCMs) with high thermal conductivity, rigid structures, and improved durability.1 Despite these enhancements, hysteresis during solidification remains a concern. Recent innovations include a core-shell structure of Sn@α-Al2O3 MEPCM that lowers the energy barrier for nucleation, effectively reducing hysteresis through the formation of localized Sn nanoparticles on an α-Al2O3 nanoparticle.2 Expanding on this, we used an Al-Cu-Si alloy for a similar MEPCM structure, achieving notable hysteresis suppression. Unlike Sn, Al-Cu-Si does not volatilize, avoiding the formation of oxide byproducts over repeated thermal cycles. These MEPCMs were calcined at 1000°C in an O2 atmosphere, developing a dense α-Al2O3 shell. However, no localized nanoparticles were detected, prompting further in-situ HAADF-STEM studies to explore hysteresis mechanisms in Al-Cu-Si@α-Al2O3 MEPCM.

Methods
Al-Cu-Si alloy (m.p. = 529 °C, ϕ ≈ 38 µm, 99.95% purity, Hikari Materials Industry Co., Ltd, Japan) was encapsulated with α-Al2O3 nanoparticles (ϕ ≈ 100-200 nm, 99.99% purity, Kojundo Chemical Laboratory Co., Ltd., Japan) using a dry synthesis method, as described in our previous study.2 The encapsulation was facilitated by a rapidly spinning rotor equipped with blades, which promoted the adherence of α-Al2O3 nanoparticles to the Al-Cu-Si microparticles. Sintering at 1000°C for 6 hours in an O2 atmosphere helped form a dense α-Al2O3 shell. For in-situ S/TEM sample preparation, a 6 × 6 µm lamella of the MEPCM was processed using FIB milling (JEM-9320 FIB, JEOL) followed by a standard lift-off procedure. A lamella of the raw Al-Cu-Si alloy was also prepared for comparative analysis. The lamella was placed on a MEMS-based microheater (FEI) with a silicon nitride heating element capable of reaching temperatures up to 1000 °C (Fig. 1). The lamella was positioned over the electron-transmissible window, and the holey film was removed by FIB milling to eliminate non-sample-derived Si X-rays. To secure and enable heating of the lamella, a 300 nm thick tungsten (W) film was deposited at the contact area between the lamella and the heating pad using FIB. S/TEM observations were performed using a Titan3 G2 60-300 (FEI) double aberration-corrected microscope, operated at 300 kV. In-situ heating observation involved acquiring a series of HAADF images with a convergence angle of 17.9 mrad. The camera length was set to 115 mm for a HAADF collection range of 51–200 mrad. The series were taken with a pixel size of 512 × 512 and a dwell time of 2 µs/pixel, resulting in an image frame rate of 787 ms/frame. The probe current was set to 44 pA. The MEMS microheater's temperature was controlled using a closed-loop feedback system to prevent temperature undershoot or overshoot, starting from room temperature and increasing to a maximum of 500 °C at a rate of 5 °C min-1, similar to the heating rates used in differential scanning calorimetry (DSC) for latent heat measurements. A series of HAADF images were taken during each temperature ramp. The temperature was maintained at each 100 °C increment until no further changes were observed, and EDX analyses were performed at each stage. The FEI heating holder's slight curvature over the microheater's window slightly compromised EDX signal counts for the 4-

quadrant Super-X windowless detectors. EDX maps were acquired with a resolution of 256 × 256 pixels, a dwell time of 20 µs, and a total of 250 – 350 frames per map.

Results

The target observation area focused on the core-shell interface structure consisting of α-Al2O3 and the Al-Cu-Si alloy. Compared to the raw Al-Cu-Si, the calcined MEPCM exhibits coarsening of intermetallic Cu2Al and Si. In-situ heating observation of the raw substrate revealed initial dendritic Si structures becoming denser and increasingly aligned with the Cu2Al structure during heating from 100 to 500 °C. This suggests a possible higher melting temperature for Cu-Si formations, which remain solid even at the eutectic melting point of 529 °C. This compound is confirmed in the MEPCM calcined at 1000 °C, where it appears as dispersed nanoparticles in the primary Al matrix. During the temperature ramp from 100 to 300 °C, the applied voltage increased linearly while a notable increase in current is observed, likely due to the thermal lattice expansion of Cu2Al, which leads to fluctuations in electrical conductivity. This was validated by rigid registration of the acquired frames, confirming an approximate size increase of 100 nm in Cu2Al.
This behavior persists until 300 °C. Thereafter, during the ramp to 400 °C, the current value nearly stabilizes, indicating that the Cu2Al phase is reaching its thermal stability limit and beginning to dissolve into the Al matrix. A continued ramp to 500 °C results in complete phase dissolution. This dissolution involves the diffusion of Cu and Al atoms out of the Cu2Al phase and into the surrounding matrix, driven by the gradient in chemical potential caused by temperature changes and the concentration gradients of Cu and Al in the different phases. Interestingly, during the complete phase dissolution, some phases from the Cu2Al adhere to the α-Al2O3 surface. Although α-Al2O3 acts as an inert barrier, surface defects and partial charges may provide sites for adsorption or chemical interactions. If the lattice constants of the dissolute phases are close enough to those of the α-Al2O3, epitaxial growth or nucleation could occur. Atomic resolution HAADF observations in the area where adhesion occurred confirm the presence of seed crystals.

Conclusions

The in-situ HAADF-STEM observations have provided valuable insights into the thermal expansion and dissolution behaviors of Cu2Al within Al-Cu-Si@α-Al2O3 MEPCM during heating. A critical observation from this study is the adhesion of dissolute phases from Cu2Al to the α-Al2O3 surface during phase transformation. This adhesion suggests a potential for epitaxial growth or nucleation at the interface, which could effectively induce nucleation in the Al-Cu-Si alloy during solidification, thereby suppressing hysteresis.

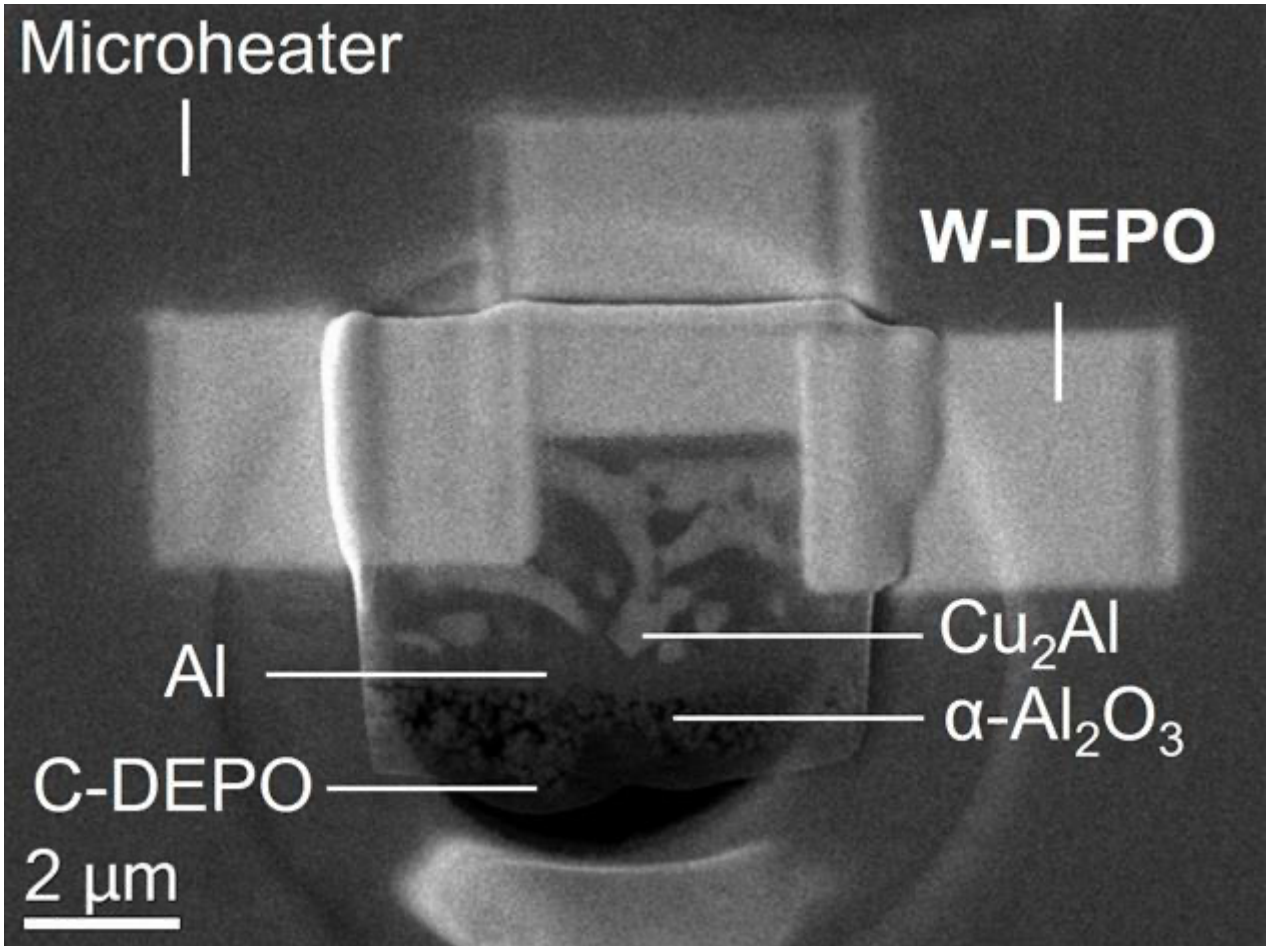

Keywords:

In-situ, MEMS, HAADF, PCM, alloy

Reference:

(1) Nomura, T.; Zhu, C.; Sheng, N.; Saito, G.; Akiyama, T. Sci. Rep. 2015, 5, 9117.
(2) Jeem, M.; Ishida, R.; Kondo, M.; Shimizu, Y.; Kawaguchi, T.; Dong, K.; Kurniawan, A.; Kunisada, Y.; Sakaguchi, N.; Nomura, T. ACS Appl Mater Interfaces 2024, 16, 3509-3519.

940

Innovative Nanoanalytical Approaches for Lithium Metal Interface Analysis

Clementine Warres[1], Philipp Karl Albrecht[1], Dr. Tarek Lutz[1], Dr. Wilfried Nisch[1]
[1]NMI Natural and Medical Sciences Institute at the University of Tuebingen, Reutlingen, Germany

Poster Group 1

Background

Lithium metal anodes are important for next generation high-energy batteries, enhancing energy density in terms of both volume and mass while remaining cost effective. They are already implemented in lithium-sulfur batteries nowadays. However Interfacial instability reactions during operation still represent a challenge for the commercialization of solid-state batteries and require further research.

Challenges in Characterization

The analytical characterization of lithium metal interfaces with high lateral resolution is essential for understanding chemical reactions. These interfaces are highly reactive in ambient air and in particular sensitive to electron and ion beam interactions at room temperature. Employing an argon filled glove box prevents Lithium from reacting with moisture and oxygen. Nevertheless, the reaction with the residual nitrogen content in argon-flooded glove boxes is often overlooked. Additionally, conventional electron microscope air locks are typically vented with nitrogen and are therefore another nitrogen contamination source when samples were transferred between microscopes.

Methods

We deposited lithium layers and other thin test layers by thermal evaporation in a vacuum glove box and flooded afterwards with pure argon gas. With this approach we achieved an oxygen-, water- and nitrogen-free environment in the glove box. Our workflow also involves nitrogen free transfer between the scanning electron microscopes (SEM) and transmission electron microscopes (TEM) under argon atmosphere as well as cryogenic electron microscopy. Chemical characterization of the interfaces with high spatial resolution is achieved by focused ion beam secondary ion mass spectroscopy (FIB-SIMS), energy dispersive x-ray spectroscopy (EDS) and electron energy loss spectroscopy (EELS).

Results and Conclusion

We demonstrate the preservation of metallic lithium via the analysis chain. We also show the possibility of depositing additional thin test layers within the glove box. The methodology and workflows shown in this work give rise to an understanding of Li metal / coating interfaces and can be adapted to study other thin coatings or reaction products sensitive to ambient conditions.

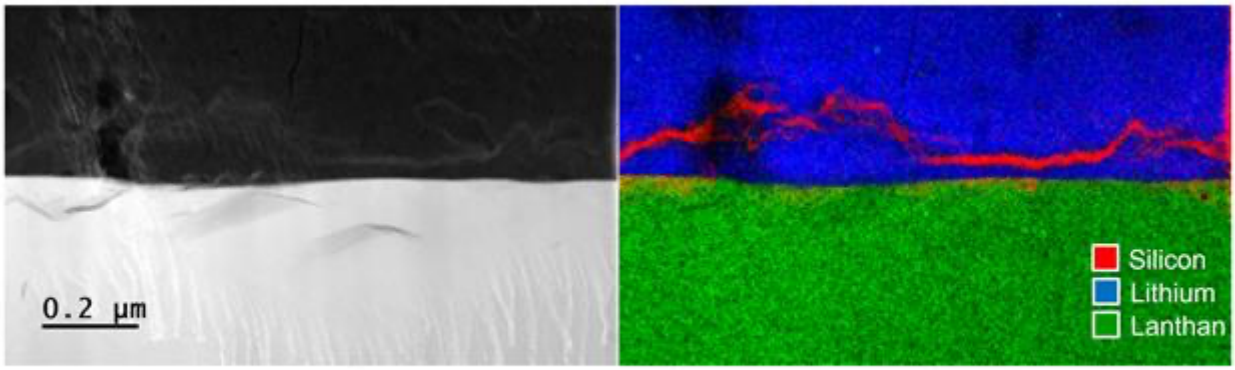

Figure 1: Scanning transmission electron microscope image with corresponding EELS elemental mapping of a lithium layer with 20 nm silicon on Lithium Lanthanum Zirconium Oxide (LLZO)

Keywords:

Li-battery
cryo-/electron-microscopy
inert-transfer
nitrogen-free
Lithium-deposition

980

Ultra-low voltage SEM observation for battery materials

Ph.D. Yutaka Nagaoka[1], Dr. Yoichiro Hashimoto[1], Mr. Toru Aiso[1], Mr. Shuhei Yabu[2], Mr. Masahiro Sasajima[3]
[1]Solution Development Dept., Hitachi High-Tech Corporation, Hitachinaka, Japan, [2]Electron Microscope Systems Design Dept., Hitachi High-Tech Corporation, Hitachinaka, Japan, [3]Software Design Dept., Hitachi High-Tech Corporation, Hitachinaka, Japan

Poster Group 1

Background incl. aims
The scanning electron microscope (SEM) observation at an ultra-low accelerating voltage can visualize strictly superficial surface of the sample with a little electron beam irradiation damage, since the electron scattering volume into the sample is extremely small. However, interpretation of the captured image becomes complicated because the voltage contrast (VC) depending on emitted electron yield changes its behavior under the ultra-low accelerating voltage conditions [1]. Previously, the VC between binders and active materials of lithium-ion battery (LIB) anodes under ultra-low accelerating voltage conditions below 50 V were studied. As the result, we reported that the VC between the binder and the active material was dramatically changed among the ultra-low accelerating voltage conditions [2]. Especially, particle-like unique contrast, which was thought to reflect the binder structure, was observed at 20 V. Although this VC was presumed to be formed by the surface potential at the specific accelerating voltage, the formation mechanism was unknown. In this study, a simplified experiment simulating the binder on the LIB anode was performed to elucidate the binder VC formation mechanism.

Methods
Styrene-butadiene-rubber (SBR) particles: the primary material of the binder, were dispersed in water. The solution with the dispersed particles were dropped onto an osmium (Os) coated Si substrate. The solution was dried at the room temperature. The SBR particles were observed at accelerating voltages below 50 V using a Hitachi SU8700 field emission SEM [3]. The correlative observation with SEM and atomic force microscope (AFM) was performed using a Hitachi AFM5300E for surface potential measurements after electron beam irradiation. The “Air protection” sample holder was used to retain the sample in vacuum at the transfer between SEM and AFM.

Results
The graphic shows the observation results of the SBR particles, representing the “binder”, on the Os-coated Si substrate at the same area captured at accelerating voltages from 10 to 50 V. The SBR showed darker signal (indicated by the red arrow in image (e)) compared to the surrounding Si substrate at 50 V. As the accelerating voltage gradually decreased to 30 V, the contrast between the SBR and the substrate was almost disappeared. When the accelerating voltage decreased to 20 V, the SBR was observed with particle-like contrast. At the accelerating voltage of 10 V, mirror phenomenon, in which the primary electrons bounced off before impacting the sample surface, occurred. This result showed that the VC of the SBR on the Si substrate showed same manner of the binder on the active material in the previous work in spite of different substrate material. To clarify the principle of the VC formation mechanism, correlative AFM observations of the SEM observed area were also executed to measure the residual surface potential. As the result, the residual surface potential of the SBR, the “binder”, was confirmed to be varied by the accelerating voltage.

Conclusion

VC formation mechanism of the binder was investigated with the simplified specimen. The surface appearances of the “binder” were observed with the SEM and the surface potentials were also measured with the AFM correlatively, and SEM accelerating voltage dependency of the residual surface potential was found.

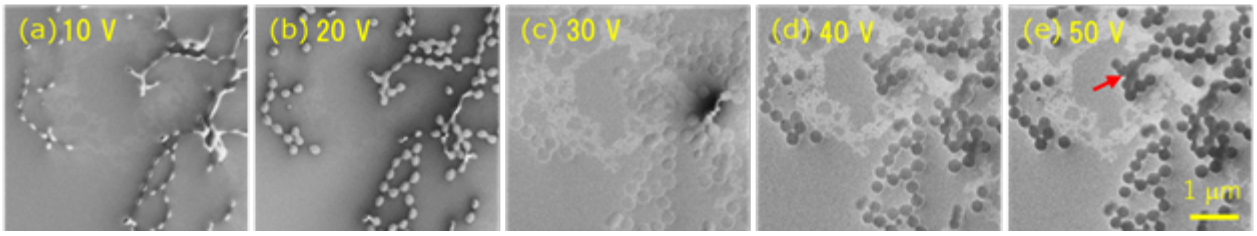

Keywords:

Ultra-low-voltage observation,Voltage contrast, Correlative observation

Reference:

[1] I. Müllerová, Scanning Microscopy 13. 1., 7-22. (1999).
[2] Y. Hashimoto et al., Microscopy and Microanalysis 29 (Suppl 1), 499-500 (2023).
[3] Y. Hashimoto et al., Microscopy Vol. 70, No. 4, 375-381 (2021).

1020

Leveraging FIB-SEM with Integrated ToF-SIMS for Comprehensive Characterization of Lithium-Ion Battery Materials

Dr. Tomáš Šamořil[1], Jiří Dluhoš[1], Jiří Honč[1], Dr. Tan Sui[2], Dr. Xuhui Yao[3]
[1]TESCAN GROUP, a.s., Brno, Czech Republic, [2]University of Surrey, Guildford Surrey, UK, [3]National Physical Laboratory, Teddington, UK

Poster Group 1

In recent years, there has been significant emphasis on enhancing lithium-ion batteries, crucial for electric vehicles, stationary storage technologies, and portable electronics. Their lifespan, particularly concerning capacity fade, is primarily influenced by electrode degradation and the deactivation of active materials. Another critical factor affecting battery lifespan and performance is the solid electrolyte interphase (SEI). Choosing the right analytical technique to study lithium-ion battery degradation and SEI properties is challenging due to the need for detailed structural and chemical composition data, including the distribution of light elements like lithium.
In this study, we utilized a unique combination of a Scanning Electron Microscope equipped with a Focused Ion Beam (FIB-SEM) and a compact Time-of-Flight Secondary Ion Mass Spectrometer (ToF-SIMS) [1,2] to explore the topography and chemical composition of both non-cycled and cycled lithium-ion battery electrodes. Our goal was to pinpoint degradation mechanisms, including parasitic chemical reactions [3]. By integrating SEM observations with ToF-SIMS and other analytical techniques such as Energy Dispersive X-ray Spectroscopy (EDS) [4] and Raman spectroscopy [5] on the same FIB-SEM system, we achieved comprehensive 2D and/or 3D characterization of lithium-ion battery materials. This approach offers insights into degradation processes, SEI properties, and electrode composition, enhancing our understanding of battery behavior at its core.

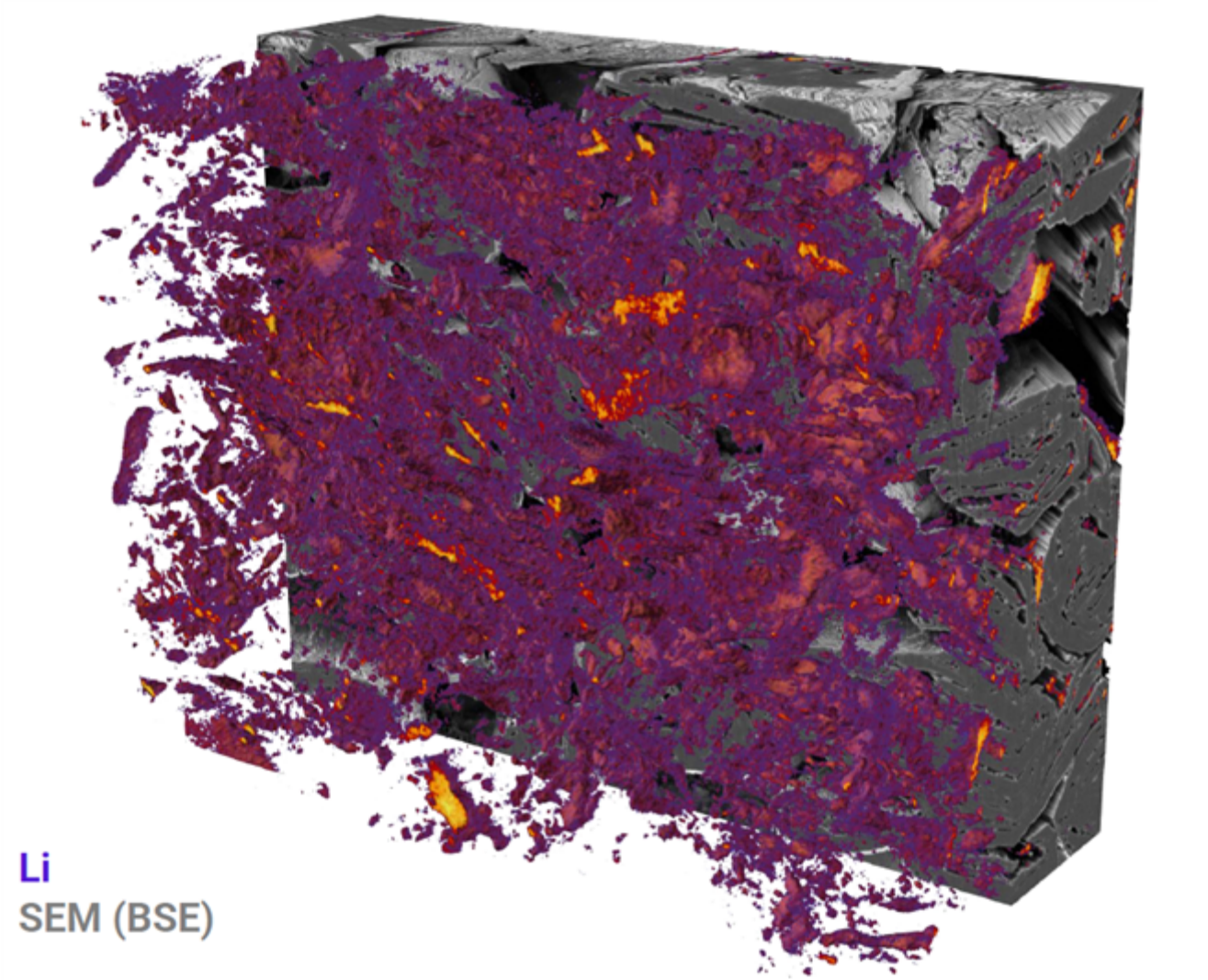

Keywords:

lithium-ion battery, FIB-SEM, ToF-SIMS, tomography

Reference:

[1] J.A. Whitby, et. al., Advances in Mat. Sci. and Eng., (2012), 1-13.
[2] D. Alberts, et. al., Instr. Sci. & Technol. 42, (2014), 432-445.
[3] Yao, et. al., Energy Environ. Mater., (2022), 662-669.
[4] T. Sui, et. al., Nano Energy 17, (2015), 254-260.
[5] D.J. Miller, et. al., Microsc. Microanal. 25, (2019), 862-863.

1030

Insights into Lithium-rich Oxides from Synthesis and Characterization Studies

Rabail Badar Abbasi[1,2,3], Dr Marjan Bele[1], Dr Giuliana Aquilanti[4], Dr Jasper Plaisier[4], Prof. dr Anton Meden[2], Dr Elena Tchernychova[1], Prof. dr Robert Dominko[1,2,3]
[1]Department of Materials Chemistry, National Institute of Chemistry, Ljubljana, Slovenia, [2]Faculty of chemistry and chemical technology, University of Ljubljana, Ljubljana, Slovenia, [3]ALISTORE-European Research Institute, Amiens, France, [4]Elettra-Sincrotrone Trieste S.C.p.A, Trieste, Italy

Poster Group 1

Lithium-ion batteries (LIBs) have dominated the market as preferred energy storage system since their commercialization. However, there is growing need to improve the system in order to accommodate the advancements in different sectors, with electric vehicles being the main driving force. Electric vehicles require high energy and power density, which translates to greater distances traveled and faster charging, respectively. In this respect high capacity and voltage cathodes are a promising path forward, and Li rich oxides (LROs) are amongst the most promising cathode materials for increasing efficiency of LIBs. In addition, the most widely studied composition of LROs, $Li_{1.2}Mn_{0.54}Co_{0.13}Ni_{0.13}O_2$, reduces the amount of nickel and cobalt, making it more environmentally friendly and less expensive. However, these cathode materials suffer from severe drawbacks of voltage decay, low initial coulombic efficiencies, transition metal migration and dissolution, oxygen loss etc. In order to target and resolve these issues, it is first important to understand the pristine structure of LROs, which is still under debate in the scientific community. There are two main hypotheses for its structure i.e., nano-domains of two phases or solid solution of a single phase. The two phases correspond to a rhombohedral $LiMO_2$ phase (space group R-3m) and a monoclinic Li_2MnO_3 phase (space group C2/m). These phases share a similar oxygen lattice, which increases the difficulty in distinguishing them from one another. As such, further studies on the structural and electrochemical properties of LROs are needed to reach its wide-scale commercialization.
In this study, we synthesized a series of LRO samples with the composition, $Li_{1.2}Mn_{0.54}Co_{0.13}Ni_{0.13}O_2$, through sol-gel synthesis. We used two different chelating agents; citric and oxalic acid, and the resulting foam was calcinated at two temperatures; 850°C and 900°C. We recorded X-ray diffraction (XRD) patterns at ~15keV (0.8265 Å), over the 2θ range of 8-60 degrees, at the MCX beamline at Elettra Synchrotron, Italy. The powder samples were measured in borosilicate glass capillary tubes (0.3mm diameter) in transmission mode. We analyzed the particles using a JEM ARM200CF, probe Cs corrected scanning transmission electron microscope (STEM), at 80kV. A GIFQuantum ER dual-EELS system (GATAN-AMETEK, Pleasanton, USA), was used for electron energy loss spectroscopy (EELS). Figure 1(a) shows the XRD pattern, in which the peaks correspond to that of a rhombohedral phase, excluding the weak reflections between ~11-15 degrees. These weak peaks correspond to a monoclinic phase and are highly asymmetric. The asymmetric peak shapes are related to the presence of stacking faults in the material. Figure 1(b) shows the STEM-High-angle annular dark-field (HAADF) image of the particle and the corresponding EELS spectra at O K-edge and Mn L-edge. Three spectra for each elemental edge are shown, moving from the center to the edge of the particle, as indicated in Figure(b). The white line of oxygen K-edge is seen to vary with depth; increasing towards the center of the particle. This change can be attributed to the change in valence state of the surrounding transition metals. On the Mn L-edge spectra, more prominent on the inner-most spectra, a shoulder appears which is similar to that seen in pure Li_2MnO_3.
By combining XRD and EELS in this study, we have shown the need to complement bulk probing techniques with local probing techniques, respectively. The weak reflection for the monoclinic phase in the XRD pattern make data analysis difficult but local EELS spectra indicate the presence of

different environments within a single particle. Our findings contribute to a deeper understanding of the pristine structure of LROs and highlights the need for multiscale characterization.
This work has received funding from the European Union Horizon 2020 research and innovation PhD program DESTINY under grant agreement No. 945357. Co-financing from the Slovenian Research Agency ARIS (core program funding P2-0423, projects J2-3050 and JV-4637) is acknowledged.

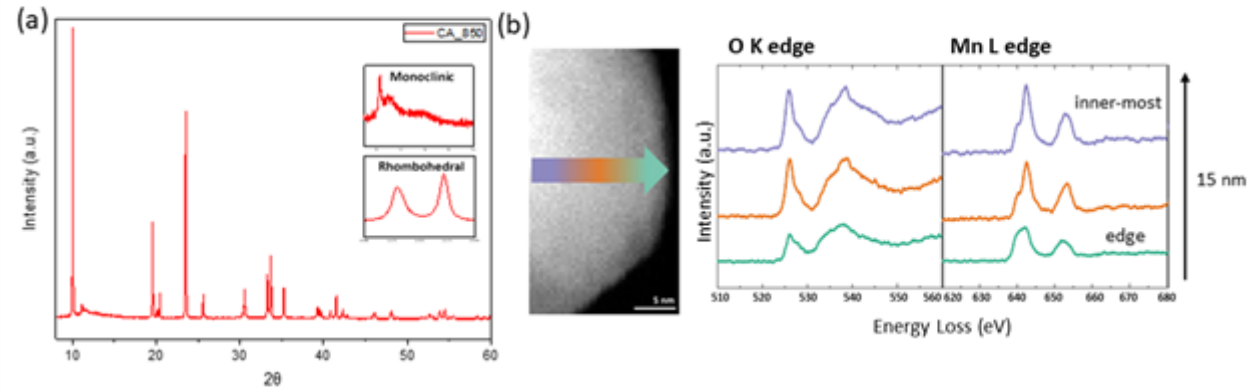

Figure 1: (a) XRD patterns with insets of monoclinic and rhombohedral regions for $Li_{1.2}Mn_{0.54}Co_{0.13}Ni_{0.13}O_2$ synthesized through citric acid assisted sol gel synthesis and calcinated at 850°C, (b) STEM-HAADF image with corresponding EELS spectra at O K-edge and Mn L-edge, as labeled, for the same sample.

Keywords:

li-rich oxides, EELS, XRD, sol-gel

Reference:

1. Jarvis, K. A., Deng, Z., Allard, L. F., Manthiram, A. & Ferreira, P. J. Atomic Structure of a Lithium-Rich Layered Oxide Material for Lithium-Ion Batteries: Evidence of a Solid Solution. Chemistry of Materials 23, 3614–3621 (2011).
2. Kim, J.-S. et al. Electrochemical and Structural Properties of xLi2M'O3·(1−x)LiMn0.5Ni0.5O2 Electrodes for Lithium Batteries (M' = Ti, Mn, Zr; 0 ≤ x ⩽ 0.3). Chemistry of Materials 16, 1996–2006 (2004).
3. A.Boulineau, L. Croguennec, C. Delmas, F. Weill, Structure of Li2MnO3 with different degrees of defects, 2010, https://doi.org/10.1016/j.ssi.2009.10.020.
4. Nakayama, K., Ishikawa, R., Kobayashi, S. et al. Dislocation and oxygen-release driven delithiation in Li2MnO3. Nat Commun 11, 4452 (2020). https://doi.org/10.1038/s41467-020-18285-z

1035

Electron microscopy studies of Ni/GDC fuel electrode in solid oxide fuel cell

Ardavan Makvandi[1], Yanting Liu[2], Dr. Heike Störmer[1], Dr. André Weber[2], Dr. Martin Juckel[3], Prof. Norbert H. Menzler[3], Prof. Dagmar Gerthsen[1]
[1]Laboratory for Electron Microscopy (LEM), Karlsruhe Institute of Technology (KIT), Karlsruhe, Germany, [2]Institute for Applied Materials - Electrochemical Technologies (IAM-ET), Karlsruhe Institute of Technology (KIT), Karlsruhe, Germany, [3]Institute of Energy and Climate Research (IEK), IEK-1: Materials Synthesis and Processing, Forschungszentrum Jülich GmbH, Jülich, Germany

Poster Group 1

To increase the commercialization of solid oxide fuel cells (SOFCs), it is necessary to reduce their cost and extend their lifetime [1]. By operating SOFCs at temperatures below 650 °C, it is possible to make use of low-cost materials and reduce the performance degradation of SOFCs [2]. However, in the case of yttria-stabilized zirconia (YSZ) electrolytes, the electrochemical performance dramatically decreases at lower temperatures due to the low ionic conductivity of YSZ, leading to a high ohmic resistance [2]. The ionic conductivity of gadolinia-doped ceria (GDC) is significantly higher than that of YSZ at temperatures as low as 500 °C [3]. Ni/GDC fuel electrodes therefore provide superior properties compared to Ni/YSZ [4]. The microstructural integrity of Ni-based fuel electrodes is necessary for the long-term operation of SOFCs. Therefore, it is necessary to understand the structural and chemical degradation mechanisms of SOFCs to enhance and predict the lifetime of SOFCs [5].
In this work, the effect of operation temperature and duration on the structural and chemical degradation of Ni/GDC fuel electrodes was studied using (scanning) transmission electron microscopy ((S)TEM) and focused-ion-beam/scanning-electron microscopy (FIB-SEM) to correlate the structural and chemical evolutions with the results of electrochemical impedance spectroscopy. By using FIB-SEM, it is possible to reconstruct the 3D structure of the porous electrode to acquire structural parameters such as tortuosity, particle size distribution, specific active area, and triple-phase boundary length. The TEM sample preparation and 3D reconstruction of the Ni/GDC fuel electrodes were carried out using a Helios G4 FX dual-beam instrument (Thermo Fisher Scientific). STEM imaging and energy-dispersive X-ray spectroscopy were performed using a Tecnai OSIRIS ChemiStem (Thermo Fisher Scientific). TEM and SEM results of the Ni/GDC fuel electrodes at different aging states indicate a significant change in the microstructure, e.g. Ni agglomeration at higher operating temperatures, leading to an increase in polarization resistance.

Keywords:

FIB, SEM, TEM, SOFC

Reference:

1. Steele, B. C. H. & Heinzel, A. Materials for fuel-cell technologies. Nature 414, 345–352 (2001).
2. Liu, Y., Juckel, M., Menzler, N. H. & Weber, A. Ni / GDC Fuel Electrode for Low Temperature SOFC and its Aging Behavior under Accelerated Stress. ECS Trans. 111, 1855–1865 (2023).
3. Zhang, J., Lenser, C., Menzler, N. H. & Guillon, O. Comparison of solid oxide fuel cell (SOFC) electrolyte materials for operation at 500 °C. Solid State Ionics 344, 115138 (2020).
4. Nenning, A., Bischof, C., Fleig, J., Bram, M. & Opitz, A. K. The relation of microstructure, materials properties and impedance of SOFC electrodes: A case study of Ni/GDC anodes. Energies 13, (2020).
5. Zekri, A., Knipper, M., Parisi, J. & Plaggenborg, T. Microstructure degradation of Ni/CGO anodes for solid oxide fuel cells after long operation time using 3D reconstructions by FIB tomography. Phys. Chem. Chem. Phys. 19, 13767–13777 (2017).

1078

Optimizing Soft X-ray Spectroscopy for Silicon Anode Lithium Mapping

M. Sc. Svenja Kalthoff[1]
[1]Fraunhofer ISE, Freiburg im Breisgau, Germany

Poster Group 1

Background incl. aims
Silicon has emerged as a promising candidate material for anodes in lithium-ion batteries due to its high theoretical capacity (about 10 times that of graphite). However, the practical use of silicon faces challenges related to its large volume expansion (~300%) upon lithiation, which leads to mechanical degradation and pulverization of the electrode over repeated charge/discharge cycles. This degradation results in loss of electrical contact, reduced cyclability, and capacity fading.
To address these issues and optimize silicon-based anodes, extensive research efforts are underway. One critical area of investigation involves understanding the distribution and behavior of lithium within silicon structures during battery operation. The distribution of lithium impacts the electrochemical performance and stability of the battery.
Various techniques are employed to study silicon-based anodes, including microscopy (e.g., scanning electron microscopy, transmission electron microscopy) for structural analysis, spectroscopy (e.g., X-ray diffraction, X-ray photoelectron spectroscopy) for chemical characterization, and electrochemical methods for performance evaluation. But the lithium distribution in the anodes cannot be found by these techniques.
However, soft X-ray emission spectroscopy (SXES) is a powerful technique that can provide detailed insights into the lithium distribution within silicon anodes with high sensitivity and spatial resolution. SXES allows researchers to map the chemical states of lithium in different states of charge (SOC) and investigate phenomena such as lithium trapping, where lithium becomes immobilized within the silicon structure, contributing to capacity loss and reduced battery efficiency over time.
By studying these fundamental processes, we aim to develop strategies to mitigate silicon degradation, enhance lithium utilization, improve battery cyclability, and ultimately advance the performance and lifespan of lithium-ion batteries. Furthermore, this study aims to establish optimal measurement conditions for SXES when analysing silicon-based anodes in lithium-ion batteries. By identifying and demonstrating the most effective measurement parameters and techniques, our goal is to streamline SXES procedures for battery research, facilitating broader adoption and use by other researchers in the field.

Methods
This research focuses on investigating silicon-based anodes derived from lithium-ion batteries fabricated in our laboratory using micrometer-sized silicon particles as the anode material. The batteries are assembled in coin cell half-cell format, featuring electrodes with a diameter of 18 mm. Assembly and subsequent disassembly for post-mortem analysis are meticulously conducted within an argon atmosphere glovebox to ensure controlled environmental conditions and prevent exposure to moisture and oxygen.
After disassembly, the electrodes undergo a thorough cleaning process using dimethyl carbonate (DMC) and are then dried under vacuum to eliminate any residual contaminants. For SXES analysis, a plane surface is essential. Therefore, a small portion of the electrode is extracted and a cross-section is meticulously prepared using the IB-19520CCP cross-section polisher from Jeol under a cooled atmosphere at -120°C. The transfer from the glovebox to the ion polisher and subsequently to the scanning electron microscope (SEM) is carried out in an inert transfer vessel to ensure that the sample remains shielded from air or moisture throughout the process.

SXES investigations are performed using a JSM-IT800 SEM equipped with the JS50XL SXES detector from Jeol. This advanced setup enables high-resolution analysis of lithium distribution and chemical states within the silicon-based anodes.

Results

Our investigation revealed significant influences of probe current, excitation voltage, and exposure time on the spectroscopy results. Identifying optimal settings for these parameters is crucial, balancing high signal intensity with minimal sample degradation during measurements. Additionally, variations in lithium (Li) distribution within the analysed particles were observed. By employing mapping techniques, we were able to spatially resolve and identify regions enriched with lithium, providing valuable insights into its distribution within the silicon-based anodes. This detailed elemental mapping enhances our understanding of lithium behavior in battery materials and underscores the importance of precise measurement conditions in SXES for comprehensive battery research.

Conclusion

In conclusion, our study underscores the significance of SXES in elucidating the complex interplay between lithium distribution and silicon-based anode performance in lithium-ion batteries. The challenges associated with silicon's volume expansion upon lithiation and subsequent mechanical degradation highlight the critical need for advanced characterization techniques to optimize battery materials.

Through our investigation, we have demonstrated the pivotal role of SXES in mapping lithium distribution with exceptional sensitivity and spatial resolution. Our findings emphasize the impact of probe current, excitation voltage, and exposure time on spectroscopy results, emphasizing the importance of optimizing measurement parameters to balance signal intensity and sample integrity. The observed variations in lithium distribution within the anode particles provide valuable insights for developing strategies to mitigate lithium trapping and enhance battery cyclability. By enhancing our understanding of lithium behavior at different states of charge, we aim to contribute to the development of more efficient and durable lithium-ion batteries.

Keywords:

SXES, Silicon-based Anodes, Lithium-Ion Battery

Reference:

[1] Y. Domi, H. Usui, A. Ando, K. Nishikawa, and H. Sakaguchi, "Analysis of the Li Distribution in Si-Based Negative Electrodes for Lithium-Ion Batteries by Soft X-ray Emission Spectroscopy," ACS Applied Energy Materials, vol. 3, no. 9, pp. 8619–8626, 2020, doi: 10.1021/acsaem.0c01238.

[2] X. Zhou, S. Qiao, N. Yue, W. Zhang, and W. Zheng, "Soft X-ray emission spectroscopy finds plenty of room in exploring lithium-ion batteries," Materials Research Letters, vol. 11, no. 4, pp. 239–249, 2023, doi: 10.1080/21663831.2022.2141586.

1085

Electron microscopy characterization of grain boundaries in Nb1-xTixFeSb based half-Heusler thermoelectric materials

Dominique Mattlat[1], Dr. Ruben Bueno Villoro[1], Dr. Chanwon Jung[1], Raana Hatami Naderloo[2], Dr. Ran He[2], Prof. Dr. Kornelius Nielsch[2], Duncan Zavanelli[3], Prof. Dr. G. Jeffrey Snyder[3], Dr. Siyuan Zhang[1], Prof. Dr. Christina Scheu[1]
[1]Max-Planck-Institute for Iron Research, Düsseldorf, Germany, [2]Leibniz Institute for Solid State and Materials Research, Dresden, Germany, [3]Northwestern University, Chicago, United States of America

Poster Group 1

Background incl. aims
Thermoelectrics are a group of semiconductors which generate electrical power by conversion of heat into electrical energy. A thermoelectric power generator requires a hot and a cold side to use the temperature gradient for this conversion of energy.
Microstructure engineering has been used in the thermoelectric material research community to reduce the phonon mean free path and thus led to reduction of thermal conductivity which is crucial for thermoelectrics. This can be done by grain refinement, i.e. reducing the grain size for more phonon scattering. The challenge remained to keep a high electrical conductivity since increasing the grain boundary fraction usually led to decrease of electrical conductivity. To achieve the desired properties in thermoelectrics, it is important to understand the dependence of the microstructure of grain boundaries and correlate it to the thermoelectric properties. For this, detailed electron microscopy investigations covering several length scales from the µm to an atomic scale need to be conducted.

Methods
Scanning electron microscopy (SEM) analysis including electron backscatter diffraction (EBSD) and energy-dispersive X-ray spectroscopy (EDX) has been done to observe the µm down to nm scale microstructure. The grain boundary characterization down to atomic scale was achieved with (scanning) transmission electron microscopy ((S)TEM). In addition, atom probe tomography (APT) was used to get a chemical analysis on the composition of the grain boundaries with highest accuracy and spatial resolution.

Results
EBSD analysis of the grain size of the Nb1-xTixFeSb based half-Heusler thermoelectric materials synthesized at two different temperatures and two different Ti contents of 5% and 20% replacing Nb revealed a significant difference related to the grain size while all samples showed a random Mackenzie distribution for the grain misorientation (see Figure 1a). The later observation means that specific low angle grain boundary types were not dominating.
To uncover this mystery and proove our hypthoesis of resistive and conductive grain boundaries, we combined APT analysis with STEM analysis at the grain boundaries. We observed a defect grain boundary phase at random grain boundaries (Figure 1b) with chemical composition and lattice parameters differing from the one of the matrix phase of the half-Heusler material. The parameters are close to an FeSb phase in all four samples (different doping content and grain size) but with an additional segragation of Ti content for the high Ti doped samples which was shown with APT (see Figure 1c). This defect grain boundary phase proved to be the reason for increased electrical conductivity by providing conductive pathways in the high Ti doped sample.

Conclusion

Scale bridging electron microscopy was key to understand the correlation between microstructure and thermoelectric properties of NbFeSb based half-Heusler p-type thermoelectric material.[1] We have revealed a way of decoupling the electrical and thermal conductivity to tune the properties for maximizing the materials performance. This way of grain boundary alloying will provide a new road map for microstructure engineering in the future and should also be applicable to other half -Heusler materials.

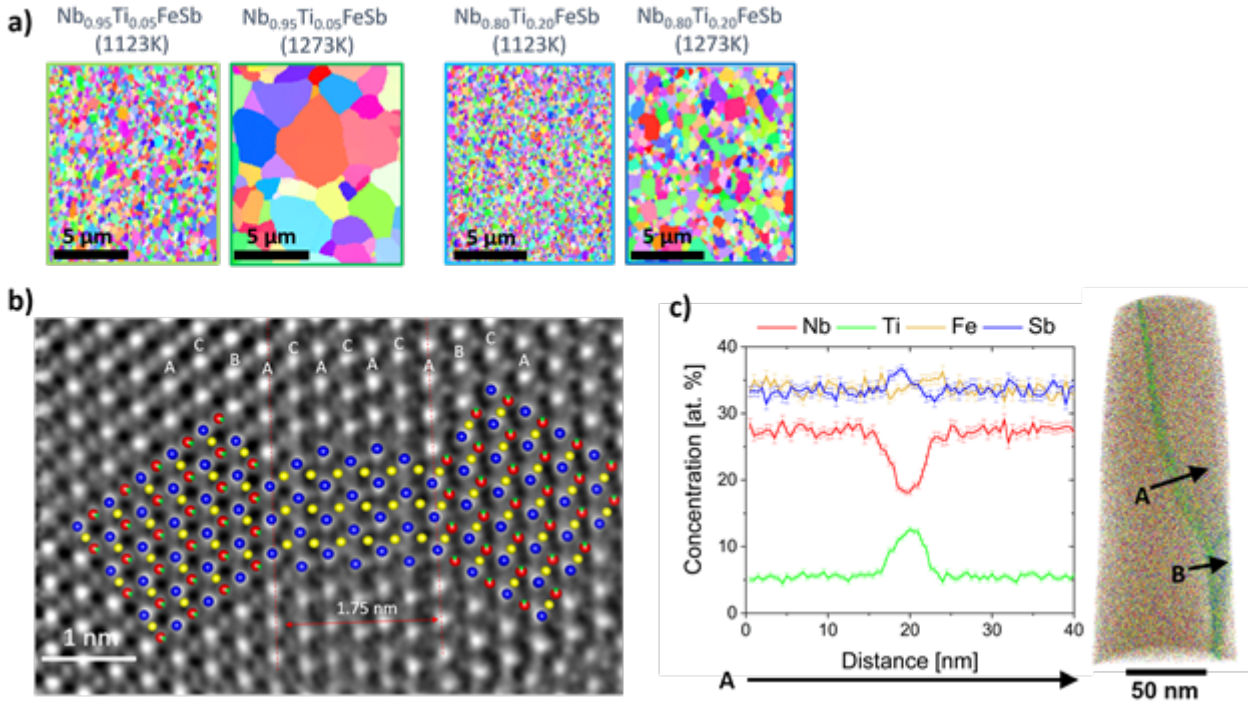

Keywords:

SEM, EBSD, STEM, APT, Thermoelectrics

Reference:

R. Bueno Villoro, D. Mattlat et al., Grain Boundary Phases in NbFeSb Half-Heusler Alloys: A New Avenue to Tune Transport Properties of Thermoelectric Materials, Advanced Energy Materials, 2204321, (2023)

1131

In-situ synthesis of thin kesterite films using high voltage TEM

Professor Klaus Leifer[1], Mr Sharath Sathyanath[1], Professor Y Gong[2], Dr Alex J. Arguijo[2], Prof Edgardo Saucedo[2], Professor S Araj[3], Professor Shun Muto[3]
[1]Uppsala University, Uppsala, Sweden, [2]Univ. Politèc. de Catalunya, Barcelona, Spain, [3]Nagoya University, Nagoya, Japan

Poster Group 1

A promising route for the synthesis of kesterite solar cell absorber layers consists in the annealing of thin layers in vapours resulting in alloys of kesterites, a route that has recently also be used for the synthesis of van der Waals materials. This straightforward annealing procedure includes several structural transformations of the absorber thin film layer such as phase transformations, diffusion processes and grain growth. The disentanglement of these different processes is difficult and TEM analysis is essential to understand the structural changes during the annealing of those materials. The best approach to follow the structural changes during the synthesis process of such kesterite materials is to carry out the related annealing steps in situ in the TEM. Since the layers have a certain thickness and the annealing must be carried out in a Se atmosphere, the high voltage TEM (HVTEM) is an appropriate method for this type of in situ annealing which we carry out in this work.

Methods
For the TEM in-situ synthesis of kesterite structures of Cu2ZnSnSe4, we used the JEOL-1000K RS HVTEM at Nagoya University. The starting materials are Cu2ZnSnS4 and AgCu2ZnSnS4, which are annealed in a Se atmosphere to obtain a Cu2ZnSnSSe phase with as high as possible Se content. The temperature is increased in steps of 50-100 °C up to 500 °C while the Se-enriched carrier gas streams along the sample surface. At each temperature ramp, the sample is analysed by electron diffraction, TEM and STEM imaging as well as by EELS spectroscopy. In addition, the TEM is equipped with a highly sensitive mass spectrometer, which enables us to analyse the gases coming from the sample during annealing.

Results
We started the synthesis either from the metallic stacks or from Cu2ZnSnS4 which are exposed to Se vapours. Though the analysis of the metallic stacks has promising results, the thickness increase of about a factor of 2 during the selenisation process made the sample so thick that it was difficult to analyse nanometric changes in the sample happening during the synthesis process. This situation changed by using thin Cu2ZnSnS4 and AgCu2ZnSnS4 films as a starting material since these films preserve their thickness during the synthesis.
During the in-situ annealing of AgCu2ZnSnS4, we observed the nucleation of the kesterite Cu2ZnSn(S)Se4 phase, which is precedented by the formation of Ag- and Se-containing nanoprecipitates. Those partially disappear during higher annealing temperatures, when the AgCu2ZnSnSe4 grains grow. By in-situ EELS analysis and post-annealing EDS measurements of the thin layers we could follow the chemical modifications of the crystallites forming a core-shell structure.
When the Cu2ZnSnS4 is synthesised, the replacement of S by Se causes an expansion of the lattice parameter. We applied a Hough transform to extract the lattice plane spacing from the diffraction patterns and conclude that in Cu2ZnSnS(4-x)Sex, Se is inserted at a concentration of 50±10 %. One goal of this annealing process is to increase the grain size to reduce the impact of grain boundaries on carrier transport. Whereas the starting kesterite has a grain size in the 10 nm range, after the annealing process, a grain size of 50 nm is reached.

Conclusion

Using in situ HVTEM synthesis of Cu2ZnSn S(1-x)Sex kesterite structures, we could successfully demonstrate the grain growth and replacement of S by Se in the kesterite crystal. This replacement reaction happens at elevated temperatures of 400-500 °C.

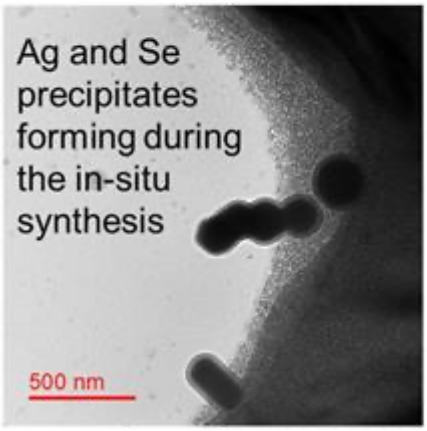

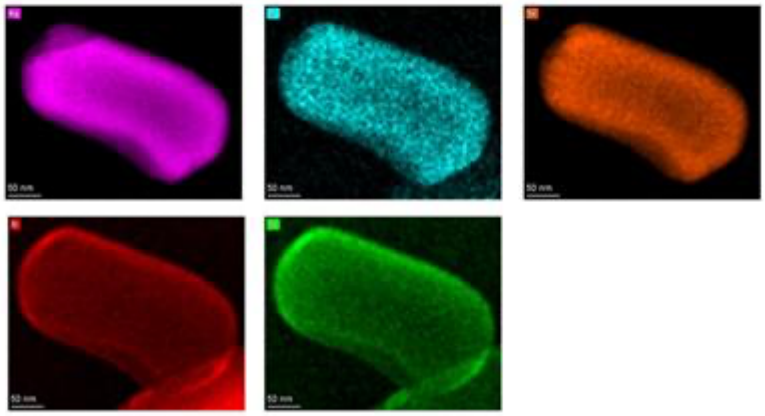

Keywords:

high voltage TEM, insitu, kesterite

1145

Interplay between microstructural properties with ionic/electronic conductivity in Na3PS4-based composite cathodes for Na-SSBs

Rana Ucuncuoglu[1], Dr. Leticia Trezecik Silvano[1], Tim Schubert[1], Prof. Dr. Volker Knoblauch[1], Dr Pinar Kaya[1]
[1]Materials Research Institute (IMFAA), Aalen University of Applied Sciences, Aalen, Germany

Poster Group 1

The potential of having high energy and power density in all-solid-state batteries (ASSBs) makes them attractive candidates for energy storage systems of the future [1]. They also have several advantages over traditional liquid electrolyte-based systems, including safety and a wide operating temperature range [2]. Furthermore, the higher abundance of sodium relative to lithium makes solid state sodium ion batteries a more cost-effective alternative [3]. One challenge is the limited ionic transport capabilities of current solid electrolytes (SE), but also the development of a suitable cathode, which is as crucial as having a promising SE for practical applications [4]. An optimized composite cathode (CC) should provide a percolating network of ions and electrons with short transport pathways and a large active interphase area between SE and cathode active material (CAM) [4,5]. Therefore, the composite cathode must be carefully built by optimizing the phase fractions between CAM, SE, and CA (conductive additive), particle characteristics, and phase distribution to ensure percolation and adequate ionic and electronic transport.
In this work, our motivation is to gain a deeper understanding of the relationship between the microstructure and the ionic/electronic conductivity of the composite cathode. Within this aim, as a CAM, NaCrO2 was mixed with the conductive matrix (CM), which consists of Na3PS4 as a SE and vapor growth carbon fiber (VGCF) as a CA. The effective ionic and electronic conductivity of the composite cathodes were measured using electrochemical impedance spectroscopy (EIS) with two different configurations (ion blocking and electron blocking). The cross-sectional microstructures of CCs were investigated via scanning electron microscopy (SEM) and FIB-tomography. Our findings revealed that reducing the Na3PS4 (SE) and VGCF (CA) content simultaneously results in a balanced ionic and electronic conductivity (70 wt. % CAM contained CC) at 10 MPa stack pressure. Additionally, both ionic and electronic conductivity values increase with increasing stack pressure. 2D microstructural information from SEM images showed slightly reduced density but a better CAM distribution by reducing CAM content. To obtain 3D information from the microstructures XRM & FIB tomography analyses will be performed and presented in this study.

Keywords:

Sodium solid-state batteries, Microstructural design

Reference:

[1] M. Clausnitzer, R. Mücke, F. Al-Jaljouli, S. Hein, M. Finsterbusch, T. Danner, D. Fattakhova-Rohlfing, O. Guillon, A. Latz, Batteries & Supercaps 2023, 6.
[2] A. L. Santhosha, L. Medenbach, T. Palaniselvam, P. Adelhelm, J. Phys. Chem. C 2020, 124, 10298.
[3] E. A. Wu, S. Banerjee, H. Tang, P. M. Richardson, J.-M. Doux, J. Qi, Z. Zhu, A. Grenier, Y. Li, E. Zhao, G. Deysher, E. Sebti, H. Nguyen, R. Stephens, G. Verbist, K. W. Chapman, R. J. Clément, A. Banerjee, Y. S. Meng, S. P. Ong, Nat Commun 2021, 12, 1.
[4] P. Minnmann, F. Strauss, A. Bielefeld, R. Ruess, P. Adelhelm, S. Burkhardt, S. L. Dreyer, E. Trevisanello, H. Ehrenberg, T. Brezesinski, F. H. Richter, J. Janek, Advanced Energy Materials 2022, 12, 2201425.

[5] T. Shi, Q. Tu, Y. Tian, Y. Xiao, L. J. Miara, O. Kononova, G. Ceder, Advanced Energy Materials 2020, 10.

1256

A systematic study on PtRu alloy composition for catalytic applications

Tonya Kloos[1], Dr. Ningyan Cheng[1], M.Sc. Miquel Vega Paredes[1], M.Sc. Alan Savan[2], Prof. Dr.-Ing. Alfred Ludwig[2], Prof. Dr. Christina Scheu[1]
[1]Max-Planck Institute for Sustainable Materials, Düsseldorf, Germany, [2]Ruhr-Universität Bochum, Bochum, Germany

Poster Group 1

Background incl. aims
In order to reduce CO2 emissions in the areas of energy supply and consumption the use of fuel cells (FC) is inevitable. The choice of the catalyst material for the electrochemical reaction to convert H2 in electricity plays a major role. For this reaction the system of PtRu catalyst nanoparticles is well studied and already used in commercial application. However, for the PtRu phase diagram at ambient temperatures empirical data is not available. Thus, only Thermo-Calc generated phase diagrams down to room temperature exist.
Until now just few compositions of the PtRu nanoparticles are investigated in terms of structure and their performance since it is challenging and time consuming to synthetize nanoparticles with different specific compositions. In this work we perform a systematic investigation on the different chemical compositions of PtRu alloys and the influence on their micro- and nanostructure using a thin film.

Methods
The thin film was deposited on an oxidized silicon wafer via combinatorial magnetron sputtering. With positioning the Pt target and the Ru target in an 180° angle to each other a geometrical concentration gradient is generated. The surface of the thin film was analyzed in a Scanning Electron Microscope (SEM) followed by Energy dispersive X-ray Spectroscopy (EDXS) to determine chemical composition and distribution of the elements. Using a focused ion beam (FIB) lamellae were lifted out on specific targeted areas. Theses were analyzed with a Transmission Electron Microscope (TEM) to obtain the local structure and composition. The software Thermo-Calc was used to generate a phase diagram of the PtRu alloy down to room temperature.

Results
The deposited thin film had a smooth surface with no macroscopic defects. The atomic concentration range goes from Pt:Ru 58:42 at % - 17:83 at % along the sample. The thickness of the thin film was determined to be 115 nm ± 3 nm based on TEM micrographs. Additionally, the TEM micrographs taken from cross sections of the thin film showed columnar grains with 13 nm ± 4 nm width and the height of the thin film. With lamellae from areas of targeted positions EDXS was performed in the TEM to verify the validity of the calculated phase diagram. EDXS maps revealed that a two-phase material exists in regions where the calculation suggests a single phase material.

Conclusion
Combinatorial magnetron sputtering can be used to create thin films with a concentration gradient. A systematic study on the influence of the chemical composition on the structure was performed. This is necessary for a follow-up investigation of the electrochemical performance and its dependence on the composition and atomic structure. Correlation of structure and electrochemical experiments is key for future catalyst design.

Keywords:

PtRu, thin film, composition, catalyst

1258

Synthesis, structural and electrochemical characterization of nanostructured Ir/TiO_2 for the oxygen evolution reaction

Yeeun Bang[1], Dr. Raquel Aymerich Armengol[2], Prof. Dr. Joohyun Lim[3], Prof. Dr. Christina Scheu[1]
[1]Max-Planck-Institute for Sustainable Materials, Düsseldorf, Germany, [2]Technical University of Denmark, Lyngby, Denmark, [3]Kangwon National University, Gangwon-do, South Korea

Poster Group 1

Background incl. aims
To reduce the problem of global warming, alternative eco-friendly energy sources such as solar cells or fuel cells should be used. For fuel cells, hydrogen is an attractive energy carrier.1) To produce hydrogen in a sustainable way, we need to improve the efficiency of hydrogen generation in electrolysers. For this, efficient and stable electrocatalysts are required. One promising class are Ir-based catalyst which are known to speed up the oxygen evolution reaction (OER) but its stability needs to be improved. 2) In our work, we want to improve the stability of Ir and reduce the amount of Ir by using TiO_2 support.

Methods
Ir/TiO_2 nanostructures were synthesized on fluorine doped tin oxide coated glass slide (FTO) using a facile hydrothermal approach. After synthesis, films were prepared for scanning electron microscopy (SEM) by using copper tape attached to an aluminum SEM holder. ZEISS Gemini SEM 500 and ZEISS Merlin FE-SEM (field emission gun) were applied for examining the morphology of samples. For the (scanning) transmission electron microscopy ((S)TEM) analysis, the nanostructures were collected on a TEM holey carbon-copper (C/Cu) grid. A JEOL 2100 and an image Cs-corrected Titan Themis 80-300 from Thermo Fisher were used for the examination.

Results
Electrochemical characterization of the films showed that higher contents of Ir lead to an improved oxygen evolution reaction activity. SEM and (S)TEM analysis revealed that Ir/TiO_2 films consist of an assembly of facetted nanowires on the FTO substrate with the facets in according to the Wulff shape. The width of the individual nanowires was evaluated and it was observed that it increased from 95 nm to 114 nm with increasing amount of Ir used during the synthesis. Electron diffraction in TEM shows that Ir/TiO_2 maintains a rutile structure independent of the Ir content. Finally, energy dispersive X-ray spectroscopy (EDS) demonstrates that small Ir clusters with a size of less than 1 nm form which are homogenously distributed. However, until now it is not yet clear whether Ir is placed on top of the TiO_2 or embedded in the TiO_2 lattice.

Conclusion
To reduce the amount of Ir catalyst for the OER, TiO_2 is used as support. By changing the amount of Ir during the synthesis, the width of the nanowires increased in proportion to the amount of Ir. It is found that Ir/TiO_2 has a rutile structure but further studies are needed to determine whether Ir is incorporated into the lattice or adsorbed on the surface.

Keywords:

Electrocatalyst,nanowires,TiO2,Ir,OER,SEM,TEM

Reference:

1) Rosen, M.A., Koohi-Fayegh, S. The prospects for hydrogen as an energy carrier: an overview of hydrogen energy and hydrogen energy systems. Energ. Ecol. Environ. 1, 10–29, 2016.
2) O. Kasian, T. Li, A. M Mingers, K. Schweinar, A. Savan, A. Ludwig, and K. Mayrhofer. Stabilization of an iridium oxygen evolution catalyst by titanium oxides. Journal of Physics: Energy, 3:034006, 2021.

1263

Nano-characterization of Sodium-ion cathodes fabricated using economically and environmentally friendly organic routes

Dr Ana M Beltran[1], Dr. Saul Rubio[1], Dr. Francisco J Garcia-Garcia[2], Mr Julio E de la Rosa[2], Dr Eva M. Pérez[2], Dr Isabel Montealegre-Meléndez[1], Dr. Cristina Arévalo[2], Dr. Juan G. Lozano[2]
[1]Departamento de Ingeniería y Ciencia de los Materiales y del Transporte, Escuela Politécnica Superior, Universidad de Sevilla, Sevilla, Spain, [2]Departamento de Ingeniería y Ciencia de los Materiales y del Transporte, Escuela Técnica Superior de Ingeniería, Universidad de Sevilla, Sevilla, Spain

Poster Group 1

Developing new materials for battery energy storage is a significant challenge and a key factor in technology. Among the limitations, new materials for more efficient cathodes have been required, but until now there is no perfect candidate. Sodium ion batteries have emerged as a promising solution, although they still present some disadvantages. In addition to new cathode materials, fabrication routes also need to be improved, and economically and environmentally friendly synthesis routes are desirable. When new candidates were sought, in this study, a promising transition metal oxide cathode for Sodium-Ion Batteries (SIBs) was characterized. The synthesis was performed following a variant of an organic synthesis approach developed within the research group [1]. This method uses metal acetates, and Vaseline (hydrophobic component) and oleic acid (surfactant). To further test this route, different combinations of hydrophilic and surfactants have now been employed to validate the use of this route for the synthesis of the cathodes. Notably, the use of non-polluting, economically and safe reagents and the generation of non-contaminant reaction by-products render this approach environmentally friendly. Moreover, it has shown speeds and efficiency higher than those of conventional dry-milling or sol-gel methods, with significant potential for scalability. Preliminary X-ray diffraction and transmission electron microscopy results confirmed the structure of the materials, similar to those obtained by other fabrications routes.

Methods

To achieve the emulsions studied in this work, metal acetates were mixed for 4 minutes in a shear mixer with the other organic compounds to be tested. Products such as coconut oil or mineral oil were used as the hydrophobic component. Whereas glycerol or, sodium dodecyl sulphate (SDS), were tested as surfactants. The achieved emulsion was heat treated for 10 hours at 900 ° C. The crystallinity of the obtained Na compounds was studied by X-ray diffraction (XRD) and the microstructure, morphology and size of the particles as well as the composition by (Scanning)Transmission Electron Microscopy ((S)TEM).

Results

After sintering, XRD was performed to investigate the structure of the synthesized particles, revealing the formation of the desirable products in all cases, similar to those obtained using other techniques, i.e., the stable P2 structure. Scanning electron microscopy revealed hexagonal-shaped particles, with sizes consistent with those in the literature [2]. EDS mapping in STEM mode was used to corroborate composition and the homogeneous distribution of elements which the particles.

Conclusions

In summary, the use of economical and common products to fabricate cathodes following this organic route is a suitable and environmentally friendly technique as well as a scalable route, while drastically decreasing mixing times down to a few minutes. Furthermore, the use of organic products guarantees that the side products are non-contaminant.

Keywords:

Sodium-batteries; cathodes; (S)TEM; nanoparticles

Reference:

Reference:
[1] F. J. García, R. Klee, P. Lavela, M. R. D. Bomio, J. L. Tirado. ChemElectroChem,2020, 7, 3528
[2] U. Maitra, R. A. House, J. W. Somerville, N. Tapia-Ruiz, J. G. Lozano, N. Guerrini, R. Hao, K. Luo, L. Jin, M.A. Pérez-Osorio, F. Massel, D. M. Pickup, S. Ramos, Xi. Lu, D. E. McNally, A. V. Chadwick, F. Giustino, T. Schmitt, L. C. Duda, M. R. Roberts, P. G. Bruce. Nature Chemistry 2018, 10, 288

1264

Epitaxial LiNi0.33Mn0.33Co0.33O2 thin films as a model cathode material system for Li-ion batteries

Dr. Elena Tchernychova[1], Blaž Jaklič[2,3], Jan Žuntar[2,3], Gregor Kapun[1,4], Prof. Dr. Matjaž Spreitzer[2], Prof. Dr. Robert Dominko[1,4,5]
[1]National Institute of Chemistry, , Ljubljana, Slovenia, [2]Jozef Stefan Institute, Ljubljana, Slovenia, [3]Jozef Stefan Institute International Postgraduate School, Ljubljana, Slovenia, [4]4Faculty of chemistry and chemical technology, University of Ljubljana, Ljubljana, Slovenia, [5]ALISTORE-European Research Institute, Amiens, France

Poster Group 1

LiNi1-x-yMnxCoyO2 (NMC) belongs to a class of layered oxide materials renowned for their solid energy storage performance, making them ideal for use as cathodes in lithium-ion batteries. NMC's structure consists of a two-dimensional layered arrangement where lithium and transition metal ions layers alternate, affecting how lithium ions move from the bulk to the surface within the crystal structure. These materials have already reached the stage of commercial performance with Tesla currently utilizing the NMC622 ($LiNi_{0.6}Mn_{0.2}Co_{0.2}O_2$) formula. However, the performance of NMC cathodes tends to degrade with battery cycling, which is linked to structural deterioration of NMC, although the precise degradation mechanisms remain poorly understood. To explore the performance and structural integrity of NMC cathodes and to understand the directional transport properties of Li ions, we created a thin film model cathode system using NMC111 ($LiNi_{0.33}Mn_{0.33}Co_{0.33}O_2$).

NMC111 thin films were grown on $SrRuO_3$/0.5% wt. Nb-doped $SrTiO_3$ (SRO/Nb) substrates with varying surface terminations by means of the pulsed laser deposition (PLD) technique. X-ray diffraction was used to confirm their epitaxial nature, showing distinct out-of-plane orientations (104), (118), and (003) corresponding to the (001), (110), and (111) substrate orientations. Detailed microstructural analysis through conventional and high-resolution transmission electron microscopy (TEM) showed twinned domains in films on (001) and (110) SRO/Nb substrates due to angled layer growth, with no twinning observed on the (111) SRO/Nb substrate. Electrochemical behavior of the produced thin films with different orientations was tested via galvanostatic cycling at different cycling rates. It revealed that crystal orientation markedly influences NMC's electrochemical performance, especially at higher charge and discharge rates, highlighting the anisotropic nature of lithium ion movement within NMC.

Acknowledgements: This work has received funding from the Slovenian Research Agency ARIS through core program funding P2-0423 and projects J2-3050 and JV-4637.

Keywords:

Thin films, Li-ion batteries, NMC

Reference:

1. T. Li, X.Yuan, L. Zhang, D. Song, K. Shi, C. Bock, Electrochemical Energy Reviews 2020, 3, 43–80

1276

Visualisation of tetrahedral Li in the alkali layers of Li-rich layered oxides

Dr Weixin Song[1,2,3], Dr Miguel Pérez-Osorio[1,2,3], Dr Jun Chen[1,2,3], Mr Zhiyuan Ding[1,3], Dr John Joseph-Marie[1,2,3], Dr Robert House[1,2,3], Prof Peter Bruce[1,2,3], Prof Peter Nellist[1,2,3]
[1]University of Oxford, Oxford, United Kingdom, [2]The Faraday Institution, Oxford, United Kingdom, [3]The Henry Royce Institute, Oxford, UK

Poster Group 1

Li-rich metal oxide cathode materials for Li-ion batteries, such as Li1.2Ni0.13Mn0.54Co0.13O2 can make use of the redox reaction of oxygen anions and transition metal (TM) cations, delivering superior capacities of over 250 mAh/g, much higher than the conventional metal oxides. However, fading in the capacity and voltage and the sluggish kinetics are significant problems for the Li-rich oxides1,2. Understanding the Li+ ion diffusion pathway is crucial for understanding the sluggish kinetics in anionic O2- redox. Li diffusion within the alkali layers undergoes a well-known, low-barrier octahedral-tetrahedral-octahedral (o-t-o) pathway3, however, it is less clear how Li diffuses in and out of the TM layers, particularly given the complex structural rearrangements which take place during O2- oxidation.

Here, we perform electron ptychography and simultaneous annular dark field imaging to directly visualise the Li in Li1.2Ni0.13Mn0.54Co0.13O2. At the end of the TM-oxidation region and before the high voltage O oxidation plateau, we observe Li occupying alkali-layer tetrahedral sites on opposite sides of the TM layers, forming Li-Li dumbbell configurations. The presence of Li at these tetrahedral sites is demonstrated by mathematical processing of the quantitative ptychographic phase contrast, see Figure 1. Density functional theory (DFT) calculations support the observation showing that tetrahedral Li-Li dumbbell configurations are lower in energy than corresponding tetrahedral TM configurations. We also observe the in- and out-of-plane TM migration as well as a partial phase transition from O3 to O1 stacking. In the O1 stacking phase, tetrahedral Li is absent, consistent with our DFT calculations indicating the O1 phase is not thermodynamically stable to accommodate tetrahedral Li. Upon further Li deintercalation to 4.8V, most tetrahedral Li is removed and we only observe a small amount of residual tetrahedral Li. After discharging to 2 V, we do not observe the reformation of tetrahedral Li but observe permanently migrated TMs occupying the alkali-layer sites. These migrated TMs may suppress the Li re-population of some vacant TM-layer octahedral sites by disfavouring Li occupation of the face-sharing tetrahedral sites. To maintain the maximum number of accessible tetrahedral Li sites and minimise the blocking of tetrahedral Li diffusion pathways, strategies to mitigate the irreversible TM migration and the O1 phase change should be employed.

Figure 1 Quantification of ptychographic phase contrast of Li1.2Ni0.13Mn0.54Co0.13O2 at a charging state of 4.45 V. (a) Ptychographic phase image marked with the alkali-layer tetrahedral sites showing contrast. The scale bar is 0.5 nm. (b) Squared phase image by squaring the ptychographic phase contrast in (a). The squared phase values around each atom are integrated using Voronoi cells to obtain the integrated squared phase (ISP). The ISP values at the alkali-layer tetrahedral site (AKtetra) and TM-layer octahedral site (TMoct) define an ISP ratio between these values. Two DFT models are used to simulate the ptychographic image and deliver the ISP ratios: (c) tetrahedral Li (Tetra_Li) model with Li ions at the tetrahedral sites. (d) tetrahedral Ni (Tetra_Ni) model with Ni ions at the tetrahedral sites. In the schematic representations of the models, grey is Ni, purple Mn, blue Co, red O and green Li. The ISP ratios calculated from the collected image in (a) and simulated images of the two DFT models within a range of thicknesses are compared in (e) and (f).

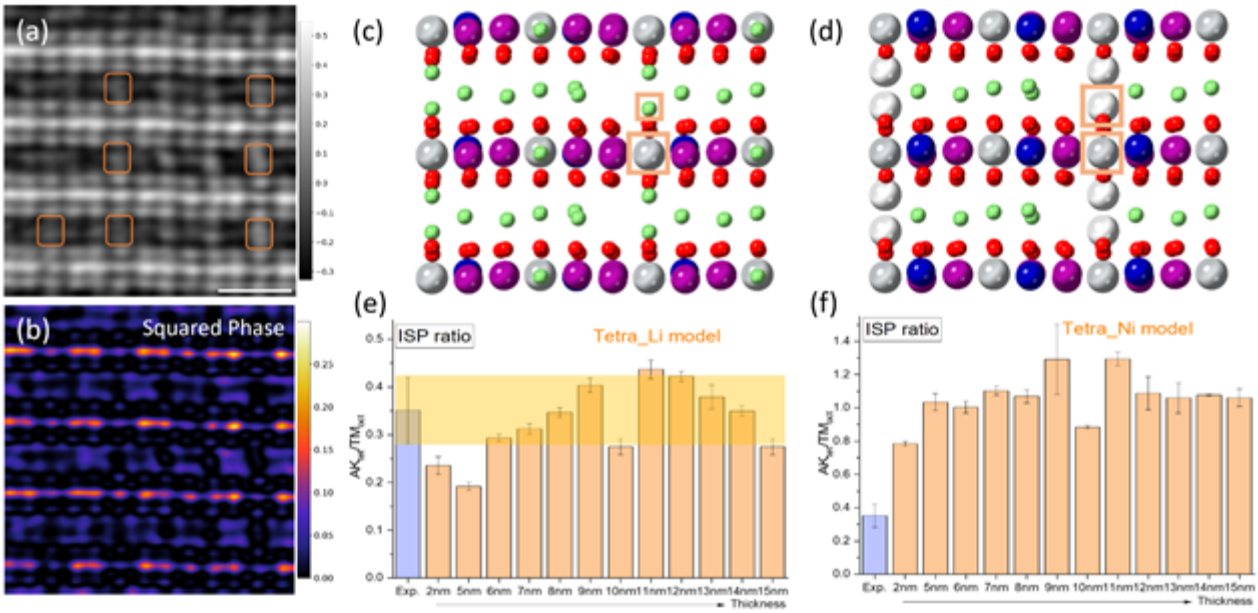

Keywords:

Li-rich metal oxide; electron ptychography

Reference:

Reference
1.House, R. A. et al. Nat Energy 5, 777, (2020).
2.Song, W. X. et al. Joule 6, 1049, (2022).
3.Kang, K., Meng, Y. S., Breger, J., Grey, C. P. & Ceder, G. Science 311, 977, (2006).
4. We acknowledge the financial support from the EPSRC (EP/K040375/1 ‘South of England Analytical Electron Microscope’), the Henry Royce Institute for Advanced Materials (EP/R00661X/1, EP/S019367/1, EP/R010145/1) and the Faraday Institution CATMAT project (FIRG016, FIRG035). We acknowledge the use of the facilities in the David Cockayne Centre for Electron Microscopy at University of Oxford.